Investigations on the selective deoxygenation of sugar alcohols over heterogeneous catalysts

TECHNISCHE UNIVERSITÄT DARMSTADT

From the Department of Chemistry at the

Technische Universität Darmstadt

approved

Dissertation

to obtain the academic degree of

Doctor-Engineer (Dr.-Ing.)

submitted by

M.Sc. Benjamin Bernhard Kühne

from Mainz

1. Referee: Prof. Dr.-Ing. Herbert Vogel

2. Referee: Prof. Dr. Markwart Kunz

Darmstadt 2018

Kühne, Benjamin Bernhard:

Investigations on the selective deoxygenation of sugar alcohols over heterogeneous catalysts

Date of submission: 11th April 2018

Date of oral exam (disputation): 25th June 2018

Darmstadt, Technische Universität Darmstadt

This dissertation was performed at the Ernst-Berl-Institut for Technical Chemistry and Macromolecular Science (Technische Universität Darmstadt) in cooperation with Südzucker's Central Department for Research, Development, and Services (CRDS) in Offstein. The experimental work was performed from 01.01.2014 to 31.12.2016 under supervision of Prof. Dr.-Ing. Herbert Vogel and Prof. Dr. Markwart Kunz.

List of publications

Partial results of this work have been published, by approval of the Department of Chemistry (represented by Prof. Dr.-Ing. Herbert Vogel), in the following contributions in advance.

Posters

B. Kühne, C. Götzelmann, H. Vogel, M. Kunz, *Heterogeneous catalyzed hydrogenolysis of sugar derivatives to oligohydroxy C4 to C6 alkanes*, 48. Jahrestagung Deutscher Katalytiker, Weimer, 11.03.-13.03.2015

B. Kühne, H. Vogel, M. Kunz, *Reaction engineering challenges – selective hydrogenolysis of sugar derivatives*, European Symposium on Chemical Reaction Engineering, Fürstenfeldbruck, 27.10.-30.10.2015

B. Kühne, S. Glasder, S. Kunz, C. Kröner, A. Haji Begli, H. Vogel, M. Kunz, *Oligohydroxy hexanes by selective hydrogenolysis from sugars*, 50. Jahrestagung Deutscher Katalytiker, Weimar, 15.03.-17.03.2017

Presentations

B. Kühne, H. Vogel, M. Kunz, *Heterogeneous catalyzes production of green C6 diols and triols*, 251st American Chemical Society National Meeting, San Diego (California), 13.03.-17.03.2016

B. Kühne, H. Vogel, M. Kunz, *Commodities from biomass by selective hydrogenolysis from sugars*, Jahrestagung Reaktionstechnik 2016, Würzburg, 02.05.-04.05.2016

Journal Papers

B. Kühne, H. Vogel, R. Meusinger, S. Kunz, M. Kunz, *Selective -C-O- hydrogenolysis over Cu based catalysts; identification of the reaction mechanism and key intermediates*, Catalysis Science & Technology, **2018**, *8*, 755-767, DOI: 10.1039/C7CY02426F

B. Kühne, S. Glasder, H. Vogel, S. Kunz, M. Kunz, *Structure-Selectivity Relationships for Polyol Hydrogenolysis over Ru Catalysts*, paper in review

Acknowledgements

My acknowledgement and gratitude goes to the following people for contribution to this work:

Prof. Dr.-Ing. Herbert Vogel and Prof. Dr. Markwart Kunz for the opportunity to perform my dissertation in the working group at TU Darmstadt and Südzucker's research department in Offstein. I am especially very grateful for the excellent personal and professional support as well as their trust and interest in my work.

Dr. Alireza Haji-Begli and Dr. Christine Kröner for all the meetings in Offstein and the many suggestions to find constructive solutions in this complicated field of research. Furthermore, I am also very appreciative for the coworkers in the departments of heterogeneous catalysis, biotechnology and instrumental analysis. I have enjoyed every visit and the teamwork developing a new chemical process including the development of analytical methods.

Prof. Dr.-Ing. Alfons Drochner, Prof. Dr. Reinhard Meusinger, and all coworkers from TU Darmstadt for the consistently friendly and pleasant atmosphere, as well as the numerous professional discussions. I particularly thank all of the student coworkers that helped contributing to this work in practical courses, as well as Bachelor and Master thesis. Great acknowledgements also go to Dr. Sebastian Kunz from the Institute for Applied and. Physical Chemistry (IAPC) at the University of Bremen for all the encouraging words and the proofreading of my papers.

Karl Kopp and the working group of Prof. Christian Hess (TU Darmstadt, Eduard-Zintl-Institute for inorganic and physical chemistry) for XPS analysis of the Cu catalysts. Our special gratitude also goes to Dr. Jörg Engstler (TU Darmstadt, Eduard-Zintl-Institute for inorganic and physical chemistry) for TEM analysis of the Cu/Al_2O_3 catalyst.

And most importantly my beautiful wife Ramona, my family, and friends for all the support over the last few years. Thank you for always encouraging me and critically reviewing this work. In particular, my gratitude goes to Artur Wiser for reviewing lots of presentations and posters and all the good times we had in the working group and numerous meetings in Germany and overseas.

Table of contents

1. Motivation

One of the major long-term challenges in the chemical industry is the replacement of fossil feedstocks with renewable resources. The term *sustainability* has taken – analog to *bio* – an inflationary trend; products are promoted to be bio-based and sustainable [Vogel2014]. In the original form, sustainability means supplying humanity with carbon-based raw materials without further exploitation of the limited fossil feedstocks provided by our planet. The most basic route occurs naturally by photosynthesis, which delivers biomass from the solar powered conversion of CO_2 with water [Vogel2014]. About 200 billion tons of renewable biomass are produced annually from this process [Lichtenthaler2004]. Carbohydrates account for roughly 75 % of this mass, with C6 and C5 building blocks (hexoses and pentoses, respectively) stored in the form or biopolymers such as cellulose, hemicellulose, starch, and inulin. The repeating units of these polysaccharides are glucose (cellulose, starch), fructose (inulin) and xylose (xylan) which can be utilized for the production of large-scale commodities (**Figure 1-1**). Transitioning from petrochemical processes into a bio-based industry is pressing, but various obstacles need to be overcome: fossil raw materials are currently more economic than renewable resources; the petrochemical process technology is exceedingly well developed and basically much different from the transformation of carbohydrates into organic chemicals [Lichtenthaler2004]. Thus, only a minor fraction (about 4 %) of the annually renewable carbohydrates is utilized. Such aspects gain more importance from the point of view of sustainable chemistry and the use of renewable feedstocks [Baerns2013]. Herein, the concept of bio refineries is not a new approach but rather the reawakening of proven methods. A hundred years ago the feedstocks of the chemical industry were based on biomass, coal and tar. The steady increase of cheap oil and gas in large quantities began in the early 20th century and displaced the traditional chemistry with entirely new processes [Lichtenthaler2004].

The different chemical routes for the production of large scale platform chemicals (intermediates) based on fossil and renewable feedstocks is simply reasoned in the molecular structure of the raw materials. Fossil raw materials such as coal, oil and natural gas generally need to be functionalized by addition of a hetero atom (e.g. oxygen and nitrogen). The hydrocarbons of various carbon-chain lengths (usually C1 to C18) are thus converted to aldehydes, ketones, alcohols, carboxylic acids or amines and gain weight. In contrast, the repeating units of carbohydrates glucose, fructose, and xylose – as well as the corresponding sugar alcohols sorbitol, mannitol, and xylitol – are over-functionalized. Each carbon atom in the C5 or C6 carbon chain is attached to an oxygen atom in form of a hydroxyl group (-C-OH) and a ketone or aldehyde group (-C=O) in the mono sugars. Hence, the conversion of such polyol compounds into products with only one or two functional groups like mono alcohols or diols requires selective defunctionalization [Palkovitz2012]. One promising route to value-added chemicals is the metal-catalyzed cleavage of -C-O- and -C-C- bonds using hydrogen (H_2) [Bond2013, Claus2006, Corma2007, Isikgor2015, Vogel2014].

Such transformation reactions of renewable feedstocks by hydrogenolysis have been investigated intensively, but mainly with focus on -C-C- bond cleavage to form short-chain polyols [Clark1958, Montassier1983, Zartman1933]. Catalysts for selective -C-C- bond cleavage of sugars to glycols (1,2-propanediol and ethanediol) with yields up to 91 wt-% are well known (**Figure 1-1**) [Schuster1989, Dubeck1984]. However, the formation of deoxygenated C6 products by selective -C-O- bond cleavage (deoxygenation) to C6 tetrols, triols and diols still requires further improvements.

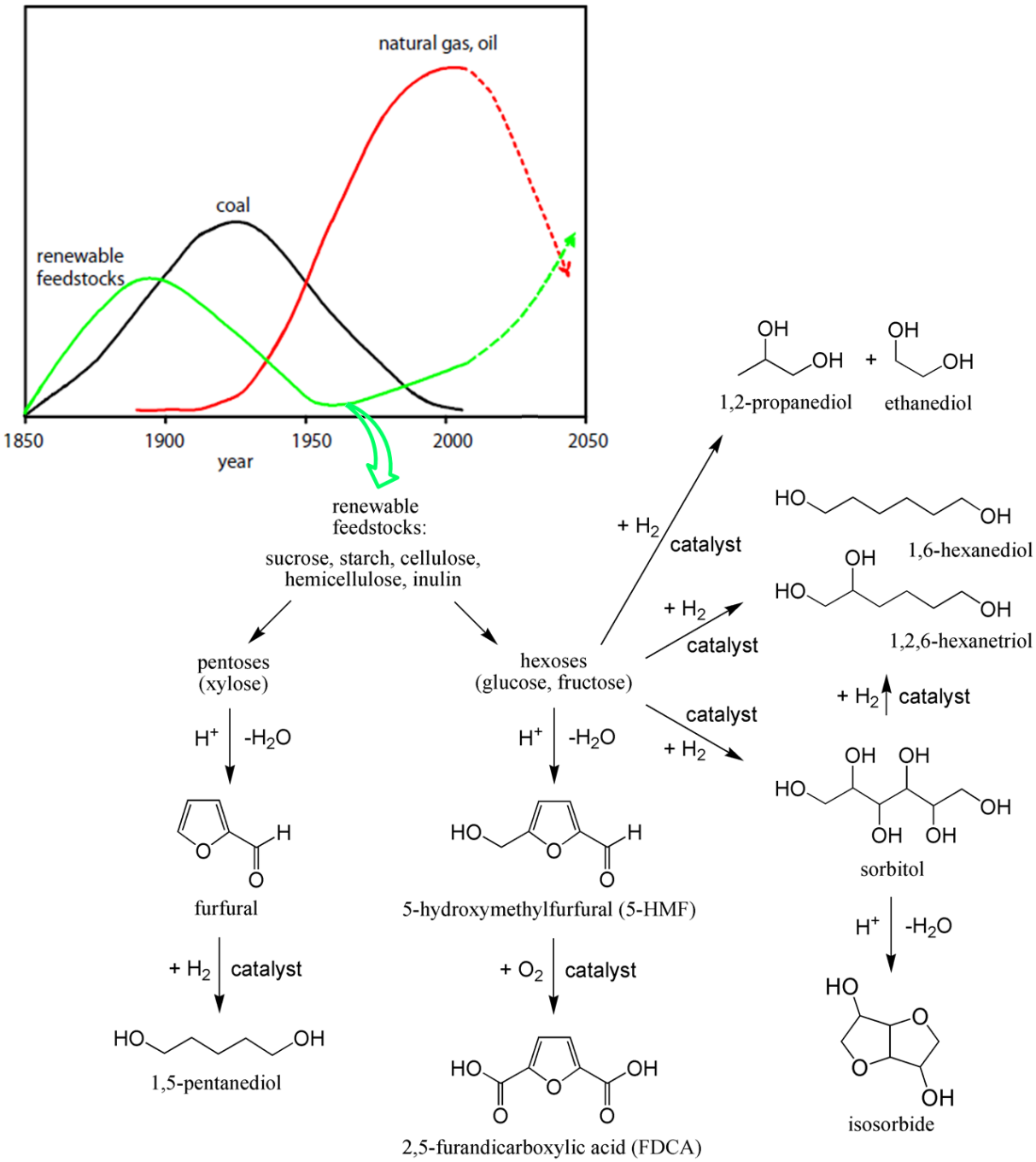

Figure 1-1: Raw materials basis of the chemical industry in historical perspective, adapted from Lichtenthaler *et al.* and potential value-added intermediates based on pentoses and hexoses [Lichtenthaler2014].

Repeated -C-O- bond cleavage from hexoses (and hexitols such as sorbitol) yields valuable deoxy C6 products such as 1,2,6-hexanetriol or 1,6-hexanediol (**Figure 1-1**). Bio-derived 1,6-hexanediol could be converted into the amine and combined with bio-derived adipic acid [Rennovia2010] for a 100 % bio-based nylon-6,6 process. 1,2,6-hexanetriol is a widely applied cross-linker in polyesters and alkyd resins [Tess1957]. Esterification of 1,2,6-hexanetriol with long-chain carboxylic acids also forms plasticizers for various polymers (e.g. polyvinylchloride) and rubbers [Whetstone1956].

Multiple petrochemical routes to 1,6-hexanediol are currently used in the industry, commonly based on butadiene or benzene [BASF1976, Musser1993, Musser2005]. 1,6-hexanediol formation via adipic acid requires four steps, starting from naphtha (benzene, see **Figure 1-2**). Likewise, the production of 1,2,6-hexanetriol from propylene would also require four synthesis steps via an acrolein-dimer, acid-catalyzed hydration and hydrogenation [Arntz2007, Schulz1950, Shell1956]. Replacing this complex chemistry by an ecofriendly one-pot reaction via selective deoxygenation from sugars or sugar alcohols would be a significant breakthrough for the use of renewable feedstocks.

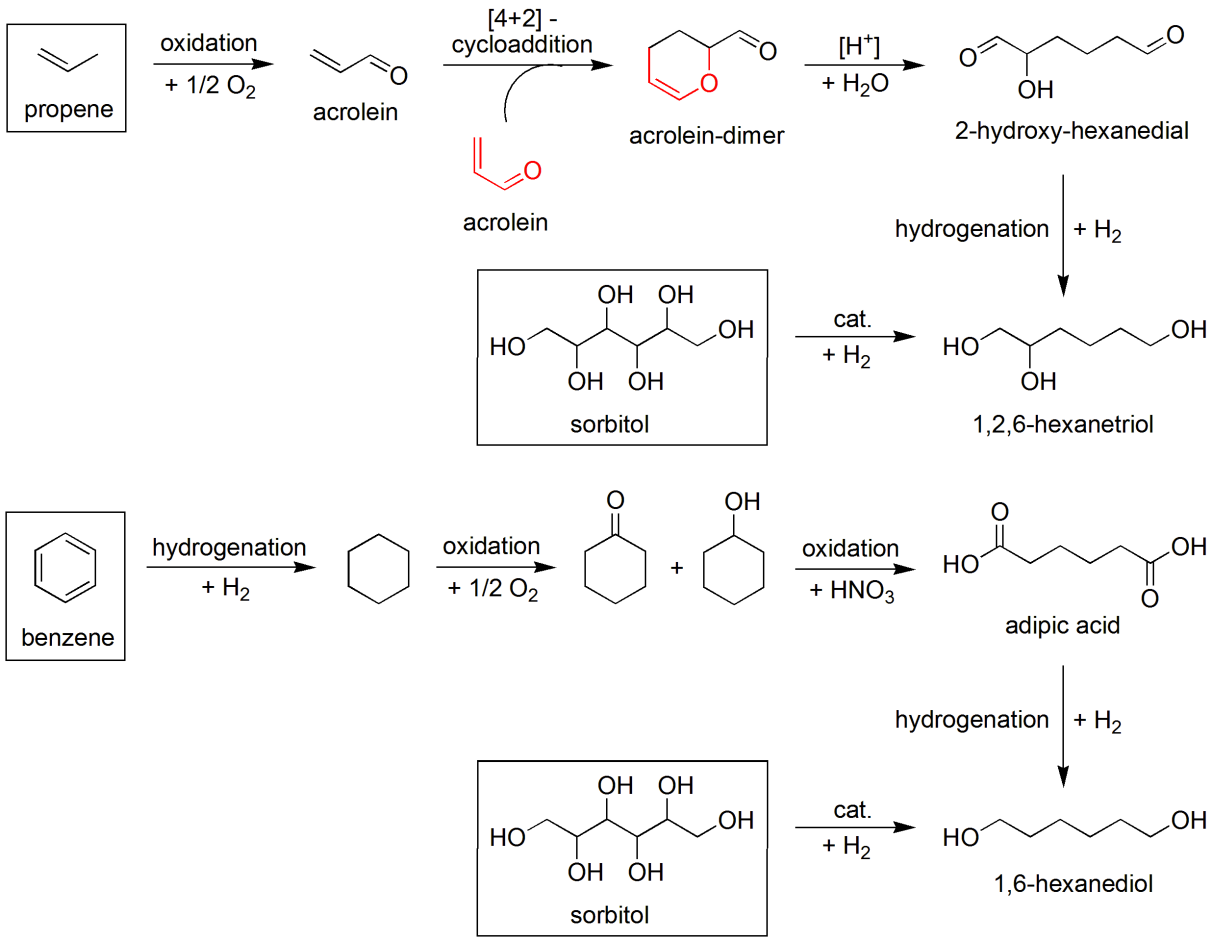

Figure 1-2: Petrochemical routes to 1,2,6-hexanetriol and 1,6-hexanediol include four synthesis steps from naphtha (propylene and benzene, respectively). Selective -C-O- hydrogenolysis (deoxygenation) from sorbitol would enable the same products in a one-pot reaction with suitable catalytic systems.

Many other deoxy C5 and C6 products are accessible from pentoses and hexoses, including 1,5-pentanediol and isosorbide, that are also suitable for the formation of polyesters and alkyd resins [Blanc2000, Huber2010, Tomishige2017]. The acid-catalyzed dehydration of xylose yields furfural which is further converted to 1,5-pentanediol via ring-opening hydrogenation over suitable catalysts (**Figure 1-1**) [Tomishige2017]. Isosorbide is obtained when the linear sugar alcohol sorbitol is used as reactant instead of xylose.

Substituting large-scale chemicals without changing the existing value chains seems partially possible with such concepts. However, many routes will require a complete re-design of value chains [Palkovitz2012]. Not only new synthesis strategies, processes, and catalysts are required. The available product spectrum from renewable feedstocks is often different from fossil raw materials. New molecular structures may substitute traditional compounds which leads to the adaptation of final products, for example, terephthalic acid versus 2,5-furandicarboxylic acid (FDCA) [Rose2011]. FDCA is identified as one of twelve future building blocks for bio-based value added chains along with glucaric acid, sorbitol, xylitol, and glycerol [Werpy2004]. The dicarboxylic acid can be obtained from oxidation of 5-HMF, which is an intermediate in the acid-catalyzed dehydration from fructose (**Figure 1-1**) [BASF2015, Furanix2014, Nikolla2011, Titirici2008]. Substitution of terephthalic acid with FDCA enables the production of polyethylene-furandicarboxylic acid (PEF instead of PET). This new polymer would be 100 % bio-based, recyclable and exhibits better gas barrier properties, mechanical strength, and heat resistance [Synvina2017].

These examples highlight the potential of selective deoxygenation reactions (-C-O- bond cleavage) for the transformations of sugars and sugar alcohols to bulk commodities. Optimizing of catalysts, process parameters and the isolation of products from reaction mixtures will be the main challenges for potential bio refinery concepts. Thus, in order to develop new industrial processes, a better understanding of the major and side reaction pathways is necessary. In particular, the mechanisms involved on the catalyst surface need to be further investigated.

2. Scope of this work

The scope of this work is to evaluate the potential for selective deoxygenation (-C-O- bond cleavage) of biomass-derived polyol compounds over heterogeneous catalysts. Standard commercial hydrogenation catalysts are applied for the hydrogenolysis of various sugars and sugar alcohols, including sucrose, glucose, sorbitol, mannitol, and xylitol. The effect of the active metal and support material are investigated for Ru, Ni and Cu based catalysts with regards to -C-O- vs. -C-C- bond cleavage properties.

It is the main goal to isolate and identify reaction intermediates to better understand the mechanisms involved in the selective -C-O- bond cleavage over Cu and Ru catalysts. Furthermore, different reaction pathways for -C-C- bond cleavage (degradation of the carbon chain) should be addressed for the different metals such as retro-aldol reactions, decarbonylation and decarboxylation. For this purpose, deoxy C6 polyols such as 1,2,6-hexanetriol as well as short-chain polyols like 1,2,4-butenetriol, 1,2-butanediol, and 1,2-propanediol are used as reactants. In particular, the effect of the number and arrangements of OH-groups in the reactant should be investigated. Mechanistic conclusions should be drawn when significant patterns are observed for a catalyst. With such conclusions selective -C-O- and -C-C- bond cleavage properties can be traced back to interactions of the polyol compounds with the active metals (Cu, Ni, and Ru, respectively) on the catalyst surface. In particular, a correlation between hydrogenation and hydrogenolysis properties of the applied catalysts should be addressed. The better understanding of the mechanisms involved on the catalyst surface should then be used to optimize the catalysts and reaction conditions (e.g. temperature and H_2 pressure) to increase the yield of deoxy C6 products.

Finally, the separation of deoxy C6 polyols from short-chain compounds such as glycols and glycerol should be investigated by comparing standard industrial downstream processes. The first method is chromatographic separation over ion-exchange resins in an aqueous solution. The potential for purification of the desired deoxy C6 products should be evaluated by variation of the ionic form of the resin (H^+ or Ca^{2+}), column temperature, and flow rate of the mobile phase. The second downstream process is liquid-liquid extraction with non-soluble polar solvents. A screening of various organic solvents and the effect of the extraction temperature should be investigated and highlighted for application in potential bio refinery concepts.

3. State of the art of science

3.1. Hydrogenolysis of polyols over heterogeneous catalysts

In this chapter various heterogeneous metal catalysts are presented with respect to their -C-O- and -C-C- bond cleavage properties for the conversion of polyols. The characteristics of commonly used metals for hydrogenolysis reactions, as well as the effect of co-catalysts and support materials are demonstrated. The main focus will be given on the optimization of catalysts and process parameters for improved -C-O- bond cleavage (deoxygenation). However, the sometimes inconsistent proposals of different authors will also be presented in this critical review. Complex degradation pathways for -C-C- bond cleavage will be presented in chapter 3.1.4.

3.1.1. Cu catalysts

Cu based catalysts have long been considered for the catalytic conversion of polyol compounds. Zartman and Adkins attempted to convert various sugars and sugar alcohols (including mannitol and sorbitol) dissolved in ethanol over a $CuCrO_x$ catalyst [Zartman1933]. The formation of deoxy C6 compounds (dehydroxylated sorbitol and mannitol) along with short-chain alcohols such as methanol, ethanol, and 1,2-propanediol was reported. Three deoxygenated C6 polyols were identified: 1,2,5-hexanetriol, 1,2,5,6-hexanetetrol, and a heterocyclic polyol formed by intramolecular dehydration. The reaction conditions were quite harsh with temperatures and pressures up to 250 °C and 300 bar H_2, respectively [Zartman1933]. A different $CuCrO_x$ catalyst was used at comparatively mild reaction conditions (180 °C and 75 bar H_2) for the conversion of sucrose, also dissolved in ethanol [Goldschmid1960]. The reaction products were 5-hydromethylfurfural (5-HMF), glycerol, erythritol, and various ketohexoses. Interestingly, the formation of deoxygenated C6 polyols was not reported. Montassier *et al.* studied the transformation of sorbitol, erythritol, and glycerol over Cu-Raney and supported noble metal catalysts [Montassier1988]. The Cu- Raney catalyst yielded mainly deoxy compounds while maintaining the carbon chain of the reactant. An unidentified hexanetetrol (presumably the 1,2,5,6-isomer) and hexanetriols were obtained from sorbitol hydrogenolysis; however, specific isomers were not reported. The C4 sugar alcohol erythritol was mainly converted to 1,2-butanediol, while glycerol yielded 1,2-propanediol with ethanediol as a minor side product [Montassier1988]. A comprehensive analysis of hexanetetrols and -triols isomers, obtained from hydrogenolysis over Cu-Raney, was reported in a patent by ADM [ADM2015]. 1,2,5,6-hexanetetrol, 1,2,5-hexanetriol, 1,2,6-hexanetriol, and 1,4,5-hexanetriol are obtained among the major products. These isomers are the same as already reported in 1933 by Zartman *et al.* using the $CuCrO_x$ catalyst (**Figure 3-1**) [Zartman1933]. An overall yield of 63 % deoxy hexitols is reported by Blanc *et al.* using Cu/ZnO (methanol synthesis catalyst) for the conversion of starch-derived hexitol mixtures [Blanc2000].

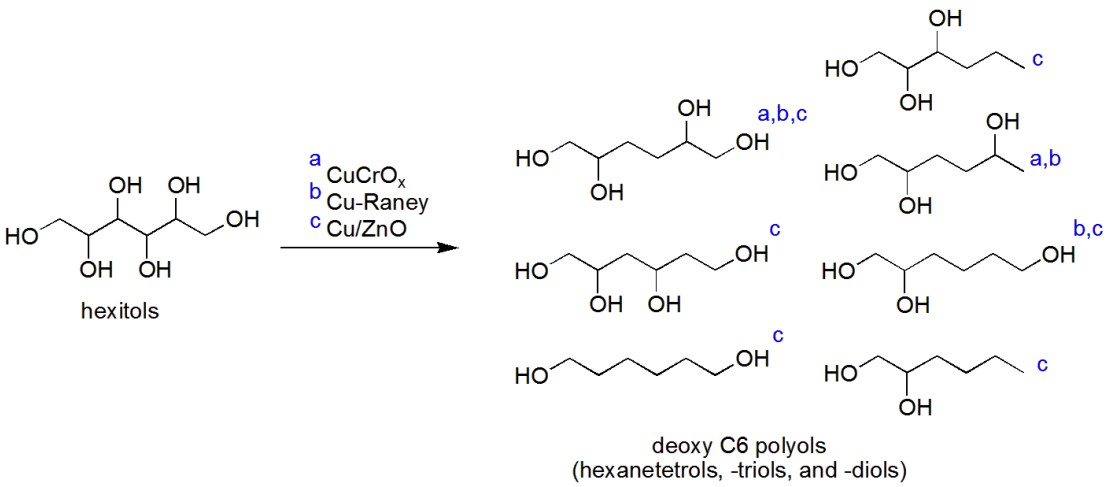

Figure 3-1: Formation of deoxy C6 polyols from hexitols (sorbitol, as well as *in situ* formed mannitol and iditol) over Cu-CrO_x [Zartman1933], Cu-Raney [ADM2015, Montassier1988], and Cu/ZnO [Blanc2000].

However, different deoxy C6 products are reported from Blanc *et al.*: 1,2,4,6-hexanetetrol, 1,2,3-hexanetriol, and 1,2,6-hexanetriol were identified among various unassigned polyols [Blanc2000]. Mechanistic concepts for the formation of these deoxy C6 compounds from hexitols over Cu were not carried out by either of the authors and are up to this date not available in literature. Montassier *et al.* only concluded mechanistic proposings for degradation reactions to short-chain polyols. This work, however, helped to elucidate most of the currently known -C-C- bond cleavage mechanisms that result from dehydrogenated species on the catalyst surface (see chapter 3.1.4). The formation of such species is attributed to special hydro-dehydrogenating properties of the Cu-Raney catalyst which leads to abstraction of H_2 during adsorption [Montassier1988]. These characteristics of Cu-Raney accord with patents from Berweiler *et al.* for dehydrogenation of alcohols to aldehydes and ketones [Berweiler2001, Berweiler2004]. Cu does not hydrogenolyze -C-C- or -C-O- bonds of polyols in aqueous phase under elevated H_2 pressure [Montassier1988]. The elimination of OH-groups results from dehydration of strongly adsorbed intermediates. Although a pathway for -C-O- bond cleavage from sorbitol to hexanetriols is not described, a dehydroxylation mechanism for the conversion of glycerol to 1,2-propanediol is presented (**Figure 3-2**).

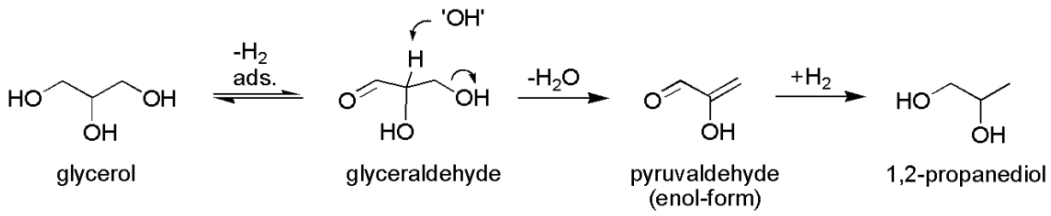

Figure 3-2: Dehydroxylation mechanism for conversion of glycerol to 1,2-propanediol as proposed by Montassier *et al.* [Montassier1988].

Adsorbed OH-groups on the catalyst that are in close proximity of dehydrogenated glycerol (glyceraldehyde) species on Cu sites are able to initiate deprotonation which leads to cleavage of an adjacent OH-group yielding the enol-form of pyruvaldehyde. Hydrogenation of this intermediate product gives 1,2-propanediol, which was found to be a stable product. This dehydration route is also supported by various other authors [Jin2015, Palkovitz2014, Wang2010]. Reactions carried out under N_2 and H_2 revealed that deoxygenation occurs on reduced copper species [Wang2010]. These results suggest that the initial dehydrogenation step of glycerol to glyceraldehyde is necessary before dehydration and hydrogenation to 1,2-propanediol take place [Palkovitz2014]. These considerations from Wang *et al.* and Palkovitz *et al.* were made for Cu catalysts modified by Zn and report up to 93 % selectivity for 1,2-propanediol [Wang2010]. Interestingly, kinetic studies using a similar Cu/ZnO catalyst consider another dehydration mechanism that does not involve initial dehydrogenation and leads to different reaction intermediates [Zhou2010]. The mechanism proposed from Zhou *et al.* was first reported by Dasari *et al.* and proposes acid-catalyzed dehydration of glycerol to acetol, which was identified as the intermediate product (see **Figure 3-3**) [Dasari2005].

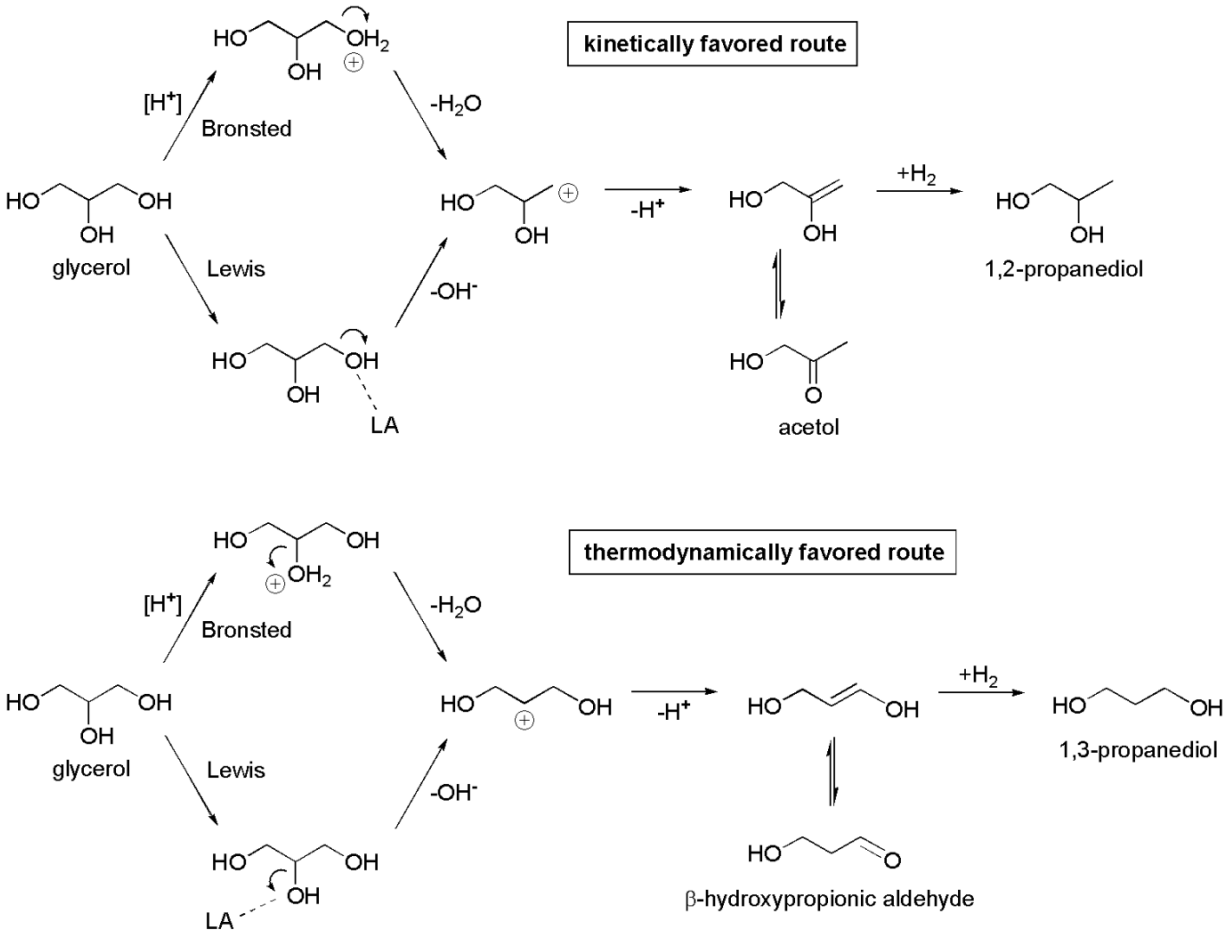

Figure 3-3: Kinetically and thermodynamically controlled dehydration of glycerol to 1,2-propanediol or 1,3-propanediol, respectively. The acid-catalyzed reactions may occur via Bronsted or Lewis acid sites on the catalyst as proposed from Dasari *et al.* [Dasari2005].

These contradicting findings by the authors show that Cu catalysts with the same composition and co-metals are able to catalyze different -C-O- bond cleavage pathways. In contrast to Montassier's initial dehydrogenation-hydrogenation step, this pathway to 1,2- or 1,3-propanediol over commercially available Cu catalysts does not involve formation of unsaturated species before -C-O- bond cleavage. Unsaturated intermediates are only formed after elimination of water (over Bronsted acid sites) or hydroxide ions (over Lewis acid sites) from glycerol. Regarding this mechanism, it is interesting that the selectivity for 1,2-propanediol from glycerol increases from around 36 to 90 % when the H_2 pressure is increased from 50 to 300 psi [Dasari2005]. This would lead to the conclusion that side reactions via unsaturated intermediates are enhanced at low pressure, e.g. retro aldol reactions. However, no such effects are discussed by the authors, probably because acetol is not able to undergo retro aldol reactions. The kinetically favored route follows dehydration of terminal OH-groups because there are easier accessible, while dehydroxylation of the secondary OH-groups is thermodynamically favored due to the more stable carbenium ion. The comparison of 1,2-propanediol and 1,3-propanediol yields concludes that the acid-catalyzed dehydration is kinetically controlled because 1,2-propanediol is always obtained in much higher quantities [Palkovitz2012]. 1,2-propanediol yields of >73 % are reported from Dasari *et al.* over $CuCrO_x$ [Dasari2005]. The dehydration step of glycerol to acetol is the rate limiting step because it is much slower than hydrogenation of acetol to 1,2-propanediol [Zhou2010].

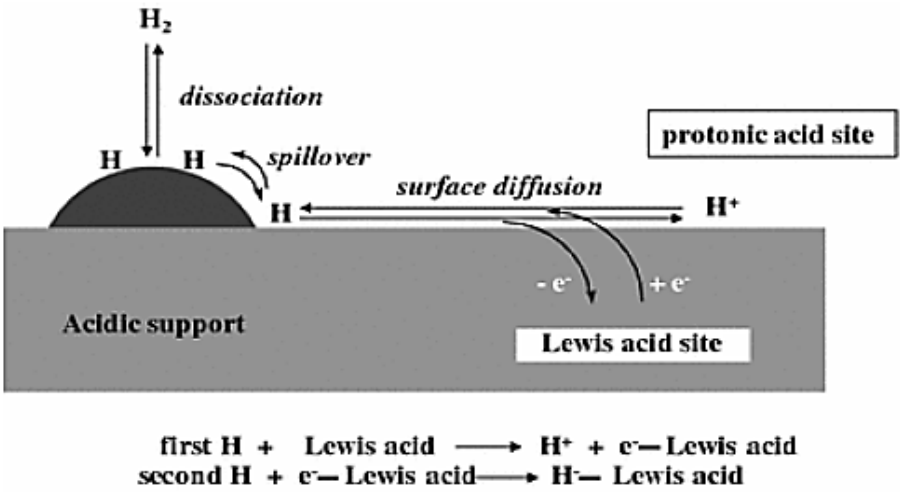

Figure 3-4: Formation of protonic acid sites on acidic supports of modified catalysts. Homolytic dissociation of H_2 on the metal surface leads to mobile hydrogen atoms that spillover to Lewis acid sites on the support. The electron transfer at these sites leads to the formation of protons [Bejile2015, Hattori2010].

The formation of Bronsted acid sites (protons) on the catalyst surface without addition of homogeneous acids, such as H_2SO_4 or HCl, is not yet well established. A concept by Hattori *et al.* proposes strong interactions between H_2 and metal catalysts modified by an acidic support (see **Figure 3-4**) [Bejile2015, Hattori2010]. Bronsted acid sites may arise from homolytic dissociation of H_2 over metals creating two hydrogen radicals. These activated species are able to spillover to the acidic support

and migrate to Lewis acid sites (electron deficient species such as oxygen defects in metal oxides), where an electron is transferred creating the proton [Hattori2010]. In contrast, the incorporation of alkaline co-catalysts or basic catalyst sites initiates -C-C- bond cleavage to short-chain polyols and even oxidation to short-chain acids [Huang2014, Jin2015]. On the one hand, the addition of $Ca(OH)_2$ promotes base-catalyzed rearrangement reactions such as the retro aldol mechanism. Huang *et al.* have shown that silica-supported Cu catalysts are responsible for dehydrogenation of xylitol to xylose and subsequent -C-C- bond cleavage yielding unsaturated C2 and C3 compounds [Huang2014]. Unsaturated intermediates in this reaction are either hydrogenated to glycols or oxidized with $Ca(OH)_2$ to glycolic acid and lactic acid [Huang2014]. The same effects were observed for hydrogenolysis of C3 to C6 sugar alcohols on modified Cu catalysts with up to 82 % glycol yields from sorbitol [Jin2015]. The strong interaction between Cu and Ca^{2+} cations in the solid support supposedly facilitates -C-C- and -C-O- bond cleavage of the sugar alcohols [Jin2015]. Surface characterization revealed that different phases promote dehydrogenation ($Ca_xCu_yAl_zO_p$) and hydrogenation (spinal $CuAl_2O_4$). A CuCoMnO catalyst by BASF gives comparable yields of up to 80 % glycols for the conversion of sucrose through the intermediates sorbitol and mannitol [Schuster1988]. The addition of Co and Mn to a Cu catalyst obviously enhances -C-C- bond cleavage in the same way.

This comparison of various Cu catalysts shows on the one hand that similar catalytic properties are possibly obtained by a combination of different supports and (metallic or acidic) co-catalysts. On the other hand, catalysts with seemingly the same metal composition such as $CuCrO_x$ can lead to totally different product distributions. While Zartman *et al.* first described deoxy C6 polyols as major products from sorbitol over such catalysts, Goldschmid *et al.* only detected short-chain polyols aside from 5-HMF [Goldschmid1960, Zartman1933]. Mechanistic models for -C-O- bond cleavage are at present only available for the conversion of glycerol to 1,2-propanediol. Some proposals suggest initial hydrodehydrogenation with subsequent dehydration [Palkovitz2014, Wang2010], while kinetic studies reveal the presence of an acetol intermediate that does not require dehydrogenation of the reactant glycerol [Zhou2010]. Obviously, different reaction pathways are possible and further studies are still required.

3.1.2. Ru catalysts / Pt group metals

Hydrogenolysis properties of catalysts based on Ru are often compared with other Pt group metals (Rh, Ir, Pd, and Pt) because of similar characteristics for -C-O- and -C-C- bond cleavage [Hibbitts2015, Miyazawa2006, Montassier1988, Palkovitz2012]. These metals are generally known to catalyze degradation reactions of polyols and alcohols that lead to formation of short-chain compounds and volatile gaseous products [Blanc2000, Deutsch2012, Hibbitts2015, Manas2015, Montassier1988, Miyazawa2006, Palkovitz2015]. Early studies from Montassier *et al.* reported that the competition between -C-O- and -C-C- bond cleavage depends on the properties of the active metal and the reaction conditions (pH level and temperature) [Montassier1983, Montassier1988]. Transition metals such as Ru initially activate polyol compounds by abstracting H_2 (dehydrogenation) during adsorption on the catalyst surface. This leads to isomerization of unsaturated intermediates via base-catalyzed enol-ketone rearrangements. The presence of dehydrogenated species becomes more statistical when the temperature is increased (from 130 to 190 °C) and enables -C-C- bonds cleavage [Montassier1983]. At neutral pH, sorbitol and other C6 polyols derived from isomerization undergo cleavage in the middle of the carbon chain yielding the C3 polyols glycerol and 1,2-propanediol. Glycerol is further converted to 1,2-propanediol via metal catalyzed -C-O- hydrogenolysis. However, 1,2-propanediol was also found to be an initial product from sorbitol and not only originating from glycerol. Thus, C3 polyols that are formed on the catalyst surface from sorbitol are able to undergo additional -C-O- bond cleavage before desorption from the catalyst occurs (**Figure 3-5**) [Montassier1983].

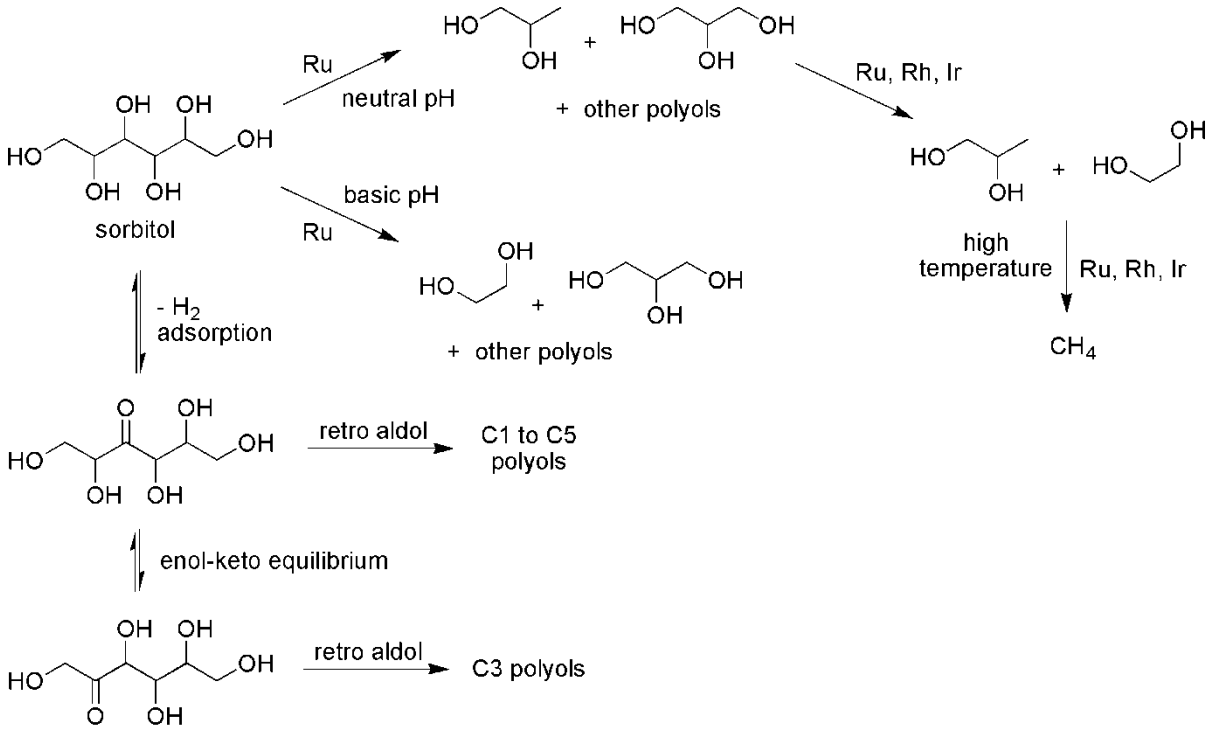

Figure 3-5: Hydrogenolysis of sorbitol over Ru catalysts at neutral and basic pH with dehydrogenated intermediates, as well as conversion of glycerol over Ru, Rh, and Ir as proposed by Montassier *et al.* [Montassier1983, Montassier1988].

At higher temperatures all bonds are potentially broken, leading to a general loss in selectivity with the formation of methane as the major product. In a basic medium, reverse aldolization leads to a vast mixture of different polyols, including C2 and C3 compounds, independently of the temperature [Montassier1983]. Further studies at neutral pH revealed that Rh and Ir have the same catalytic properties as Ru and finally convert polyols to hydrocarbons, mainly methane [Montassier1988]. Mechanistic investigations on the role of an Ir catalyst have shown that the transition metal enables multiple pathways under H_2 pressure, e.g. dehydration, degradation and even oxidation of polyols via unsaturated intermediates on the catalyst surface [Manas2015]. Mechanistic details of these reactions are described in chapter 3.1.4.

The formation of 1,2-propanediol from glycerol via selective -C-O- bond cleavage over noble metal catalyst was the subject of investigations by many research groups [Dasari2005,Miyazawa2006, Shinmi2010]. Dasari *et al.* and Miyazawa *et al.* proposed a mechanism that describes direct dehydration of glycerol to acetol, which is hydrogenated to 1,2-propanediol over supported Ru, Pd, and Pt. In contrast to the catalytic route according to Montassier *et al.*, an initial dehydrogenation to unsaturated species is not required (**Figure 3-6**).

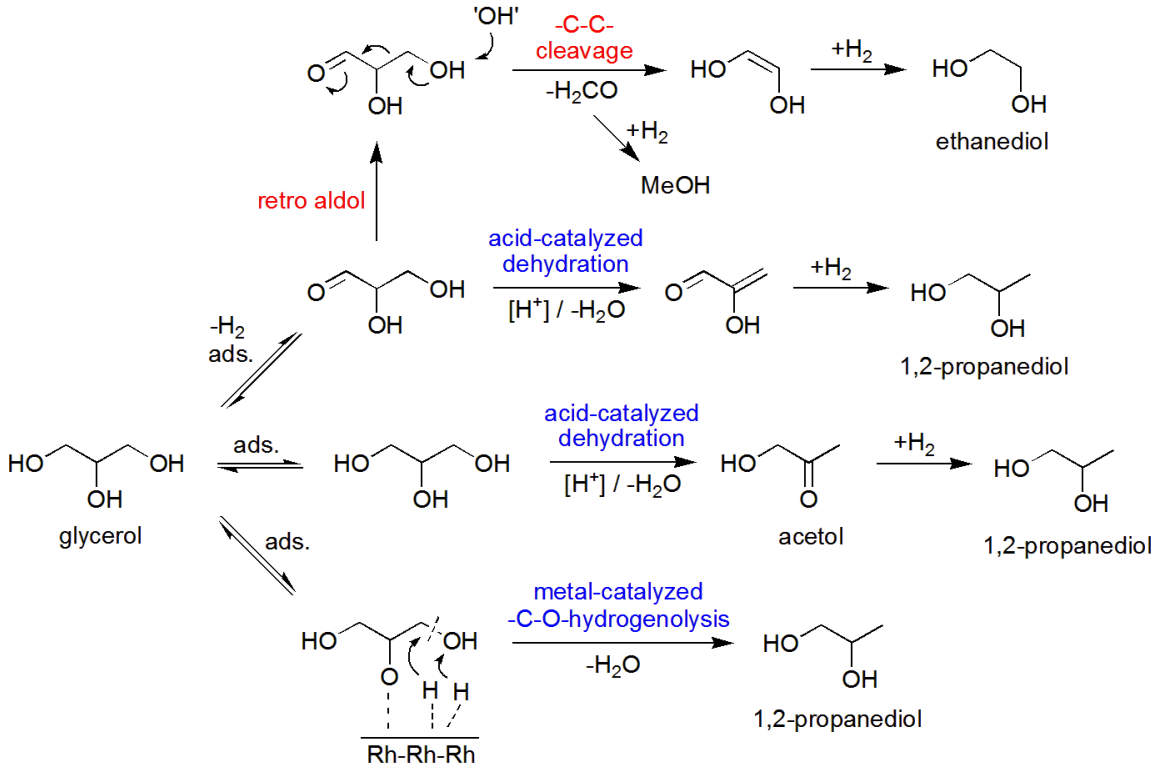

Figure 3-6: Mechanisms for the conversion of glycerol to 1,2-propanediol or ethanediol via unsaturated intermediates according to Montassier *et al.* [Montassier1988]. The dehydration route to acetol was proposed by Dasari *et al.* and Miyazawa *et al.* [Dasari2005, Miyazawa2006], whereas the metal-catalyzed -C-O- hydrogenolysis is adapted from Shinmi *et al.* [Shinmi2010].

This is a contradiction to the well described dehydrogenating characteristics of these metals [Hibbitts2015, Montassier1988], in particular for Ru catalysts [Deutsch2012 , Montassier1983, Montassier1991, Palkovitz2015]. However, the presented mechanism is based on the identification of the acetol intermediate that can only be formed when glycerol is not dehydrogenated [Dasari2005]. The reaction pathways are proposed for various noble metal catalysts in combination with homogeneous and heterogeneous acids (H_2SO_4, HCl, and acidic Amberlyst resin) [Miyazawa2006]. Glycerol undergoes dehydration to acetol, which is subsequently hydrogenated to 1,2-propanediol. Thus, combining acidic co-catalysts with supported platinum group metals such as Ru, Rh, Pd, and Pt also shows good -C-O- bond cleavage properties. 1,2-propanediol is even further converted to 1-propanol over Ru, demonstrating strong -C-O- bond cleavage properties similar to the Rh catalyst presented by Shinmi *et al.* [Miyazawa2006, Shinmi2010]. However, significant differences in the conversion of glycerol are reported. Carbon-supported Ru with the addition of the solid acid Amberlyst resin is much more effective for dehydration of glycerol to 1,2-propanediol and 1-propanol than Rh, Pd, and Pt or the homogeneous acids H_2SO_4 and HCl [Miyazawa2006]. The authors explain the special properties of the Ru catalyst with Ru-OH species for dehydration along with the strong acidic Amberlyst. Degradation reactions are proposed to occur over the noble metal catalysts but detailed mechanisms are not presented for -C-C- bond cleavage reactions. Interestingly, a detailed comparison of the reactants used by Miyazawa *et al.* reveals that degradation does not occur over acetol or propanal [Miyazawa2006]. The carbon yield for the hydrogenated products 1,2-propanediol and 1-propanol, respectively, are >99 mol-%. Retro aldol reactions are not possible for these two reactants because of the requirement of 1,3-diol functionalities. However, the degradation of ethanediol is reported, which has to be metal-catalyzed because this compound is not able to follow the retro aldol reaction either.

Shinmi *et al.* proposed yet another mechanism via direct -C-O- hydrogenolysis over an Rh catalyst that does not require initial dehydrogenation of the reactant (**Figure 3-6**) [Shinmi2010]. Strong interactions between glycerol and the active metal are described with adsorption over alkoxide species. A vicinal (adjacent) free OH-group is then cleaved in what seems to be a hydride-shift reaction. Hence, heterolytic dissociation of H_2 has to occur on the catalyst surface leading to protons and hydride like species. The supported Rh catalyst yields equimolar amounts of 1,2-propanediol and 1-propanol at moderate reaction conditions (120 °C and 80 bar H_2 pressure). Specific interactions between polyols and noble metals on the catalyst surface for selective -C-O- bond cleavage are also proposed from Palkovitz *et al.* [Palkovitz2015]. The selective metal-catalyzed dehydration of terminal OH-groups from hexitols (C6 polyols, e.g. sorbitol) to 6-deoxy hexitols is reported and traced back to specific interactions with the Ru surface following an E2-mechanism (**Figure 3-7**). According to the authors, terminal OH-groups adsorb on the catalyst surface without dehydrogenation to an aldehyde, similar to the proposed mechanism from Shinmi *et al.* [Palkovitz2015, Shinmi2010]. An adsorbed OH-group on the Ru surface in close proximity then initiates deprotonation of the α-carbon atom with subsequent

dehydroxylation of the terminal OH-group. Hydrogenation of the 1-en (or 6-en, respectively) intermediate yields the 1-deoxy or 6-deoxy hexitol. The molecular structure of these compounds was determined using the 6-deoxy sugar rhamnose [Palkovitz2015]. Hydrogenation of this reducing sugar yielded exactly the same isomers of 6-deoxy hexitols (1,2,3,4,5-hexanepentols) as obtained from hydrogenolysis of hexitols.

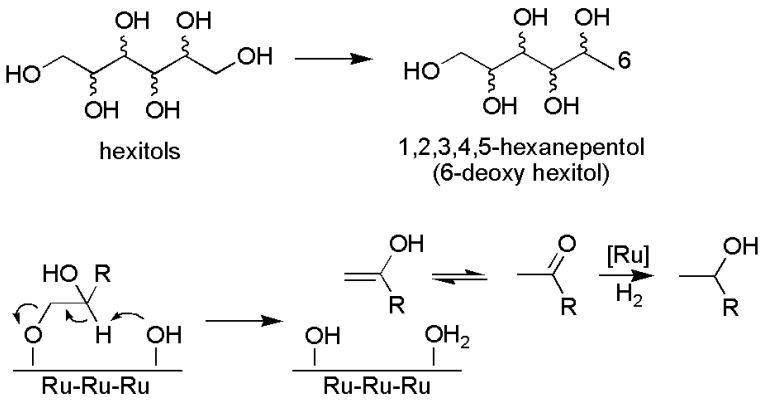

Figure 3-7: Dehydration of terminal OH-groups following an E2 mechanism with subsequent hydrogenation to a 6-deoxy hexitol as proposed by Palkovitz [Palkovitz2015].

Investigations on the occurrence of -C-C- bond cleavage revealed that mainly pentitols (C5 polyols) are obtained from hexitols (C6 polyols). In principle, the retro aldol reaction can cleavage all -C-C-bonds depending on the site of dehydrogenation [Palkovitz2015]. However, the formation of C5 polyols as the major product can only be attributed by selective cleavage of the carbon backbone (terminal C in the carbon chain) via decarbonylation. Hence, CO and the hydrogenation product methane (CH_4) are obtained as C1 compounds in the gas phase. The same observations were made by Deutsch *et al.* for hydrogenolysis of C3 to C6 polyols over carbon-supported Ru [Deutsch2012, Palkovitz2015]. This leads to a mechanism as shown in **Figure 3-8** with an initial interaction of the carbonyl double bond with Ru and subsequent cleavage of the terminal -C-C- bond.

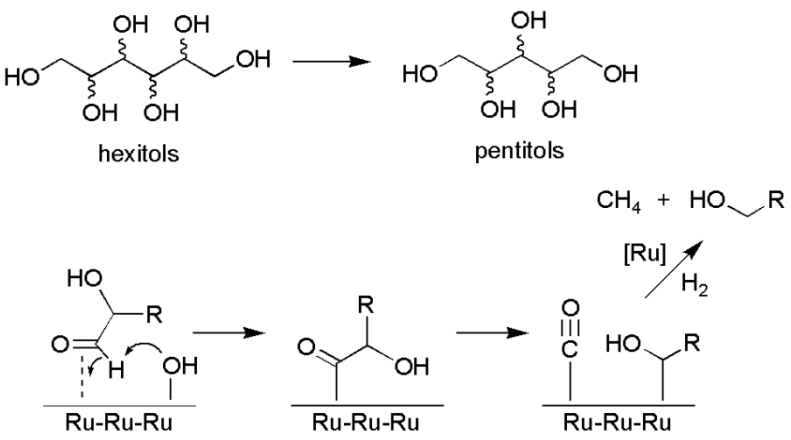

Figure 3-8: Proposed mechanism for decarbonylation of hexitols over Ru catalysts as proposed by Palkovitz *et al.* [Palkovitz2015]. The deprotonation of the carbonyl C atom was adapted to complete the atom balance.

These results are in line with studies from Hibbitts *et al.* who reported similar catalytic properties for Ru, Ir, and Pt catalysts regarding the competing -C-O- and -C-C- bond cleavage of alcohols and aldehydes [Hibbitts2015]. The noble metals preferably showed degradation of the carbon backbone by decarbonylation. 1-butanol, for instance, is converted to propane and CO (as well as methane, obtained from CO hydrogenation). This accords with mechanistic studies from Huber *et al.* and Vilcocq *et al.* for supported Pt catalysts, which have clearly shown that -C-C- bond cleavage is catalyzed by the active metal (see chapter 3.1.3) [Huber2010, Vilcocq2014]. Interestingly, Blanc *et al.* revealed that Ru and Pt do not always have the same catalytic properties. C1 to C3 hydrogenolysis products with large amounts of hydrocarbons, mainly methane, are reported for hydrogenolysis of sorbitol over Ru [Blanc2000]. The carbon yield (or total organic carbon: TOC) in the aqueous product solution was only 57 % of the initial amount, which means that 43 wt-% of the applied sorbitol reactant were lost in form of volatile hydrocarbons. Decreasing the reaction temperature only decreased the rate of sorbitol conversion without suppression of -C-C- bond cleavage reactions. In contrast, Pt and Pd catalysts are supposedly not active for breakage of the carbon chain. These metals exhibited weak hydrogenolysis properties and thus, yielded mainly C6 cyclic ethers by intramolecular dehydration [Blanc2000].

The comparison of these reports from literature shows that the proposings for -C-C-hydrogenolysis activity of noble metals are sometimes contradictory. This further shows that the understanding of hydrogenolysis reactions is highly complicated. Hence, it has to be considered that the properties of heterogeneous catalysts depend on multiple parameters: active metal, support, promoters (co-catalysts) and reaction conditions (e.g. temperature, H_2 pressure). A great example is the modification of a Ru catalyst with sulfur, as shown in a patent from Dubeck [Dubeck1984]. Unmodified Ru generally produces a large quantity of methane, whereas the sulfide-modified catalyst yields up to 91 % glycols (ethanediol and 1,2-propanediol) without further -C-O- and -C-C- bond cleavage to volatile hydrocarbons. More examples of catalyst modification, such as the optimization of the support, active metal or the addition of co-catalysts are described in the following chapter.

3.1.3. Other transition metals and acidic co-catalysts

Modified noble metal catalysts based on Ru, Rh, and Ir show great potential for selective -C-O- bond cleavage when combined with acidic co-catalysts such as electron deficient supports or transition metals. In the last decade, the effect of adding promoters like Re, Mo, W was investigated in detail by many authors [Liu2014, Ma2008, Ma2009, Ma2010, Shinmi2010, Tomishige2014]. Shinmi *et al.* investigated the promotion of silica-supported Rh with Re, Mo, and W for the conversion of glycerol to 1,2-propanediol and 1-propanol [Shinmi2010]. Degradation reactions are more expressed over the unmodified Rh catalyst, especially at low H_2 pressure. In contrast, adding these transition metals clearly improves the selectivity to the desired products in the following order: Re >> Mo > W. Modification with Re enhances -C-O- bond cleavage to 1,2-propanediol and suppresses side reactions, even under the low H_2 pressure and high reaction temperature where Rh/SiO_2 shows degradation of glycerol [Shinmi2010]. At 85 % conversion, the combined selectivity for 1,2- and 1,3-propanediol as well as 1- and 2-propanol is higher than 95 %. The main products are 1,2-propanediol and 1-propanol (**Figure 3-9**), whereas only trace amounts of degradation products are reported. This promoting effect is maximized for a ratio of Re/Rh = 0,5 and attributed to synergistic effects of both metals that lead to strong interactions of glycerol and the catalyst surface. An excess addition of Re decreased the catalytic performance, which is in line with previous reports that pure ReO_x/SiO_2 shows no activity for the hydrogenolysis of glycerol [Shinmi2009]. Similar promoting effects for Re are shown by Ma *et al.* for the modification of Ru based catalysts [Ma2008, Ma2009, Ma2010]. Supported Ru (Ru/Al_2O_3, Ru/C and Ru/ZrO_2) exhibits higher activity and selectivity for the conversion of glycerol to 1,2-propanediol and 1-propanol when $Re_2(CO)_{10}$ is added [Ma2008].

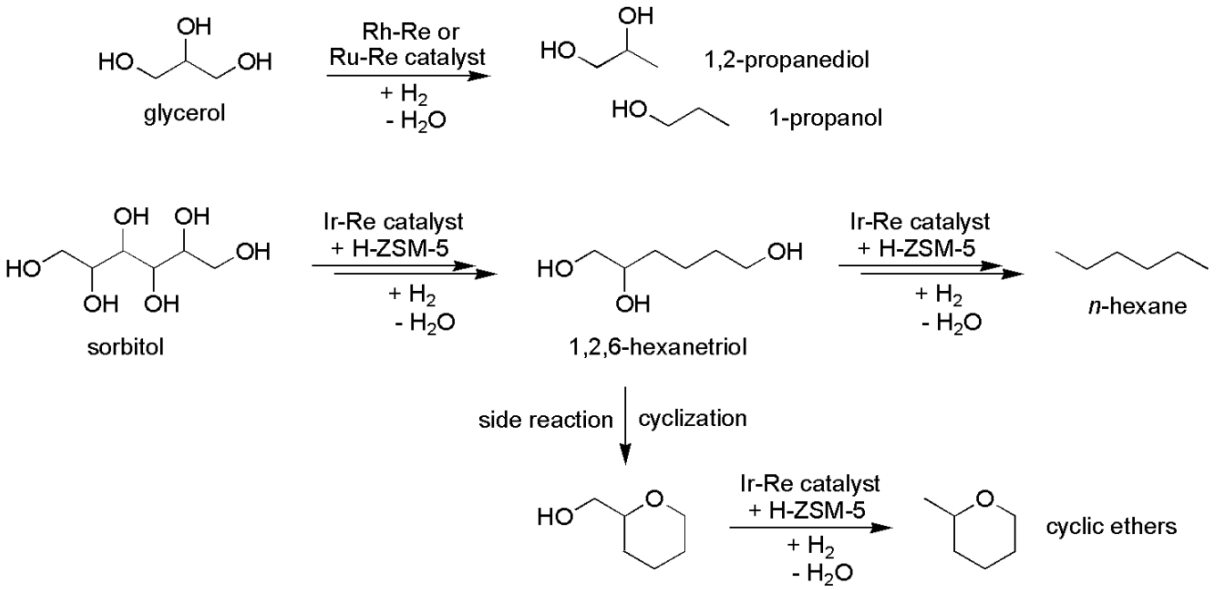

Figure 3-9: Hydrogenolysis of glycerol to 1,2-propanediol and 1-propanol over Rh-Re and Ru-Rh catalysts [Ma2008, Shinmi2010]. Sorbitol is converted to *n*-hexane over Ir-ReO_x/SiO_2 in combination with an acidic H-ZSM-5 zeolite [Liu2014, Tomishige2014].

These excellent -C-O- bond cleavage properties could be further enhanced by addition of the acidic H-ZSM-5 zeolite as co-catalyst in a biphasic solvent system (dodecane and water) [Tomishige2014]. A Re-modified Ir catalyst was combined with the acidic zeolite and yielded 98 % propane from glycerol at moderate 120 °C. In the same way, C4, C5, and C6 sugar alcohols were converted to the corresponding *n*-alkanes with 94 to 96 % yield. Mechanistic studies propose the same hydride-like species on the catalyst surface, as originally reported from Shinmi *et al.* [Shinmi2010] and shown in **Figure 3-6** in the previous chapter. The heterolytic dissociation of H_2 into H^+ and H^- over Ir-Re clusters leads to Bronsted acid sites (H^+) for dehydration and H^- species that substitute the OH-group, which enables the selective -C-O- bond cleavage of polyols [Tomishige2011, Tomishige2012, Tomishige2017]. Following this pathway, even glucose, cellobiose, and cellulose are converted to n-hexane with at least 83 % yield [Liu2014, Tomishige2013, Tomishige2014]. The acidic H-ZSM-5 zeolite enables hydrolysis of the cellulose polymer and water-soluble oligosaccharides. Glucose monomers are subsequently hydrogenated to sorbitol and completely dehydroxylated to *n*-hexane (**Figure 3-9**) [Liu2014]. The only setback is the comparatively low conversion rate with very long reaction times of 72 to 114 h [Tomishige2014], which is most presumably related to the biphasic solvent system and the poor solubility of hydrophilic alcohols and polyols in the alkane solvent.

Conversion of sorbitol over pure H-ZSM-5 and other zeolites (e.g. H-Beta) yields the cyclic ethers sorbitan and isosorbide via intramolecular dehydration [Kobayashi2015, Otomo2015]. Yields of up to 76 % are reported, with isosorbide as the stable final product. Further -C-O- bond cleavage for this cyclic deoxy C6 polyol only occurs when a hydrogenation metal is applied for ring-opening hydrogenolysis. These reactions were investigated several authors over bifunctional Pt catalysts that combine acidic properties for dehydration with hydrogenation properties for excessive -C-O- bond cleavage (**Figure 3-10**) [Huber2010, Vilcocq2014, Wang2016]. Supported Pt over acidic silica-alumina (SiO_2-Al_2O_3), zirconia-titania (ZrO_2 + TiO_2-WO_x), or niobia ($NbOPO_4$) is able to dehydroxylate all OH-groups and yield up to 70 % *n*-hexane from sorbitol. These results are almost comparable to the presented Re-modified catalysts and conversion rates are much higher because the Pt catalysts do not require an *n*-alkane as co-solvent. Hence, limitations due to solubility of polyol compounds are not the case. However, much higher temperatures are require for -C-O- bond cleavage activity with up to 240 °C at 37 bar H_2 [Vilcocq2014]. Practically the same reaction conditions are required for Ni-doped Z-HSM-5/MCM-41 catalysts with 240 °C at 40 bar H_2 and *n*-hexane yields are also the same [Zhang2014]. Mechanistic studies for these catalytic systems revealed that the dehydration of sorbitol to isosorbide is attributed to the acidic support. The dianhydro compound (isosorbide) is obtained as the main product from sorbitol when only the acidic support is used as catalyst without doping of a hydrogenation metal (here: Pt) [Huber2010]. When the same support is doped with Pt, isosorbide is converted to 1,2,6-hexanetriol via ring opening -C-O- bond cleavage. The activation energy of sorbitol dehydration is about 73 kJ/mol, whereas the ring-opening hydrogenolysis of isosorbide to 1,2,6-hexanetriol is the rate-determining step with about 148 kJ/mol [Wang2016]. The 1,2,6-hexanetriol

then undergoes both -C-O- and -C-C- bond cleavage reactions yielding alkanes as well as short-chain polyols such as glycols [Huber2010, Wang2016]. Formation of cyclic ethers from 1,2,6-hexanetriol by acid-catalyzed intramolecular dehydration is also observed, which accords with results from Shanks *et al.* using zeolites, amorphous silica-alumina (SiO_2-Al_2O_3), and niobias (Nb_xO_y) [Shanks2014]. These cyclic ethers also convert to alkanes and short-chain polyols via Pt catalyzed -C-O- and -C-C- bond cleavage, similar to sorbitan and isosorbide [Huber2010]. Degradation of polyols over Pt finally leads to CO_2, whereas alkanes are stable towards -C-C- bond cleavage [Huber2010, Vilcocq2014].

Hence, formation of long-chain alkanes from sugar alcohols is possible with substantially different heterogeneous catalysts that combine acid-catalyzed cleavage of OH-groups (or dehydration to form cyclic ethers) and hydrogenation properties of metal catalysts.

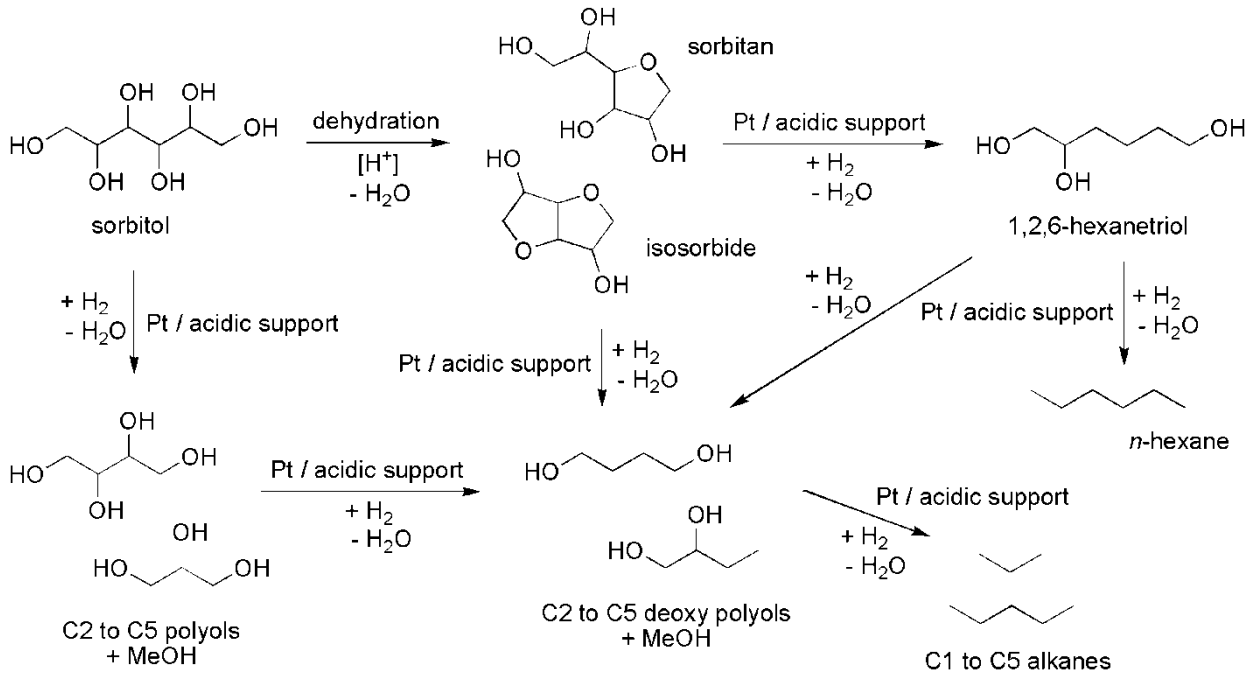

Figure 3-10: Hydrogenolysis of sorbitol to *n*-hexane over Pt catalysts on acidic supports such as SiO_2-Al_2O_3 or ZrO_2 + TiO_2-WO_x. The initial dehydration is acid catalyzed and leads to cyclic ethers sorbitan and isosorbide [Huber2010, Vilcocq2014, Wang2016].

3.1.4. Degradation mechanisms for -C-C- bond cleavage

Metal catalysts are characterized by different hydrogenolysis properties as described in the previous chapters. However, all of the most commonly used metals (Cu, Ru, Ni, Rh, Ir, Pt) have in common that polyols (e.g. glycerol, sorbitol) are partly dehydrogenated during adsorption which leads to -C-C- bond cleavage (see **Figure 3-11**, **Figure 3-12**, **Figure 3-13**, and **Figure 3-14**). The formation of un-saturated aldehydes or ketones occurs in a quasi-equilibrated dehydrogenation step [Berweiler2001, Berweiler2004, Clark1958, Deutsch2012, Gallegos2013, Hattori2010, Hibbitts2015, Huang2014, Huber2010, Jin2015, Liu2010, Manas2015, Maris2007a, Maris2007b, Montassier1983, Montassier1988, Montassier1991, Palkovitz2014, Vilcocq2014, Wang1995, Zhang2016]. The unique properties of the active metals then determine which of the many possible -C-C- bond cleavage pathways take place during conversion of these intermediates.

Retro aldol, retro Claisen, retro Michael, and Cannizzaro reaction

Rearrangement reactions such as the retro aldol reaction have been proposed as the main degradation pathway for Cu catalysts [Huang2014, Jin2015, Liu2010, Montassier1988, Montassier1991, Palkovitz2014, Wang1995, Zhang2016], Ru [Gallegos2013, Maris207a, Maris2007b, Montassier1983, Montassier1988, Montassier1991, Deutsch2012], Ni [Clark1958, Wang1995], Rh [Montassier1988, Shinmi2010], Ir [Manas2015, Montassier1988] and Pt [Huber2010, Maris2007a, Maris2007b, Vilcocq2014]. Adsorption of glycerol leads to glyceraldehyde or dihydroxyacetone via dehydrogenation (**Figure 3-11**) that can both convert into the other by base-catalyzed isomerization. Glyceraldehyde is able to undergo -C-C- bond cleavage via the retro aldol reaction yielding ethanediol and methanol [Maris2007a, Maris2007b, Montassier1988]. This mechanism was initially proposed by Montassier *et al.* because formaldehyde was identified as an intermediate product. The deprotonation of the terminal OH-group is possibly induced by adsorbed OH-groups on the catalyst surface [Montassier1988].

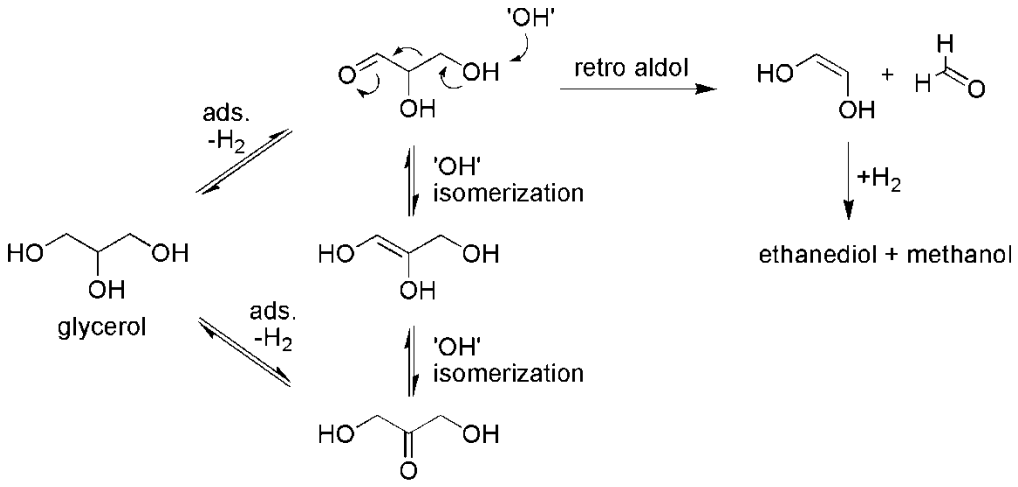

Figure 3-11: Quasi-equilibrium dehydrogenation step during adsorption of glycerol and adapted retro aldol mechanism from Montassier and Maris *et al.* [Maris2007a, Maris2007b, Montassier1988]. 'OH': adsorbed hydroxyl species on the catalyst surface.

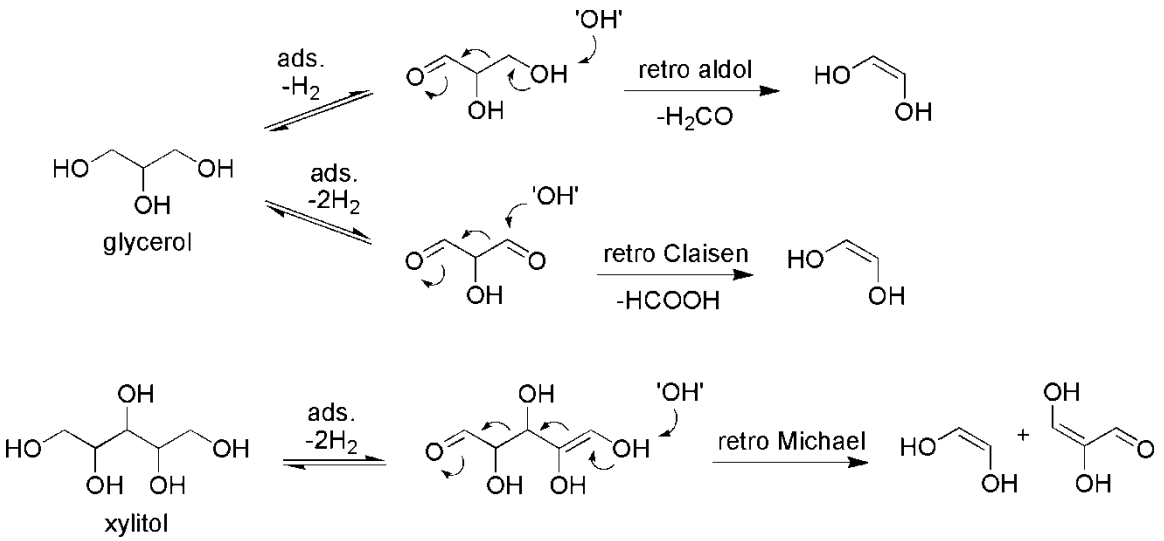

Figure 3-12: Degradation of glycerol and xylitol by the retro Claisen and retro Michael pathway, respectively, adapted from Montassier *et al.* [Montassier1988].

Alkaline co-catalysts such as $Ca(OH)_2$ are not necessary for this base-catalyzed reaction step. Interestingly, formic acid was found as an intermediate product instead of formaldehyde when Cu-based catalysts were applied for glycerol hydrogenolysis [Montassier1988]. This was explained by the retro Claisen mechanism as an additional reaction pathway over Cu which leads to formation of formic acid (**Figure 3-12**). However, the retro Claisen reaction requires a second dehydrogenation step to form the Dicarbonyl precursor, which is thermodynamically unfavorable at high H_2-pressures according to Wang *et al.* [Wang1995]. Furthermore, the second dehydrogenation step is in competition with dehydration of the monocarbonyl intermediate (-C-O- bond cleavage). The dehydration is thermodynamically and kinetically more favorable and thus, should lead to deoxy products rather than formic acid [Wang1995]. Since formic acid was identified by Montassier *et al.* as by-product in glycerol hydrogenolysis reactions, Wang *et al.* proposed that the acid may be produced from the Cannizzaro reaction of formaldehyde [Wang1995]. Formaldehyde is oxidized to formic acid while other carbonyl compounds are reduced to alcohols, which accords with the proposed mechanism from Manas *et al.* (see **Figure 3-14**) [Manas2015]. The Cannizzaro reaction is greatly enhanced by transition metal co-catalysts as reported by Maitlis and Cook [Maitlis1981]. Aldehydes such as acetaldehyde are more rapidly converted to the corresponding acid over transition metals than base-induced reactions. Hence, the normally base-catalyzed disproportion reaction is very likely to occur in a non-alkaline medium. This means that formaldehyde, produced from the retro aldol reaction, can be easily converted to formic acid [Wang1995]. The same argument was made for degradation of C5 polyols or larger compounds (**Figure 3-12**) [Montassier1988].

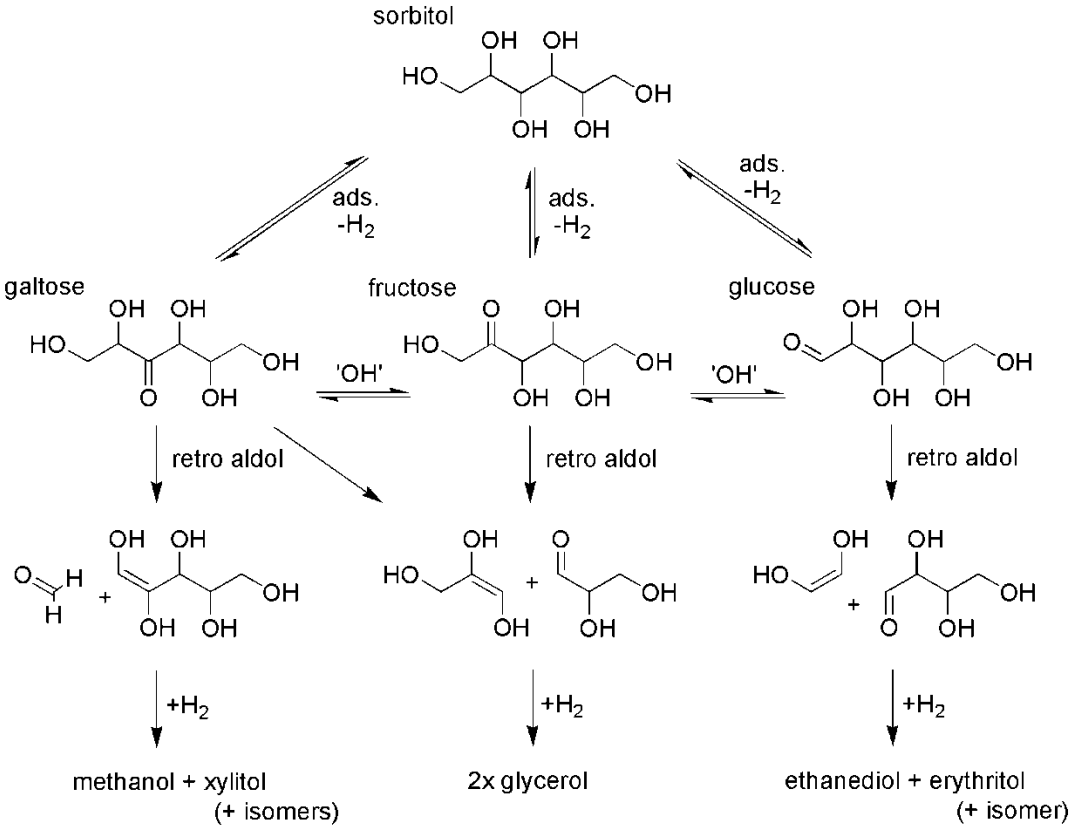

Figure 3-13: Quasi-equilibrated dehydrogenation step during adsorption of sorbitol and adapted retro aldol mechanism from Montassier [Montassier1988, Montassier1991], Huber [Huber2010], Palkovitz [Palkovitz2014], and Manas *et al.* [Manas2015]. 'OH': adsorbed hydroxyl species on the catalyst surface.

This critical comparison of reaction pathways is endorsed by other authors [Palkovitz2012] and thus, the retro aldol reaction in combination with other rearrangement reactions have been accepted as the main -C-C- bond cleavage mechanism over C3 to C6 polyols. Manas *et al.* elucidated the formation of short-chain polyols as well as deoxy products and acids from sorbitol by a combination of -C-C- bond cleavage steps [Manas2015]. The sugar alcohol is dehydrogenated to glucose (aldehyde), fructose (ketone), and galtose (ketone) during adsorption (**Figure 3-13**). The reducing sugars convert into other sugars by tautomerization. These transient products on the catalyst surface undergo -C-C- bond cleavage via the retro aldol reaction to form different short-chain polyols, depending on the position of the carbonyl group in the unsaturated sugar. Glucose yields C5, C4, C2, and C1 products, whereas the retro aldol reaction from fructose leads to C3 compounds [Huber2010, Manas2015, Montassier1983, Palkovitz2014]. C5 and C4 polyols are possibly further decomposed by repeated retro aldol reactions into C1 to C3 compounds. Parallel side reactions include base-catalyzed oxidation of aldehydes to acids or intra- and intermolecular Cannizzaro reactions (**Figure 3-14**) [Huang2014, Manas2015, Zhang2016]. For example, glyceraldehyde can be converted to pyruvaldehyde by dehydration. This dicarbonyl compound can be either hydrogenated to 1,2-propanediol or transformed to lactic acid by an intramolecular Cannizzaro reaction. Another mechanism from Zhang *et al.* proposes base-catalyzed oxidation of pyruvaldehyde to lactic acid by $Ca(OH)_2$ [Zhang2016].

Interestingly, substitution of $Ca(OH)_2$ with alkaline $La(OH)_3$ yields mainly 1,2-propanediol and thus, enhances the hydrogenation of pyruvaldehyde. Lactic acid is only obtained in trace amounts. Moreover, sorbitol is primarily converted to C2 and C4 compounds over $La(OH)_3$, with only small amounts of C3 fragments, and among them pyruvaldehyde, as side products. Hence, the alkalinity of the reaction mixture is not the decisive factor for the formation of lactic acid. The formation of lactic acid and other acids rather seems to be a result of complex interactions between the unsaturated sugars and metal ions. This is in agreement with results from Vogel *et al.* regarding the production of lactic acid from carbohydrates by addition of Co(II), Ni(II), Cu(II), or Zn(II) in subcritical water [Vogel2005].

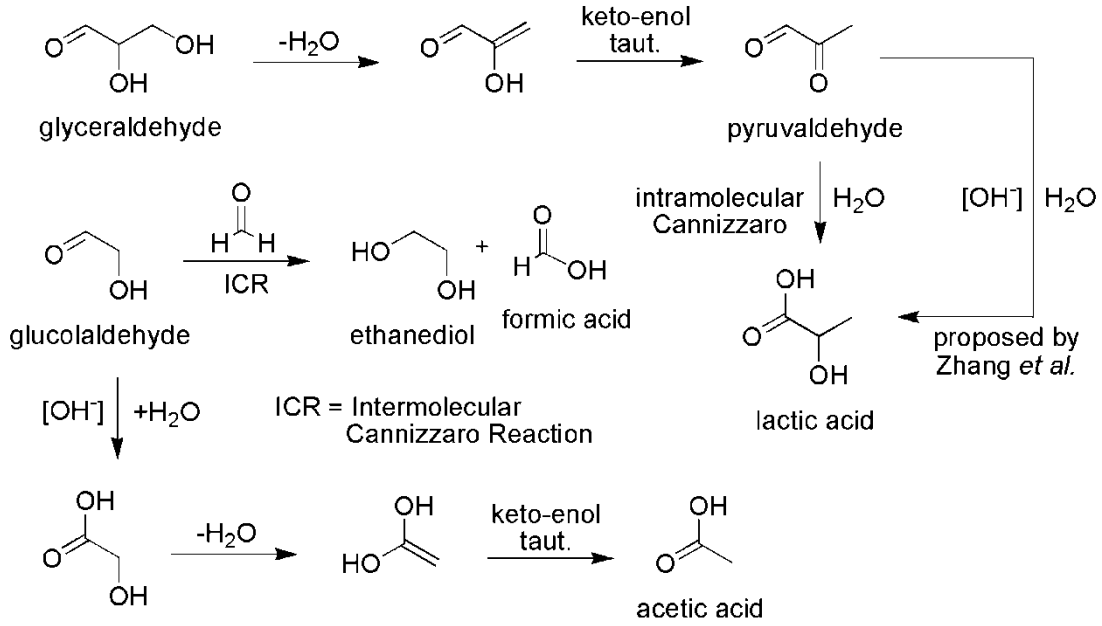

Figure 3-14: Formation of C1 to C3 acids from unsaturated intermediates via dehydration, tautomerization, intra- and intermolecular Cannizzaro reaction adapted from Manas *et al.* [Manas2015] and alkaline-catalyzed acid formation as proposed by Zhang *et al.* [Zhang2016].

Formation of CO_2 by decarboxylation

The formation of such acids is also of great interest regarding the formation of CO_2 in polyol hydrogenolysis reactions. Kornberg proposed that acids, in particular *ß*-keto acids, are quite unstable and undergo spontaneous decarboxylation in aqueous solution [Kornberg1948]. The same is observed for the sugar based intermediate 2,5-fucandicarboxylic acid at temperatures above 180 °C [Furanix2012]. Furthermore, it is proposed by many authors that CO_2 also results from dehydrogenation of formic acid over metal catalysts [Manas2015, Palkovitz2014, Vilcocq2014]. Both mechanisms are shown in **Figure 3-15**. Formic acid is possibly formed as an intermediate product by the Cannizaro reaction (see **Figure 3-14**), or methanol reforming with repeated dehydrogenation steps as proposed by Nielsen *et al.* [Nielsen2013]. The conversion of methanol to CO_2 by subsequent dehydrogenation in aqueous solution was initially proposed for a homogeneous Ru catalyst and adapted for a heterogeneous Cu catalyst by Palkovitz *et al.* [Palkovitz2014].

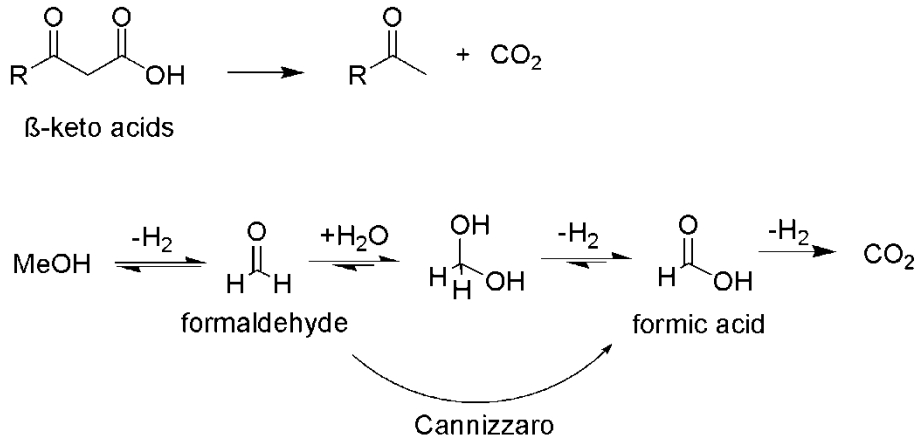

Figure 3-15: Formation of CO_2 by decarboxylation from *ß*-keto acids, adapted from Kornberg *et al.* [Kornberg1948] or methanol reforming [Nielsen2013, Palkovitz2014].

Formation of CO from decarbonylation

Detailed studies on the conversion of sorbitol over Ru have shown that hydrogen is preferably abstracted from terminal OH-groups, rather than internal OH-groups, to form aldehydes instead of ketones [Deutsch2012, Palkovitz2015]. These aldehydes are rapidly converted via decarbonylation, indicating that decarbonylation is the main decomposition pathway. Retro aldol reactions are also possible, but decarbonylation remains the dominant -C-C- bond cleavage reaction [Deutsch2012, Palkovitz2015]. A clear indication is the formation of methane that results from hydrogenation of CO. The formation of methane from methanol, which is the C1 product obtained from retro aldol reactions, is not described. Alcohols such as 1-butanol, 1-propanol, and ethanol follow the same degradation pathways over Ru, Ir, Pd, and Pt catalysts (**Figure 3-16**) [Davis1987, Hibbitts2015, Sexton1982]. The conversion of polyols and alcohols via decarbonylation not only competes with other degradation reactions such as the retro aldol reaction or decarboxylation. The -C-C- bond cleavage pathways also compete with -C-O- bond cleavage via dehydration or metal-catalyzed -C-O- hydrogenolysis [Hibbitts2015, Palkovitz2015, Shinmi2010]. However, Hibbitts *et al.* have shown that decarbonylation rates of 1-butanol are about 10 times higher than -C-O- bond cleavage to *n*-butane [Hibbitts2015].

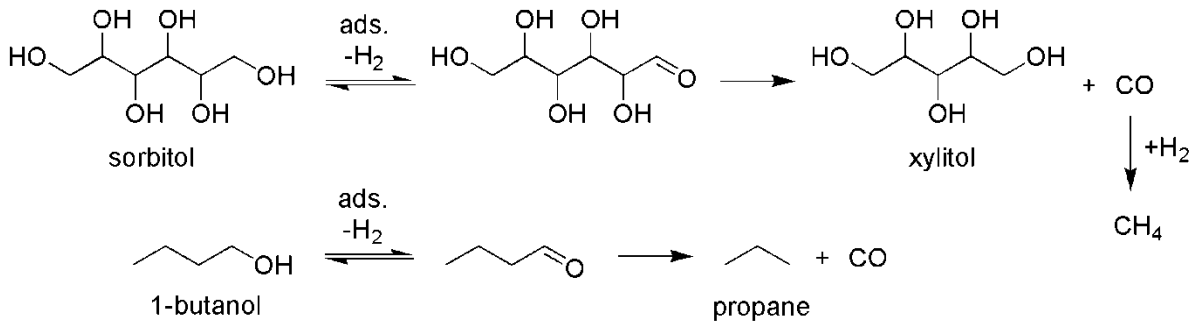

Figure 3-16: Decarbonylation of sorbitol to xylitol and CO with subsequent hydrogenation to methane, adapted from Deutsch *et al.* and Palkovitz *et al.* [Deutsch2012, Palkovitz2015]. 1-butanol converts to propane and CO, respectively [Hibbitts2015].

These characteristic properties of the group VIII metals are attributed to strong interactions of an activated carbon atom, vicinal to the aldehyde group, with the metal surface [Davis1989, Hibbitts2015]. The vicinal oxygen atom weakens the -C-C- bond of the carbon backbone (in the terminal -C-C=O group) and finally leads to formation of CO [Hibbitts2015]. The -C-C- bond activation does not occur without the vicinal oxygen from the aldehyde group and thus, alkanes are stable towards -C-C- bond cleavage over Ru [Hibbitts2015] and Pt catalysts [Hibbitts2015, Huber2010]. In contrast, Cu exhibits low decarbonylation rates because the activation of -C-C- bonds in aldehyde intermediates is weakly expressed over group IX metals [Hibbitts2015].

Finally, it should be mentioned that CO in aqueous solution should also convert to CO_2 via the water-gas shift reaction, even when H_2 is present during hydrogenolysis reactions [Deutsch2012]. However, CO_2 was neither detected during sorbitol hydrogenolysis [Palkovitz2015] or conversion of alcohols [Hibbitts2015]. Hence, the formation of certain degradation products seems to depend on the applied catalysts and reaction conditions. This comparison shows on the one hand that degradation routes via decarbonylation, decarboxylation and rearrangement reactions (e.g. retro aldol and Cannizzaro reaction) are highly complex. On the other hand, certain undesired products can obviously be avoided by optimization of specific parameters, which enables the possibility to suppress side reactions.

3.2. Hydrogenation of isomaltulose

The hydrogenation of isomaltulose (palatinose^{TM}) over standard commercial heterogeneous catalysts based on Ru, Ni, and Cu is used in this thesis as a reference for the hydrogenation activity of the applied catalysts. Rapid hydrogenation of unsaturated intermediates (in hydrogenolysis reactions) is required in order to suppress degradation reactions of polyols as described in the previous chapters 3.1.1, 3.1.2, and in particular in chapter 3.1.4. The correlation between hydrogenation properties and the activity for -C-O- and -C-C- bond cleavage is investigated to better understand the reactions involved in the hydrogenolysis of polyols. Most of the provided catalysts from Südzucker (supported Ru and various Ni-Raney and Cu-Raney catalysts) are used commercially for the hydrogenation of isomaltulose. Hence, a general over of this process is presented hereafter.

Isomaltulose is a reducing disaccharide, containing a glucose and fructose building block. It is obtained from sucrose by enzymatic transglucosidation [Kunz2002]. In this rearrangement reaction, the α-1,2-bond in sucrose (α-D-glucopyranosyl-1,2-β-D-fructofuranose) is converted into the thermodynamically more stable α-1,6-bond of isomaltulose (α-D-glucopyranosyl-1,6-D-fructofuranose). The anomeric C2 in the fructose building block is now able to convert into the open-chain keto form, which enables hydrogenation over a heterogeneous catalyst (**Figure 3-17**) [Kühne2013, Kunz2002].

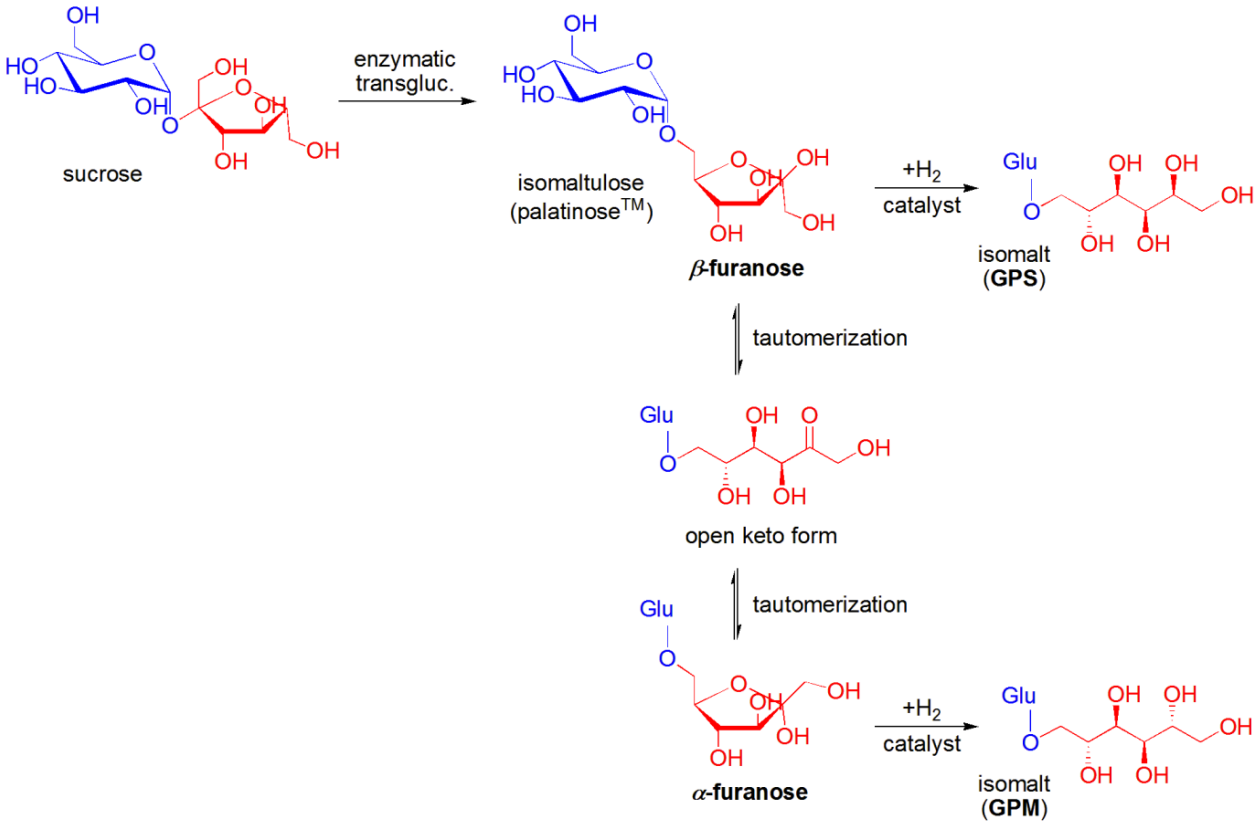

Figure 3-17: Conversion of sucrose to isomaltulose by enzymatic transglucosidation and subsequent hydrogenation to isomalt, a mixture of the two epimers GPS (glucopyranosyl-sorbitol) and GPM (glucopyranosyl-mannitol) [Kühne2013, Kunz2002].

Usually, this reaction is carried out in a fixed bed reactor at elevated H_2 pressure (150 to 300 bar) and temperatures between 70 and 120 °C [Kunz2002, Südzucker1998]. Hydrogenation of fructose yields sorbitol and mannitol. Similarly, adding H_2 to isomaltulose leads to the formation of GPS (α-D-glucopyranosyl-sorbitol) and GPM (α-D-glucopyranosyl-mannitol). Two different observations are made when comparing Ru, Ni, and Cu based catalysts. On the one hand, Ru is generally considered to be more active for hydrogenation of sugars than Ni or Cu [Arena1992, Makkee1985]. On the other hand, different amounts of the two epimers sorbitol and mannitol are obtained from fructose or isomaltulose, respectively. Ru based catalysts yield up to 67 % sorbitol [Heinen2000, Makkee1985, Kuusisto2005, Schichtel2009], whereas over Cu mannitol is obtained in 67 % yield. Ni in contrast gives approximately equimolar amounts of both epimers [Ruddlesden1981]. Makkee *et al.* suggested that the preferred hydrogenation to specific epimers is attributed to interactions of the two anomeric fructofuranose species (α- and β-form) with the catalyst surface. Hydrogenation of the β-form leads to inversion of the configuration at the anomeric C2 and thus, yields mannitol. Likewise, the α-form is converted to sorbitol (**Figure 3-18**) [Makkee1985]. It is proposed that the cyclic fructofuranose adsorbs on a Cu surface via three OH-groups at the 1-, 2- and 5-position (ether bond). Hydrogenation occurs by addition of a hydride-like species on the Cu surface from the anti-ring-O side which leads to the inversion of the configuration [Makkee1985]. Hence, the preferred hydrogenation to sorbitol over Ru catalysts results from preferred adsorption of α-fructofuranose (and α-fructofuranose building block in isomaltulose). In contrast, adsorption of the β-form is preferred on a Cu surface [Makkee1985, Ruddlesden1981]. If hydrogenation only occurred via the open-chain keto form, addition of H_2 to the planar carbonyl group would give equal amounts. Thus, specific interactions between the sugars (polyols) and active metals are required.

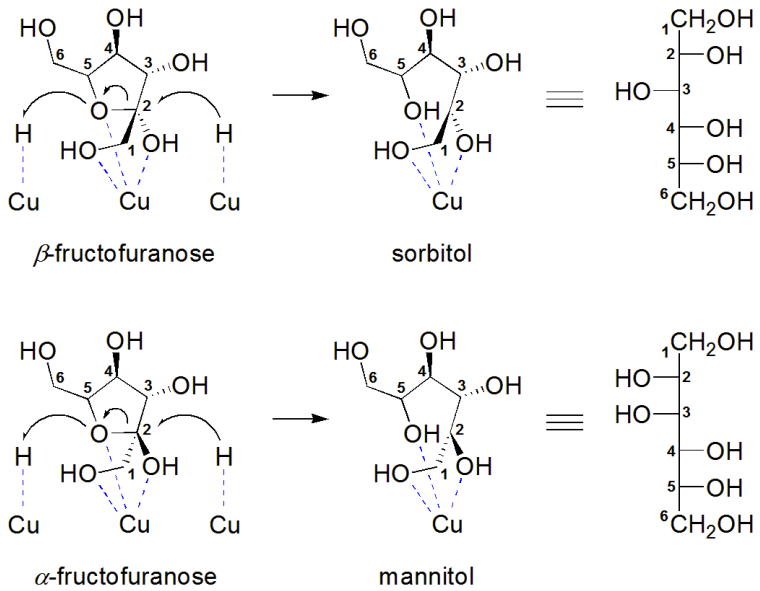

Figure 3-18: Hydrogenation of β-fructofuranose to sorbitol and α-fructofuranose to mannitol on a Cu surface as adapted from Makkee *et al.* [Makkee1985].

3.3. Downstream processing / Separation of polyols

The chromatographic separation of sugars and sugar alcohols (referred to as polyhydroxy compounds) on functionalized materials was first described in the 1950s by several patents [Blann1950, Khym1958, Paley1950]. This method makes use of differences in the adsorption affinity of carbohydrates (e.g. sucrose, glucose, galactose, rhamnose) for a given adsorbent, usually in powdered form, which is packed in a column. The adsorbed sugars begin to move down or along the column as an adsorption zone, or band, that spread out on the columns in a series of separate zones arranged in descending order of their respective adsorption affinities for the adsorbent used [Lew1950]. The first detailed investigation for the separation of sugars and sugar alcohols (e.g. sorbitol, mannitol, and galactitol (dulcitol)) was performed over an anion exchange resin that exploits strong adsorption of negatively charged polyol-borate-complexes (**Figure 3-19**) [Khym1958]. The formation of such acidic borate complexes (I), (II), and (III) is well known [Makkee1985]. The correspondent anions, formed by deprotonation in the aqueous solution, adsorb on the positively charged amines (here: quaternary amines) of the strong base anion exchange resin. In order for the polyols to combine with the borate ions, they must have at least one OH-group in close proximity of a second OH-group. The differences in adsorption affinities are attributed to the many isomeric forms of the polyols and the respective differences in the arrangement of OH-groups.

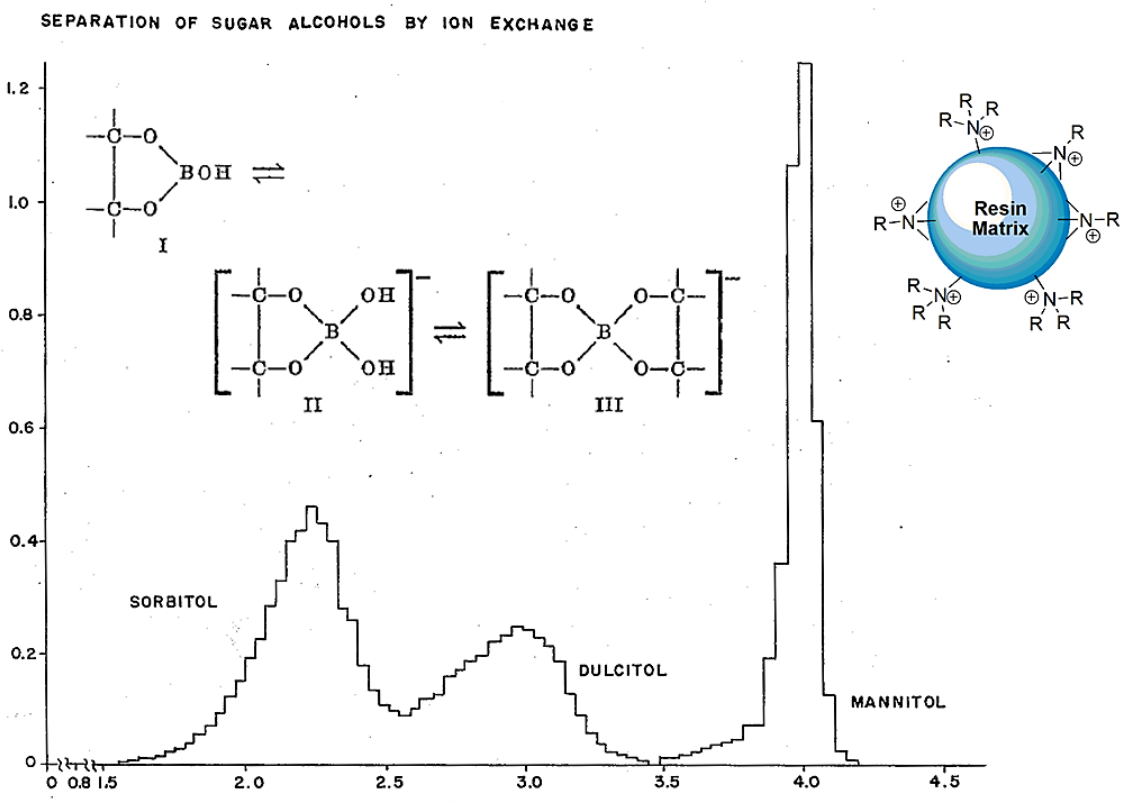

Figure 3-19: Adsorption bands of sorbitol, galactitol (dulcitol), and mannitol after chromatographic separation over an anion exchange resin. The separation of the sugar alcohols is achieved by separating the negatively charged borate complexes (I), (II), and (III) that adsorb on the positively charged resin [Khym1958].

A pair of adjacent OH-groups (vicinal) can be arranged in a *cis* or *trans* configuration. Furthermore, reducing sugars can exist in an open chain structure and various five-membered (furanoid) and six-membered (pyranoid) rings. Generally, it is found that polyols with a *cis* configuration have greater affinity for borate complex ion formation and that the same arrangement in a furanoid ring is more suitable for adsorption than the pyranoid ring [Khym1958]. However, the various isomeric forms of sugars are simultaneously existent in an aqueous solution and convert to another in an equilibrium state. The ratio of these isomers depends on pH, ratio of borate to sugar or sugar alcohol, the absolute concentration of the sugar, and the temperature [Khym1958, Makkee1985]. This enables the separation of various polyol mixtures with the right adjustment of the chromatography conditions.

In a mechanistic studies for the formation of polyol-boron-complexes by Makkee *et al.* it was found, that the addition of Ca^{2+} ions inhibits the boron-complexes completely [Makkee1985]. Hence, the affinity of polyols for binding to Ca^{2+} ions has to be even stronger, which accords with investigations from Angyal *et al.* [Angyal1979]. This effect is used for the separation of sugars and sugar alcohols over Ca^{2+} functionalized acid cation exchange resins [AlEid2006, Angyal1979, Hashimoto1983, Pronin1987]. Two adjacent acidic groups (e.g. sulfonic acid, HSO_3) in the deprotonated form are able to complex Ca^{2+} ions that enable direct interaction with polyols in the mobile phase (**Figure 3-20**) [Dow2016].

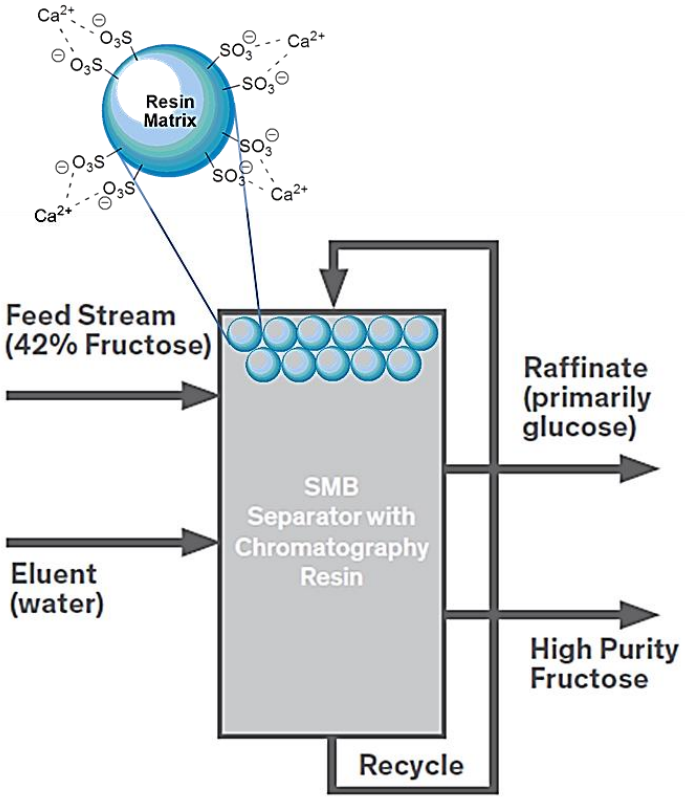

Figure 3-20: Simulated moving bed enrichment of high fructose corn syrup over Ca^{2+} functionalized cation exchange resins, as adapted from Dow [Dow2016].

This process is currently the commercial standard for separation of sugars, in particular glucose/fructose mixtures [Südzucker1991]. In the industrial process a simulated moving-bed (SMB) adsorber is used that connects twelve or more single columns with the cation exchange resin in Ca^{2+} form. The columns are connected with valves and pumps so that the moving of the stationary phase can be simulated for a continuous operation. Reaction conditions for purification of fructose from corn syrup are 60 to 70 °C and pH levels between 4.0 and 6.5 [Dow2016]. With this chromatographic system enrichment of fructose from 42 wt-% in the feed stream up to 95 wt-% in the isolated product stream is achievable. The separation is possible because fructose interacts more strongly with the Ca^{2+} ions bound to the resin than glucose. Hence, fructose in the mobile phase moves slower through the packed bed than glucose (**Figure 3-21**). Oligosaccharides (DP2, DP3, and DP4) that have not been further converted to mono saccharides do not fit into the small openings between the polymer chains of the resin. These side products from hydrolysis are easily separated from the feed stream because they are rapidly flushed through the packed bed and leave the column first.

It also has to be noted, that the strong cation exchangers enable excellent separation of glucose and fructose in the H^+ form (HSO_3), or rather the deprotonated bisulfite (SO_3^-), without Ca^{2+} loading of the resin. High purities of >99 % can be achieved in a semi-continuous counter current system of twelve connected columns [Barker1984].

The interactions of sugars with the stationary phase are then rather attributed to the formation of intermolecular H-bonding between the OH-groups of glucose/fructose and the sulfonic acid.

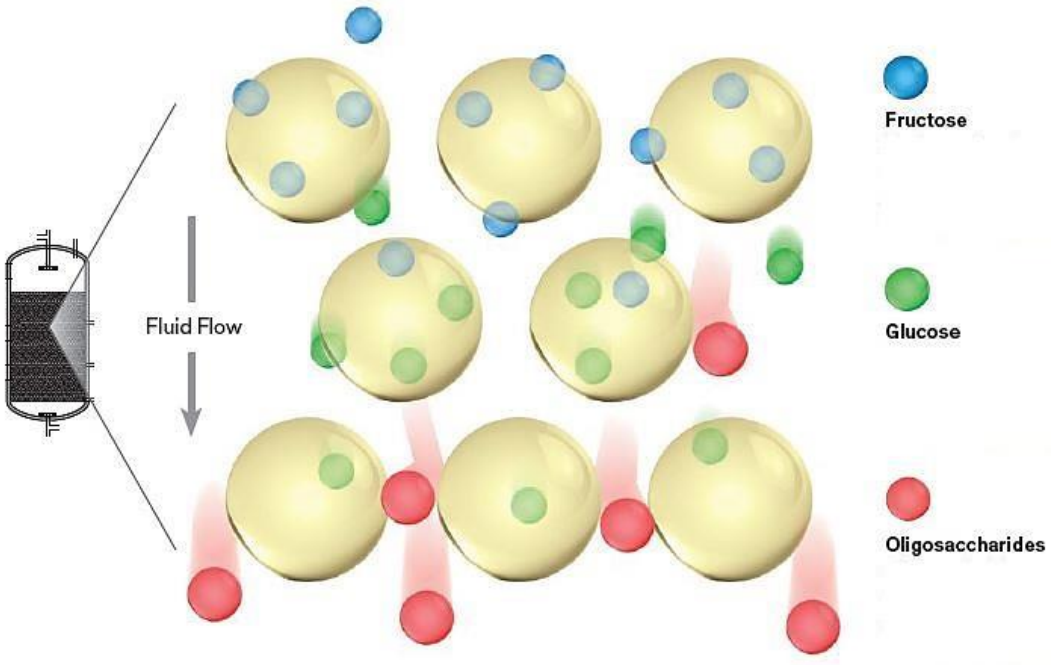

Figure 3-21: Chromatographic separation of fructose from glucose and oligosaccharides. Oligosaccharides are excluded from the resin based on size and elute first, followed by glucose. Fructose elutes last due to stronger interactions with the Ca^{2+} ions bound to the resin [Dow2016].

A second great advantage of cation exchange resins is the enhanced stability compared to anionic resins. Two major degradation processes are known to decompose anion exchange resins. The first one is auto-oxidation of the polymer matrix in the resin by the attack of oxygen, dissolved in water [Barker1984, Michaud1990]. Other oxidants such as chlorine anions, UV light, and strong acids (e.g. nitric and chromic acid) combined with heat also speed the de-cross-linking process. The breakdown of the cross-linked polymer backbone finally leads to a weakening of the bead, causes it to swell and lose capacity. Metallic ion impurities such as Fe^{2+} and Cu^{2+} are known to enhance this reaction. Hence, leaching of catalysts commonly used for hydrogenation (e.g. Cu-Raney) needs to be avoided. Also, dissolved oxygen levels below 0.1 ppm (with a maximum of 0.5 ppm) are required to maintain resin performance and maximize the resin lifetime [Dow2016]. The second known process for degradation of anionic resins is known as mechanical fouling, where the resin pores are blocked (fouled) by microorganisms that are present in water [Barker1984]. Cation exchange resins also suffer from these decomposition mechanisms. However, the sulfonic acid groups on polystyrene-polymer beads that are commonly used for strong acidic resins are very stable and lifetimes are much higher than 2-5 years [Michaud1990].

4. Experimental

4.1. Hydrogenolysis experiments in a batch-reactor

All reactions were performed in a stainless steel autoclave (Berghof, BR-700 series, 990 mL) in temperature, H_2-pressure, and hexitol concentration dependent experiments. The reaction mixture was vigorously stirred at 600 rpm at all reactions using an external gas distribution stirrer. The temperature was varied between 160 and 220 °C for Ru and Ni catalysts as well as the solid acid H-ZSM-5 zeolite, whereas for Cu catalysts a change from 180 to 220 °C was performed. The heterogeneous catalysts were filled in catalyst basked of 50 to 150 mL size (**Figure 4-1**). For each experiment the autoclave was filled with 500 mL of the reactant solution (varying from 7.5 to 30 wt-% hexitols or sugars in deionized water; if not mentioned otherwise 7.5 wt-% hexitols were used), sealed and flushed with three times at 40 bar H_2 to remove residual air. Subsequently a pressure of approximately 100 bar H_2 was adjusted and the autoclave was heated up under constant stirring to reaction temperature. This led to a pressure increase from 100 to for example 150 bar when heated to 180 °C. Hence, the pressures discussed reflect the system pressure obtained under reaction conditions. The H_2 pressure was varied from 0 to 200 bar H_2, whereas in the case of an inert atmosphere we used 25 bar of argon. Samples were taken at various time intervals to measure the product distribution. In blind experiments, the same procedure was performed without a heterogeneous catalyst (empty catalyst basket). No reaction occurred; hence, the polyol compounds are stable in an aqueous solution at the applied reaction conditions. The only exceptions are the reducing sugars glucose and fructose, which slowly tend to polymerization at temperature above 150 °C.

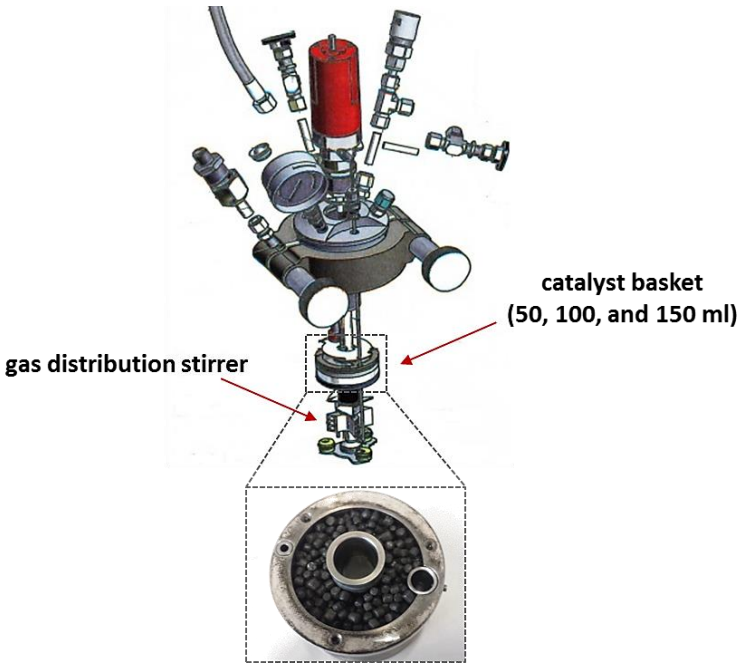

Figure 4-1: Batch reactor for hydrogenolysis reactions, equipped with a gas distribution stirrer and catalyst basket of various sizes.

The calculation of the carbon yield in the liquid phase is based on the following equation:

$$Y_{c,\,liq}\,(\%) = \frac{n_{c\,(reactant)} + \sum n_c^{GC-detected}(liq.)}{n^0_{c\,(reactant)}}\; x\; 100 \qquad \text{Eq. 1}$$

Carbon yield in the gas phase is based on the following equation, with the assumption that the amount of undetectable products as shown in (**Figure 4-2**) is negligible:

$$Y_{c,\,gas}\,(\%) = 100 - \frac{n_{c\,(reactant)} + \sum n_c^{GC-detected}(liq.)}{n^0_{c\,(reactant)}}\; x\; 100 \qquad \text{Eq. 2}$$

Conversion of the reactants was calculated based on the following equation:

$$X_c\,(\%) = \left(1 - \frac{n_{c\,(reactant)}}{n^0_{c\,(reactant)}}\right) x\; 100 \qquad \text{Eq. 3}$$

All isomeric hexitols in the reaction mixture (sorbitol, mannitol, galactitol and iditol) were considered as hexitol reactants.

The calculation of the selectivity is based on the following equation:

$$S_c\,(\%) = \frac{\sum n_c^{GC-detected}(liq.)}{n^0_{c\,(reactant)} - n_{c\,(reactant)}}\; x\; 100 \qquad \text{Eq. 4}$$

A variety of isomeric deoxy hexitols (hexane pentols, tetrols, triols and diols) was found. For each group of deoxy hexitols we defined a cumulative selectivity in which all isomeric hexane pentols, tetrols, triols and diols are accumulated.

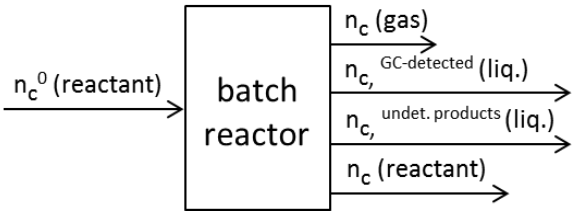

Figure 4-2: Classification of hydrogenolysis products into liquid and gaseous phase products based on analysis methods.

Sucrose (purity >99 %), invert sugar syrup (equimolar mixture of glucose and fructose, purity >95 %), sorbitol (>99 %), mannitol (>99 %), rhamnose (99 %) and xylitol (99 %) were provided by Südzucker. The 1,2,5,6-hexanetetrol was isolated from various product solutions (purity 75 %). 1,2,6-hexanetriol (96 %), 1,2,4-butanetriol (>90 %), 1,2-butanediol (>98 %), 2,3-butanediol (98 %), glycerol (>99 %), 1,2-propanediol (99 %), 1,3-propanediol (98 %), ethanediol (>99 %), isosorbide (dianhydro-D-glucitol, 98 %), ethanol (99 %) and methanol (99 %) were purchased from Sigma-Aldrich.

The heterogeneous catalysts (molded as granulate, spheres, and in cylindrical tablets) were applied in catalyst baskets with a volume of 50 to 150 mL (**Figure 4-1**). If not mentioned otherwise the 100 mL sized catalyst basked was used. All catalysts were used for hydrogenation of isomaltulose (at least 30 h on stream time) prior to hydrogenolysis reactions in order to remove soluble inorganic species that may originate from the catalyst preparation. The catalyst preconditioning was necessary to exclude effects arising from impurities on the fresh catalyst that catalyze undesired side reactions. Ru based catalysts with over alumina support (Al_2O_3) and activated carbon (C) were applied (**Table 4-1**). The Cu catalysts comprised of alumina supported Cu, different Raney-type catalysts that consist of Cu/Al alloys and a Cu/ZnO bulk catalyst (methanol synthesis catalyst). A standard Ni-Raney and Mo promoted Ni-Raney catalyst were also provided from Südzucker, as well as two modified Ni zirconia (ZrO_2) catalysts. Two different solid acid catalysts were compared in form of H-ZSM-5 and H-Beta zeolites, both in the H^+ form with a module (molar Si:Al ratio) of 30.

Table 4-1: Heterogeneous metal catalysts and zeolites used as solid-acid catalysts for hydrogenolysis of sugars and sugar alcohols.

Catalyst	Provided from
2 wt-% Ru/C	Südzucker AG
1,5 wt-% Ru/Al_2O_3	Südzucker AG
13 wt-% Cu/Al_2O_3	Sigma Aldrich
Cu/ZnO	Alfa Aesar
Cu-Raney	Südzucker AG
Ni-Raney	Südzucker AG
Mo promoted Ni-Raney	Südzucker AG
$Ni/ZrO_2/WO_3$	Südzucker AG
$Ni/ZrO_2/Mn_2O_3$	Südzucker AG
H-ZSM-5 Zeolite	Clariant
H-Beta Zeolite	Clariant

GC analysis of products in the liquid phase

C2 to C6 polyols ranging from ethylene glycol to hexitols were analyzed using an Agilent 6890 gas chromatograph (GC) with a fused silica capillary column (RXI-5sil MS, 40 m x 0.18 mm, ID*0.18 µm df, FID or MS detector). The liquid samples are prepared before analysis by silylation with bis(trimethylsilyl)amine. A temperature-programmed injector was used and heated from 80 °C to 300 °C at a heating rate of 15 °C min^{-1}. The injection volume of the sample was 1µL. Helium was used as carrier gas (Linde 5.0, purity >99.999 %) with a flow rate of 4.7 mL min-1. GC peaks were assigned to specific polyols by GC-MS analysis and comparison with reference compounds. The quantification of hexanepentols and -tetrols was carried out using response coefficients of hexitols. The concentration of hexane triols was measured using the response coefficient of 1,2,6-hexanetriol. Mono alcohols, aldehydes and ketones were quantified by headspace analysis because the GC method does not allow the detection of mono alcohols and unsaturated compounds. All of the described steps were executed at the Südzucker laboratory for GC and HPLC analysis in Offstein. Specific hexanetriols, -tetrols and -pentols were identified by ^{13}C-NMR analysis (Bruker BioSpin GmbH, DRX-500 NMR spectrometer) in the group of Dr. Reinhard Meusinger at TU Darmstadt. The evaluated data is shown in the appendix in chapter 9.1.

IR analysis of gaseous products

Volatile hydrocarbons, carbon dioxide (CO_2), and methane (CH_4) were detected by IR spectroscopy at ambient temperature without quantification (Bruker ALPHA FT-IR-spectrometer, spectral range from 500 to 4000 cm-1). However, the integral of the IR bands was found to reflect the trends expected from the calculated carbon yield: experiments with low (calculated) carbon yield showed large signals for volatile products as shown in **Table 4-2** and **Figure 4-3**.

Table 4-2: Carbon yield as calculated in Eq. 1 for products in the liquid phase (GC detected C2 to C6 polyols) after hydrogenolysis of mannitol over Ru/Al_2O_3 at 150 bar H_2 and 5 h reaction time. The calculation accuracy is rounded to ± 1 %. This should suffice because response coefficients for hexanepentols and –tetrols are estimated, which probably leads to a deviation of about ± 2 %.

Temperature / °C	Carbon yield / %
160	66
180	41
200	27
220	13

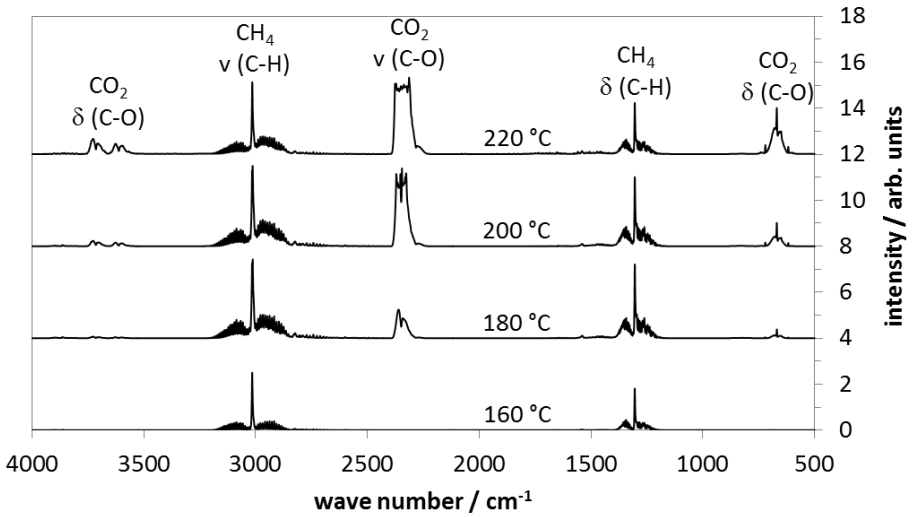

Figure 4-3: Standard reference IR spectra of the gas phase analysis with detection of carbon dioxide (CO_2) and methane (CH_4), both obtained from hydrogenolysis of mannitol over Ru/Al_2O_3 at 150 bar H_2 and 5 h reaction time. The amount of gaseous products increases with the reaction temperature, which correlates with the decrease in the carbon yield as shown in **Table 4-1**.

4.2. Ion-exchange chromatography

The chromatographic separation of the C2 to C6 polyol compounds obtained from hydrogenolysis of sugars and sugar alcohols is performed in a tempered Crannich-column (length: 100 cm, inner diameter: 5 cm). A standard Dowex 99Ca/320 cation exchange resin is used as the stationary phase in either the H^+ or $Ca2^+$ form as shown in **Figure 4-4**. The resin was provided by Südzucker in the Ca^{2+} form and transferred into the H^+ form by washing with a 5 wt-% chloric acid solution (HCl). The procedure was as follows:

The column was washed with twice the bed volume (approximately 3,8 liters) of the aqueous chloric acid solution at a flow rate of half a bed volume per hour. Afterwards, it was washed with deionized water at the same flow rate until the conductivity of the eluent, measured at the end of the column, was below 10 µS/cm. The regeneration of the column was performed in the same way after about 50 to 60 experiments.

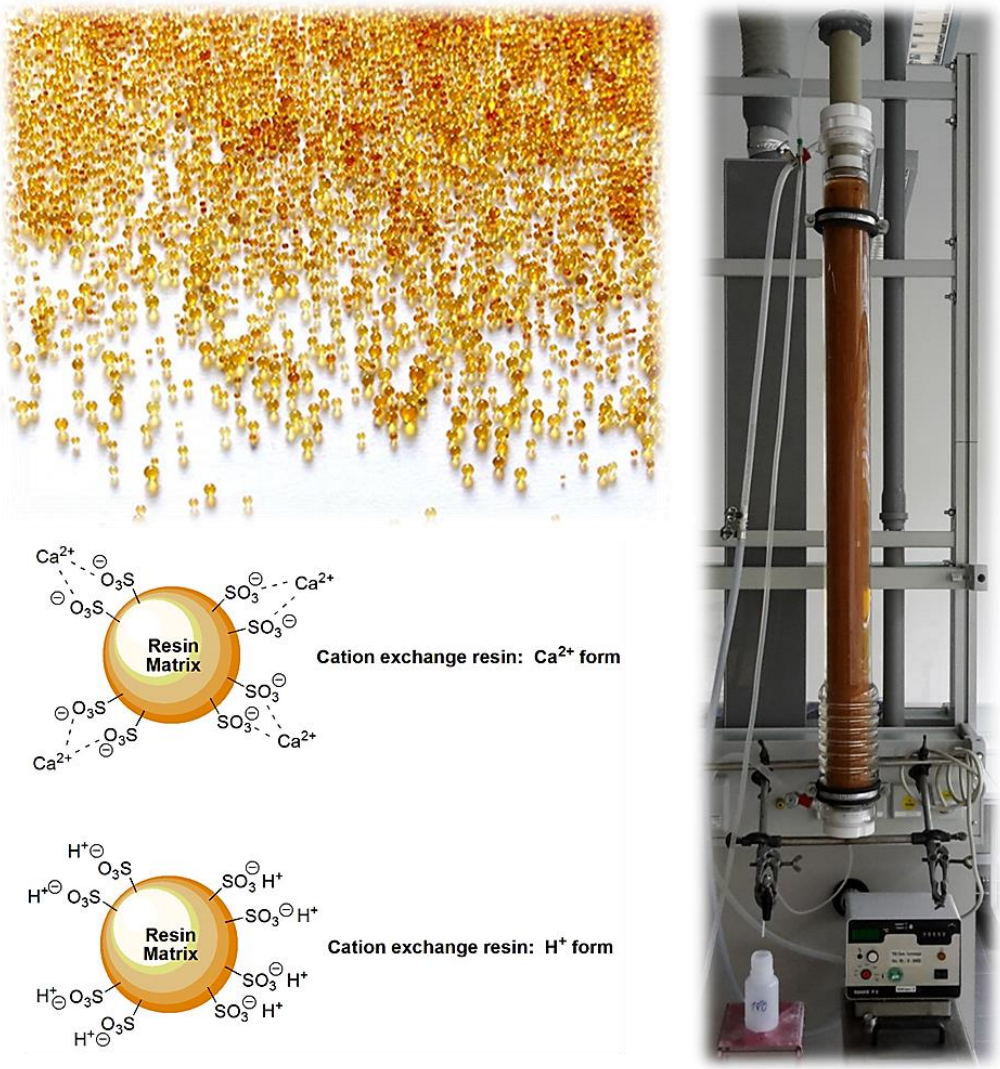

Figure 4-4: Chromatography column packed with a cation exchange resin with sulfonic acid groups in the H^+ form or complexed Ca^{2+} ions.

Deionized and degased water was used as the mobile phase (eluent) in all experiments. The eluent was heated to 10 °C above the temperature of the column. Chromatography experiments were usually carried out at 50 to 70 °C, which leads to severe degasing of the eluent when it is not heated first to remove the dissolved air. Prior to an experiment the column was heated to the assigned temperature for at least 30 min at a constant flow rate of 10 mL/min. The liquid sample, a mixture of different C2 to C6 polyols obtained from sugar hydrogenolysis, is injected at the head of the column at once to start an experiment. If not stated otherwise, 20 mL of high the concentrated viscous polyol solution (about 75 to 80 wt-% polyols) are injected. Afterwards, the constant flow of 10 mL/min of the mobile phase continued. The first separated products are obtained after about 90 to 120 min, depending on the carbon chain length and amount of OH-groups of the molecule. The retention times of the deoxy hexitols with two to five OH-groups and C3 polyols increase in the following order:

C6 pentols < C6 tetrols = C3 triols < C6 triols = C3 diols < C6 diols

A new liquid sample is collected each 5 min (50 mL) and used for GC analysis in order to obtain a detailed chromatogram for the separation of the C2 to C6 polyols. Each chromatography is repeated at least twice to validate the observed effects on the separation when either the temperature, flow rate, or the amount of injected polyol solution is changed. Furthermore, the model compounds glycerol and 1,2,6-hexanetriol to investigate if the complex mixture of polyols impacts the retention time (**Figure 4-5**). Additional chromatographic experiments were performed with a 300 cm column (inner diameter 2,5 cm). Due to the limitation of height in the laboratory two 150 cm columns are connected to enable this version of chromatography column.

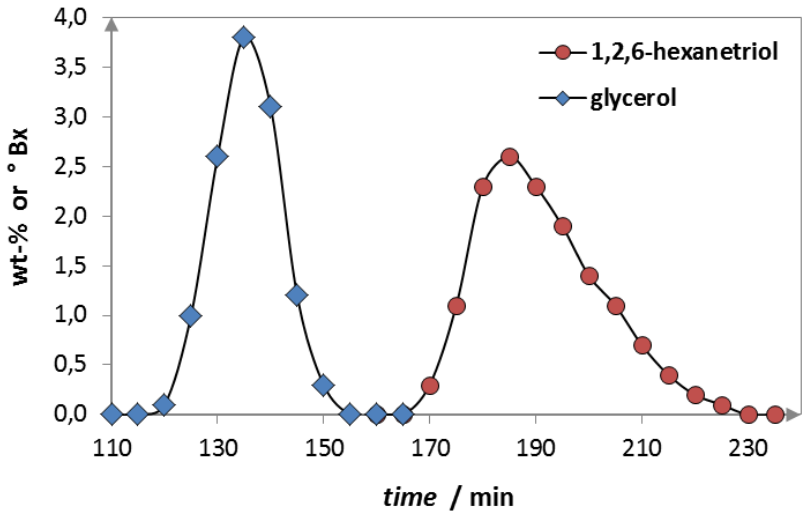

Figure 4-5: Chromatographic separation of glycerol and 1,2,6-hexanetriol mixture (20 mL with 78 wt-% of polyols) in a 100 cm column (inner diameter: 5 cm) packed with Dowex 99/320 cation exchange resin in the H^+ form at 50 °C.

4.3. Liquid-liquid extraction

The extraction of deoxy hexitols (C6 triols and diols) that have undergone multiple -C-O- bond cleavage reactions should be significantly less hydrophilic than hexitols such as sorbitol and mannitol that comprise of six OH-groups. It is expected that short-chain polyols such as glycerol or 1,2-propanediol (C3 compounds) are also much more hydrophilic than C6 diols and triols because they carry the same amount of OH-groups but are much smaller. Hence, the increasing hydrophobic properties of deoxygenated carbon atoms possibly enable the extraction of the desired deoxy C6 products. 1,6-hexanediol, 1,2,6-hexanetriol, mannitol and glycerol are dissolved in deionized water with a concentration of 7.5 wt-% each (and 30 wt-% polyols in total). 30 g of this raffinate are extracted with various solvents and in different amounts as shown in **Table 4-3**. These solvents (extractants) are chosen because they are not soluble in water. Other potential alcoholic solvents such as methanol, ethanol, 1- and 2-propanol are soluble in water and cannot be separated from the raffinate. Thus, they are not suitable for liquid-liquid extraction. In each experiment, a glass separation funnel is filled with the raffinate and 5, 10, 15, 30 or 45 g of the solvent at 25 and 50 °C. The separation funnel is shaken vigorously for 30 s followed by a short break to enable separation of the aqueous and the organic phase. This procedure is repeated five times in total to ensure equilibrium separation of the dissolved polyols in the two phases. Both phases are then separated and analyzed by GC analysis to validate the separation and calculate distribution coefficients for each solvent.

Table 4-3: Solvents used for the extraction of the model compounds 1,6-hexanediol and 1,2,6-hexanetriol from 30 g of an aqueous polyol mixture (raffinate). The aqueous solution contains 1,6-hexanediol, 1,2,6-hexanetriol, glycerol, and mannitol in a concentration of 7.5 wt-% each.

Solvent	Extraction temperature 25 °C Amount / g	Extraction temperature 50 °C Amount / g
1-butanol	45	45
	30	30
	15	15
	10	10
	5	5
1-pentanol	45	45
	30	30
	15	15
	10	10
	5	5
1-hexanol	45	45
	30	30
	15	15
	10	10
	5	5

4.4. Hydrogenation of isomaltulose

Various heterogeneous Ru, Cu, and Ni catalysts were applied for hydrogenation of isomaltulose to determine the activity for hydrogenation of ketoses (**Table 4-4**). A serious of five experiments with the same catalyst was performed at the same reaction conditions (70 °C, 150 bar H_2 and 3 h reaction time) in the previously described batch reactor (section 4.1). 500 mL of a 30 wt-% isomaltulose solution in deionized water, which accounts for 1M isomaltulose, are filled in the autoclave, sealed and flushed with three times at 40 bar H_2 to remove residual air. Subsequently a pressure of 150 bar H_2 is adjusted and the autoclave is heated up under constant stirring (600 rpm) to reaction temperature. In contrast to the hydrogenolysis experiments, no pressure increase is observed because the reaction is carried out at only 70 °C. Liquid samples were taken at 20, 40, 60, 120, and 180 min and analyzed by HPLC analysis to calculate conversion rates and thus, the specific hydrogenation activity for each catalyst. The catalysts are weight after washing with water (when they are still wet) in order to compare the specific activity. This is necessary because Ni-Raney is pyrophor and cannot be weighed in the dry state.

Table 4-4: Heterogeneous catalysts based on Ru, Cu, and Ni used for hydrogenation of isomaltulose and corresponding weight in a 100 mL basket used for activity experiments.

Catalyst	Weight / g
2 wt-% Ru/C	109,4
1,5 wt-% Ru/Al_2O_3	124,0
13 wt-% Cu/Al_2O_3	157,3
Cu-Raney	204,5
Ni-Raney	222,8
$Ni/ZrO_2/WO_3$	159,2
$Ni/ZrO_2/Mn_2O_3$	124,8

HPLC analysis

All samples are analyzed in Offstein using a Dr. Maisch Repro Gel Ca^{2+} column (300 mm x 8 mm, ID 9 µm, polystyrene-divinylbenzene resin functionalized with sulfonic acid groups in the Ca^{2+} form heated to 80 °C) in an Agilent 1100 chromatograph. The injection volume of the sample was 10 µL and the duration of an analysis run 40 min. For detection of the sugars and sugar alcohols an Agilent RID detector (type G1362A 1260) was used. The limit of quantitation is 0,1 % and the reproducibility of such HPLC analysis experiments is between 99.5 and 100.6 %.

The analysis of the reactant solution comprising of 30 wt-% isomaltulose was performed using an amino-type Reprosil carbohydrate column (250 mm x 4.6 mm, ID 5 µm, ultra-pure silica gel modified with amino groups) at ambient temperature. The eluent is an acetonitrile and water mixture (with a ratio of 68:32 vol-%) at a flow rate of 1.4 mL/min. The injection volume of the sample was 10 µL and the duration of an analysis run 15 min. The same Agilent RID detector (type G1362A 1260) was used as in the analysis of the hydrogenation products.

5. Results and discussion

5.1. Hydrogenolysis of sugar alcohols

This chapter describes the effects of various heterogeneous catalysts and operating parameters on the hydrogenolysis of sugar alcohols, notably sorbitol and mannitol (hexitols), and other polyols. The following aspects regarding -C-O- and -C-C- bond cleavage will be discussed in separate chapters.

5.1.1. Effect of the catalyst (active metal as well as support material) and reaction temperature for known hydrogenation catalysts and zeolites, molded as granulate, spheres, and cylindrical tablets.

5.1.2. Selective -C-O- bond cleavage over Cu catalysts; identification of intermediate deoxy C6 products and final (stable) deoxy C6 products from sugars and sugar alcohols.

5.1.3. Reaction mechanism for -C-O- bond cleavage, in particular with regards to the OH-group arrangement in the reactant. Herein, various C2 to C6 poly alcohols are screened over the Cu-Raney catalyst that is presented in chapters 5.1.1 and 5.1.2.

5.1.4. Selective -C-C- bond cleavage over Cu catalysts, contrasting the retro aldol reaction to decarbonylation and decarboxylation. The importance of hydrogenation properties and the effect of the H_2 pressure on the suppression of degradation reactions (via unsaturated intermediates) are discussed based on the proposed mechanism from chapter 5.1.3.

5.1.5. Selective -C-C- bond cleavage over Ru catalysts, in particular decarbonylation. Various polyols are screened over the supported Ru catalyst that is presented in chapter 5.1.1.

The parameters, that affect -C-O- and -C-C- bond cleavage the most, are then highlighted to show how the catalyst and process parameters can be optimized for higher yields of specific deoxy C6 polyols form sugar alcohols.

5.1.1. Effect of the catalyst and reaction temperature

Cu, Ni and Ru catalysts show a fundamentally different product distribution for the conversion of hexitols. All reactions were performed at 150 bar H_2 with mannitol as the model compound for C6 sugar alcohols (7.5 wt-% aqueous solution) because of the molecule's symmetry. Herein, Cu-Raney shows promising -C-O- bond cleavage properties while maintaining the C6 carbon chain. In contrast, supported Cu and Ru catalysts primarily cleave -C-C- bonds to yield short-chain polyols. Ni catalysts are inactive for hydrogenolysis reactions at moderate temperatures (below 200 °C) and catalyze degradation of the carbon chain to CO_2 as the major reaction when the temperature is increased.

Ru based catalysts

Supported Ru catalysts are the most active and already show high conversion at 160 °C. About 70 % and 80 % of the applied mannitol is converted with the activated carbon and alumina-supported Ru catalyst, respectively (**Figure 5-1**). The main products are C5 polyols along with formation of gaseous C1 products, in particular CH_4. The amount of detected C5, C4 and C3 polyols in descending order gives evidence that the -C-C- bond cleavage occurs gradually from C6 to C5, C4, C3, and C2 polyols. Finally, all polyols are converted to volatile C1 compounds. At higher temperatures barely any products are found in the liquid phase, but significant amounts of CO_2 and CH_4 are detected by gas phase IR analysis (see **Figure 5-36** in chapter 5.1.5). Hence, degradation of the carbon chain is the dominant reaction pathway over supported Ru. Deoxy C6 polyols are only formed as minor side products. Interestingly, only terminal OH-groups are cleaved via the E2-mechanism as was shown in **Figure 3-8** in chapter 3.1.2 (literature section) [Palkovitz2015]. However, only trace amounts of these C6 products are yielded at full conversion. The product distribution is similar for both Ru catalysts, indicating that effects of the different supports are negligible. The -C-C- bond cleavage reactions are solely catalyzed by the active metal (Ru) as shown in detail in chapter 5.1.5.

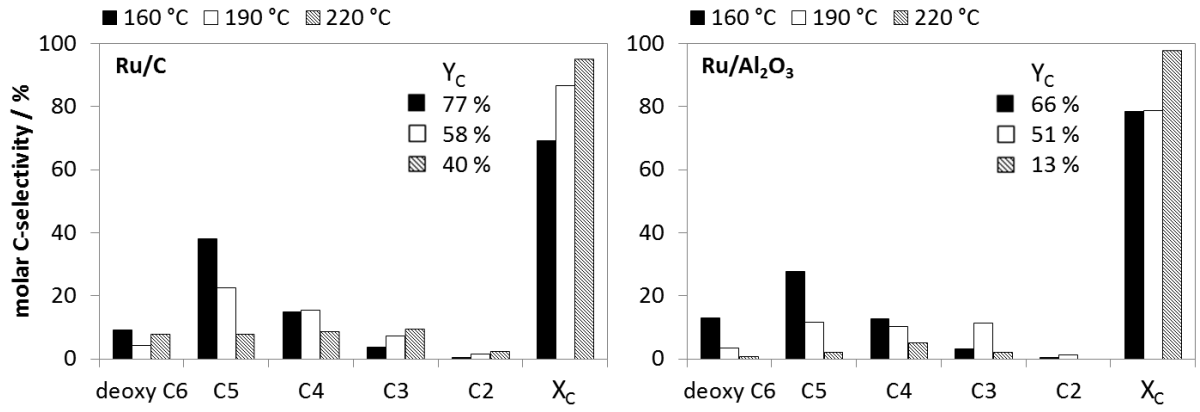

Figure 5-1: Conversion of mannitol and selectivity to polyols of different carbon chain length for Ru/C (left) and Ru/Al_2O_3 (right) at different temperatures, 150 bar H_2 pressure and 5 h reaction time. Y_C: as defined in equation 1 in chapter 4.1.

Cu based catalysts

Different catalytic properties are observed for the Cu catalysts (**Figure 5-2**). They are less active and show negligible conversion at 160 °C. Thus, Cu catalysts are tested at higher temperatures starting from 180 °C with an increase up to 220 °C. Cu/Al_2O_3 shows primarily -C-C- bond cleavage reactions to C3 polyols, with 1,2-propanediol as the main product. The isomeric 1,3-propanediol was not detected. The supported catalyst only possesses weak -C-O- bond cleavage properties with 11 % selectivity to deoxygenated hexitols (deoxy C6 polyols). In contrast, Cu-Raney mainly performs the desired -C-O- cleavage to deoxy C6 products at 180 °C, including hexanepentols, -tetrols, -triols and -diols as shown in chapter 5.1.2, with a molar carbon selectivity of 75 %.

The selectivity for deoxygenation reactions decreases at the expense of more -C-C- bond cleavage when the reaction temperature is increased to 220 °C. Similar to the Raney-type, Cu/ZnO exhibits good -C-O- bond cleavage properties with deoxy C6 polyols as the main products. However, the maximum selectivity is about 52 % at 180 °C and also decreases when reaction is conducted at higher temperature. At 220 °C only 39 % selectivity are obtained at complete conversion. The degradation of hexitols over Cu follows -C-C- bond cleavage to primarily C3 polyols. Interestingly, only very minor concentrations of C4 and C5 polyols are detected for all Cu catalysts. Glycerol and 1,2-propanediol are the major side products, suggesting retro aldol reactions from hexitols and deoxy hexitols as the main degradation route. CO_2 is the only volatile C1 product when Cu-Raney, Cu/ZnO and Cu/Al_2O_3 are applied; no methane or other hydrocarbons are detected. The carbon yield in the liquid phase at 220 °C is significantly lower for Cu-Raney (72 %), Cu/ZnO (80 %), and Cu/Al_2O_3 (75 %) compared to experiments at 180 °C (95, 90 and 88 %, respectively). However, the carbon yield for these catalysts is still much higher compared to Ru (max. 40 %, **Figure 5-1**) and Ni at 220 °C (max. 58 %, **Figure 5-4** and **Figure 5-5**). Based on these results, Cu-Raney is the catalyst of choice for selective -C-O- bond cleavage and applied for further studies to investigate the reaction mechanism and find the optimum reaction conditions (e.g. H_2 pressure and polyol concentration).

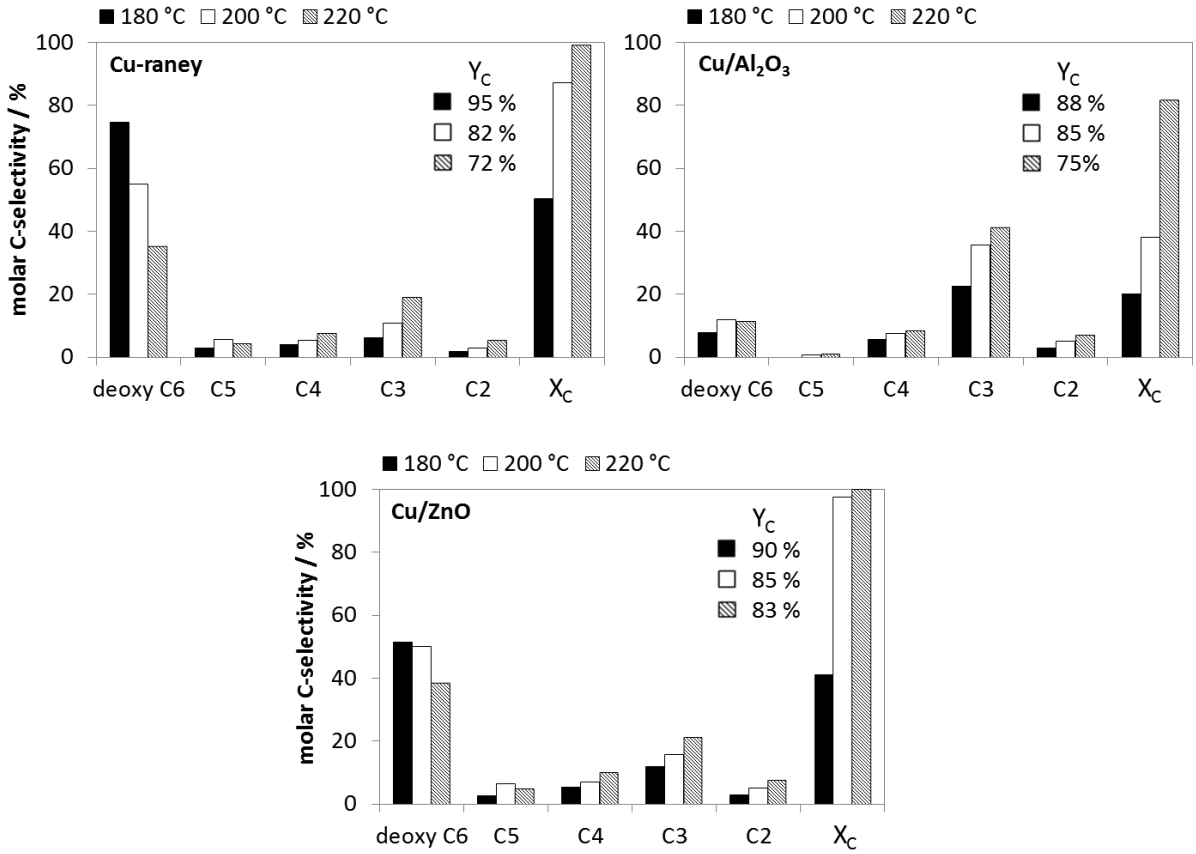

Figure 5-2: Conversion of mannitol and selectivity to polyols of different carbon chain length for 100 mL of a Cu-Raney catalyst, Cu/Al_2O_3 and Cu/ZnO at different temperatures, 150 bar H_2 pressure and 5 h reaction time. Y_C: as defined in equation 1 in chapter 4.1.

The comparison of the supported Cu/Al_2O_3 catalyst to both bulk-Cu catalysts shows that the hydrogenolysis activity is much lower with only about 80 % conversion, even at 220 °C. Furthermore, degradation reactions are much more pronounced. The formation of short-chain products, in particular C3 polyols (glycerol and 1,2-propanediol), is predominantly attributed to non-catalytic retro aldol elimination of the C6 sugar alcohols [Montassier1988, Palkovitz2014, Wang1995]. This reaction pathway competes with the -C-O- bond cleavage and seems to be much more favored when Cu/Al_2O_3 is used.

The degradation could be attributed either to the alumina-support or on the low catalytic activity, which enhances the contribution of retro aldol reactions (**Figure 5-3**, additional degradation routes are shown in detail in chapter 5.1.4). However, it is unlikely that Al_2O_3 enhances such base-catalyzed reactions because oxygen defects in the support should lead to (Lewis-) acidic properties. In fact, pure Al_2O_3 without Cu showed no conversion at all. Hence, the enhanced -C-C- bond cleavage has to be related to the formation of unsaturated intermediates over Cu that initiate degradation reactions.

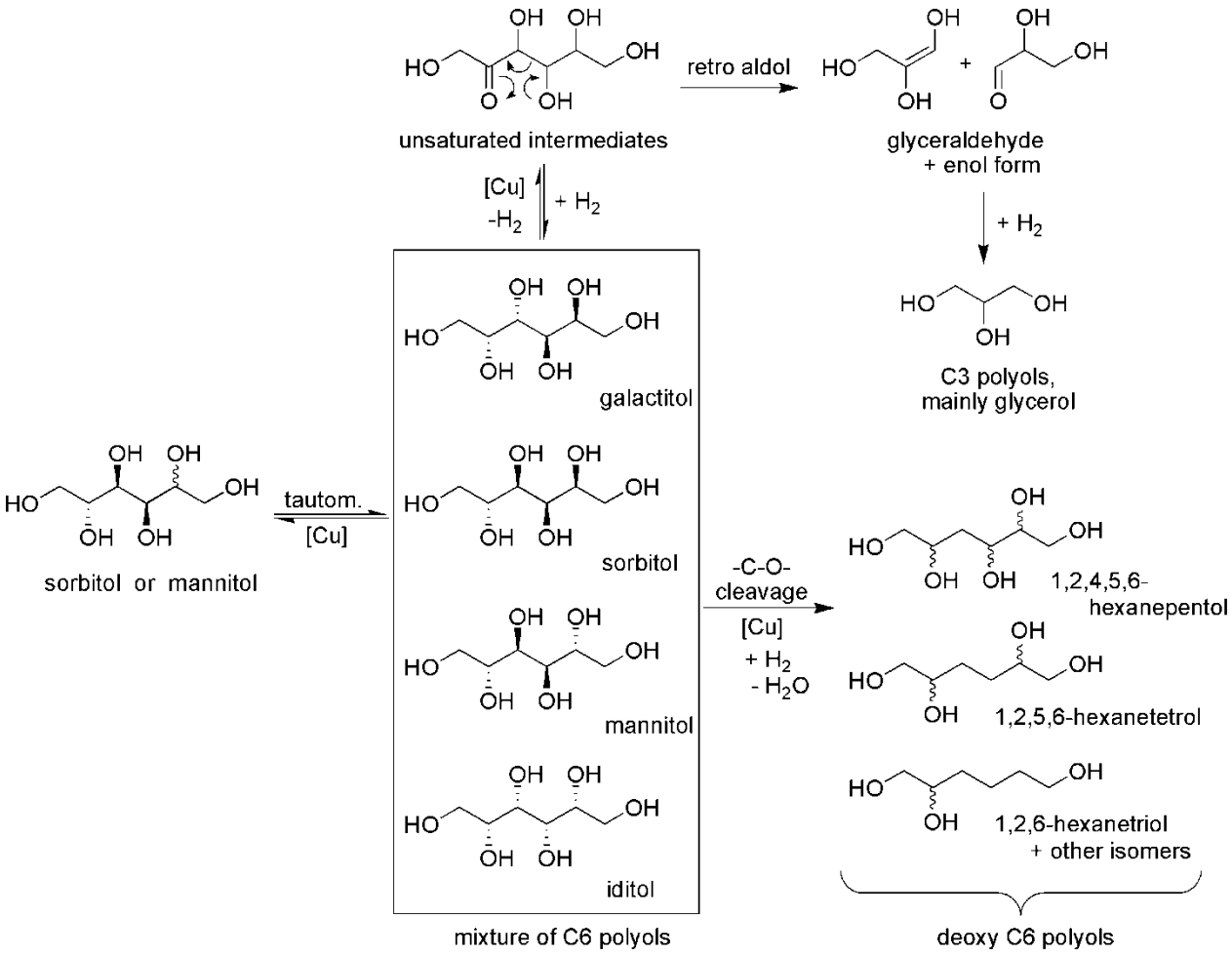

Figure 5-3: Cu-catalyzed tautomerization of sorbitol or mannitol into a mixture of C6 polyols (hexitols) and -C-O- bond cleavage to deoxy C6 polyols. The -C-C- bond cleavage to C3 polyols occurs as a non-catalytic side reaction initiated from unsaturated intermediates.

Polyols are known to undergo dehydrogenation to aldehyde and ketone intermediates during adsorption over supported Cu/Al_2O_3 [Palkovitz2014] and Cu-Raney [Berweiler2001, Berweiler2004, Wang1995]. These unsaturated intermediates enable the retro aldol reaction and thus, need to be re-hydrogenated as quickly as possible (**Figure 5-3**). Cu-Raney is about three times more active for the hydrogenation of ketones than Cu/Al_2O_3 (model compound: isomaltulose, a reducing sugar with a fructose building block, see **Figure 5-24** in chapter 5.1.4). Hence, we propose that side reactions like the retro aldol reaction are more expressed over Cu/Al_2O_3 because the unsaturated intermediates, that initiate -C-C- bond cleavage, have a longer residence time on the catalyst surface. Such unsaturated species perform degradation without the catalyst and thus, hydrogenation of these intermediates has to be improved to suppress -C-C- bond cleavage. This would shift the equilibrium towards -C-O- bond cleavage. Cu-Raney exhibits better hydrogenation properties and thus, the selectivity to undesired short-chain polyols is much lower.

In addition to the comparatively low hydrogenation activity, Cu/Al_2O_3 shows significant signs of deactivation at hydrogenolysis conditions (up to 220 °C at 150 bar H_2). The structure of the supported catalyst seems to collapse as the BET surface area is strongly decreased from 176 m^2/g (fresh catalyst) to 8 m^2/g after 30 h reaction time at temperatures between 180 and 220 °C. The rapid deactivation of supported Cu catalysts is a well-known phenomenon at such conditions [Montassier1995]. In contrast, the surface area for Cu-Raney remains about the same with 34 m^2/g before and 28 m^2/g after 200 h time-on-stream at 180 to 220 °C just like it's activity and selectivity.

Ni based catalysts

A standard commercial Ni-Raney catalyst shows only marginal conversion at temperatures below 220 °C. The few detected products comprised of deoxy C6 polyols and C5 polyols such as xylitol and arabitol, similar to Ru catalyzed reactions. Complete conversion is observed at 220 °C, but barely any products are identified in the liquid phase with a carbon yield of only 13 % (**Figure 5-4**). Ni-Raney with a Mo promoter on the other hand showed 52 % selectivity for deoxy C6 polyols at 160 °C. Although this catalyst is not as selective for -C-O- bond cleavage as Cu-Raney, it is already active at 160 °C whereas Cu-Raney only started to show conversion at about 180 °C. The Mo promoted catalyst also shows complete conversion at 190 °C, whereas the standard Raney-type is still inactive. However, even with Mo-promoter a significant decrease in deoxygenation selectivity occurred at higher temperatures. The carbon yield in the liquid phase was reduced to only 26 % at 220 °C due to excessive -C-C- bond cleavage, showing properties that are rather comparable to Ru based catalysts than to Cu.

A similar effect is observed when a Ni/zirconia bulk catalyst is doped with WO_3 and Mn_2O_3, respectively. The $Ni/ZrO_2/WO_3$ catalyst provided by Südzucker exhibits -C-O- bond cleavage with 50 to 55 % selectivity for deoxy C6 polyols at 160 and 190 °C (**Figure 5-5**). In contrast, the substitution of WO_3 with Mn_2O_3 changes the catalytic properties significantly. Barely any deoxy C6 polyols are detected in the liquid phase when $Ni/ZrO_2/Mn_2O_3$ is applied for the conversion of hexitols. The main products are C3 polyols with about 35 % at 190 °C. At 220 °C both Ni zirconia catalysts show complete conversion which is attributed to excessive -C-C- bond cleavage to CO_2 and CH_4.

These results show that Ni catalysts can be modified to increase the selectivity for deoxygenation reactions, but only with a moderate effect. At temperatures above 200 °C the catalytic properties are again more comparable to Ru.

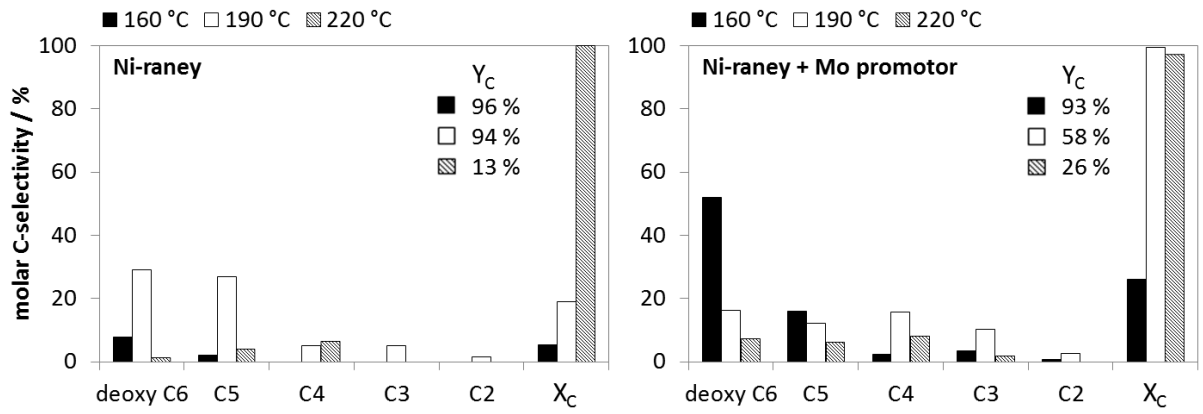

Figure 5-4: Conversion of mannitol and selectivity to polyols of different carbon chain length for Ni-Raney (left) and Ni-Raney with a Mo promoter (right) at different temperatures, 150 bar H_2 pressure and 5 h reaction time. Y_C: as defined in equation 1 in chapter 4.1.

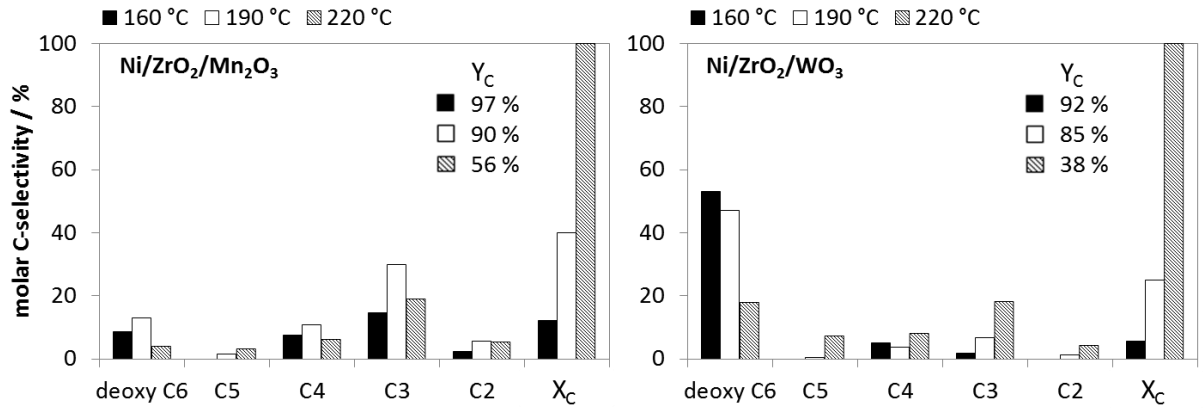

Figure 5-5: Conversion of mannitol and selectivity to polyols of different carbon chain length for $Ni/ZrO_2/Mn_2O_3$ (left) and $Ni/ZrO_2/WO_3$ (right) at different temperatures, 150 bar H_2 pressure and 5 h reaction time. Y_C: as defined in equation 1 in chapter 4.1.

Zeolites / solid-acid catalysts

The conversion of mannitol over an H-ZSM-5 zeolite (solid-acid catalyst) yields cyclic deoxy C6 polyols (**Figure 5-6**). The special catalytic properties enable -C-O- bond cleavage via intramolecular dehydration while maintaining the C6 carbon chain. H-ZSM-5 and H-beta type zeolites are known catalysts for the dehydration of sorbitol and mannitol into cyclic ethers [Kobayashi2015, Otomo2015]. First, the anhydro-hexitols sorbitan (1,4-anhydro sorbitol) and mannitan (1,4-anhydro mannitol) are obtained by an acid-catalyzed intramolecular dehydration from sorbitol and mannitol, respectively. They are transient intermediates and further converted to the dianhydro compounds isosorbide and isomannide. Isosorbide yields between 76 and 80 % are reported from sorbitol [Kobayashi2015, Otomo2015] which is in line with an isomannide yield of 75 % from mannitol in our experiments.

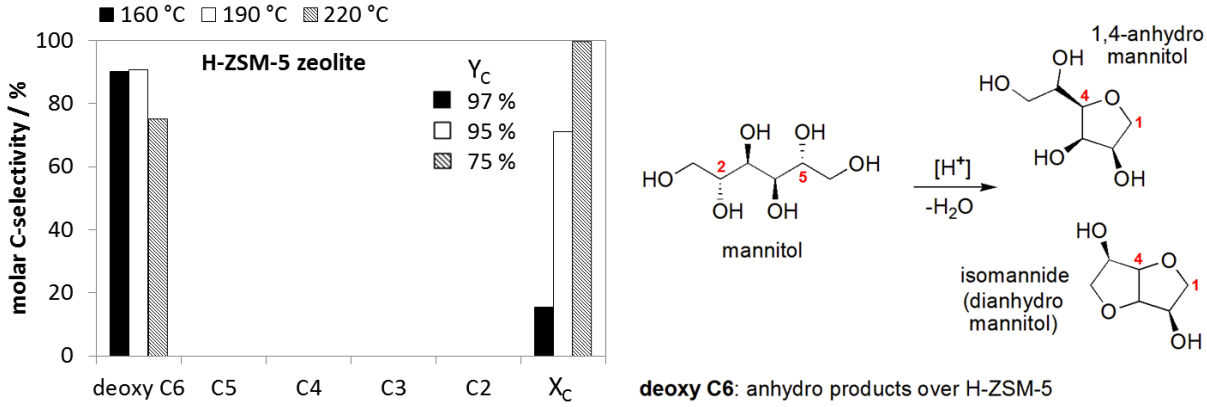

Figure 5-6: Conversion of mannitol and selectivity to polyols of different carbon chain length over a H-ZSM-5 zeolite at different temperatures, 150 bar H_2 pressure and 5 h reaction time. Y_C: as defined in equation 1 in chapter 4.1.

At 190 °C the selectivity for deoxy C6 products is about 90 % at 71 % conversion. Increasing the temperature to 220 °C lowers the selectivity for isomannide to 75 % at full conversion. This decrease in selectivity is attributed to enhanced side reactions at temperatures above 200 °C [Li2013]. When mannitol is used as the reactant, the major side reaction leads to a 2,5-anhydro product. The formation of such a by-product from sorbitol does not occur due to the unfavorable steric arrangement of the OH-groups at the 2- and 5-position (**Figure 5-7**) [Li2013, Yamaguchi2014]. 2,5-anhydro mannitol is undesired because it does not convert to isomannide. It is probably responsible for the formation of side products such as 5-HMF and humines, similar to acid-catalyzed fructose dehydration. These compounds are not detected with GC-analysis and thus, lead to a carbon loss of 25 % shown in **Figure 5-6**. Linear deoxy polyols, as well as short-chain C2 to C5 polyols are not detected. Hence, hydrogen induced hydrogenolysis of -C-O- bonds or degradation reactions (-C-C- bond cleavage) such as the retro aldol reaction do not occur over solid-acid H-ZSM-5 catalyst.

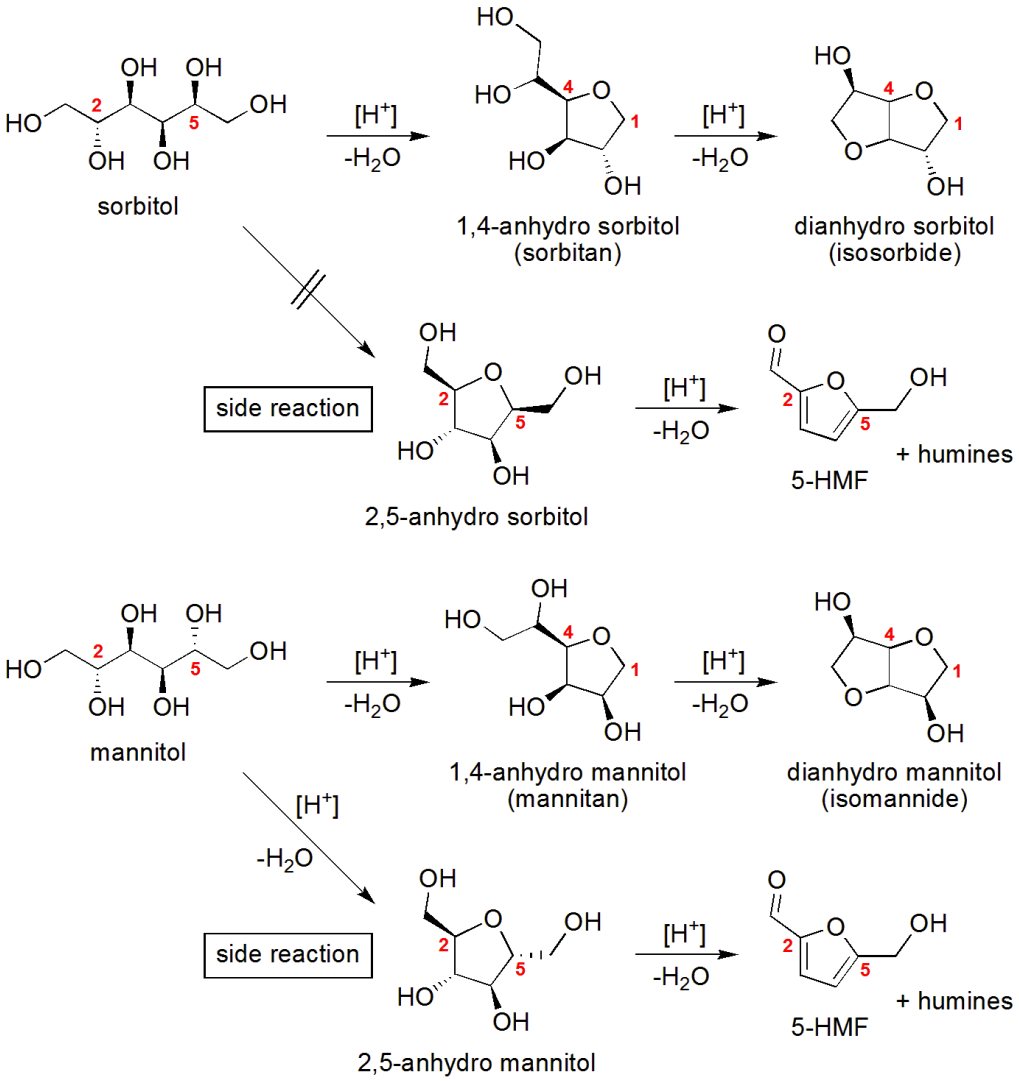

Figure 5-7: Acid-catalyzed dehydration of sorbitol and mannitol to 1,4-anhydro products and finally dianhydro compounds. Formation of a 2,5-anhydro ether is also possible for mannitol because of the OH-group arrangement at the 2- and 5-position.

Further studies with other hexitol reactants and a detailed identification of side products were not performed because anhydro compounds are not the desired deoxy C6 products. However, in addition to H-ZSM-5, a H-Y zeolite with the same module (molar Si:Al ratio) of 30 was applied for the conversion of mannitol. This Y-type solid-acid catalyst decomposed and showed no conversion which accords with literature that the Y-type zeolites are unstable under water at the chosen reaction conditions (160 to 220 °C) [Ravenelle2010]. Such alumosilicates are primarily used for applications and reactions in the gas phase.

5.1.2. Selective -C-O- bond cleavage over Cu catalysts

Our results show that Cu-Raney exhibits appreciable -C-O- bond cleavage properties for the production of linear deoxy C6 polyols. A detailed study with focus on the intermediate products after each -C-O- bond cleavage step was performed in order to achieve a better understanding for the reaction pathways. It has to be noted that the conclusions drawn from our investigations are primarily valid for the described process parameters.

Many transient deoxy C6 polyols are formed C6 sugar alcohols over Cu-Raney. However, only a few final products are obtained that are not further converted at the chosen conditions (180 °C and up to 200 bar H_2). Hexanepentols are obtained after the first -C-O- bond cleavage and further converted to hexanetetrols (**Figure 5-8** and **Figure 5-9**). Two constitutional isomers are identified: 3-deoxy and 6-deoxy hexitols in a molar ratio of 8:1. The mechanistic interpretation of these results in chapter 5.1.3 elucidates why the 3-deoxy product is obtained in much greater amounts than the 6-deoxy isomer. **Figure 5-9** shows that the concentration of hexanepentols reaches a maximum at 7.5 h, indicating that they are further converted to lower polyhydric products over time. They are a transient intermediates and fully converted to hexanetetrols after 25 h reaction time. Side reactions via -C-C- bond cleavage also take place yielding glycerol along with the glycols 1,2-propanediol and ethanediol. Glycerol is also an intermediate product and further transformed to both glycols by -C-O- and -C-C- bond cleavage, respectively.

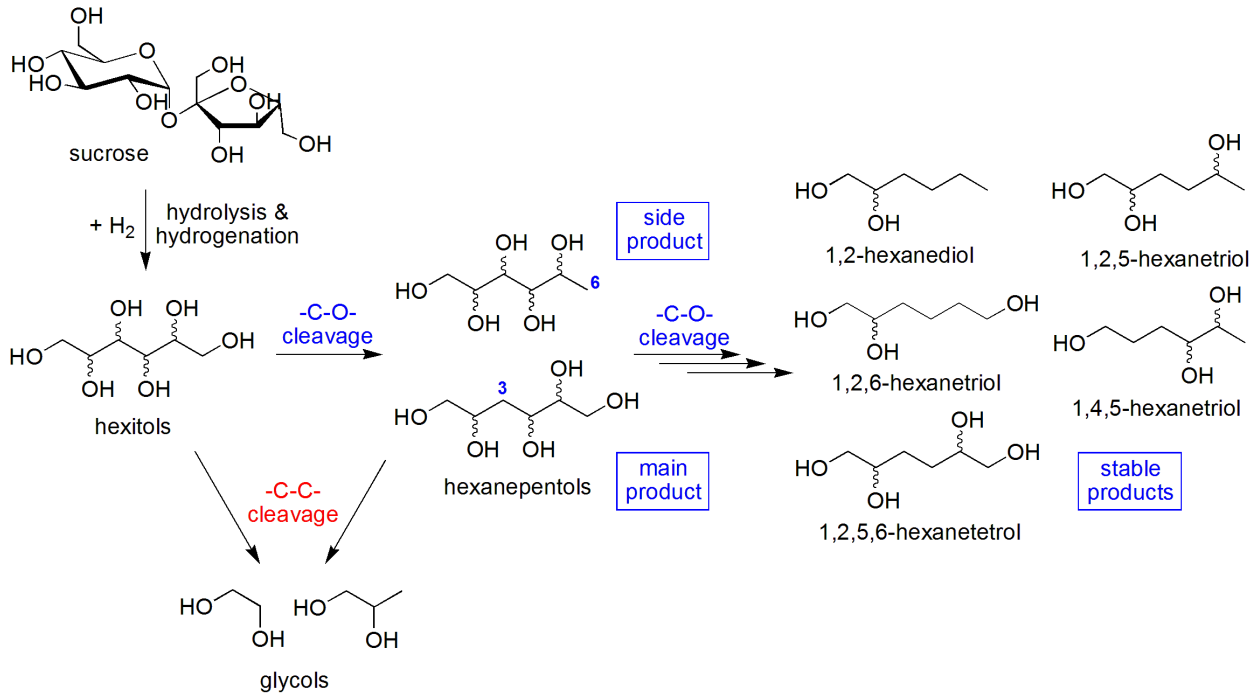

Figure 5-8: Hydrogenolysis of hexitols over Cu-Raney to stable deoxy C6 products (1,2,5,6-hexanetetrol, three hexanetriols and 1,2-hexanediol) via -C-O- cleavage at 180 °C and 150 bar H_2. The glycols ethanediol and 1,2-propanediol are the major side products from -C-C- bond cleavage after 40 h reaction time.

The concentration of hexanetetrols also reaches a maximum between 15 to 20 h (**Figure 5-9**) and decreases over an extended reaction time, indicating that these products are also intermediates. However, one hexanetetrol identified as the 1,2,5,6-isomer by ^{13}C-NMR analysis is not further converted. This product is stable towards -C-O- and -C-C- bond cleavage and accounts for 28 mol-% of all products in the liquid phase after 40 h reaction time. Other hexanetetrol isomers, of which seven are detected by GC-MS in comparatively low amounts, are further transformed to hexanetriols after a third -C-O- bond cleavage step.

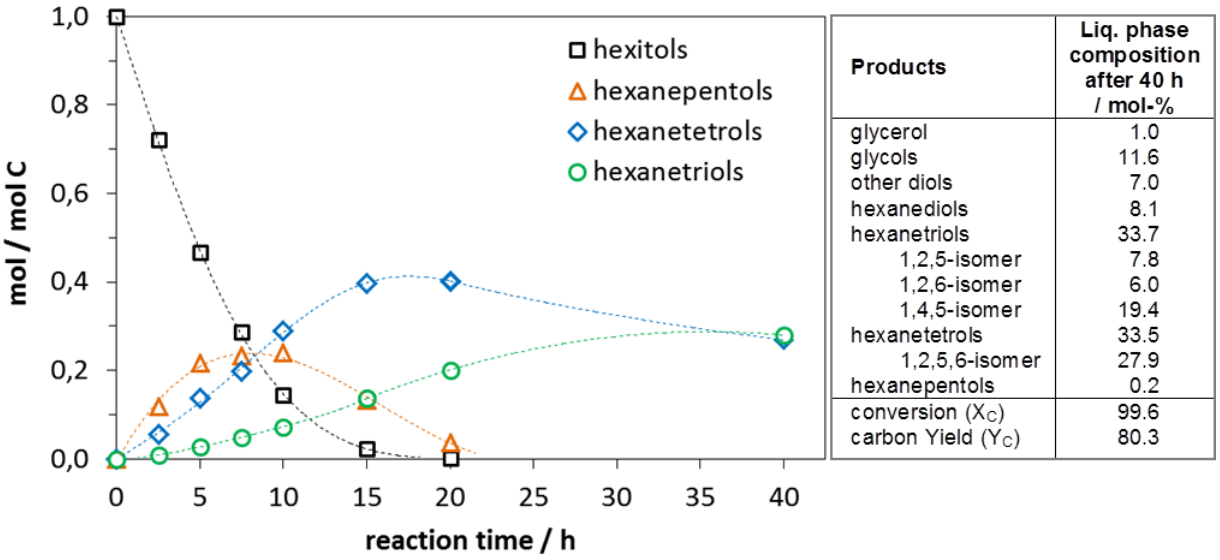

Products	Liq. phase composition after 40 h / mol-%
glycerol	1.0
glycols	11.6
other diols	7.0
hexanediols	8.1
hexanetriols	33.7
1,2,5-isomer	7.8
1,2,6-isomer	6.0
1,4,5-isomer	19.4
hexanetetrols	33.5
1,2,5,6-isomer	27.9
hexanepentols	0.2
conversion (X_C)	99.6
carbon Yield (Y_C)	80.3

Figure 5-9: Product distribution for hydrogenolysis of hexitols as a function of reaction time over Cu-Raney (50 mL catalyst basket which equals about 100 g) at 180 °C and 150 bar H_2.

Three stable hexanetriols are obtained: the 1,2,5-, 1,2,6- and 1,4,5-isomers. The concentration of these products steadily increases up to 34 mol-% after 40 h reaction time. A 1,2,3-hexanetriol as described by Blanc *et al.* is not formed [Blanc2000]. The only hexanediol obtained in noticeable concentrations was the 1,2-isomer (8 mol-%, **Figure 5-9**). Other products such as the 1,6-hexanediol are only detected in minor amounts. The liquid phase composition shows that final products are oligohydroxy compounds with two vicinal OH-groups and at least two adjacent methylene groups (**Figure 5-8**). We conclude that deoxy C6 polyols are not further converted when OH-groups are separated by at least two methylene groups. These final products are stable towards -C-O- and -C-C- cleavage.

The product distribution does not differentiate when sorbitol or mannitol are applied as reactant. This shows that the steric orientation of the OH-groups (R- or S-configuration) in stereo isomers does not affect the deoxygenation (more specifically: the position of the carbon atom in the reactant where -C-O- bond cleavage occurs). Tautomerization on the catalyst surface occurs already at 150 °C when the batch reactor is heated to the reaction temperature of 180 °C and thus, leads to a mixture of at least four hexitols before the first -C-O- bond cleavage step takes place.

The four detected hexitols are sorbitol, mannitol, galactitol and iditol (**Figure 5-10**). However, at least one additional undetected hexitol epimer has to be present in the aqueous solution (altritol or talitol) because iditol cannot derive from sorbitol, mannitol or galactitol directly. Furthermore, the mono- and disaccharides glucose, fructose (applied in an equimolar mixture known as invert sugar) and sucrose also yield the same products with comparable conversion and selectivity for each deoxy C6 product. This is probably attributed to hydrogenation reactions that already start at 70 °C when the batch reactor is heated up. Hence, the aqueous solution comprises of the same hexitols mixture when -C-O- hydrogenolysis starts at 180 °C. Hydrolysis of sucrose into the glucose and fructose monomers occurs without adding an acid (**Figure 5-8**). This is promising because the raw materials of sugar based feedstocks can be used directly as the reactant.

The reproducibility of these experiments was investigated in a long-term stability study of Cu-Raney with 40 repeated experiments of 20 h reaction time. No change in activity or selectivity was observed. The selectivity of 75 % for deoxy C6 polyols at 5 h as shown in **Figure 5-2** in chapter 5.1.1 describes a cumulative parameter for the sum of all deoxy C6 polyols, including hexanepentols. However, as they are further converted to hexanetetrols and -triols, degradation to short-chain polyols also takes place. A decrease in the overall selectivity for deoxy C6 polyols from 75 % to 65 % is observed when the reaction time is increased from 5 to 20 h. The catalytic properties of the Cu-Raney catalyst did not change even after a total of more than 800 h time-on-stream (**Figure 5-11**). Conversion and product distribution (selectivity) for each 20 h experiment are the same.

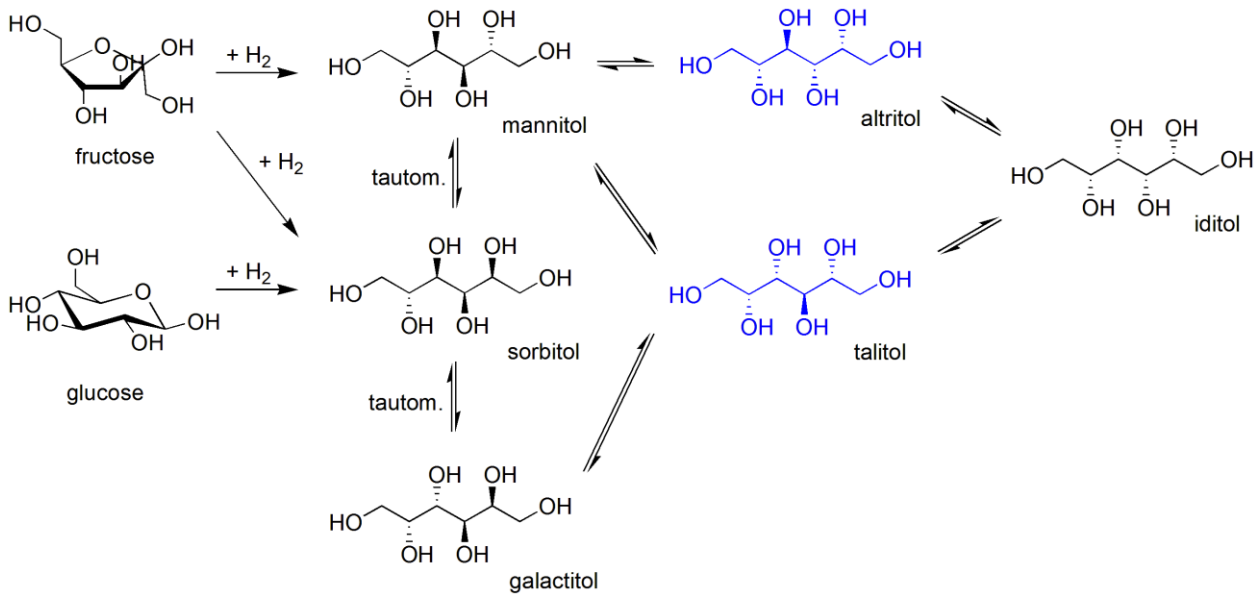

Figure 5-10: Hydrogenation of glucose and fructose to sorbitol and mannitol and tautomerization into other hexitols at temperatures between 70 and 150 °C and 150 bar H_2. The epimers altritol and talitol shown in blue are not detected by GC analysis. However, at least one of both hexitols has to be present in the aqueous solution because iditol is detected, which cannot derive from sorbitol, mannitol or galactitol directly.

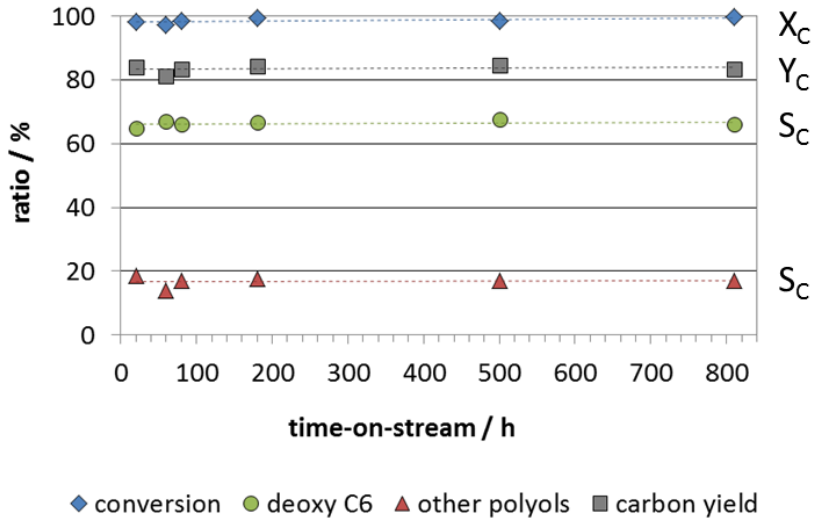

Figure 5-11: Cu-Raney shows no deactivation for hydrogenolysis of hexitols over a total reaction time of 800 h, achieved by 40 experiments with 20 h reaction time each, at 180 °C and 150 bar H_2. S_C describes the selectivity for deoxy C6 polyols (green dots: hexanepentols, -tetrols, -triols, and -diols) and other polyols (red dots: C2 to C5 polyols). Y_C is the carbon yield for all GC-detected products and X_C the conversion of hexitols.

5.1.3. Reaction mechanism for -C-O- bond cleavage; effect of OH-group arrangement

Due to the deactivation of the Cu/Al_2O_3 catalyst, the effect of OH-group arrangement on hydrogenolysis activity was only investigated for Cu-Raney. **Figure 5-12** shows that the steric orientation of OH-groups in different stereoisomers does not affect the activity or selectivity for -C-O- bond cleavage reactions. Independent of the reactant (pure mannitol or sorbitol), a similar hexitol mixture of mannitol, sorbitol, galactitol, and iditol is obtained for reaction periods between 2.5 and 5 h. Sorbitol is the main stereoisomer in this mixture, followed by mannitol. Galactitol and iditol are formed in smaller amounts. All four hexitols are converted at comparable rates and the formation rates of deoxy C6 products are also similar.

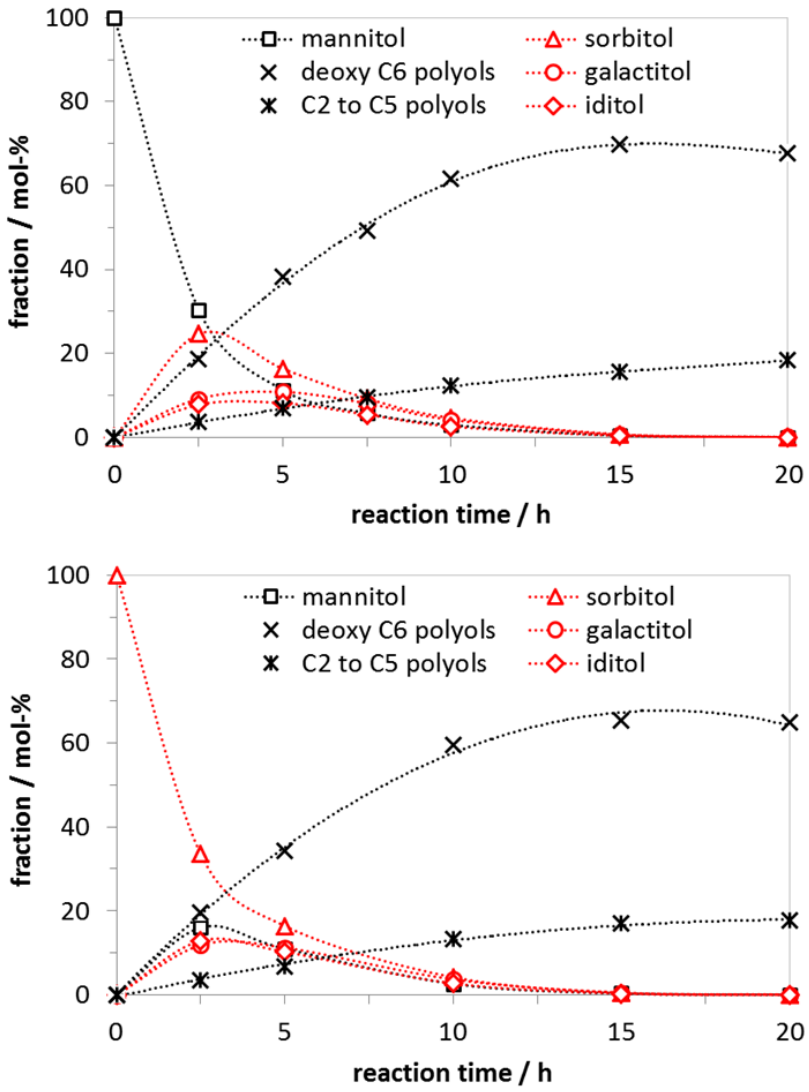

Figure 5-12: Isomerization and hydrogenolysis of mannitol (top) and sorbitol (bottom) over Cu-Raney at 180 °C and 150 bar H_2. Independent of the reactant, the isomerization products galactitol and iditol are formed in comparable amounts and also converted at approximately the same rate as mannitol and sorbitol.

However, the arrangement of OH-groups in the deoxygenated reaction intermediates strongly affects the hydrogenolysis pathway and thus, the selectivity to specific deoxy C6 polyols. In order to investigate how the selective -C-O- bond cleavage over Cu-Raney occurs, we have categorized numerous polyols into different types based on similarities in the molecular structure (**Figure 5-13**) and studied the dependency of deoxygenation reactions from the structure of the reactant. Type A polyols consist of at least three adjacent OH-groups with glycerol as the smallest possible compound of this category. The type B polyols consist of two vicinal OH-groups at the 1- and 2-position and an adjacent methyl or methylene group at the 3-position when the carbon chain is longer than two carbon atoms (e.g. 1,2-propanediol and 1,2-butanediol). 2,3-butanediol does not consist of terminal OH-groups but rather two adjacent OH-groups in the middle of the molecule (type C).

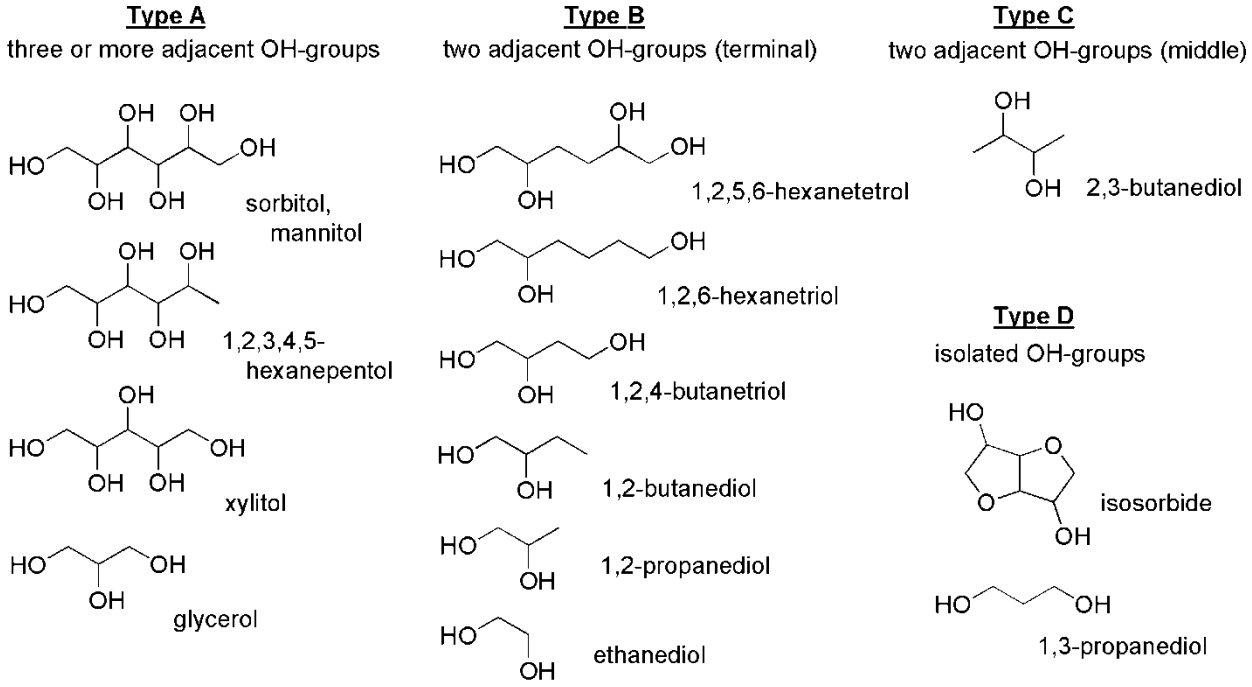

Figure 5-13: Classification of polyols into types A to D, based on the arrangement of OH-groups.

The type D polyols isosorbide and 1,3-propanediol are also diol compounds but con-sist of isolated OH-groups. The application of these different reactants enables the investigation how the number and the arrangement of OH-groups affects -C-O- and -C-C- bond cleavage over Cu catalysts. Our study reveals that both conversion and selectivity for Cu catalyzed -C-O- bond cleavage strongly depend on the number and arrangement of the OH-groups within the molecule. Sugar alcohols with three or more adjacent OH-groups (e.g. glycerol or hexitols, type A) are highly reactive and more effectively converted than compounds with only two adjacent OH-groups (type B and C polyols) or isolated OH-groups (type D) as shown in **Table 5-1**. Comparison of the conversion (X_C / %) reveals that type B polyols are rather stable towards -C-O- and -C-C- bond cleavage over Cu-Raney.

The carbon chain length does not seem to affect the hydrogenolysis activity as long as the reactant only comprises of vicinal OH-groups at the 1- and 2-position. Ethanediol, 1,2-propanediol, and 1,2-butanediol show only very low conversion (1 to 12 %). When the reactant carries an additional OH-group, the distance between the third OH-group and the vicinal OH-groups at the 1- and 2-position determines the reactivity for -C-O- bond cleavage. For example, the third OH-group in 1,2,6-hexanetriol is separated from the OH-groups at the 1- and 2-position by three methylene groups. In 1,2,5,6-hexanetetrol the distance to the next OH-group is two methylene groups. Both compounds are only weakly converted (10 and 4 %, respectively), similar to ethanediol, 1,2-propanediol, and 1,2-butanediol. In contrast, the third OH-group in 1,2,4-butanetriol is only separated by one methylene group and this reactant shows much higher conversion (48 %).

Table 5-1: Reactivity of various polyols over Cu-Raney (100 mL catalyst basket which equals about 200 g of catalyst; 500 ml of an 7.5 wt-% aqueous solution which equals about 42.5 g of each reactant) at 180 °C, 150 bar H_2 and 20 h reaction time.

Structure	Reactant	X / %	$Y_{c,liq}$ / %	$Y_{c,loss}$ / %	Reactivity
	Three or more adjacent OH-groups (type A)				
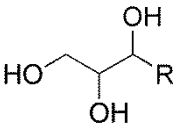	Sorbitol	100	83	17	very high
	Mannitol	100	86	14	very high
	1,2,3,4,5-hexanepentol	75	80	20	high
	Xylitol	96	81	19	very high
	Glycerol	77	92	18	high
	Two adjacent OH-groups (terminal position, type B)				
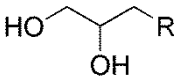	1,2,5,6-hexanetetrol	4	96	4	very low
	1,2,6-hexanetriol	10	91	9	very low
	1,2,4-butanetriol	48	85	15	moderate
	1,2-butanediol	8	92	8	very low
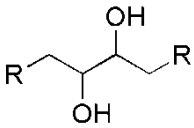	1,2-propanediol	12	89	11	very low
	Ethanediol	1	99	1	very low
	Two adjacent OH-groups (internal position, type C)				
	2,3-butanediol	1	99	1	very low
	Other polyols with isolated OH-groups (type D)				
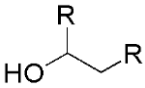	1,3-propanediol	20	82	18	low
	Isosorbide	9	92	8	very low

Interestingly, the only deoxy product obtained from 1,2,4-butanetriol hydrogenolysis over Cu-Raney is 1,2-butanediol. Hence, the OH-group at the 4-position is also preferably cleaved whereas the vicinal OH-groups at the 1- and 2-position are stable towards -C-O- bond cleavage (**Figure 5-14**). Based on this comparison of the type B polyols we conclude that the number of OH-groups in a reactant only seems to affect the hydrogenolysis activity when OH-groups are in close proximity. Furthermore, we conclude that vicinal OH-groups at the 1- and 2-position of a reactant are more stable.

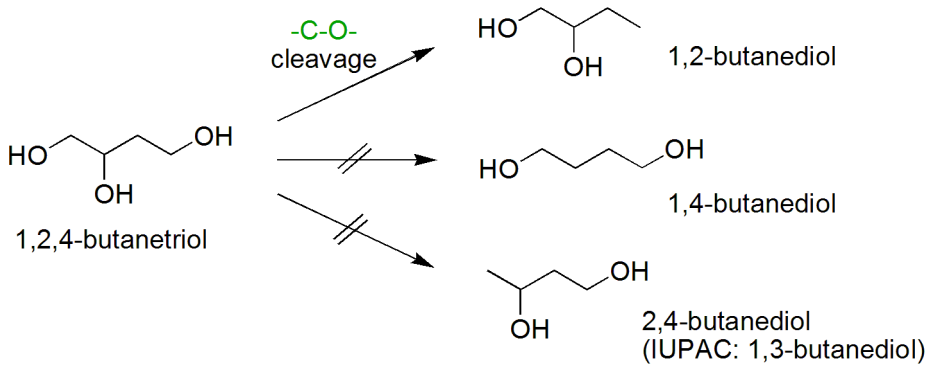

Figure 5-14: Selective -C-O- bond cleavage of 1,2,4-butanetriol over Cu-Raney at 180 °C and 150 bar H_2.

The type C polyol 2,3-butanediol consists of vicinal OH-groups in the middle of the molecule with adjacent methyl groups on both sides. This reactant also shows negligible conversion (1 %), similar to 1,2-butanediol. The same very low reactivity is seen for isosorbide, consisting of isolated OH-groups (type D polyol), and a conversion of only 9 %. The conversion of 20 % for 1,3-propanediol is mainly attributed to -C-C- bond cleavage via retro aldol elimination yielding ethanol and methanol. The carbon loss ($Y_{C,loss}$ / %) of 18 % as shown in **Table 5-1** accounts for these mono alcohols. As the GC method used to analyze di-, tri-, and tetrols does not allow the detection of mono alcohols, ethanol and methanol were detected and quantified separately by additional headspace analysis. In contrast to 1,3-propanediol, isosorbide and vicinal diols are not able to follow the retro aldol reaction and thus, show less conversion.

Type A polyols with three or more adjacent OH-groups show much higher reactivity than type B, C and D polyols (**Table 5-1**). Sorbitol, mannitol and xylitol are almost completely converted (96 to 100 %). The main products are deoxy C6 polyols and deoxy C5 polyols when xylitol is used as reactant, respectively. Glycerol and the 1,2,3,4,5-hexanepentol show conversions of 75 and 77 %, respectively. A comparison of the pentols 1,2,3,4,5-hexanepentol and xylitol indicates that the presence of terminal methyl groups has a negative effect on the hydrogenolysis activity. Both reactants comprise of five adjacent OH-groups with one additional methyl group in 1,2,3,4,5-hexanepentol. We attribute this methyl group is a hindrance in the interaction be-tween OH-groups of the reactant and the Cu surface. Makkee *et al.* proposed that reducing sugars such as fructose preferably adsorb on a Cu catalyst with specific OH-groups, in particular at the 1- and 2-position (**Figure 5-15**) [Makkee1985]. Based on our results, we assume that polyols adsorb similarly via at least two OH-groups, including the terminal position. Consequently, a methyl group as in 1,2,3,4,5-hexanepentol has a negative effect on the adsorption because the reactant can only adsorb from one side. In contrast, xylitol can adsorb from both sides via two vicinal OH-groups which results in the higher conversion compared to 1,2,3,4,5-hexanepentol.

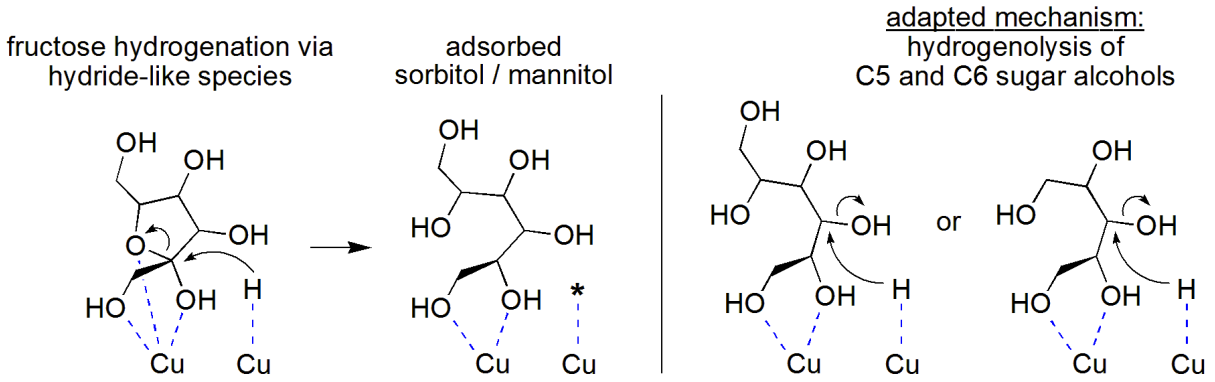

Figure 5-15: Adsorption of fructose on a Cu surface and hydrogenation to sorbitol and mannitol via hydride-like species as proposed by Makkee *et al.* (on the left) [Makkee1985]. The adapted mechanism proposes adsorption of C5 and C6 sugar alcohols via two vicinal OH-groups in a five-membered ring, similar to a chelating complex (right). The free OH-group in closest proximity is then cleaved via substitution with a hydride-like species.

Herein, the adsorbed OH-groups seem to be inert towards -C-O- bond cleavage which is probably attributed to the stable five-membered ring in the chelating complex with Cu (**Figure 5-15**). This is in agreement with a postulated mechanism from Shinmi et al. regarding deoxygenation from glycerol to 1,2-propanediol [Shinmi2010], where the adsorbed OH-groups are not cleaved and only the adjacent free OH-groups are deoxygenated. Our proposing would also explain the negligible conversion of the type B polyols (e.g. 1,2-butanediol, 1,2,6-hexanetriol and 1,2,5,6-hexanetetrol). When these compounds are adsorbed via the two OH-groups at the 1- and 2-position, there are no free OH-groups in close proximity to the catalyst that could undergo -C-O- bond cleavage. All other diols (type C and D) also do not have free OH-groups left for -C-O- bond cleavage and therefore are not effectively converted.

The side reactions over Cu-Raney are mainly -C-C- bond cleavage to short-chain polyols via retro aldol reactions. Formation of gaseous C1 products, in particular CO_2, is only significant when polyols comprise of more than two adjacent OH-groups. **Figure 5-16** shows that only traces of volatile C1 products are detected when type B, C, and D polyols are used as reactants. In contrast, the type A compounds (e.g. glycerol) undergo degradation to CO_2 in larger quantity. We attribute this to the requirement of a 1,3-diol arrangement of OH-groups for decarboxylation as discussed in more detail in chapter 5.1.4. Type A polyols with at least three adjacent OH-groups allow such reactions whereas the type B, C, and D polyols are not able to follow these degradation pathways. Hence, the OH-group arrangement in the reactant does not only affect deoxygenation reactions but also degradation via different -C-C- bond cleavage mechanisms.

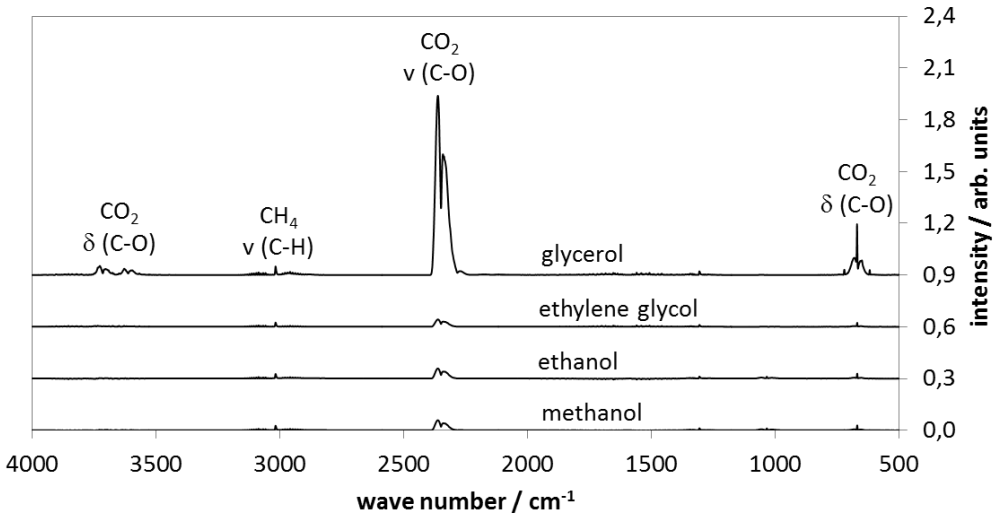

Figure 5-16: IR spectra of the gas phase composition for hydrogenolysis reactions of various hydroxy compounds over Cu/Al_2O_3 at 220 °C, 150 bar H_2 and 5 h reaction time.

Reaction mechanism for consecutive -C-O- bond cleavage from hexitols to hexanetriols

Based on the results from the previous chapter, the selective -C-O- bond cleavage of type A polyols such as sorbitol and mannitol was studied for the Cu-Raney catalyst. Our analysis of reaction intermediates reveals that the hydrogenolysis of hexitols to deoxy products (hexanepentols, -tetrols, and -triols) occurs via multiple consecutive -C-O- bond cleavage steps. Hexanepentols (monodeoxy compounds) are the first transient product while hexanetetrols (dideoxy polyols) and -triols (trideoxy polyols) are produced from these intermediates as was shown in **Figure 5-9**. The liquid phase composition after 40 h reaction time shows that the main product is 1,2,5,6-hexanetetrol. This isomer is the only hexanetetrol obtained in large amounts. Similarly, the mixture of hexanetriols only comprises of three isomers (1,2,5- / 1,2,6- / 1,4,5-isomers). It is remarkable that only four deoxy C6 polyols account for more than 60 mol-% of the applied carbon from mannitol. These products have to derive from selective -C-O- bond cleavage pathways. Combined GC- and NMR-analysis shows that only two hexanepentols are formed by the initial -C-O- bond cleavage step over Cu-Raney. The first deoxygenation predominantly occurs at the 3-position (**Figure 5-17** and **Figure 9-1** to **8-5** in the appendix). 6-deoxy hexitols (1,2,3,4,5-hexanepentols) are also identified but only as a minor side product in small amounts. These are the same stereoisomers as obtained from hydrogenation of the 6-deoxy hexose rhamnose (see **Figure 9-3** and **Figure 9-4** in the appendix).

In a recent study by Palkovitz *et al.* it was shown that the deoxygenation of terminal OH-groups is not acid-catalyzed but rather a metal-catalyzed reaction via the E2 mechanism [Palkovitz2015]. This reaction was initially proposed for Ru catalysts but it seems also plausible for Cu. However, the 3-deoxy and 6-deoxy hexitols are formed in a ratio of about 8:1, which means that the E2 mechanism is not the dominant -C-O- bond cleavage pathway over Cu-Raney. 2-deoxy hexitols (or 5-deoxy, respectively) are not detected which reflects the special catalytic properties of Cu. We attribute this large excess of 3-deoxy products to the favored adsorption via the vicinal OH-groups at the 1- and 2-position with -C-O- bond cleavage of the adjacent OH-group (see **Figure 5-15** and **Figure 5-17**). Four stereoisomers of 3-deoxy hexitols are detected with GC analysis which corresponds to the four detected hexitols: sorbitol, mannitol, galactitol, and iditol. The next -C-O- bond cleavage step should yield a 3,4-dideoxy hexitol as the main product (1,2,5,6-hexanetetrol, see **Figure 5-18** and **Figure 9-6** to **8-10** in the appendix). According to our mechanism, adsorption can now occur at the 5- and 6-position with -C-O- bond cleavage of the adjacent OH-group at the 4-position. This reaction is basically the same as the first -C-O- cleavage step, just repeated from the other side of the molecule. This proposed mechanism would explain why 1,2,5,6-hexanetetrol is the main product in the liquid phase. In a side reaction, 3-deoxy hexitols may also undergo direct -C-O- bond cleavage at the 4-position, when adsorbed via the 1- and 2-position, as was shown by hydrogenolysis of 1,2,4-butanetriol (**Figure 5-14**).

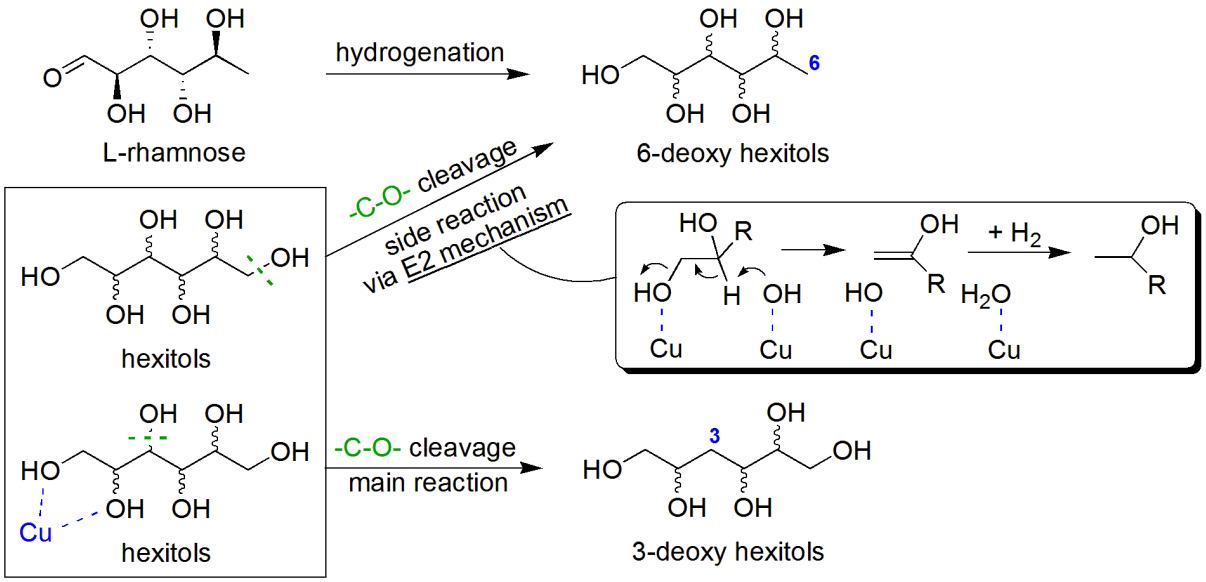

Figure 5-17: Selective -C-O- bond cleavage of hexitols over Cu-Raney. Only two constitutional isomers are detected: 3-deoxy hexitols as the main products and 6-deoxy hexitols as side products. The formation of 6-deoxy products via the E2 mechanism is adapted from Palkovitz *et al.* [Palkovitz2015].

The further conversion of the 3-deoxy and 6-deoxy hexitols via the E2 mechanism and our proposed mechanism for the cleavage of internal OH-groups should yield three different dideoxy hexitols (**Figure 5-18**). This is in line with combined GC-MS and NMR analysis which shows that only three constitutional isomers are formed. The 3,4-deoxy hexitol (1,2,5,6-hexanetetrol) is the main product and the 3,6-dideoxy hexitol (1,2,4,5-hexanetetrol) is the major side product (see **Figure 9-9** to **9-11** in the appendix). The structure of the third isomer could not be identified with NMR analysis, but it is expected to be the 2,3-dideoxy hexitol (1,4,5,6-hexanetetrol). The 3,6-dideoxy hexitol may be formed from the 3-deoxy intermediate along the E2 mechanism. A second route to the 3,6-dideoxy hexitol could be the adsorption via the 4- and 5-position with -C-O- bond cleavage of the adjacent terminal OH-group at the 6-position. When the OH-group at the 2-position is cleaved instead, the 2,3-dideoxy hexitol is obtained.

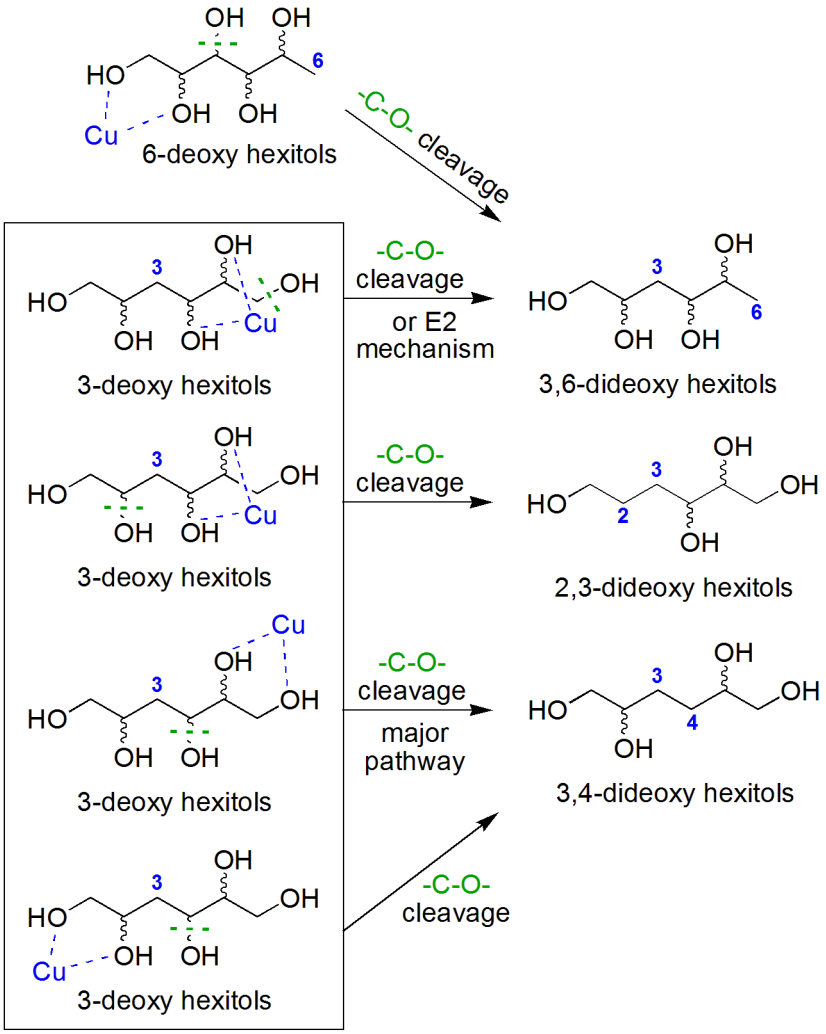

Figure 5-18: Selective -C-O- bond cleavage of 3-deoxy and 6-deoxy hexitols over Raney-Cu. Our proposed mechanism invovles adsorption via vicinal OH-groups with cleavage of an adjacent OH-group or an OH-group with one methylene group distance. This leads to only three possible dideoxy products (hexanetetrols).

Figure 5-19 shows that the 3,6-dideoxy and 2,3-deoxy product are only intermediates and further converted to hexanetriols. The 3,6-dideoxy hexitol leads to 1,2,5- or 1,4,5-hexanetriol, whereas the 2,3-dideoxy hexitol yields the 1,4,5- or 1,2,6-hexanetriol. Other hexanetriols are not detected. The formation of 1,2,6-hexanetriol is also possible from ring-opening hydrogenolysis of cyclic ethers such as isosorbide. The product mixture was checked for these intermediates, but not even trace amounts were detected. Hence, the selective -C-O- bond cleavage over Cu-Raney only seems to occur via linear deoxy C6 polyols.

The 1,2,5,6-hexanetetrol and the three hexanetriols (1,2,5- / 1,2,6- / 1,4,5-isomers) consist of vicinal OH-groups and two adjacent methylene groups, similar to the OH-group arrangement of the type B polyols shown **Figure 5-13** and **Table 5-1**. Thus, we conclude that this is a stable configuration over Cu and such polyols do not undergo further -C-O- bond cleavage.

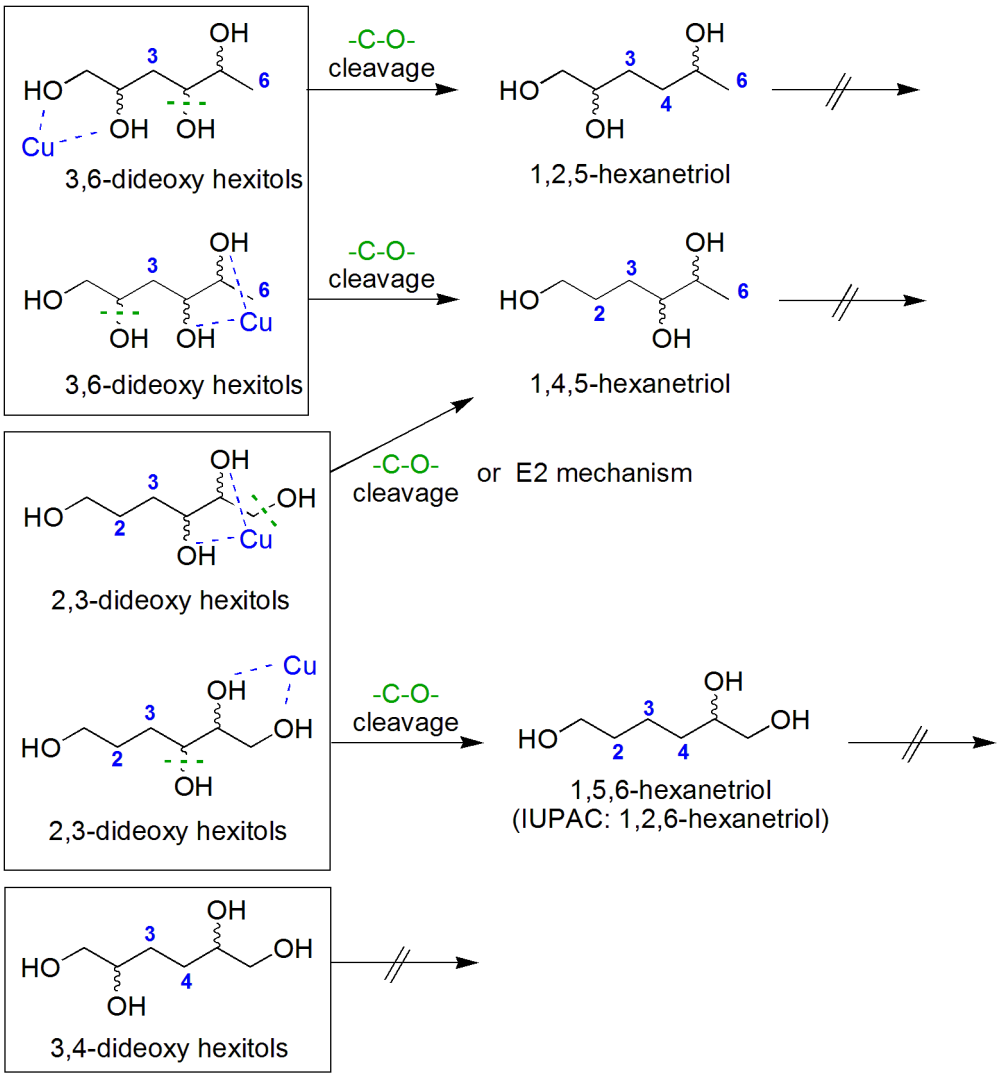

Figure 5-19: Selective -C-O- bond cleavage of 3,6-dideoxy and 2,3-dideoxy hexitols over Raney-Cu. Our proposed mechanistic model leads to three hexanetriols. The 3,4-deoxy hexitols are stable and not further converted.

Likewise, the deoxygenation of xylitol should yield 1,2,5-pentanetriol (**Figure 5-20**). A detailed analysis of tautomerization products (arabitol and ribitol) and the respective diastereomers after -C-O- bond cleavage showed exactly the same results as described for the C6 and C4 polyols previously. Two stereoisomers are obtained from xylitol, ribitol and arabitol after cleavage of the OH-group at the 3-position. The second -C-O- bond cleavage step either eliminates the OH-group at the 2-position or the 4-position. Both pathways lead to the same stereo isomer (a pair of enantiomers) as the final product, which is validated by GC and ^{13}C-NMR analysis. These investigations underline the selectivity of -C-O- bond cleavage over Cu-Raney, again.

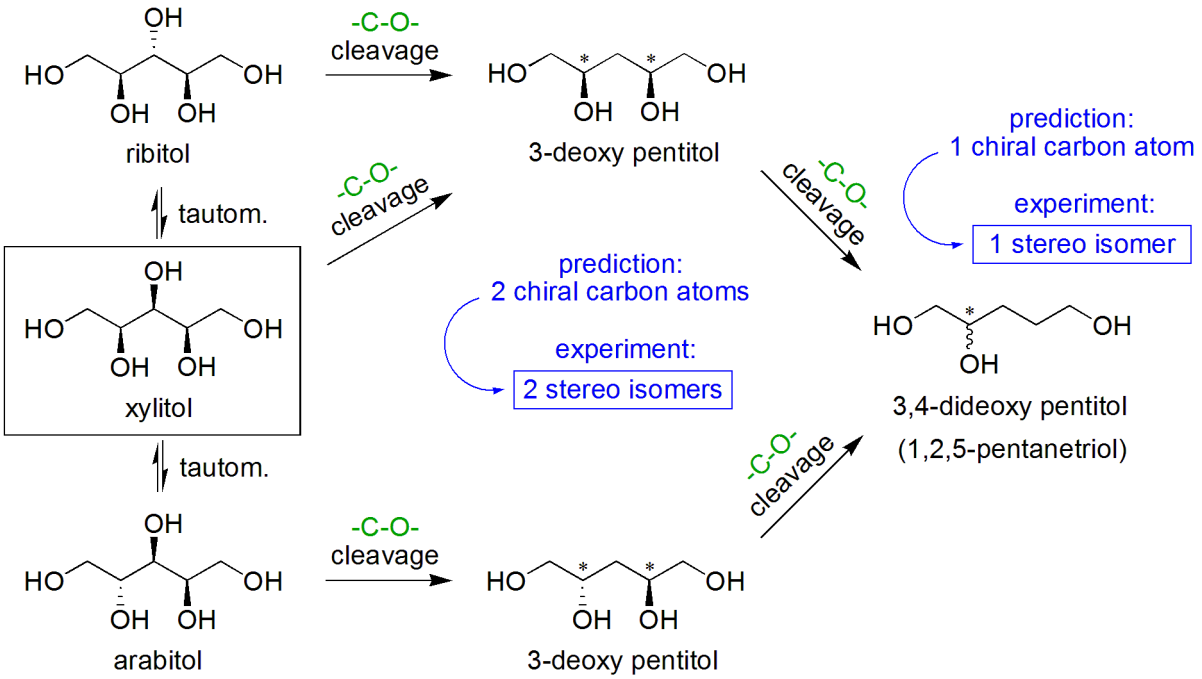

Figure 5-20: Selective -C-O- bond cleavage of xylitol over Raney-Cu. Formation of tautomerization and deoxygenation products, with separation of stereo isomers, is validated with combined GC and ^{13}C-NMR analysis. The predicted diastereomers are in line with the detected products and yield the final product 1,2,5-pentanetriol.

We conclude that stable final products consist of two vicinal OH-groups with two neighboring methylene groups. Products with this arrangement of OH-groups are not further converted via -C-O- or -C-O- bond cleavage (**Figure 5-21**). We attribute this special catalytic property of Cu-Raney to preferred adsorption of vicinal OH-groups in polyols. We further propose that the reactivity of -C-O- hydrogenolysis in additional free OH-groups decreases in the following order:

1. Cleavage of an adjacent OH-group is the most likely reaction.
2. Cleavage with one methylene group distance is less likely than 1.
3. Cleavage with two or three methylene groups in between OH-groups is very unlikely to occur.

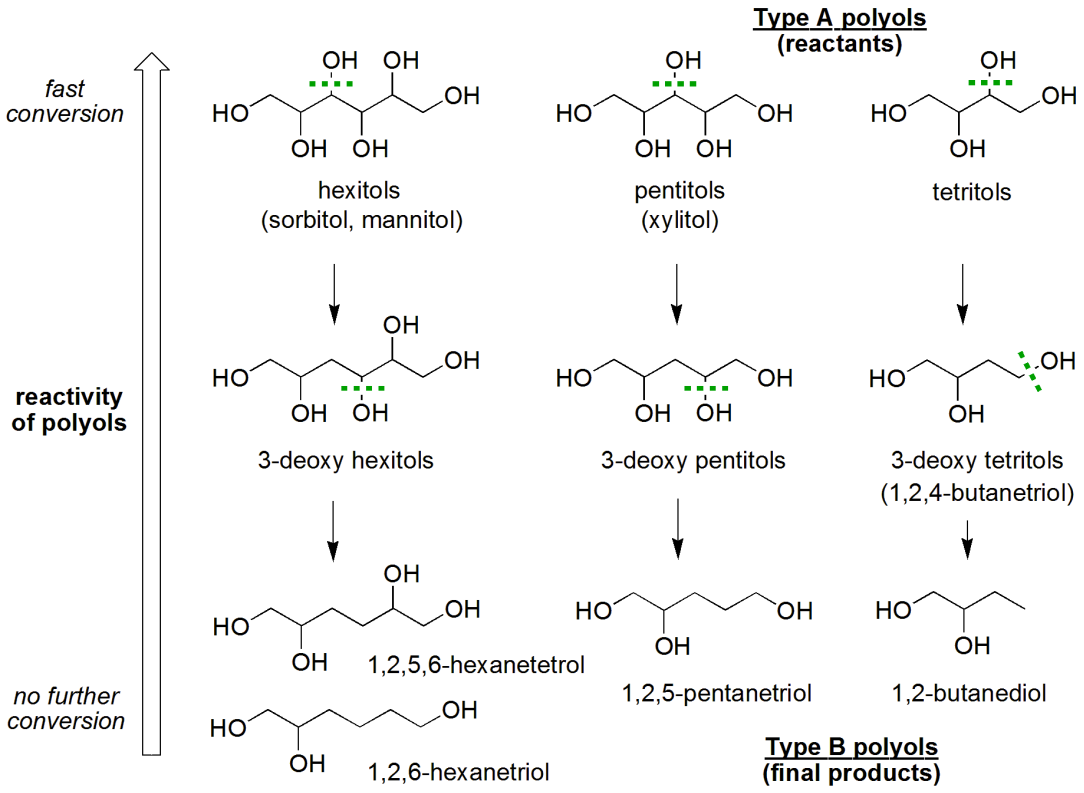

Figure 5-21: Reactivity of OH-groups over Cu catalysts for -C-O- bond cleavage. The final products consist of two vicinal OH-groups and two adjacent methylene groups, independent of the carbon chain length of the reactant.

The selective formation of 3-deoxy polyols after the first -C-O- bond cleavage is a strong indication that the deoxygenation reaction is metal-catalyzed as shown in the proposed mechanism (**Figure 5-18**, **Figure 5-19**, and **Figure 5-20**). Another known pathway for the formation of deoxy compounds is dehydrogenation to unsaturated intermediates and dehydration (**Figure 5-22**). This route is most commonly proposed for -C-O- hydrogenolysis from glycerol to 1,2-propanediol [Liu2010, Montassier1988, Palkovitz2014]. In fact, 3-deoxy hexitols could be formed from sorbitol or mannitol along this pathway as well. The predominant unsaturated species after adsorption has to be a 2-keto (or 5-keto) intermediate. We conclude this from the product distribution shown in **Figure 5-2** which clearly shows that the major side products over Cu are C3 polyols, in particular glycerol. Cleavage between the C3 and C4 bond, which yields two equivalents of glycerol (**Figure 5-22**), can only occur via such a 2-keto (or 5-keto) polyol. However, the adaptation of this dehydrogenation/dehydration pathway is not possible for the selective -C-O- bond cleavage of pentitols and tetritols. This route would lead to 4-deoxy products from such 2-keto (or 5-keto) intermediates. However, tetritols (e.g. erythritol) and pentitols (e.g. xylitol) clearly show that 3-deoxy products are formed after the first -C-O- bond cleavage step as shown in **Figure 5-21**. Hence, deoxygenation over Cu seems to be a metal-catalyzed reaction.

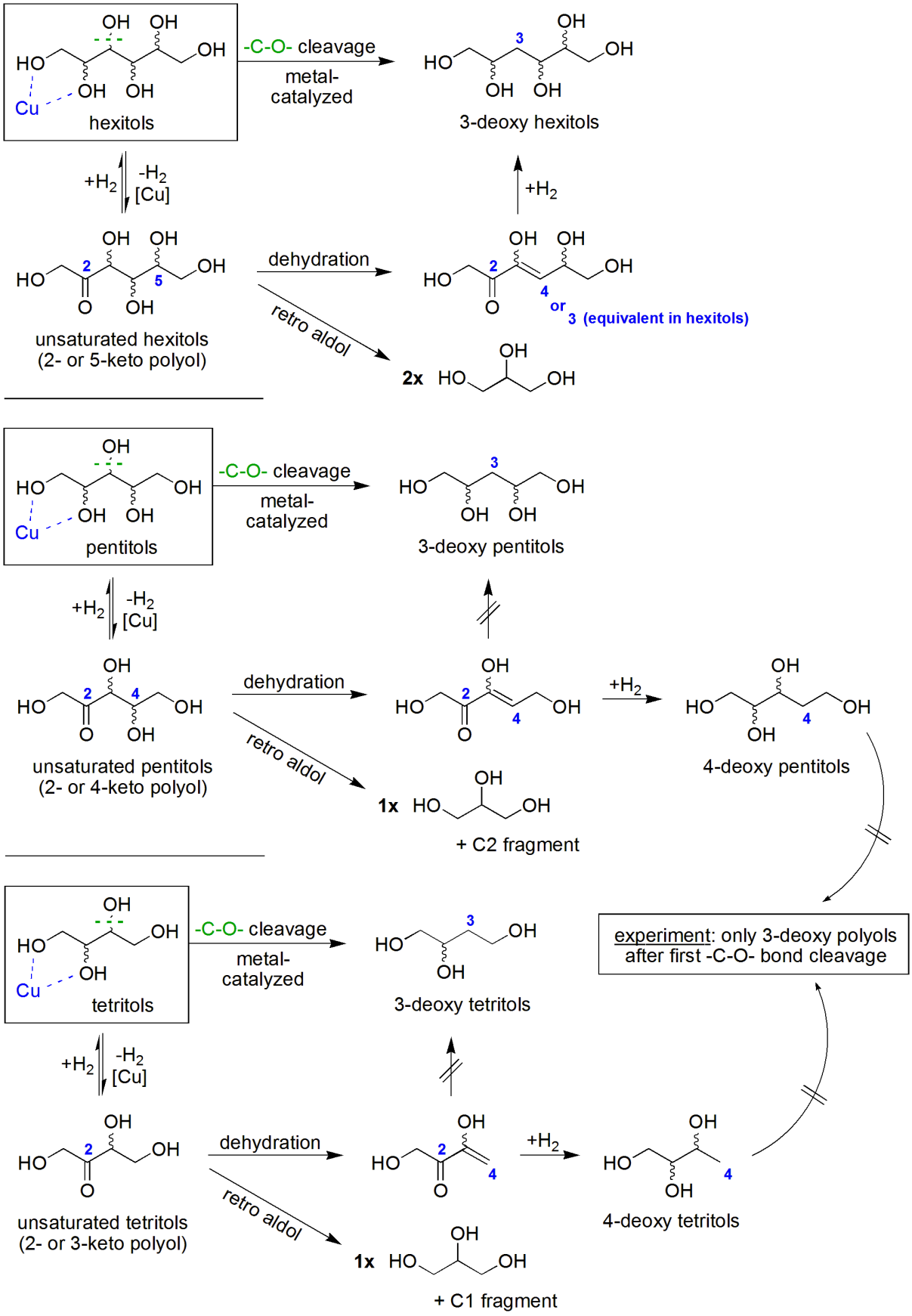

Figure 5-22: Comparison of metal-catalyzed -C-O- bond cleavage and dehydration from unsaturated intermediates shows that different deoxy polyols are obtained. Hence, the metal-catalyzed reaction has to be the most dominant pathway.

5.1.4. Reaction pathways for -C-C- bond cleavage over Cu

The comparison of the supported Cu/Al_2O_3 catalyst and Cu-Raney (bulk-catalyst) in chapter 5.1.1 showed that degradation reactions are much more pronounced using supported Cu. However, the deactivation of this catalyst was also pointed out, which clearly indicates that the -C-C- bond cleavage reactions are not catalyzed by the support. The degradation is rather attributed to the formation of unsaturated intermediates over Cu that initiate non-catalytic -C-C- bond cleavage reactions. Polyols are known to undergo dehydrogenation to aldehyde and ketone intermediates during adsorption over Cu/Al_2O_3 [Palkovitz2014] and Cu-Raney [Berweilter2001, Berweiler2004, Wang1995]. Such unsaturated intermediates enable cleavage of -C-C- bonds via the retro aldol reaction [Wang1995, Palkovitz2014] and thus, need to be re-hydrogenated as quickly as possible (**Figure 5-23**).

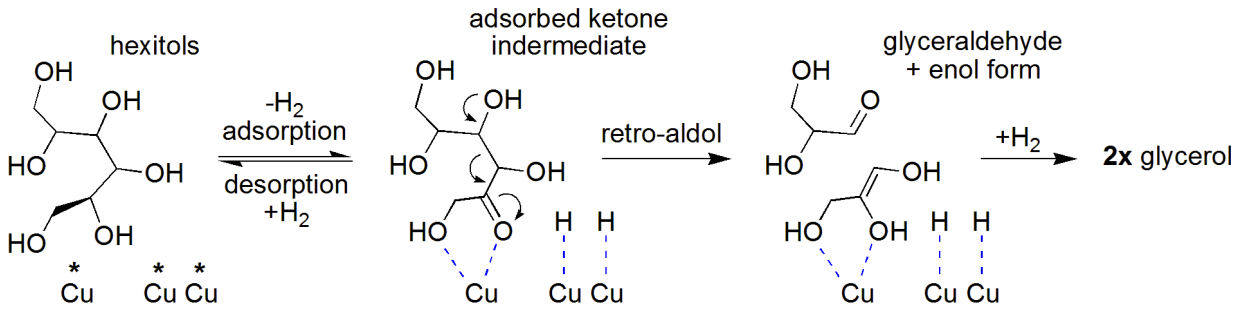

Figure 5-23: Adsorption of hexitols as ketone intermediates over Cu catalysts. Such unsaturated compounds initiate degradation via the retro aldol reaction.

For this purpose, the hydrogenation rate of isomaltulose (with a fructose building block) over Cu-Raney and the supported Cu catalyst was examined under identical reaction conditions. Cu-Raney was about three times more active for hydrogenation of the ketone reactant than the supported Cu catalyst (**Figure 5-24**). Hence, we propose that side reactions like the retro aldol reaction are more expressed over supported Cu because the unsaturated intermediates, that initiate -C-C- bond cleavage are less likely to be re-hydrogenated. Such unsaturated species degrade in the absence of any catalyst and thus, hydrogenation of these intermediates has to be improved to suppress -C-C- bond cleavage. Cu-Raney exhibits better hydrogenation properties and thus, degradation reactions are greatly suppressed.

The same correlation is seen between the applied H_2-pressure and the formation of short-chain polyols over Cu-Raney. **Figure 5-25** shows that the selectivity for C2 to C5 polyols from -C-C- bond cleavage is almost increased by a factor of two when low H_2 pressures are applied. Furthermore, at 25 bar H_2 and at inert atmosphere (25 bar argon), less than 60 mol-% of the converted carbon in the hexitol reactant is found in either deoxy hexitols or short-chain polyols. Other products such as unsaturated compounds (e.g. aldehydes and ketones) are formed. Even C2 and C3 acids are detected, e.g. acetic acid

and lactic acid, (see **Figure 9-16** in the appendix) as well as C6 sugar acids (gluconic acid and saccharinic acid). The amount of these "oxidized" products is significantly lowered when higher H_2 pressure is applied. In accordance, the selectivity for short-chain polyols also decreases at elevated H_2 pressures. Conversely, the selectivity for deoxy C6 polyols steadily increases from 51 mol-% at 50 bar to 76 mol-% at 200 bar. These results reveal that fast hydrogenation of unsaturated intermediates under high H_2 pressure is crucial in order to maintain the C6 carbon chain of sugar alcohols and suppress -C-C- bond cleavage reactions. This leads to higher selectivities for deoxy C6 polyols.

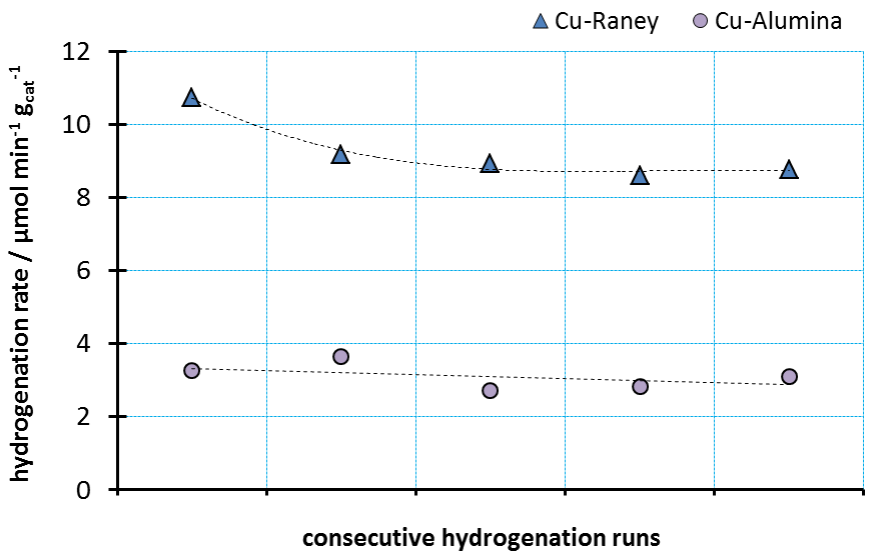

Figure 5-24: Conversion rates for Cu-Raney and the Cu/Alumina for the hydrogenation of isomaltulose (fructose building block) at 70 °C and 150 bar H_2. The hydrogenation rate is standardized per one gram of catalyst.

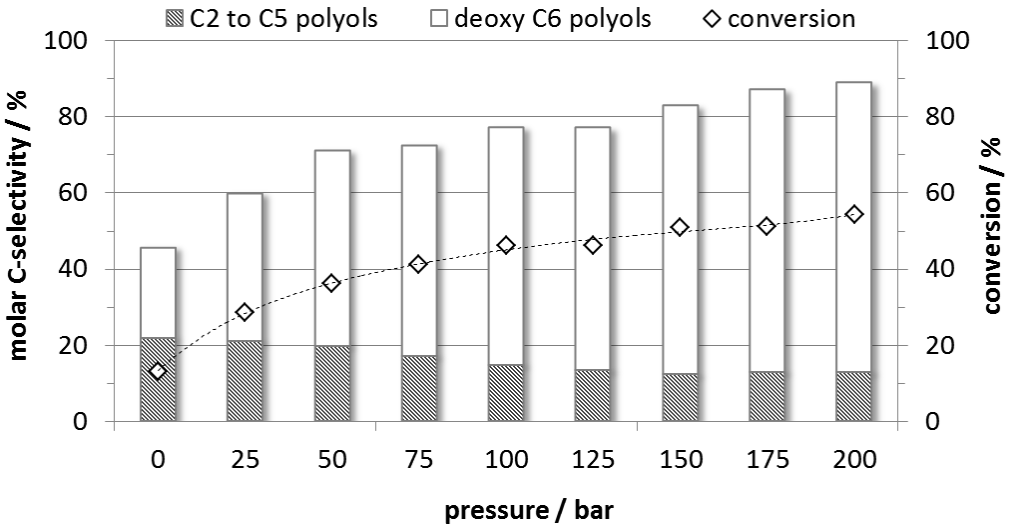

Figure 5-25: Effect of H_2 pressure on the conversion of mannitol (7.5 wt-% aqueous solution) and selectivity towards deoxy C6 polyols and short-chain polyols (C2 to C5) over Cu-raney (about 200 g catalyst) at 180 °C and 5 h reaction time.

The same correlation between these two parameters is observed when the hexitol concentration is increased at a constant H_2 pressure. The -C-O- bond cleavage selectivity decreases with increasing concentration of sugar alcohols at a constant temperature (180 °C) and pressure (150 bar, see **Figure 5-26**). We assume that polyols and H_2 competitively adsorb on the catalyst surface leading to higher sugar alcohol coverage and as a result to a lower coverage of H_2. This effect is unfavorable for high selectivity of deoxy C6 polyols. Interestingly, the selectivity for short-chain products (C2 to C5) does not inversely increase; it is rather constant indicating no increase in -C-C- bond cleavage. These results were confirmed by reproducibility tests with four repeated experiments for each hexitol concentration. The results are similar to experiments performed with 7.5 wt-% hexitols and low H_2 pressure (below 50 bar). When the selectivity for deoxy C6 polyols and short polyols do not add up to 100 mol-%, and the formation of gaseous products (verified by IR-analysis) does not account for the carbon loss, unsaturated compounds are probably formed in a larger amount.

Hence, the H_2 coverage on the catalyst surface seems to correlate with the hydrogenation of unsaturated species and thus, -C-C- bond cleavage by retroaldolization and other side reactions. Operating hydrogenolysis reactions at higher hexitols concentration would therefore require a higher H_2 pressure in order to increase the H_2 coverage and improve the selectivity of deoxygenated hexitols.

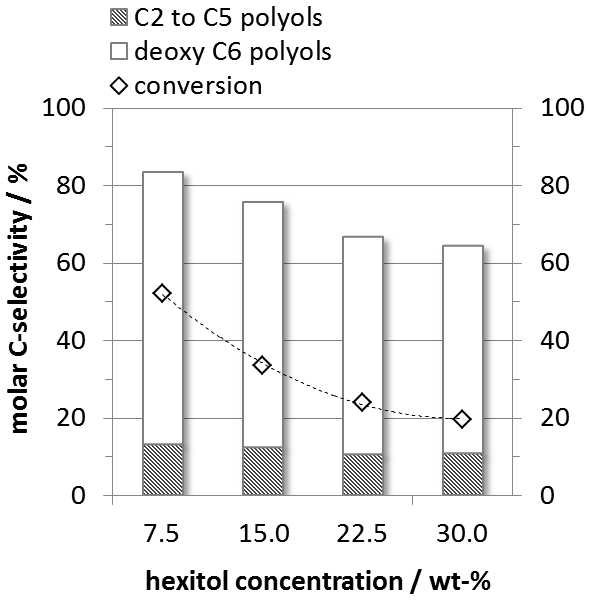

Figure 5-26: Effect of hexitol concentration on the selectivity for deoxy C6 polyols and other short-chain polyols (C2 to C5 compounds) in hydrogenolysis reactions of hexitols over Cu-Raney (about 200 g catalyst) at a constant 150 bar H_2, 180 °C and 5 h reaction time. The amount of mannitol reactant that was applied for each experiment, varied between 42.5 and 170 g (corresponding to 500 mL of an aqueous mannitol solution with 7.5 to 30 wt-% concentration).

The formation of aldehyde and ketone intermediates during adsorption is a quasi-equilibrated step as was shown in **Figure 5-23** in the beginning of this chapter. The hydrogenation in this equilibrium (e.g. of a ketone) is much faster than the hydrogenolysis of -C-O- bonds or degradation via -C-C- bond cleavage. The hydrogenation of isomaltulose (a reducing sugar, ketone) shows a conversion rate limitation due to limited H_2 diffusion when the stirring rate of the batch reactor is varied. In contrast, the relative hydrogenolysis rate of sugar alcohols (reactant: mannitol) to deoxy C6 products or short-chain polyols, respectively, is much slower. This reaction also requires hydrogenation of an adsorbed unsaturated intermediate that shows similar properties to reducing sugars such as isomaltulose. However, the hydrogenolysis reaction is not rate limited by the supply/diffusion of H_2 and rather limited by the comparatively slow -C-O- or -C-C- bond cleavage rate. We conclude these proposings from a comparison of relative conversion rates at different stirring speeds, ranging from 0 to 1200 rpm (**Figure 5-27**). With an increased stirring speed, the diffusion layer thickness around the catalyst surface, through which the H_2 dissolves in the liquid phase, should decrease. Thus, dissolved H_2 is able to diffuse to the catalyst more quickly. If this H_2 diffusion is the rate limiting step, the conversion rate should depend strongly on the diffusion layer thickness and consequently on the stirring rate in the batch reactor. No reaction occurs when the mechanical stirrer is not switched on (0 rpm). When the aqueous solution is stirred, an increase in the relative conversion rate is observed for the hydrogenolysis and hydrogenation reaction with a maximum at 1200 rpm, which is thus normed to 100 %. However, the two reactions show significantly different dependence on the stirring rate between 300 and 900 rpm.

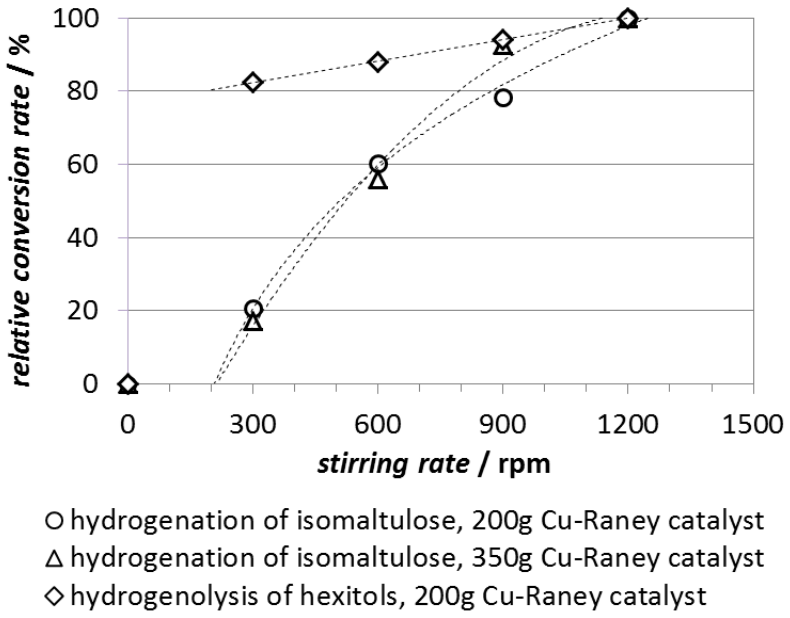

Figure 5-27: Effect of stirring rate on relative conversion rates for hydrogenation of isomaltulose (70 °C and 150 bar H_2) and hydrogenolysis of hexitols (180 °C and 150 bar H_2) using the same Cu-Raney catalyst. The hydrogenation reactions were compared based on conversion rates over 3 h reaction time as described in chapter 4.4, while the relative conversion rate for hydrogenolysis experiments was calculated based on the conversion after 5 h reaction time (see chapter 4.1).

The relative conversion rate for hydrogenolysis reactions decreases linearly to about 85 % at 300 rpm (**Figure 5-27**). In order to reproduce the measured values, four experiments at 600 rpm were performed with a ± 5 % deviation for the conversion rate. Hence, the linear decrease from 100 % at 1200 rpm to 85 % at 300 rpm is not significant. Linear regression should give a relative conversion rate of about 75 % at 0 rpm. However, since this is not the case, the relative turnover rate between 0 and 300 rpm has to decrease drastically.

In contrast, the relative conversion rate for hydrogenation reactions significantly decreases between 1200 and 300 rpm (with isomaltulose as a model compound for reducing sugars). A series of five experiments was carried out with different amounts of catalyst (about 200 and 350 g Cu-Raney) for reproducibility studies. **Figure 5-27** shows that the relative conversion rate is reduced to 60 % at 600 rpm and only about 15 to 20 % at 300 rpm. The hydrogenation of reducing sugars is decisively influenced by the mixing of the reactor which accords with results from Makkee *et al.* who studied the hydrogenation of fructose and glucose over silica-supported Cu [Makkee1985]. These effects are not influenced by the amount of catalyst. From these results we conclude that the rate limiting step for the hydrogenation reaction is the supply of H_2 and thus, the diffusion limitation. In contrast, the effect is much less pronounced for the hydrogenolysis of sugar alcohols. The rate limitation is probably attributed to comparatively slow -C-O- and -C-C- bond cleavage (**Figure 5-28**). In this context it has to be kept in mind that an increase of the hydrogenolysis rate by raising the reaction temperature above 180 °C is undesirable because side reactions to short-chain polyols are more pronounced.

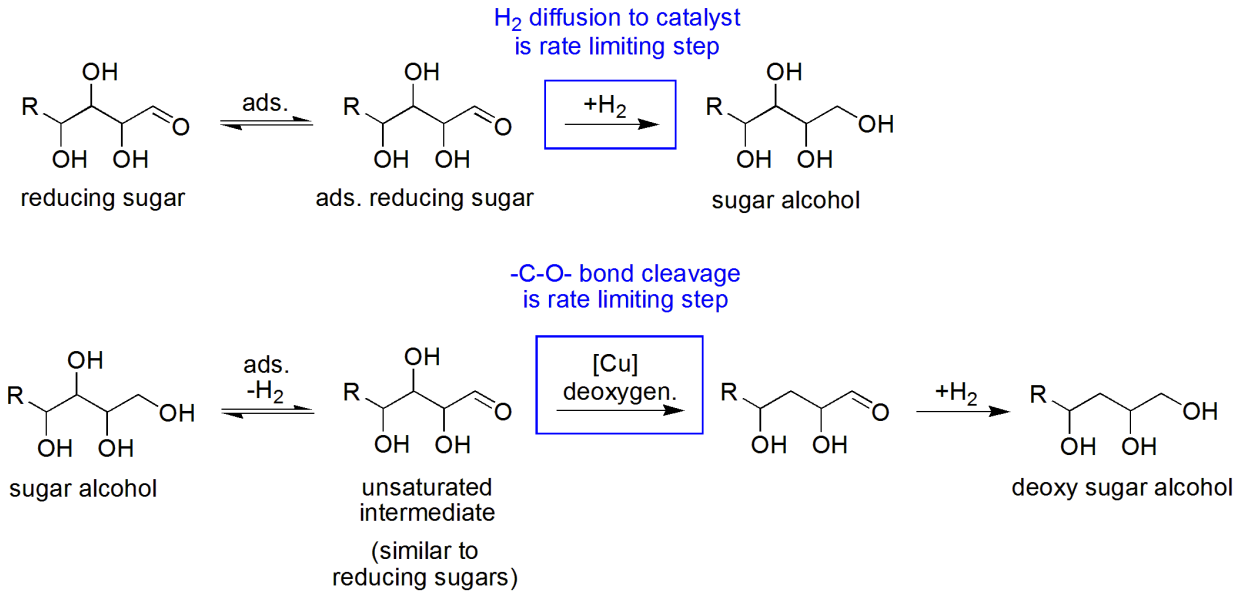

Figure 5-28: Comparison of rate limiting steps for the hydrogenation of reducing sugars to sugar alcohols and -C-O- bond cleavage of unsaturated intermediates (that show similar properties to reducing sugars) with subsequent hydrogenation.

CO_2 formation over Cu catalysts

The formation of CO_2 is another -C-C- bond cleavage reaction that needs to be re-duced in order to obtain high yields of deoxygenated C6 polyols from sugars. Significant amounts of CO_2 are only detected when polyols with a minimum of three adjacent OH-groups are used as reactant (type A). Based on these results we compared different possible routes for CO_2 formation that are initiated by dehydrogenation of the reactant. The presence of unsaturated products was validated by GC analysis, as well as isomerization of polyols, that occurs via these sp2-hybridized intermediates. CO_2 may result from one of three possible reaction pathways:

1. Decarboxylation from carboxylic acids at >180 °C [Furanix2012], in particular unstable 3-keto-acids [Kornberg1948]. Several 3-hydroxy-acids (aldonic acids) that potentially convert to 3-keto-acids via adsorption at the catalyst are detected.
2. Decarbonylation from aldehydes followed by water-gas shift reaction to CO_2.
3. Conversion of C6 polyols to methanol via -C-C- bond cleavage (e.g. by retro aldol reactions) with subsequent reforming of methanol to CO_2 [Palkovitz2014].

Multiple routes for the formation of 3-hydroxy-acids are possible in aqueous solution using a Raney-type Cu catalyst at temperatures up to 220 °C. And although Cu-Raney is a hydrogenation catalyst, it also possesses dehydrogenation properties [Berweiler2001, Berweiler2004]. The aldehyde intermediates on the catalyst surface are possibly hydrated to an acetal in aqueous solution with subsequent dehydrogenation to acids (path 1) similar to the methanol reforming mechanism (**Figure 5-29**). The conversion of aldohexoses, e.g. glucose, into sugar acids in the presence of hydroxide anions is also well-known (path 2) [deWit1978, deWit1981, Isbell1969]. Aldehyde intermediates show the same properties as reducing sugars and thus, are also possibly converted into sugar acids via this route because the auto-dissociation of water at 220 °C automatically leads to comparatively large amounts of hydroxide species. Furthermore carbonyl compounds are able to follow the Cannizzaro reaction to form carboxylic acids (path 3) [Wang1995]. Intramolecular reactions from β-keto-aldehydes are known for the formation of lactic acid [Manas2015] or saccharinic acids (monodeoxy aldonic acids) [Isbell1944]. Various acids (formic acid, acetic acid, and lactic acid) were also detected in our experiments along with saccharinic acids (**Figure 9-16** and **Figure 9-17** in the appendix). Such reactions are known to take place under H_2 atmosphere because the oxidation of the C1 carbon occurs via dehydrogenation and condensation over common hydrogenation catalysts [Deng2010]. In fact, gluconic acid is a known side product in glucose hydrogenation reactions [Arena1992].

On the other hand, decarbonylation of an aldehyde intermediate over Cu catalysts can be excluded as a degradation mechanism because the aldehydes, formed during adsorption over Cu, would give much higher yields of CO_2. Especially ethanediol and ethanol would show larger amounts of CO_2 because adsorption always leads to an aldehyde intermediate. However, for these compounds the yield of gaseous products is negligible (see **Figure 5-16** in chapter 5.1.3). The same is observed for methanol; barely any CO_2 is detected. Consequently, methanol reforming to CO_2 does not seem to occur over Cu as previously proposed by Palkovitz *et al.* [Palkovitz2014]. The degradation of sorbitol to CO_2 rather seems to follow one of the routes shown in **Figure 5-29** via an acid intermediate.

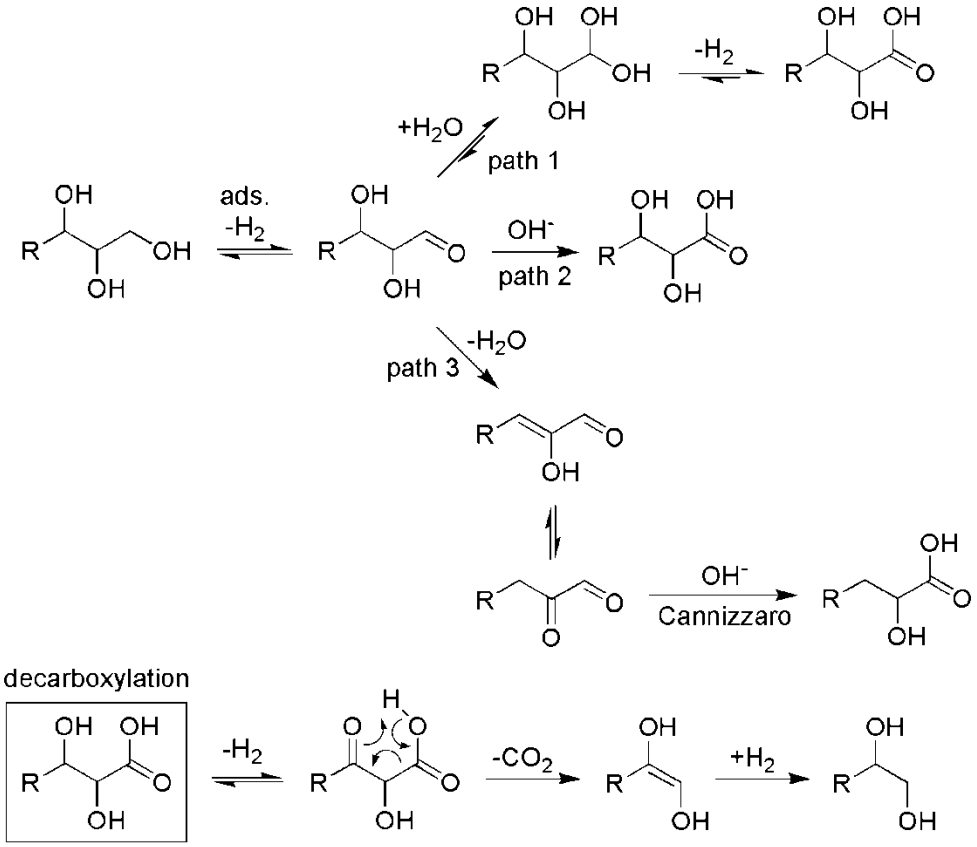

Figure 5-29: Formation of 2-hydroxy and 3-hydroxy (or 3-keto) acids and subsequent decarboxylation over Cu.

Decarboxylation is most likely to occur via 3-hydroxy or rather 3-keto acids that are obtained from an additional dehydrogenation step over Cu. The mechanism for the cleavage of the terminal -C-C- bond resembles the retro aldol reaction. Test experiments with gluconic acid as reactant confirm significant carbon loss due to formation of large amounts of CO_2 (**Figure 5-30**). The acid seems to be more reactive towards degradation. In comparison to mannitol and sorbitol much more CO_2 is formed after 5 h reaction time (220 °C and 150 bar H_2). Hence, sugar acids formed from mannitol and sorbitol in side reactions will be rapidly converted to CO_2.

Based on these results we conclude that CO_2 formation from sugar alcohols and glycerol over Cu based catalysts occurs via decarboxylation from sugar acids. This accords very well with the known and fast decarboxylation of the "sugar acid" FDCA (2,5-furan-dicarboxylic acid) at temperatures above 180 °C [Furanix2012].

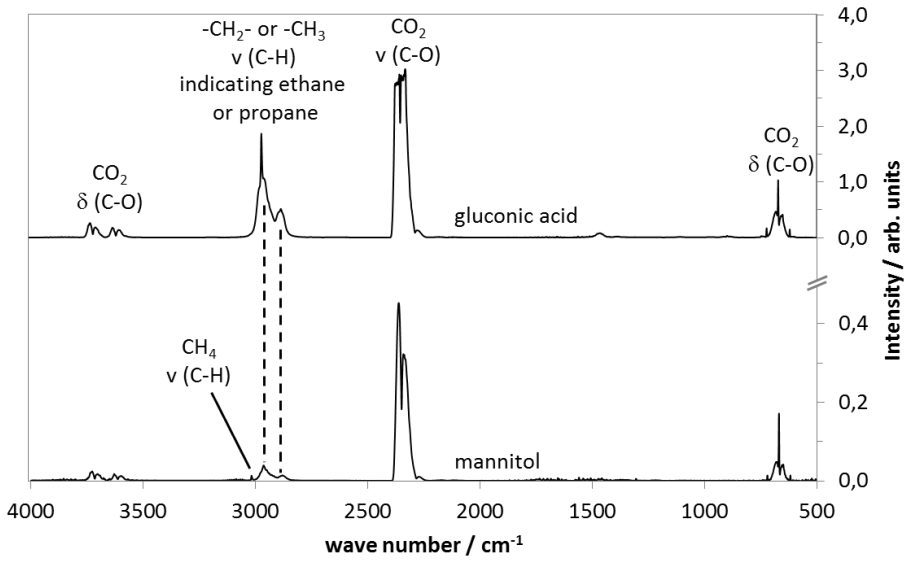

Figure 5-30: IR spectra of the gas phase composition for hydrogenolysis reactions of mannitol and gluconic acid on Cu/Al_2O_3 at 220 °C, 150 bar H_2 and 5 h reaction time.

5.1.5. Selective -C-C- bond cleavage over Ru catalysts

In contrast to Cu based catalysts, Ru primarily catalyzes hydrogenolysis of terminal -C-C- bonds when the terminal backbone carries an OH-group. Another difference to Cu catalysts is that the hydrogenolysis reactions do not show a strong dependence on the arrangement of the OH-groups within the reactant. Almost all reactants with two adjacent (or isolated) OH-groups are readily converted, e.g. glycerol and all other polyols with three or more adjacent OH-groups (**Table 5-2**). This is in agreement with a detailed mechanistic study on different sugar alcohols by Palkovitz *et al.* [Palkovitz2015]. Rapid decarbonylation was found to be the main reaction pathway for all reactants. Additionally, deoxygenation of terminal OH-groups via the E2 mechanism (see **Figure 3-8** in chapter 3.1.2) was shown to be a side reaction. However, reaction intermediates with different amounts of methylene groups (1,2,4-butanetriol or 1,2,6-hexanetriol) were not investigated. In table 2, the comparison of such compounds is shown according to similarities in the arrangement of OH-groups. All hydroxy compounds with a terminal OH-group show conversions between 70 and >99 %. Polyols with a C6 carbon chain (mannitol, the 1,2,3,4,5-hexanepentol, and 1,2,6-hexanetriol) give the highest conversion of 93 to >99 %.

Hence, in contrast to Cu the conversion over Ru does not correlate to the number of OH-groups in the reactant but rather the carbon chain length. Furthermore, C2 to C4 glycols (ethanediol, 1,2-propanediol, and 1,2-butanediol) show practically identical behavior with 70 % conversion each, while 2,3-butanediol does not comprise of terminal OH-groups and therefore shows significantly lower conversion (15 %). The same applies for the cyclic isosorbide but the effect is less pronounced (59 % conversion). Consequently, polyols with terminal OH-groups are more readily converted due to fast decarbonylation.

Table 5-2: Reactivity of various polyols and alcohols over Ru/Al_2O_3 (100 mL catalyst basket which equals about 140 g of catalyst; 500 ml of an 7.5 wt-% aqueous solution which equals about 42.5 g of each reactant) at 180 °C, 150 bar H_2. The reaction time was 2,5 h for 1,2,6-hexanetriol and 5 h for all other reactants.

Structure	Reactant	X / %	$Y_{c,liq}$ / %	$Y_{c,loss}$ / %	**Reactivity of polyols**
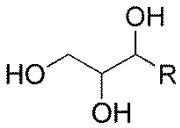	**Three or more adjacent OH-groups (type A)**				
	Mannitol	93	41	59	very high
	1,2,3,4,5-hexanepentol	96	26	74	very high
	Glycerol	74	34	66	high
	Two adjacent OH-groups (terminal, type B)				
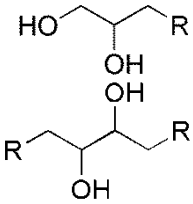	1,2,6-hexanetriol	100	34	66	very high
	1,2-butanediol	70	30	70	high
	1,2-propanediol	72	30	70	high
	Ethanediol	72	29	71	high
	Two adjacent OH-groups (middle of molecule, type C)				
	2,3-butanediol	15	85	15	low
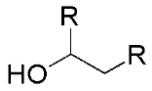	**Other polyols (type D)**				
	1,3-propanediol	74	27	73	high
	Isosorbide	59	43	57	moderate

This finding correlates with the large amounts of volatile C1 products (CO_2 and CH_4) obtained for all hydroxy compounds that comprise of terminal OH-groups. The carbon loss ($Y_{c,loss}$ / %) in **Table 5-2** accounts mainly for these gaseous products, along with trace amounts of mono alcohols such as ethanol and methanol. As the GC method does not allow the detection of mono alcohols, these products were detected and quantified separately by additional headspace analysis. The gas phase composition for the model compounds glycerol, ethanediol (ethylene glycol), ethanol and methanol is shown in **Figure 5-31** and practically identical. The only difference is the lack of CO_2 when methanol was used as reactant. We attribute this to direct conversion of methanol to methane by -C-O- bond cleavage.

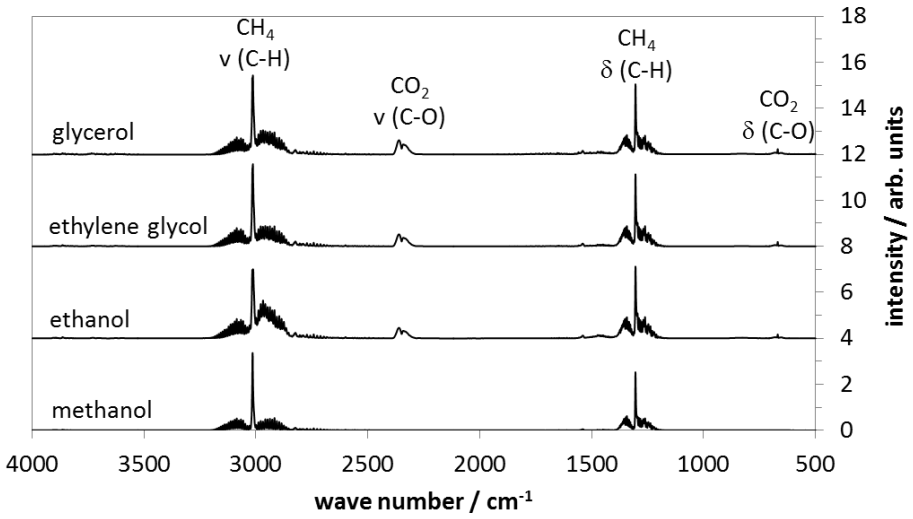

Figure 5-31: IR spectra of the gas phase composition for hydrogenolysis reactions of methanol, ethanol, ethanediol and glycerol over Ru/Al_2O_3 at 180 °C, 150 bar H_2 and 5 h reaction time.

The comparison of different reactants over supported Ru shows that all hydroxy compounds with a terminal OH-group are degraded via decarbonylation with subsequent water-gas shift reaction to CO_2. Successive -C-C- bond cleavage of terminal hydroxymethyl groups (-C-OH) is the main reaction pathway. However, with these results alone it is not possible to determine which -C-C- bond is preferably broken if both carbon backbones in the polyol carry an OH-group. For this purpose we studied the hydrogenolysis of 1,2,6-hexanetriol, as well as 1,2- and 2,3-butanediol with a focus on reaction intermediates that finally lead to CO and CH_4.

Ru catalyzed decarbonylation of 1,2,6-hexanetriol

The metal-catalyzed decarbonylation was investigated using the model compound 1,2,6-hexanetriol with both an isolated and a vicinal terminal OH-group. Adsorption of alcohols and polyols over Ru occurs primarily via one terminal OH-group [Deutsch2012, Hibbitts2015, Palkovitz2015]. The initiating equilibrium step is the formation of an aldehyde species by dehydrogenation. These unsaturated species on the catalyst surface (C-C=O) formed enable -C-C- bond cleavage by formation of CO. Using 1,2,6-hexanetriol as model compound allows to study if decarbonylation occurs preferably at the isolated or vicinal terminal hydroxymethyl group (-C-OH). It is important to note that a 1,2,6-arrangement of OH-groups does not allow retroaldolization. Therefore, this mechanism can be excluded.

Our results show that the first decarbonylation only occurs at the isolated hydroxymethyl group (6-position). 1,2-pentanediol is found as the major product in the liquid phase, whereas no traces of the 1,5-isomer are detected (**Figure 5-32**). This allows a clear distinction between the three possible -C-C- bond cleavage reactions next to a -C-OH group.

- C1/C2 scission via decarbonylation would lead to 1,5-pentanediol and a C1-fragment (upper path).
- C2/C3 scission produces ethanediol and n butanol (lower path).
- Decarbonylation of the isolated OH-group between the C5/C6 carbon leads to 1,2-pentanediol and a C1-compound (middle path).

The lack of ethanediol or 1,5-pentanediol leads to the conclusion that -C-C- bonds with an isolated hydroxymethyl group (-C-C-OH) are preferably cleaved. This is in agreement with high decarbonylation activity for conversion of alkanols over a Ru based catalyst [Hibbitts2015]. A terminal carbonyl group (-C=O) weakens the adjacent -C-C- bond which results in the high preference of decarbonylation compared to -C-C- bond cleavage in the middle of the molecule. 1,2-pentanediol then follows the same reaction pathway with cleavage of the terminal -C-C- bond to form *n*-butanol and another C1-fragment. C2/C3 scission can be excluded as no traces of ethanediol are found, even at an extended reaction time. The final product is the hydrocarbon propane, which is stable towards further degradation over Ru under applied reaction conditions and detected with IR analysis.

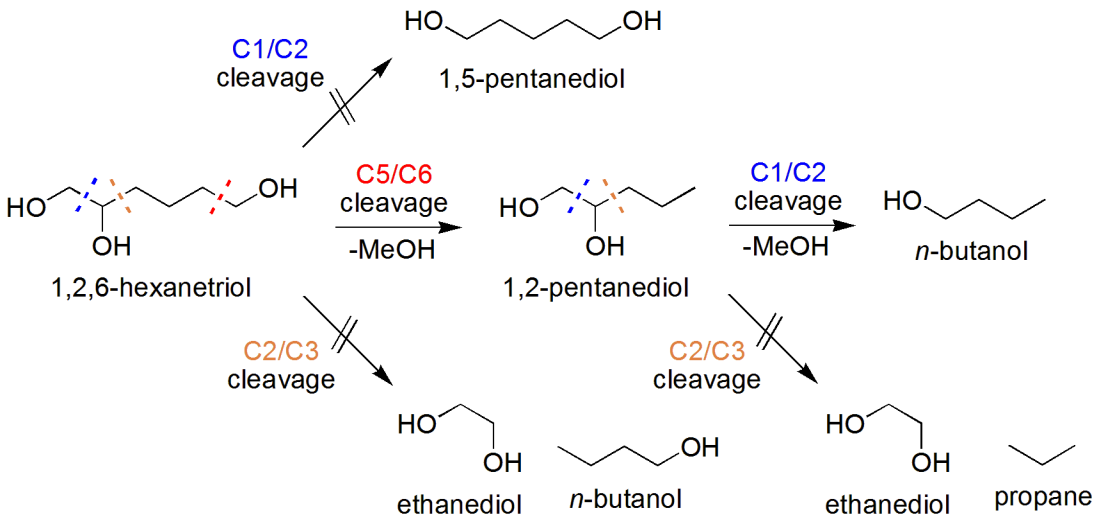

Figure 5-32: Comparison of metal-catalyzed -C-C- bond cleavage reactions as found for hydrogenolysis of 1,2,6-hexanetriol over Ru/Al_2O_3 at 180 °C and 150 bar H_2.

Ru catalyzed decarbonylation of 1,2- and 2,3-butanediol

Another comparison regarding the selectivity for -C-C- bond cleavage reactions is performed using 1,2- and 2,3-butanediol as reactants. The latter does not contain any terminal OH-groups and is hence unable to form an aldehyde (terminal carbonyl group). Consequently the -C-C- bond in the middle of the molecule is expected to be cleaved first (**Figure 5-33**) which is less favorable as shown for 1,2,6-hexanetriol. In a second step the resulting ethanol is degraded following subsequent decarbonylation to CH_4 and CO which is hydrogenated to also form CH_4. Thus, methane is the only final volatile C1 product when 2,3-butanediol is the reactant (**Figure 5-34**).

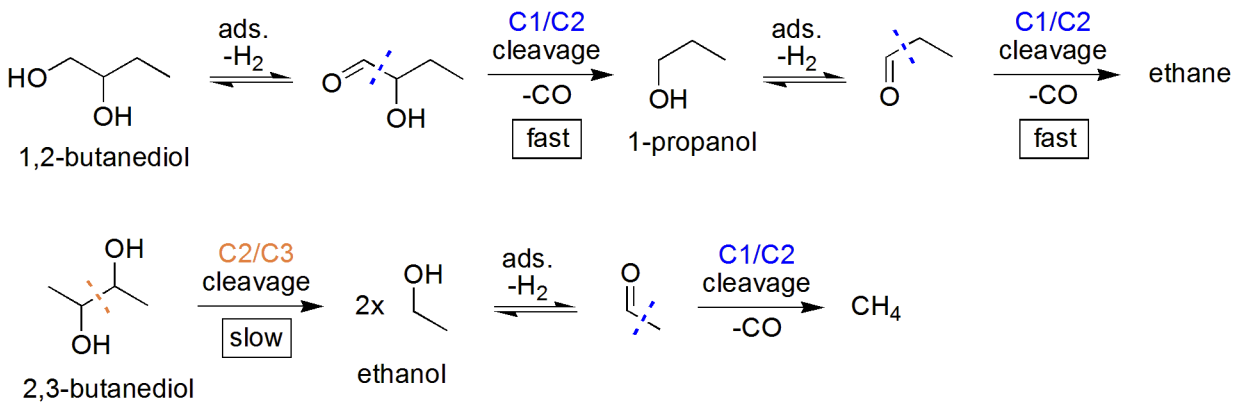

Figure 5-33: Comparison of metal-catalyzed -C-C- bond cleavage reactions in dependence of hydroxyl groups as found for hydrogenolysis of 1,2- and 2,3-butanediol on Ru/Al_2O_3 at 180 °C and 150 bar H_2.

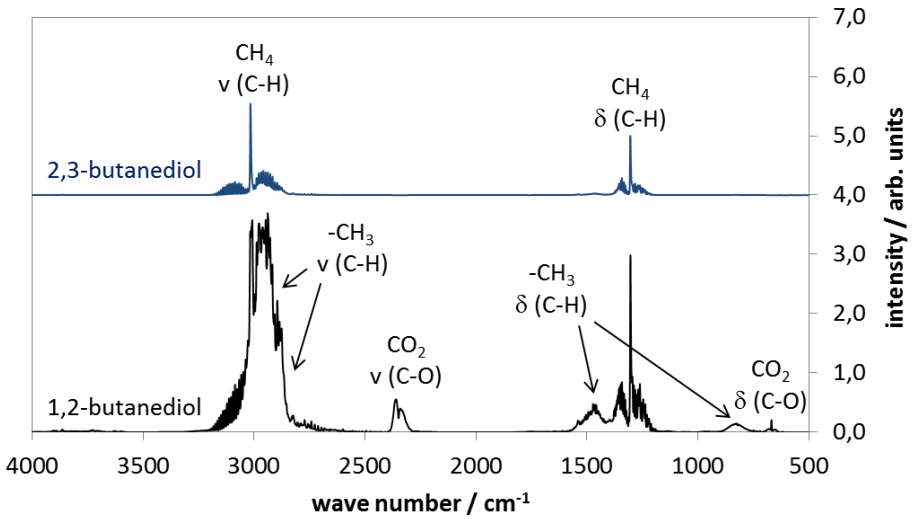

Figure 5-34: IR spectra of the gas phase composition for hydrogenolysis reactions of 1,2- and 2,3-butane diol over Ru/Al_2O_3 at 180 °C, 150 bar H_2 and 5 h reaction time.

In contrast to 2,3-butanediol, the stereo isomer 1,2-butanediol is able to degrade along the decarbonylation mechanism right away and gives much greater amounts of methane (**Figure 5-34**). Decarbonylation of 1,2-butanediol finally results in the formation of ethane after the second -C-C- bond cleavage step (the methyl groups of ethane are visible in the IR spectra). The hydrocarbon is again stable towards further degradation over Ru, similar to formation of propane from 1,2,6-hexanetriol hydrogenolysis. Consequently, the -C-C- bond next to a terminal hydroxymethyl group (-C-C-OH) is preferably cleaved over a -C-C- bond next to a hydroxymethyl group in the middle of the molecule.

Methane formation over supported Ru

The degradation of polyols and mono alcohols over Ru follows decarbonylation to CO with two potential reaction pathways leading to the final product CH4.

- Direct hydrogenation of CO to CH_4 (and other hydrocarbons) [Kellner1981].
- Conversion of CO to CO_2 following the water-gas-shift reaction that significantly favors the thermodynamically more stable CO_2 at the conditions chosen (180 °C and 150 bar H_2).

A catalytic route to CO_2 via retroaldolization of polyols to methanol with subsequent reforming is also described [Montassier1988, Nielsen2013, Palkovitz2012]. However, no CO_2 was found when methanol is used as reactant. This indicates that methanol is directly converted to methane by -C-O- bond cleavage. In contrast, the IR spectra for ethanol, ethanediol and glycerol are virtually identical (as was shown in **Figure 5-31**) and show small amounts of CO_2 next to large amounts of CH_4. This is a clear indication that methane is produced from CO_2. Hence, CO originates from decarbonylation of the polyols as the main reaction pathway and converts to CO_2, which is finally hydrogenated to methane (CH_4).

These results for decarbonylation over Ru are in agreement with mechanistic studies on the Ru catalyzed hydrogenolysis of alkanols [Hibbitts2015] and polyols [Palkovitz2015]. Interestingly, CO_2 is not mentioned as a volatile product in any of the studies. In contrast, we did not detect CO and only found CO_2 as the second volatile gaseous product besides CH_4. We conclude that CO is both directly hydrogenated to CH_4 and converted to the thermodynamically more stable CO_2 via the water-gas shift reaction (**Figure 5-35**). All reactants, mono alcohols (with the exception of methanol) and polyols are able to follow this reaction pathway. We studied the influence of the reaction temperature on the CO_2 formation and hydrogenation to CH_4 (**Figure 5-36**). Both reactions have to be much faster than decarbonylation as no traces of CO were detected in any experiment. At 160 °C only CH_4 was detected

whereas at higher temperatures an increasing amount of CO_2 was found. The lack of CO_2 at 160 °C may be explained by a higher rate for CO hydrogenation to CH_4 than CO conversion to CO_2. The shift reaction should also already occur at 160 °C as Ru catalysts are known to convert CO to the thermodynamically favored CO_2 at such temperatures [Ford1977, Ford1979, Ford1981]. Thus, hydrogenation of CO to CH_4 over alumina-supported Ru has to be even faster than the shift reaction. At 180 °C and higher temperatures, the water-gas shift reaction rate is enhanced and CO is then not only hydrogenated to CH_4 but preferably converted to CO_2. This effect is clearly visible by increasing CO_2 amounts as shown in **Figure 5-36**.

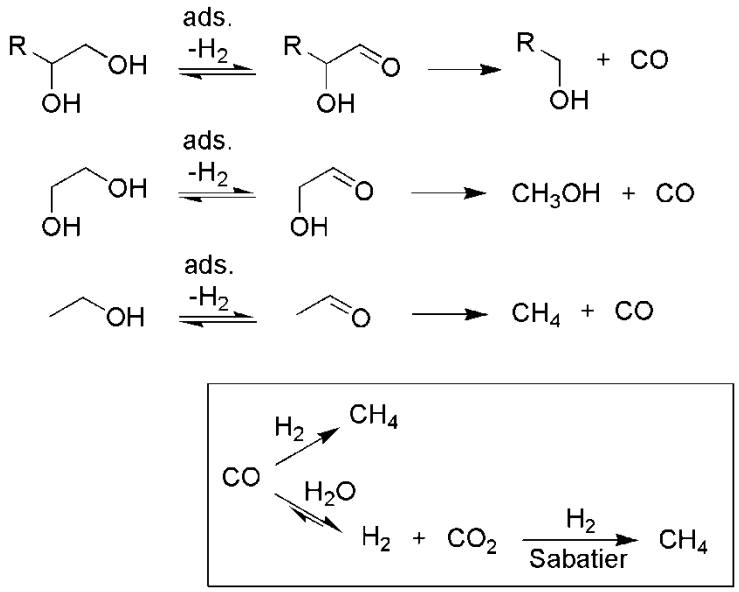

Figure 5-35: Degradation reactions for ethanol, ethylene glycol and larger polyols following decarbonylation to CO with subsequent hydrogenation to methane or conversion to CO_2.

The reaction temperature obviously has a strong effect on the rate of decarbonylation, hydrogenation and the CO_2 formation. The controversial reports in the literature about either possible shift of CO to CO_2 [Deutsch2012] or the lack of CO_2 [Palkovitz2015] using a Ru/C catalyst seem to depend on the applied reaction temperature. Deutsch *et al.* performed all reactions at temperatures between 205 to 240 °C [Deutsch2012], whereas the mechanistic study of Palkovitz *et al.* was conducted at 150 °C [Palkovitz2015]. In order to test for this hypothesis, we converted sorbitol at 150 °C and 60 bar H_2 using also a Ru/C catalyst and did not detect CO_2 similar to the published results from Palkovitz *et al.* Consequently, the lack of CO_2 [Palkovitz2015] is probably attributed to the lower reaction temperature. Therefore, the reaction mechanism should be the same in both Palkovitz's and Deutsch's proposed reactions and the detection of CO_2 is not related to another degradation pathway. Instead it rather depends on the temperature-dependent shift of CO to CO_2 and hydrogenation to CH_4.

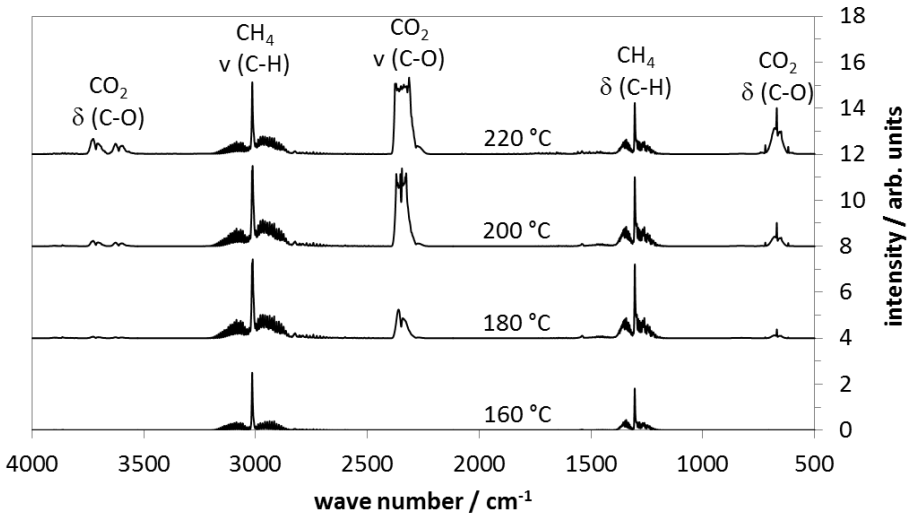

Figure 5-36: IR spectra of the gas phase composition for hydrogenolysis reactions of mannitol over Ru/Al_2O_3 dependent on reaction temperature at 150 bar H_2 and 5 h reaction time.

5.2. Downstream-processing

Two downstream-processes are investigated for the separation of deoxy C6 polyols and undesired short-chain polyols (side products). First, the purification of sugars and sugar alcohols using ion-exchange chromatography over functionalized resins is studied. Afterwards, the potential of liquid-liquid extraction with organic solvents is evaluated utilizing the different polar characteristics of deoxy C6 polyols (comprising of nonpolar methylene groups) and short-chain polyols.

5.2.1. Ion-exchange chromatography

Separating deoxy C6 polyols and short-chain polyols, e.g. glycols and glycerol, over functionalized resins seems promising because the different molecular structures will probably interact differently with the resin and thus, result in a good separation. The following parameters are studied using model compounds and the real product mixture after hydrogenolysis of sugar alcohols:

1. Loading of the resin with or Ca^{2+} ions
2. Dimensioning of the chromatography column (height/diameter ratio)
3. Flow rate

The evaluation of the column functionalization is performed using a Dowex99/320 resin in the Ca^{2+}-form and H^{+}-form, respectively (after washing the Ca^{2+}-resin with two equivalents of chloric acid to obtain the H^{+}-form). **Figure 5-37** shows that the Ca^{2+}-functionalized column is not suitable for the separation of the polyol mixture because all products are eluted similarly over a broad range. On the other hand, the H^{+}-resin clearly shows different retention times for the different products (**Figure 5-38**). In particular, the different deoxy C6 polyols are separated according to the number of remaining OH-groups in descending order. Hexanepentols are eluted first with a maximum concentration at 135 min, indicating that the interactions with the resin are the weakest. Afterwards, hexanetetrols are eluted with a maximum concentration at 155 min retention time. Hexanetriols are retained much longer than the other deoxy C6 compounds (maximum concentration at 185 min) and thus, seem to interact much stronger with the resin. A significant retardation due to strong binding to the resin could be explained by nonpolar interactions of the methylene groups with the nonpolar resin material (polystyrene). Also, the hydrate shell of the different deoxy C6 polyols should increase with the number of OH-groups which potentially enhances the diffusion through the packed material. This would also account for glycerol and glycols, comprising of three and two OH-groups, respectively. Hence, the hydrate shell of glycerol is larger and glycerol is eluted much earlier than glycols indicating that the hydrate shell of polyols is significant for interactions with the column.

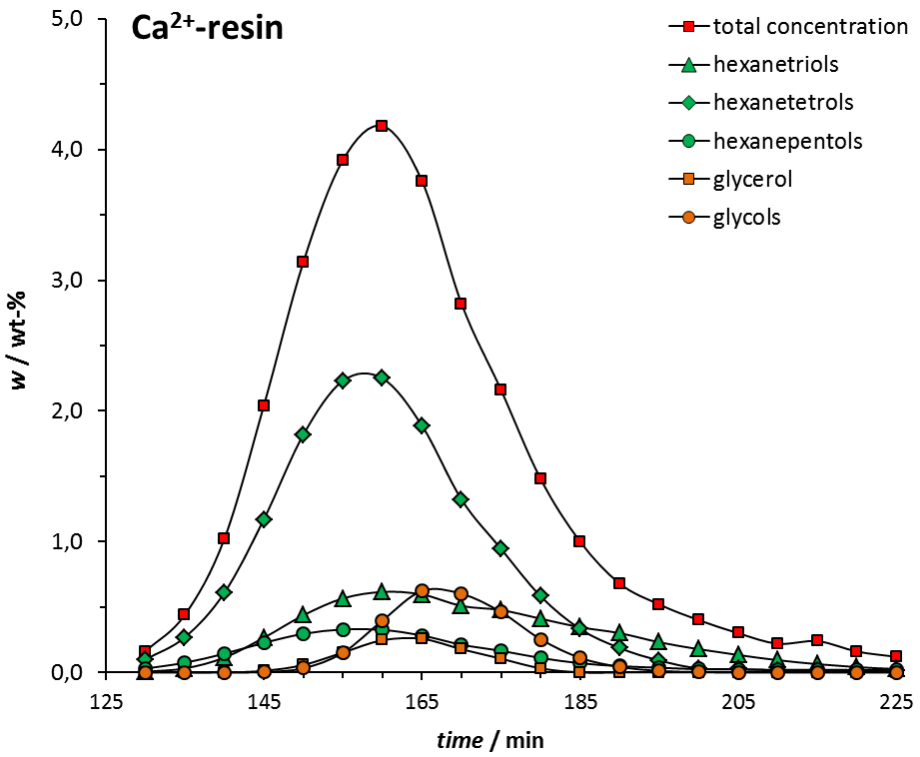

Figure 5-37: Chromatographic separation of a polyol mixture, obtained from hydrogenolysis of hexitols over Cu-Raney, using a Dowex99/320 resin in the Ca^{2+}-form at 60 °C and a flow rate of 10 mL/min. The quantity of polyols is 16 g and the column dimensions are: 96 cm packed height and 5 cm diameter.

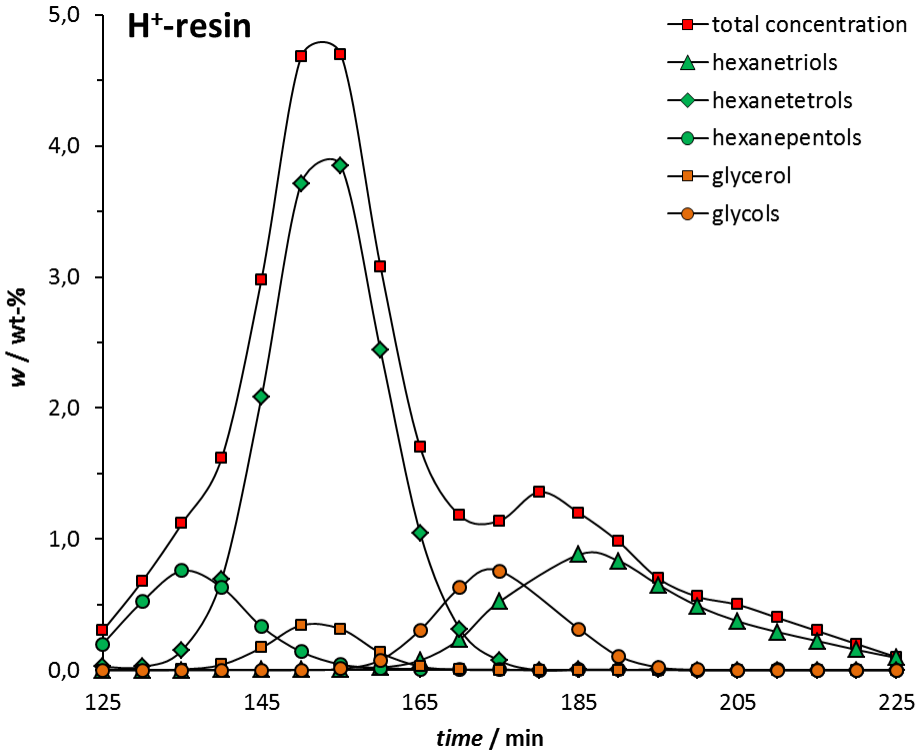

Figure 5-38: Chromatographic separation of a polyol mixture, obtained from hydrogenolysis of hexitols over Cu-Raney, using a Dowex99/320 resin in the H^{+}-form at 60 °C and a flow rate of 10 mL/min. The quantity of polyols is 16 g and the column dimensions are: 96 cm packed height and 5 cm diameter.

It is important to note that for a potential technical application the two bands for hexanepentols and glycerol can be neglected because full conversion over Cu-Raney leads to compounds with two vicinal OH-groups and adjacent methylene or methyl groups (see reaction mechanism in chapter 5.1.3). Hence, only the bands of hexanetetrols (mainly consisting of the 1,2,5,6-isomer), hexanetriols and glycols will be left which simplifies the chromatography.

One parameter to enhance this process is the optimization of the column temperature. **Figure 5-39** shows that a temperature optimum is found at 60 °C. Increasing the column temperature from 40 to 60 °C clearly sharpens the bands and counteracts the co-elution. The chromatogram at 40 °C seems to display one major fraction with significant "tailing". Hexanetetrols and glycerol are eluted at the same time and mainly account for this first fraction of products. At 60 °C the second band/fraction, which mainly consists of hexanetriols, becomes visible.

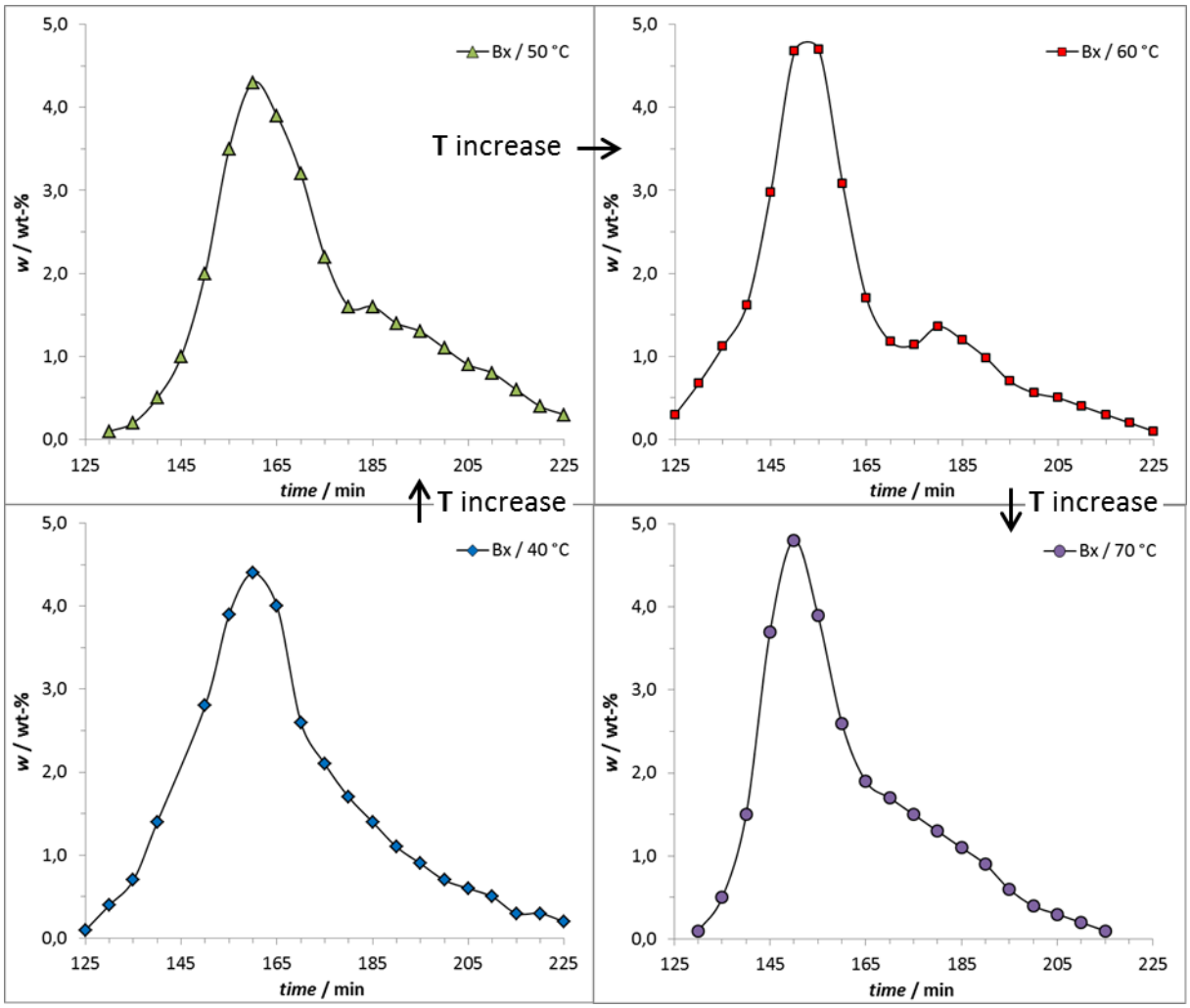

Figure 5-39: Effect of the column temperature on the chromatographic separation of a polyol mixture, obtained from hydrogenolysis of hexitols over Cu-Raney, using a Dowex99/320 resin in the H^+-form at a flow rate of 10 mL/min. The quantity of polyols is 16 g and the column dimensions are: 96 cm packed height and 5 cm diameter. The temperature are: 40 °C (bottom left), 50 °C (top left), 60 °C (top right), and 70 °C (bottom right).

The separation of these products noticeably improves at higher temperature. However, at 70 °C the chromatogram resembles more the separation at 40 °C. We attribute this to degassing because the glass column showed significant amounts of gaseous bubbles with a diameter of up to 8 mm throughout the packed column.

Another parameter to improve the separation is the column geometry. If the chromatographic column (100 cm / 5 cm) is lengthened at the expense of the diameter (300 cm / 2.5 cm), the separation deteriorates significantly although the amount of resin, flow rate and temperature stay the same (**Figure 5-40**). While both experiments are carried out at 60 °C the chromatogram when using the long and narrow column looks more like the separation at 40 °C as shown in **Figure 5-39**. There seems to be only one fraction with very strong "tailing". We attribute this to undesired wall effects that cause back mixing and consequently counteract the separation.

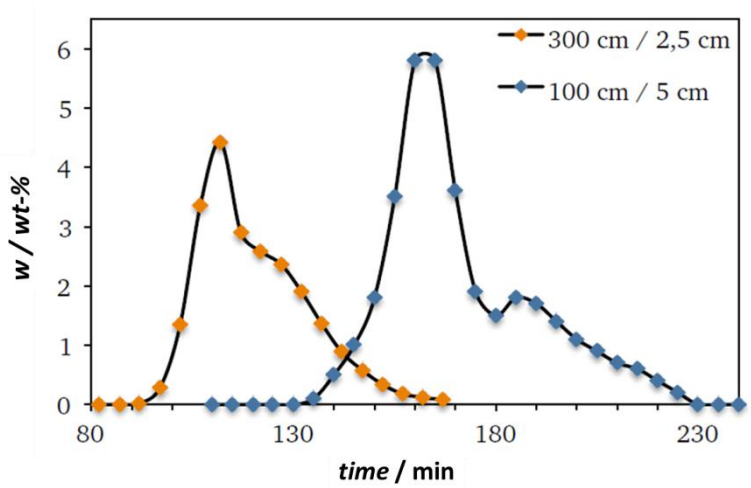

Figure 5-40: Effect of the column dimensions (height/diameter ratio) on the separation of a "real" polyol mixture as obtained from the hydrogenolysis of hexitols. The column is heated to 60 °C and filled with the same Dowex resin in the H^+-form as described in the previous experiments. The flow rate was 10 mL/min in both experiments.

The effect of the column temperature and column capacity is also further studied with the model compounds glycerol and 1,2,6-hexanetriol because they precisely represent one of each major bands fractions (**Figure 5-38**). As glycerol elutes similar to the 1,2,5,6-hexanetetrol the results can also be transferred to better understand the separation between hexanetetrols and -triols. The comparison of the chromatograms for the pure compounds and polyol mixtures shows that the retention times are not affected by the presence of other polyols (**Figure 5-41**). Also, a base line separation between the two compounds is visible which means that the separation is ideal. When the quantity of the injected polyol mixture is approximately doubled from 15.8 to 32.5 g the two compounds cannot be separated adequately because co-elution occurs at a retention time of 170 min. The maximum capacity of the column seems to be already achieved at the starting point of the experiments.

A discontinuous single-column chromatography no longer enables a base line separation and thus, for the purification of 1,2,6-hexanetriol a multi-column process such as simulated-moving-bed (SMB) chromatography would be necessary. Interestingly, glycerol shows much more pronounced "tailing" when the quantity of the injected sample is doubled whereas the shape of the 1,2,6-hexanetriol band is the same. Increasing the temperature of the column from 50 to 60 °C, and finally 70 °C, also has no effect on the shape of the 1,2,6-hexanetriol band. However, glycerol starts to show "fronting" at 70 °C and an overall shift to longer retention times. At 50 °C a maximum of 5.5 wt-% is observed at 140 min, which is moved to about 155 min at 70 °C (**Figure 5-41**).

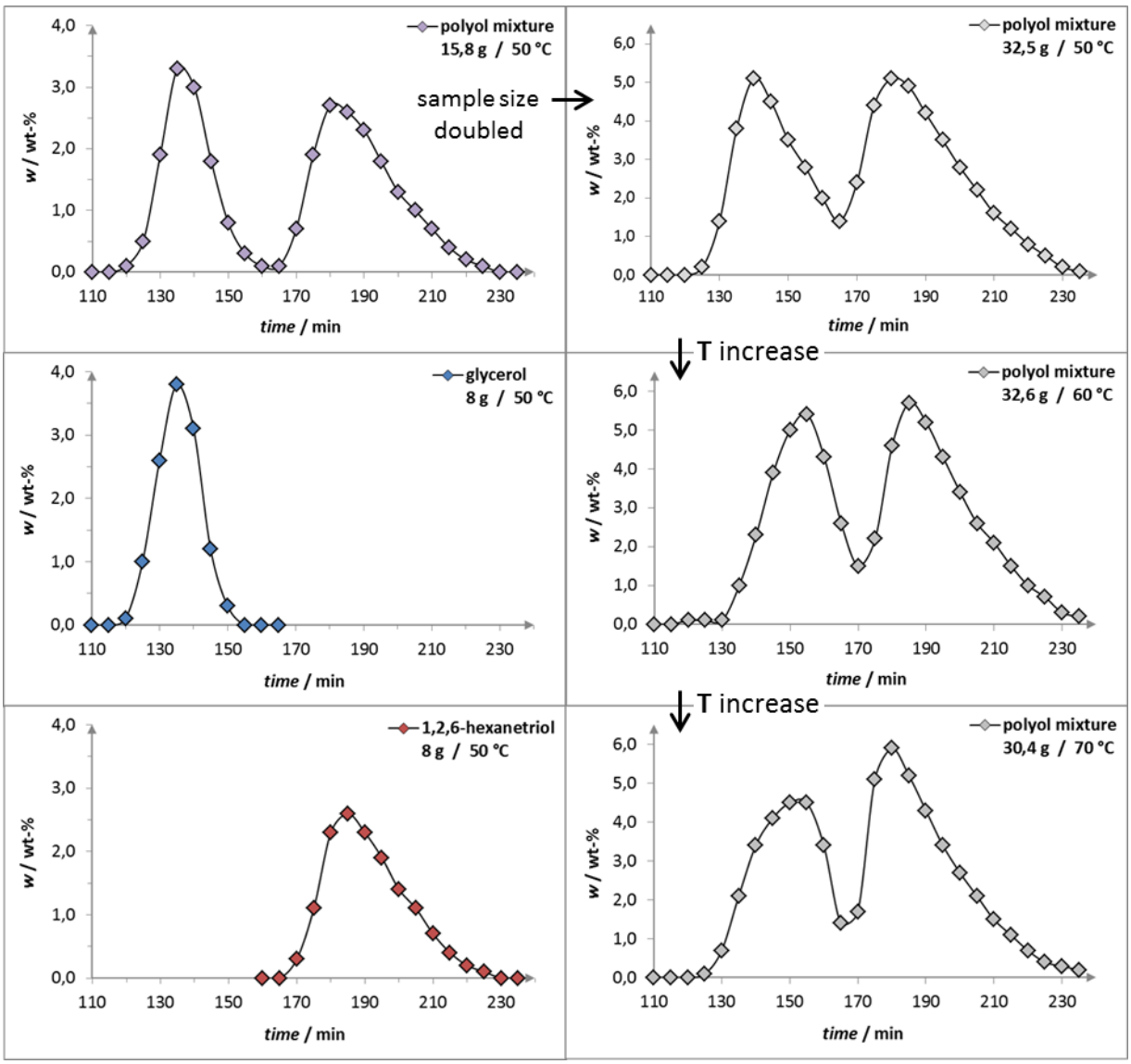

Figure 5-41: Chromatogram of pure 1,2,6-hexanetriol at 50 °C (bottom left), pure glycerol at 50 °C (center left), and a 1,2,6-hexanetriol/glycerol mixture at 50 °C (top left). The quantity of each polyol is 8 g in both the pure solution and mixture (adding to combined 15.8 g). Chromatogram of 1,2,6-hexanetriol/glycerol solutions with a doubled sample size at 50 °C (top right), 60 °C (center right), and 70 °C (bottom right). The flow rate was 10 mL/min in all experiments.

Hence, the improvement of polyol separations by increasing temperature is a limited effect. The co-elution of both model compounds, glycerol and 1,2,6-hexanetriol, cannot be prevented by simply raising the temperature form 50 to 70 °C.

Figure 5-42 shows that the flow rate in the chromatography column has a much greater impact on the separation of these polyols. The reduction of the flow rate leads to a significant optimization of the separation. Three separated bands (fractions) instead of one fraction with strong "tailing" are visible when the flow is changed from 10 mL/min to 1.25 mL/min. Lower flow rates result in a better separation and no negative effects regarding longitudinal diffusion are observed.

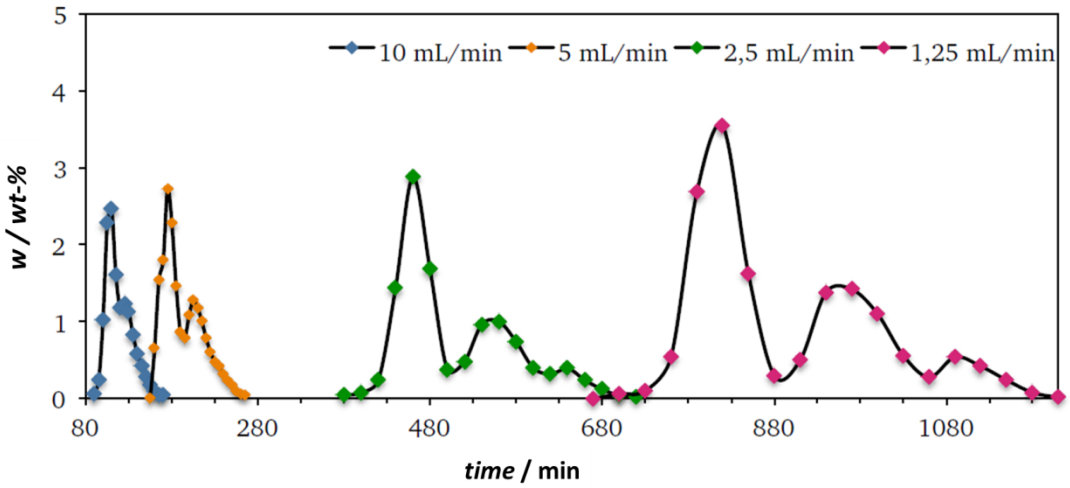

Figure 5-42: Effect of the flow rate on the separation of a "real" polyol mixture as obtained from the hydrogenolysis of hexitols. The column (300 cm height / 2.5 cm diameter) is heated to 60 °C and filled with the same Dowex99/320 resin in the H^+-form as described in the previous experiments.

5.2.2. Extraction of deoxygenated polyols

In addition to chromatographic separation, the purification of deoxy C6 polyols from a C3/C6 polyol mixture (using model compounds) is evaluated using liquid-liquid extraction with non-soluble polar organic solvents, e.g. linear mono alcohols. The hydrophily of deoxy C6 polyols decreases with each -C-O- bond cleavage and the hydrophobic character increases with the number of nonpolar methylene groups. Hence, desired products such as 1,6-hexanediol and 1,2,6-hexanetriol should be possibly extracted from a polyol mixture with short-chain diols (e.g. glycerol) because glycerol and similar compounds do not comprise of nonpolar carbon atoms. Solvents that consist of polar OH-groups and a nonpolar linear carbon chain, e.g. 1-butanol, 1-pentanol, and 1-hexanol seem promising for this approach (**Figure 5-43**).

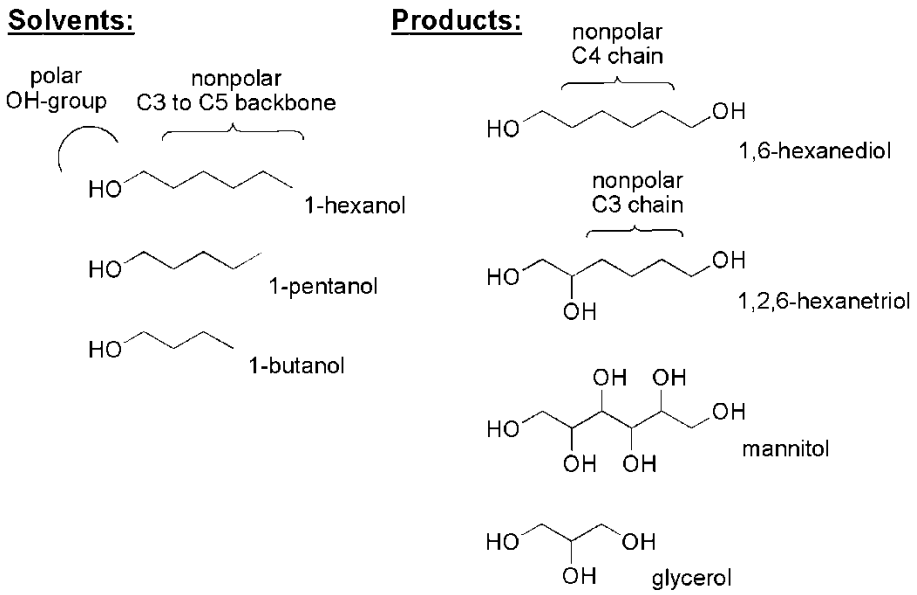

Figure 5-43: Molecular structure of deoxy C6 polyols (model compounds) and undesired glycerol / mannitol, as well as promising solvents (extractants: 1-butanol to 1-hexanol).

The results for the selective extraction of deoxy C6 polyols from complex polyol mixtures using linear mono alcohols are shown in **Figure 5-44** and **Figure 5-45**, respectively. **Figure 5-44** shows that the distribution coefficient for 1,6-hexanediol increases linearly with the concentration of the organic solvent (linear mono alcohol) in the alcohol/water mixture. This effect is much more pronounced for 1-butanol compared to 1-pentanol and 1-hexanol. The distribution coefficient for 1,6-hexanediol in 1-butanol decreases from 3.3 at 60 wt-% to 2.3 at 25 wt-%. In comparison, the distribution coefficient for 1,6-hexanediol in 1-pentanol is only reduced from 2.7 at 60 wt-% to 2.5 at 25 wt-%. Hence, 1-pentanol is more suitable for the extraction of 1,6-hexanediol when the solvent concentration in the alcohol/water mixture is below 33 wt-%. Similar to 1-pentanol, the extraction of 1,6-hexanediol with 1-hexanol is also only marginally affected by the concentration of the solvent in the separation funnel. Furthermore, it is desirable that 1-pentanol and 1-hexanol show an increasing affinity for the extraction of 1,2,6-hexanetriol at low solvent concentrations. The two solvents also perform only negligible extraction of the undesired polyols glycerol and mannitol. The distribution coefficients for these two compounds are below 0.1 in all experiments and only marginally affected by the solvent concentration in the alcohol/water mixture (**Figure 5-45**). In contrast, 1-butanol extracts about three times more of these undesired polyols. This effect is most pronounced when only comparatively low concentrations of the solvent (below 33 wt-%) are used for the extraction in a separation funnel. The distribution coefficient for glycerol and mannitol significantly decreases when the ratio for 1-butanol in the alcohol/water mixture is raised.

Based on these results 1-butanol seems promising the selective extraction of 1,6-hexanediol from an aqueous solution when a high ratio of solvent/water (60 wt-% 1-butanol / 40 wt-% water) is applied. However, from an economical and sustainable point of view the amount of organic solvent should be as low as possible in an extraction process. In this context 1-pentanol is most suitable because it exhibits the highest distribution coefficients for 1,6-hexanediol at low solvent concentration (**Figure 5-44**) and only negligible extraction of glycerol and mannitol (**Figure 5-45**). 1-hexanol is also suitable, but shows an overall lower affinity for the extraction of polyols. This is probably related to the longer nonpolar carbon chain.

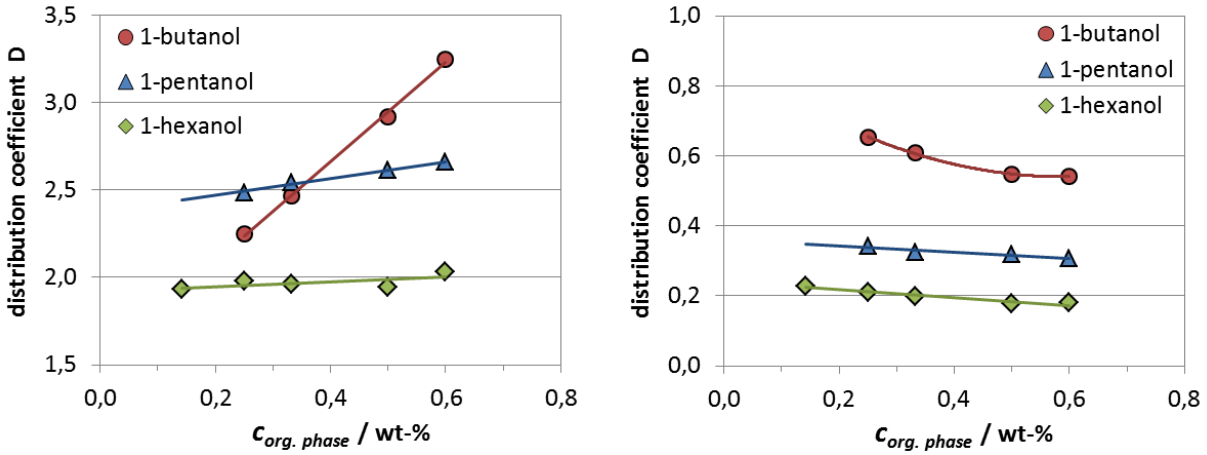

Figure 5-44: Correlation between the concentration of the organic phase in the mixer and distribution coefficients for 1,6-hexanediol (left) and 1,2,6-hexanetriol (right) in alcohol/water mixtures at 25 °C. 30 g of an aqueous solution containing 7.5 wt-% of glycerol, 1,6-hexanediol, 1,2,6-hexanetriol, and mannitol are extracted with 1-butanol, 1-pentanol, and 1-hexanol, respectively.

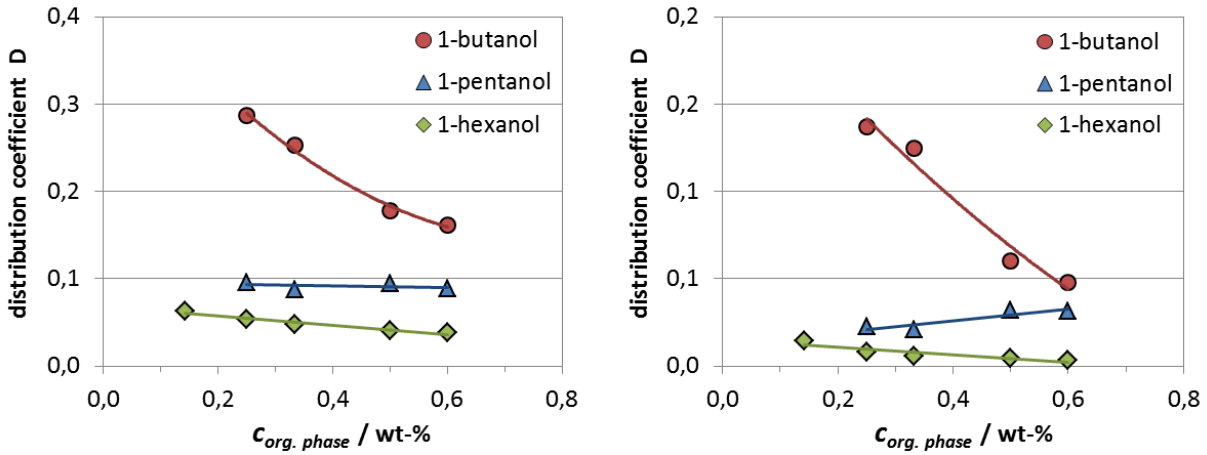

Figure 5-45: Correlation between the concentration of the organic phase in the mixer and distribution coefficients for glycerol (left) and mannitol (right) in alcohol/water mixtures at 25 °C. 30 g of an aqueous solution containing 7.5 wt-% of glycerol, 1,6-hexanediol, 1,2,6-hexanetriol, and mannitol are extracted with 1-butanol, 1-pentanol, and 1-hexanol, respectively.

Increasing the temperature of the solvent and aqueous polyol mixture (raffinate) from 25 to 50 °C leads to an improved extraction (**Figure 5-46**). All solvents show increased distribution coefficients for 1,6-hexanediol. Interestingly, the most enhanced transfer of 1,6-hexanediol into the organic phase is observed for 1-pentanol. This effect is even more pronounced when the ratios for the amount of extracted desired products (1,6-hexanediol and 1,2,6-hexanetriol) compared to glycerol and mannitol are compared (resembling the quality of the extraction, **Figure 5-47**).

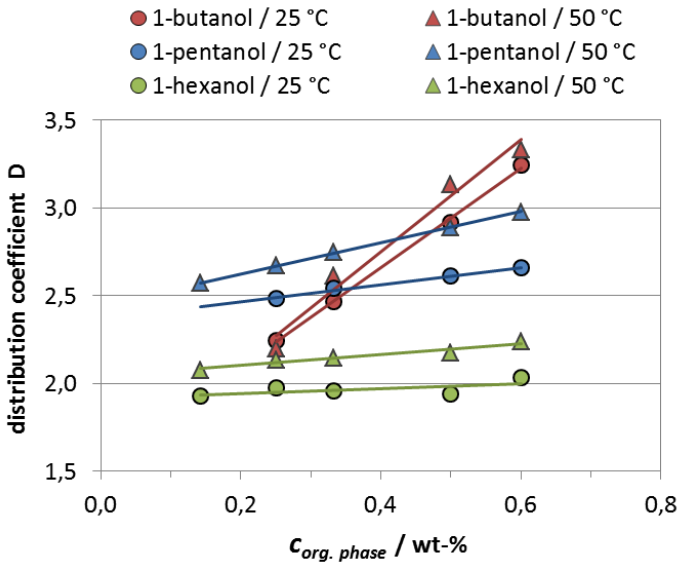

Figure 5-46: The correlation between the concentration of the organic phase in the mixer and distribution coefficients for 1,6-hexanediol in alcohol/water mixtures at 25 °C as shown in **Figure 5-44** is compared to extraction at 50 °C. 30 g of the same an aqueous solution are extracted with 1-butanol, 1-pentanol, and 1-hexanol.

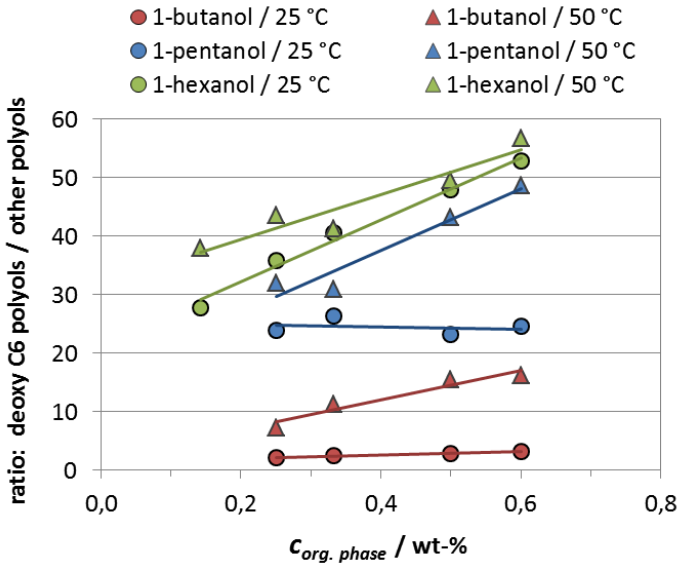

Figure 5-47: Ratio for the extraction of 1,6-hexanediol and 1,2,6-hexanetriol (deoxy C6 polyols) compared to glycerol and mannitol (other polyols) in alcohol/water mixtures at 25 and 50 °C. 30 g of an aqueous solution with 7.5 wt-% of each polyol are extracted with 1-butanol, 1-pentanol, and 1-hexanol.

Using 1-hexanol as solvent at 25 or 50 °C enables the best separation with a ratio of up to 55 in favor of extracted deoxy C6 polyols. This means that the desired products are 55 times more preferably isolated (on a molar basis) by extraction. 1-pentanol shows almost the same characteristics at 50 °C with a linear increase at higher solvent concentrations up to a ratio of 45. Interestingly, an extraction with 1-pentanol at 25 °C is unaffected by the concentration of the solvent in the mixer and the ratio between desired deoxy C6 polyols and undesired glycerol/mannitol is only about 25 (**Figure 5-47**). This shows that the extraction with 1-pentanol as solvent is strongly affected by the temperature.

1-pentanol and 1-hexanol are both very promising for the selective extraction of deoxy C6 polyols from aqueous polyol mixtures at 50 °C. The final purification of the extracted deoxy C6 polyols from the organic phase presumably occurs via evaporation of the mono alcohol. From this point of view, 1-pentanol should be even more favorable than 1-hexanol because distillation of the solvent is more economical (boiling point from 1-pentanol at 1 atmosphere is 138 °C compared to 157 °C for 1-hexanol). Furthermore, 1-pentanol is less viscous than 1-hexanol and thus, more easily to handle. In this regard a two-step cross-current extraction with 1-pentanol was performed with a moderate solvent concentration of 33 wt-% (15 g of fresh solvent compared to 30 g of aqueous raffinate) in the mixer/settler. **Figure 5-48** shows that about 75 wt-% of dissolved 1,6-hexanediol are already extracted after the first step. An overall yield of 95 wt-% are obtained with two steps with an additional 38 wt-% for 1,2,6-hexanetriol. In contrast, only 10 wt-% of the undesired glycerol are transferred into the organic phase and only trace amounts of mannitol. These results show that the separation of deoxy C6 polyols from short-chain polyols in hydrogenolysis reactions is feasible using a liq.-liq. extraction process.

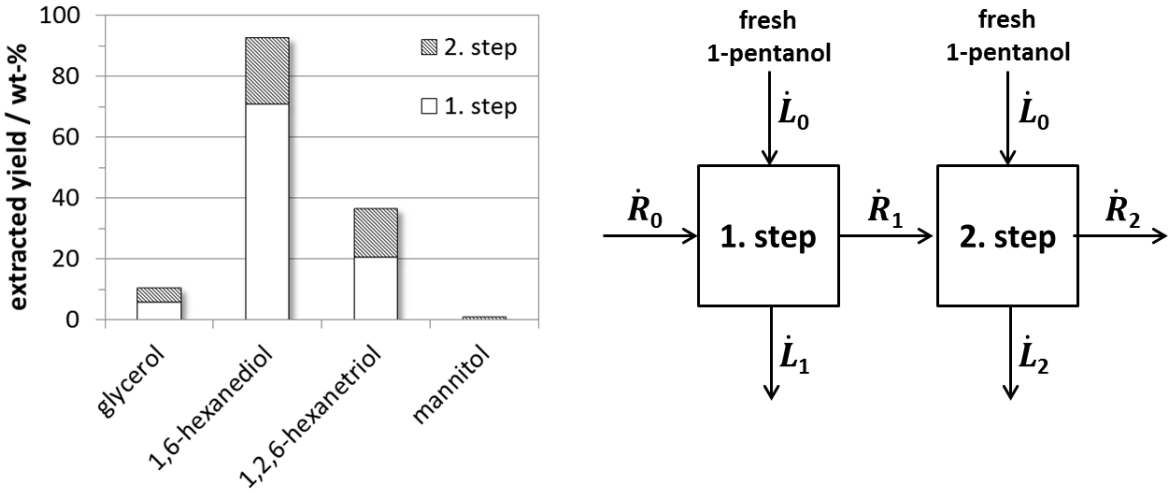

Figure 5-48: Extracted yields of the four model compounds glycerol, 1,6-hexanediol, 1,2,6-hexanetriol and mannitol from an aqueous solution with 1-pentanol at 25 °C in a cross-current extraction. 30 g of the aqueous solution with 7.5-wt of each polyol were extracted consecutively with 15 g of the fresh solvent (1-pentanol).

6. Conclusions and Thesis

The scope of this thesis is the investigation of the heterogeneously catalytic deoxygenation (-C-O- bond cleavage) of sugars and sugar alcohols using high pressure H_2. This catalytic process is very promising for the conversion of renewable feedstocks to large-scale chemicals and to substitute petrochemical products with bio-based compounds. Short-chain polyols such as glycols (ethanediol and 1,2-propanediol) are easily accessible from naphtha. However, important petro-based polyol compounds with a longer carbon chain, such as 1,6-hexanediol or 1,2,6-hexanetriol, require at least four synthesis steps. Replacing this complex chemistry with a one-pot reaction via selective -C-O- bond cleavage from sugars would be a significant breakthrough for the use of renewable feedstocks.

For this purpose, commercially available hydrogenation catalysts based on Ru, Ni, and Cu were applied for the conversion of biomass-derived sugar alcohols. The catalytic properties were studied and optimized by variation of the reaction temperature between 160 and 220 °C as well as H_2 pressures between 0 and 200 bar. Based on the experimental results of this work the following characteristics of the applied heterogeneous catalysts are presented:

- Ru based catalysts are the most active and already exhibit -C-O- and -C-C- bond cleavage at a moderate 160 °C. However, the -C-C- hydrogenolysis via decarbonylation is the dominant reaction leading to undesired C5 polyols and volatile C1 products. This reaction is metal-catalyzed and thus, not affected by the catalyst support (here: activated carbon / alumina).

- Ni based catalysts are inactive for hydrogenolysis reactions below 200 °C. The conversion of sugar alcohols is negligible. At 220 °C all Ni catalysts show complete conversion and perform excessive -C-C- bond cleavage to C1 products (CO_2 and CH_4), showing properties that are comparable to Ru.

- Cu-Raney shows good -C-O- bond cleavage properties while maintaining the C6 carbon chain. A selectivity of 76 mol-% for deoxy hexitols is obtained at 54 % conversion (at 180 °C and 150 bar H_2). In comparison, a Cu/ZnO bulk catalyst exhibits a selectivity of 52 mol-% for deoxy hexitols at 41 % conversion under the same conditions.

- Cu-Raney maintains the same catalytic activity and selectivity for >800 h on-stream (no deactivation during all tests), promising high potential for an industrial application. At full conversion the liquid phase consists of 34 mol-% hexanetetrols (major product: 1,2,5,6-isomer), 34 mol-% hexanetriols (1,2,5-, 1,2,6-, and 1,4,5-isomers) and 8 mol-% hexanediols (major product: 1,2-isomer).

A mechanistic study using the Raney-Cu catalyst shows that certain OH-groups of sugar alcohols are preferably cleaved. A mechanism is proposed leading to the following theses:

- Adsorption of polyol compounds over Cu occurs via two OH-groups, preferably at the 1- and 2-position (chelate complex with Cu), with cleavage of a free OH-group in close proximity.

- The reactivity for deoxygenation of a third OH-group decreases in the following order: adjacent OH-group > one methylene group distance > two methylene groups distance

- Hydroxy compounds with at least two methylene groups between the OH-groups are rather stable under the chosen reaction conditions (180 to 220 °C at 150 bar H_2). These special catalytic properties of Cu-Raney result in the formation of specific 3,4-dideoxy compounds such as 1,2,5,6-hexanetetrol and 1,2,5- or 1,2,6-hexanetriol (**Figure 6-1**).

A supported Cu catalyst shows the same characteristics but yields larger amounts of short-chain polyols by degradation via unsaturated intermediates. These undesired side reactions are presumably increased because of weak hydrogenation properties of the catalyst that allows unsaturated intermediates on the catalyst surface to exist longer and initiate -C-C- bond cleavage. The detection of sugar acids (aldonic acids such as gluconic acid) and saccharinic acids suggests the following -C-C- bond cleavage pathways:

- CO_2 formation is a side reaction over Cu and probably attributed to decarboxylation from a 3-hydroxy acid or rather 3-keto acid intermediate.

- Such acid intermediates are formed from adsorbed aldehyde species on the catalyst surface in aqueous solutions at temperatures above 180 °C. The dehydrogenation properties of Cu-Raney initiate this side reaction pathway.

- Dehydrogenation properties of Cu-Raney are probably attributed to the affinity of Cu to strongly adsorb H_2 and thus, enabling the abstraction of H_2 from sugar alcohols to form aldehyde species - even at 150 H_2 pressure.

- To improve the catalyst selectivity for deoxy C6 polyols and maintain the C6 carbon chain, better hydrogenation properties are required. The unsaturated aldehyde and ketone intermediates on the catalyst surface need to be re-hydrogenated as quickly as possible.

- For this purpose better saturation of the catalyst with H_2 is required and thus, working at higher H_2 pressures (e.g. up to 300 bar) should increase the catalyst selectivity.

Figure 6-1 summarizes the proposed mechanisms for the selective -C-O- bond cleavage of sugar alcohols to 3-deoxy and 3,4-dideoxy products as well as side reactions to short-chain polyols (C1 to C5 polyols). The selective deoxygenation is possible because polyols preferably adsorb via two vicinal OH-groups at the 1- and 2-position, forming a five-membered ring similar to a chelate complex. Free OH-groups in close proximity to the catalyst surface (or rather to activated hydrogen on the catalyst) are subsequently cleaved. Another characteristic of Cu is the adsorption of polyols after an equilibrium step of dehydrogenation-hydrogenation which leads to unsaturated intermediates. Unsaturated ketones as shown in **Figure 6-1** can be easily converted to an aldehyde by keto-enol tautomerization. Aldehydes are possibly transformed to sugar acids via the Cannizzaro reaction and undergo rapid decarboxylation, yielding a C5 polyol and CO_2. Other -C-C- bond cleavage pathways include retro aldol reactions via aldehyde or ketone intermediates forming C1 to C5 polyols [Kühne2018].

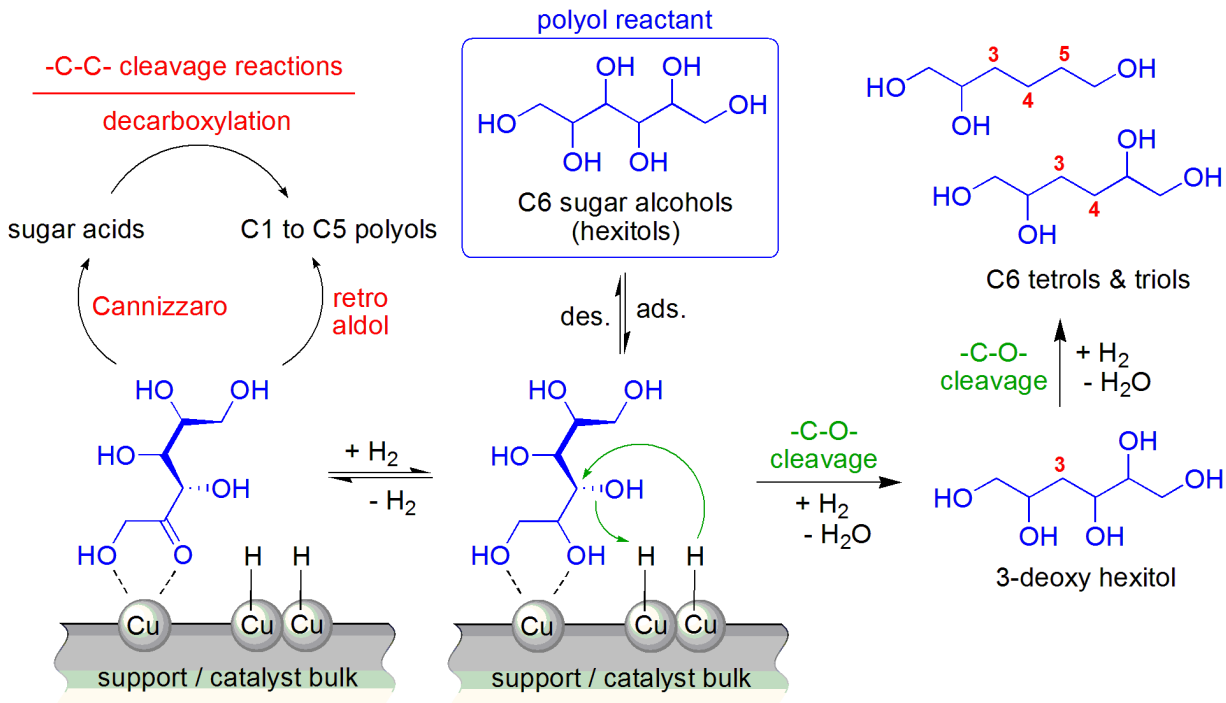

Figure 6-1: Adsorption of sugar alcohols on the surface of a Cu catalyst with selective –C-O- bond cleavage mechanism to specific 3-deoxy and 3,4-dideoxy products. Different side reaction pathways via –C-C- bond cleavage are initiated from unsaturated intermediates on the catalyst surface. This figure is adapted from [Kühne2018].

Downstream-Processing

The separation of deoxy C6 polyols and short-chain polyols seems feasible with both investigated downstream-processes: ion-exchange chromatography and liquid-liquid extraction. The extractive method shows deoxy C6 polyols (model compounds 1,2,6-hexanetriol and 1,6-hexanediol) are up to 55 times better dissolved in the organic phase than short-chain polyols (model compound glycerol) when linear mono alcohols such as 1-pentanol and 1-hexanol are used as solvent. However, this process only allows the separation of deoxy C6 polyol mixtures.

In contrast, chromatographic separation shows effective separation of hexanepentols, -tetrols, -triols, and -diols. The following results are obtained with an H^+-functionalized ion-exchange resin (Dowex99/320 with sulfonic acid groups):

- Retention times of deoxy C6 polyols increase in the following order:
  Hexanepentols < -tetrols < -triols < -diols

- This effect may be attributed to nonpolar interactions of methylene groups in deoxy C6 polyols with the poly-styrene resin material. Additionally, the hydrate shell increases with the number of OH-groups in the molecule and thus, enhances the diffusion through resin.

- Two major fractions are obtained from a hydrogenolysis product mixture over Cu-Raney, depending on the flow rate of the mobile phase. The first one includes 1,2,5,6-hexanetetrol, the second one the mixture of hexanetriols (1,2,5- , 1,2,6- , and the 1,4,5-isomer), and the third fraction consists of hexanediols, mainly the 1,2-isomer (**Figure 6-2**).

- Hexanediols, mainly the 1,2-isomer, are co-eluted with hexanetriols at higher flow rates (5 to 10 mL/min) or obtained in a small third fraction at flow rates below 5 mL/min. Thus, the flow rate of the mobile phase has a strong effect on the separation over the H^+ functionalized resin.

- The optimum column temperature for good separation is 60 °C. Lower temperatures seem to have a negative effect on the interactions with the column because the bands (fractions) show tailing and increased co-elution. Temperatures above 60 °C do not further increase the separation, which is probably attributed to degassing of the mobile phase.

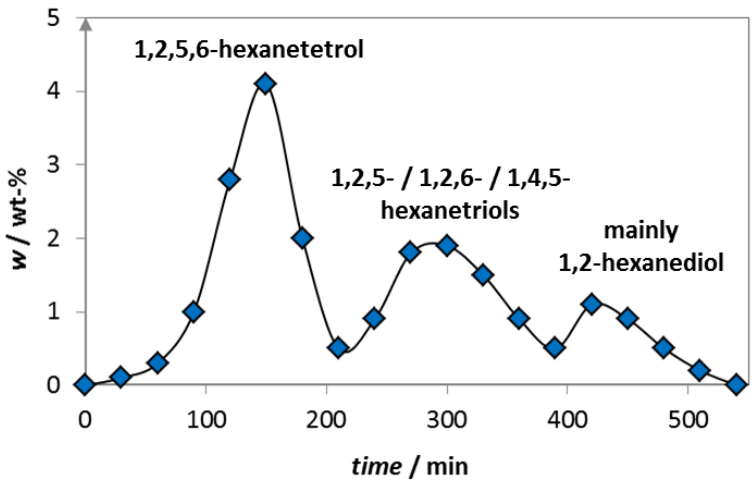

Figure 6-2: Chromatographic separation of a C6 tetrols, triols, and diols mixture as obtained from hydrogenolysis of hexitols over Cu-Raney. The separation was performed using a H^+-functionalized resin (Dowex99/320) at 60 °C.

Potential applications

The mixture of hexanetriols could be integrated into the value chains of 1,2,6-hexanetriol, e.g. as a cross-linker in alkyd resins [Tess1957], polyesters or polyurethanes. Other possible applications are humectants or solvents. 1,2,5,6-hexanetetrol comprises of new chemical properties with a fourth OH-group – in particular, with two vicinal OH-groups – in the C6 carbon chain. Possible applications are polyesters, polyurethanes or plasticizers when esterified with long-chain carboxylic acids (**Figure 6-3**). Ethers of 1,2,5,6-hexanetetrol could also potentially serve as a new bio-based high-boiling solvent. The 1,6-dimethyl-ether would be an analogue of 1-methoxy-2-propanol (two 1-methoxy-2-propanol ethers connected via the C3 backbone), a large-scale solvent for paints and coatings distributed as Solvenon® PM [BASF2016] or Dowanol™ PM [Dow2015]. The predicted boiling point would be around 330 °C and the melting point 40 °C (predicted by ChemDraw Ultra, Version 8.0). Another product with great potential for application would be the epoxide from the two vicinal diol groups (1,2-anhydro-5,6-anhydro-hexanetetrol) [Jang2007, Murthy2006] for epoxide resins.

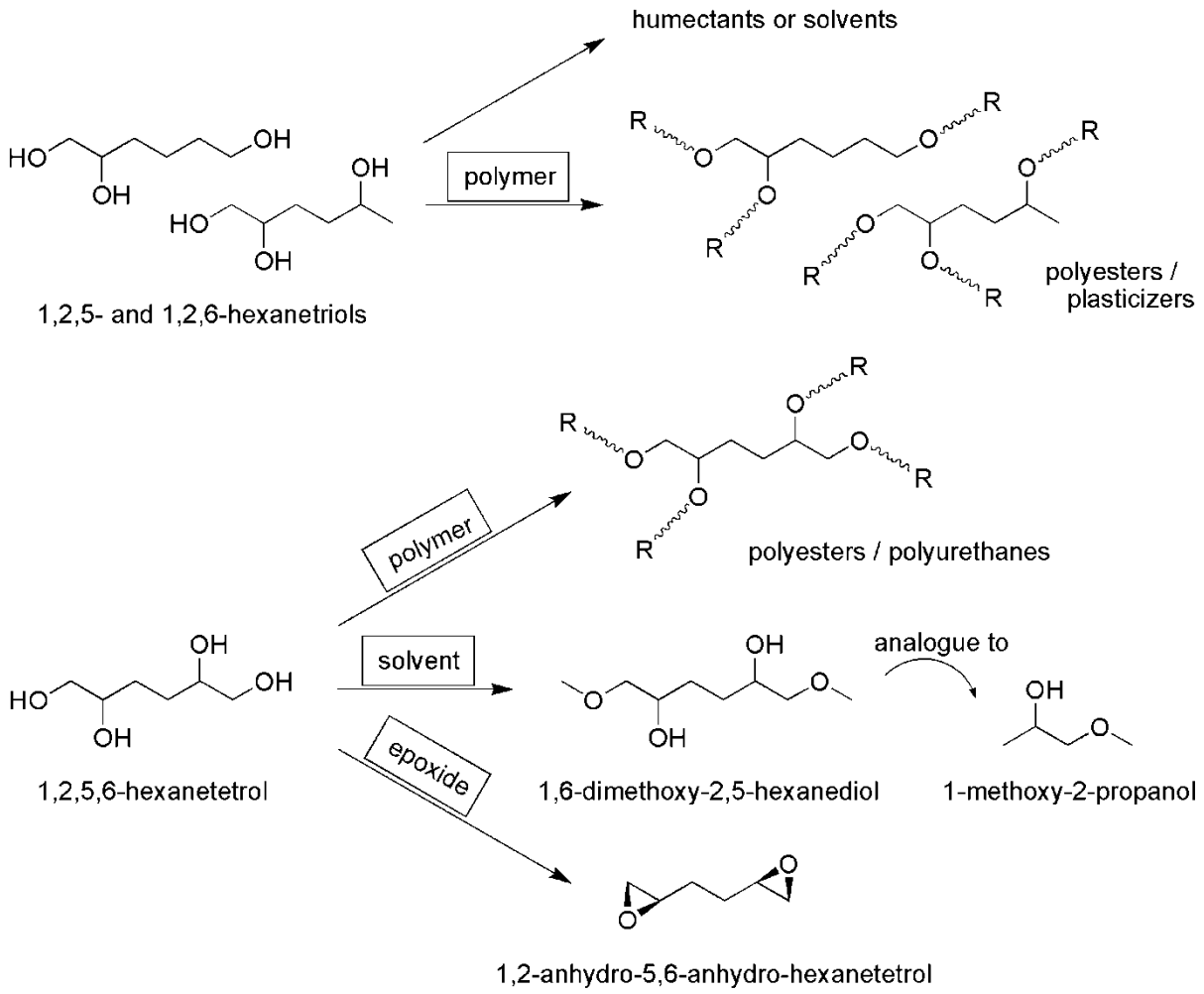

Figure 6-3: Possible applications for hexanetriols as polymers/plasticizers or humectants/solvents and various applications for the 1,2,5,6-hexanetetrol.

7. Outlook – Conceptual process design for an industrial chemical plant

The feasibility of a potential industrial application for sugar based hexanetriols (e.g. 1,2,6-hexanetriol) and the 1,2,5,6-hexanetetrol can be estimated with a process concept that shows the required units for an industrial process (**Figure 7-1**). Starting from invert sugar, an equimolar glucose / fructose mixture obtained from sucrose hydrolysis, eight units are necessary to obtain pure hexanetriols, 1,2,5,6-hexanetetrol, and glycols (ethanediol and 1,2-propanediol). The reaction section is highlighted in green and involves three units: hydrogenation, hydrogenolysis, and CO_2 absorption with H_2 recycle.

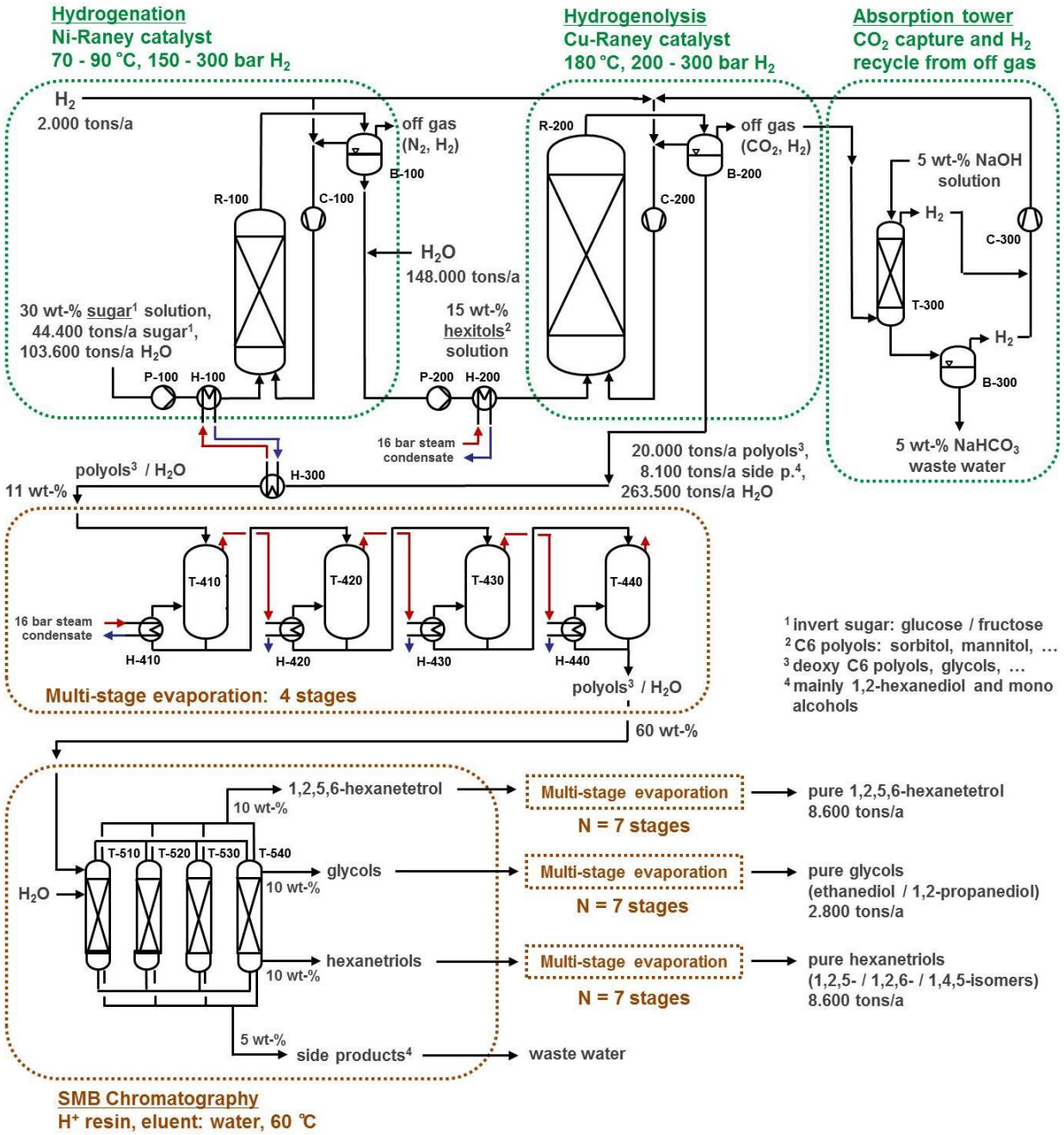

Figure 7-1: Conceptual process design based on laboratory data for conversion of sugars (invert sugar: eq. glucose/fructose mixture) into 1,2,5,6-hexanetetrol, glycols, and hexanetriols.

Five additional units are required for downstream-processing, including SMB chromatography for separation of the products and four heat-coupled multi-stage evaporators (highlighted in brown in **Figure 7-1**). The first step in this process concept is the hydrogenation of sugars into hexitols (sorbitol and mannitol) with subsequent hydrogenolysis (deoxygenation) to deoxy hexitols in a second reactor. Each of the reaction units includes a tube reactor (R-100, R-200), high-pressure pump (P-100, P-200), heat exchanger (H-100, H-200), flash tank (B-100, B-200) for separation of H_2, and a high-pressure compressor (C-100, C-200) to recycle the valuable hydrogen. The off gas from the hydrogenolysis reaction (in the flash tank B-200) includes H_2 and CO_2 which could be washed in an absorption tower (T-300, 3rd unit) with an alkaline NaOH-solution to remove CO_2 and recycle H_2. The aqueous polyol solution obtained from the hydrogenolysis step includes the desired deoxy products 1,2,5,6-hexanetetrol and hexanetriols (1,2,5- / 1,2,6- / 1,4,5-hexanetriol) along with the glycols ethanediol and 1,2-propanediol. The concentration of polyols is about 12 wt-% due to the cleavage of oxygen (mass loss). This stream is concentrated up to 60 wt-% in a heat-coupled 4-stage evaporation unit and separated in a series of connected chromatography columns known as a SMB unit: simulated moving bed. Three product streams are obtained that need to be in a 7-step evaporation unit, each, to remove water and obtain the pure products. Side products from hydrogenolysis, that are not purified, are mainly 1,2-hexanediol and mono alcohols. The diluted aqueous solution from the SMB unit could be transferred for waste water treatment - along with the waste $NaHCO_3$ solution from the absorption tower T-300. Hence, a total of eight units seem to be necessary to establish an industrial process for the production and downstream processing of deoxy polyols based on sugars.

The conceptual process design shows that two major challenges need to be solved. One economical challenge is the heavy dilution of hexitols (15 wt-%) in the hydrogenolysis reactor R-200 in order to obtain acceptable selectivity for the desired deoxy polyols over Cu-Raney. It was shown in **Figure 5-26** that the selectivity for hexanetriols and the 1,2,5,6-hexanetetrol decreases when the concentration of the reactant (hexitols) is increased. Thus, the concentration of hexitols in the hydrogenolysis reactor R-200 should not exceed 15 wt-%. However, this requires heating of large amounts of water up to temperatures where hydrogenolysis takes place (180 °C) and also removal of large amounts of water in the downstream process. Furthermore, the SMB unit uses water as eluent which also needs to be evaporated to obtain pure products. The removal of water is performed in four multi-stage evaporation units. The requirement of these units results in significant fixed and operating costs, in particular steam costs (**Table 7-1**). Hence, the energy amounts for the expensive heating of water and subsequent evaporation would be significant so that heat-coupling in such a process is crucial. Heat-coupling in evaporation units by repeatedly using compressed steam form one tower (e.g. T-100) to heat the bottom of the next tower (e.g. T-200) is a commercial standard in the sugar industry [Südzucker2011]. Energy savings of about 50 % and more are possible in a heat-coupled multi-stage evaporator when compared to one large single tower, depending on the number of stages in one unit [Luyken2018].

Another challenge is the optimization of the catalyst for the hydrogenolysis reaction. The selectivity to valuable products and the conversion rate need to be improved. It was shown in **Figure 5-9** that the molar fraction of 1,2,5,6-hexanetetrol, hexanetriol, and glycols is about 77 mol-% from the product mixture in the liquid phase. However, the overall C-balance in the liquid phase is 80 mol-% which means that the overall selectivity is only 62 mol-%. It also needs to be taken into account that the cleavage of multiple -C-O- bonds (deoxygenation) eliminates mass from sugars. Hence, the required amount of sugar to produce a certain capacity of deoxy polyols per year is much larger. This results in significant raw material costs as shown in **Table 7-1**.

Table 7-1: Estimation of investment (fixed costs) and operating costs for a 20.000 tons chemical plant based on the conceptual process design shown in **Figure 7-1**. Operating costs include prices for depreciation (dependent on the desired payback of the invested fix costs, OSBL), maintenance, raw materials (sugars and hydrogen), steam, and waste water treatment. Prices for each matter of expense are taken from [Vogel2002] and adjusted to 2018 by consideration of inflation rates as shown in chapter 9.4.1.

Investment (fixed costs) for capacity of 20.000 tons per year			
ISBL: ~ 95.000.000 €, location-independent capital investment as calculated in chapter 9.4.1			
OSBL: ~ 126.000.000 €, invest including auxiliary plants , see chapter 9.4.1 (1.33 x ISBL)			
Production costs – average case – based on average costs for industrial countries			
Description / assumptions	Matter of expense	€ / kg	Reference for cost determination
Payback of OSBL in 10 years	depreciation	0.63	[Vogel2002, Zevnik1963]
5 % of OSBL per year	maintenance	0.32	[Vogel2002, Zevnik1963]
Based on 44.400 tons/a of sugars	raw materials (sugar)	0.91	[Vogel2002]
Price average in Europe	hydrogen	0.13	[Boulamanti2017]
Factor of 0.5 for heat-coupling	steam	0.49	[Luyken2018, Vogel2002]
Side products are not burnt	waste water treatment	0.55	[Vogel2002]
	total production costs	**3.03**	
Production costs – best case – based on lower costs in specific countries			
Description / assumptions	Matter of expense	€ / kg	Reference for cost determination
Payback of OSBL in 12 years	depreciation	0.48	[Vogel2002, Zevnik1963]
3 % of OSBL per year	maintenance	0.19	[Vogel2002, Zevnik1963]
Based on 44.400 tons/a of sugars	raw materials (sugar)	0.91	[Vogel2002]
Price in USA (~30 % of Europe)	hydrogen	0.04	[Boulamanti2017]
Factor of 0.25 for heat-coupling	steam	0.25	[Luyken2018, Vogel2002]
Side products are not burnt	waste water treatment	0.55	[Vogel2002]
	total production costs	**2.43**	

The investment (ISBL and OSBL) for a 20.000 tons chemical plant is calculated using the method of specific units under consideration of each unit's complexity as shown in chapter 9.4.1 in the appendix [Vogel2002, Zevnik1963]. **Table 7-1** shows the total production costs are mainly driven by the raw material costs, in particular for sugars, depreciation (for a payback of the 126 Mio. € investment (OSBL) in ten or twelve years), and steam costs. Such calculations have a deviation of about ± 30 % to ± 60 % and only allow rough estimations [Vogel2002].

Hence, the two depicted cases – average and best case – are strongly dependent on the desired payback time for invested capital (OSBL) as well as the design and heat-coupling of the evaporation units. Lowering the energy amount (and thus, the required steam amount) for the evaporation of water has a much stronger effect on the total production cost than the variation of hydrogen costs in different countries. Cost savings achieved from lower hydrogen prices in the USA compared to average costs that are calculated for several other countries [Boulamanti2017] have a minor impact on the manufacturing costs. It can be concluded that 1,2,5,6-hexanetetrol, hexanetriols, and glycols would probably cost between 2.43 and 3.03 €/kg, which equals 2.430 and 3.030 €/ton, respectively. In comparison to an approach for conversion of lignocellulosic biomass (C5 and C6 sugars) into 1,5-pentanediol (PDO) and 1,6-hexanediol (HDO) by Huber *et al.* that shows a minimum selling price of 4.089 $/ton [Huber2017], the prices shown in **Table 7-1** are significantly lower.

Finally, in order to assess the feasibility of this conceptual process, it has to be noted that conversion rates, calculated from the laboratory data, are about 30-times faster for the hydrogenation of sugars compared to the hydrogenolysis of hexitols (see **Figure 9-34** from chapter 9.4.3 in the appendix). This means that the hydrogenolysis reactor R-200 would have to be 30-times larger than the hydrogenation reactor R-100 (about 270 m³ compared to 9 m³) because of much larger required catalyst amounts, which is not feasible. Hence, the hydrogenolysis catalyst needs to be improved in order to enable an industrial realization. So far, Cu-Raney shows unique catalytic properties in laboratory experiments but the commercialization of the presented conceptual process is not possible with this catalyst. On the positive side, an enhanced hydrogenolysis (deoxygenation) catalyst will not only enable the large scale production of sugar-derived deoxy polyols, but also lower the operating costs.

8. References

[ADM2015] K. Stensrud, C.-C. Ma, Synthesis of reduced sugar alcohols, furan derivatives, Archer Daniels Midland Company, Patent WO 2015156802 A1, **2015**

[AlEid2006] S. M. Al Eid, *Chromatographic separation of fructose from date syrup*, International Journal of Food Sciences and Nutrition, **2006**, *57 (1-2)*, 83-92

[Angyal1979] S. J. Angyal, G. S. Bethell, R. J. Beveridge, *The separation of sugars and of polyols on cation-exchange resins in the calcium form*, Carbohydrate Research, **1979**, *73*, 9-18

[Arena1992] B. J. Arena, *Deactivation of ruthenium catalysts in continuous glucose hydrogenation*, Applied Catalysis A: General, **1992**, *87 (2)*, 219-229

[Arntz2007] D. Arntz, A. Fischer, M. Höpp, S. Jacobi, J. Sauer, T. Ohara, T. Sato, N. Shimizu, H. Schwind, *Acrolein and Methacolein*, Ullmann's Encyclopedia of Industrial Chemistry, Wiley-VCH, Weinheim, **2007**

[Baatz2007] C. Baatz, *Entwicklung von Goldkatalysatoren für den Einsatz in der Glucoseoxidation*, Dissertation, TU Braunschweig, **2007**

[Baerns2013] M. Baerns, A. Behr, A. Brehm, J. Gmehling, H. Hofmann, U. Onken, A. Renken, K.-O. Hindrichsen, R. Palkovitz, *Technische Chemie*, 2. Auflage, Wiley-VCH, **2013**

[Barker1984] P. E. Barker, G. A. Irlam, E. K. E. Abusabah, *Continuous chromatographic separation of glucose-fructose mixtures using anion-exchange resins*, Chromatographia, **1984**, *18 (10)*, 567-574

[BASF1976] R. Kummer, *Manufacture of 1,6-hexanediol from butadiene*, BASF SE, Patent US 3947503, **1976**

[BASF2015] R. Backes, B. Blank, A. Kindler, C. Feldner, *Production of 5 hydroxymethylfurfural (HMF) from hexose solutions in the presence of steam*, BASF SE, Patent US 9169227 B2, **2015**

[BASF2016] BASF SE, *Solvenon® PM*, Technical Information, May **2016**

[Bejile2015] A. N. Bejile, *Copper based catalysts in the selective dehydration of polyols*, Dissertation, Iowa State University, **2015**

[Berweiler2001] M. Berweiler, D. Ostgard, K. Seelbach, *Geformter Festbett Raney-Kupferkatalysator zur Verwendung bei der Dehydrierung von Alkoholen*, Degussa AG, Patent EP1127613 A1, **2001**

[Berweiler2004] M. Berweiler, M. Höpp, R. Vanheertum, W. Girke, *Raney-Kupferkatalysator zur Dehydrierung von Alkoholen*, Degussa AG, Patent EP1382389 A1, **2004**

[Blanc2000] B. Blanc, A. Bourrel, P. Gellezot, T. Haas, P. Taylor, *Starch-derived polyols for polymer technologies: preparation by hydrogenolysis on metal catalysts*, Green Chemistry, **2000**, *2*, 89-91

[Blann1950] W. A. Blann, W. W. Durant, *Sugar purification process*, Patent US2522022 A, **1950**

[Bond2013] J. Q. Bond, D. M. Alonso, J. A. Dumesic, *Catalytic Strategies for Converting Lignocellulosic Carbohydrates to Fuels and Chemicals,* Aqueous Pretreatment of Plant Biomass for Biological and Chemical Conversion to Fuels and Chemicals: 61-102, **2013**, Wiley

[Boulamanti2017] A. Boulamanti, J. A. Moya, *Production costs of the chemical industry in the EU and other countries: Ammonia, methanol and light olefins*, Renewable and Sustainable Energy Reviews, **2017**, *68*, 1205-1212

[Clark1958] I. T. Clark, *Hydrogenolysis of sorbitol,* Industrial and Engineering Chemistry, **1958,** Vol. 50 (*8)*, 1125-1126

[Claus2004] P. Claus, Y. Önal, S. Schimpf, *Structure sensitivity and kinetics of D-glucose oxidation to D-gluconic acid over carbon-supported gold catalysts*, Journal of Catalysis, **2004,** *223*, 122-133

[Claus2006] P. Claus, G. H. Vogel, *Die Rolle der Chemokatalyse bei der Etablierung der Technologieplattform "Nachwachsende Rohstoffe"*, Chemie Ingenieur Technik, **2006,** *8*, 991-1012

[Corma2007] A. Corma, S. Iborra, A. Velty, *Chemical Routes for the Transformation of Biomass into Chemicals*, Chemical Reviews, **2007**, *107*, 2411-2502

[Dasari2005] M. A. Dasari, P.-P. Kiatsimkul, W. R. Sutterlin, G. J. Suppes, *Low-pressure hydrogenolysis of glycerol to propylene glycol*, Applied Catalysis A: General, **2005**, *281*, 225-231

[Davis1987] J. L. Davis, M. A. Barteau, *Decarbonylation and decomposition pathways of alcohol's on Pd(111)*, Surface Science, **1987**, *187 (2-3)*, 387-406

[Davis1989] J. L. Davis, M. A. Barteau, *Polymerization and decarbonylation reactions of aldehydes on the Pd(111) surface*, Journal of the American Chemical Society, **1989**, *111 (5)*, 1782-1792

[Davis2007] R. J. Davis, W. C. Ketchie, Y.-L. Fang, M. S. Wong, M. Murayama, *Influence of gold particle size on the aqueous-phase oxidation of carbon monoxide and glycerol*, Journal of Catalysis, **2007**, *250*, 94-101

[Deng2010] T. Y. Deng, Y. Sun, H. Liu, *Cellulose conversion to polyols on supported Ru catalysts in aqueous basic solution*, Science China Chemistry, **2010**, *53 (7)*, 1476-1480

[Deutsch2012] K. L. Deutsch, D. G. Lahr, B. H. Shanks, *Probing the ruthenium-catalyzed higher polyol hydrogenolysis reaction through the use of stereoisomers*, Green Chemistry, **2012**, *14*, 1635-1642

[DeWit1978] G. de Wit, J. J. de Vlieger, A. C. Kock-van Dalen, A. P. G. Kieboom, H. van Bekkum, *Catalytic dehydrogenation of reducing sugars in alkaline solution at ambient conditions*, Tetrahedron Letters, **1978**, *15*, 1327-1330

[DeWit1981] G. de Wit, J. J. de Vlieger, A. C. Kock-van Dalen, R. Heus, R. Laroy, A. J. van Hengstum, A. P. G. Kieboom, H. van Bekkum, *Catalytic dehydrogenation of reducing sugars in alkaline solution*, Carbohydrate Research, **1981**, *91*, 125-138

[Dow2015] The Dow Chemical Company, *Dowanol™ PM Glycol Ether*, Product Safety Assessment, November **2015**

[Dow2016] The Dow Chemical Company, *Dowex Monosphere Chromatography Resins for Starch Sweetener Purification*, Water & Process Solutions, Form No. 177-03580, *Rev. 2*, December **2016**

[Dubeck1984] M. Dubeck, G. G. Knapp, *Two stage hydrogenolysis of carbohydrate to glycols using sulfide modified ruthenium catalyst in second stage*, Patent US4476331, **1984**

[Ford1977] R. M. Laine, R. G. Rinker, R. C. Ford, *Homogeneous catalysis by ruthenium carbonyl in alkaline solution: the water gas shift reaction*, Journal of the American Chemical Society, **1977**, *99 (1)*, 252-253

[Ford1979] C. Ungermann, V. Landis, S. A. Moya, H. Cohen, H. Walker, R. G. Pearson, R. G. Rinker, P. C. Ford, *Homogeneous Catalysis of the Water Gas Shift Reaction by Ruthenium and Other Metal Carbonyls, Studies in Alkaline Solutions*, Journal of the American Chemical Society, **1979**, *101 (20)*, 5922-5929

[Ford1981] P. C. Ford, *The water gas shift reaction: homogeneous catalysis by ruthenium and other metal carbonyls*, Accounts of Chemical Research, **1981**, *14 (2)*, 31-37

[Furanix2012] C. M. De Diego, W. P. Schammel, M. A. Dam, G. J. M. Gruter, *Method for the preparation of 2,5-fucandicarboxylic acid and esters thereof*, Furanix Technologies B. V. (now Synvina C. V.), Patent US 2012/0283452 A1, **2012**

[Furanix2014] C. M. De Diego, M. A. Dam, G. J. M. Gruter, *Method for the preparation of 2,5-furandicarboxylic acid and for the preparation of the dialkyl ester of 2,5-furancicarboxylic acid*, Furanix Technologies B. V. (now Synvina C. V.), Patent US 8865921 B2, **2014**

[Gallegos2013] E. Gallegos-Suarez, M. Pérez-Cadenas, A. Guerrero-Ruiz, I. Rodriguez-Ramos, A. Arcoya, *Effect of the functional groups of carbon on the surface and catalytic properties of Ru/C catalysts for hydrogenolysis of glycerol*, Applied Surface Science, **2013**, *287*, 108-116

[Goldschmid1960] H. R. Goldschmid, A. S. Perlin, *Hydrogenolysis of carbohydrates*, Canadian Journal of Chemistry, **1960**, *38*, 2178-2186

[HajiBegli2007] A. Haji Begli, C. Baatz, N. Thielecke, U. Prüsse, K.-D. Vorlop, *Supported gold catalyst*, Südzucker AG Patent WO2007017157 A1, **2007**

[Hashimoto1983] K. Hashimoto, S. Adachi, H. Noujima, H. Maruyama, *Models for the separation of glucose/fructose mixture using a simulated moving-bed*, Journal of Chemical Engineering of Japan, **1983**, *16 (5)*, 400-406

[Hattori2010] H. Hattori, *Solid Acid Catalysts: Roles in Chemical Industries and New Concepts*, Topics in Catalysis, **2010**, *53* (7-10), 432-438

[Heeres2009] H. Heeres, R. Handana, D. Chunai, C. B. Rasrendra, B. Girisuta, H. J. Heeres, *Combined dehydration/(transfer)-hydrogenation of C6-sugars (D-glucose and D-fructose) to γ-valerolactone using ruthenium catalysts*, Green Chemistry, **2009**, *11*, 1247-1255

[Heinen2000] A. W. Heinen, J. A. Peters, H. van Bekkum, *Hydrogenation of fructose on Ru/C catalyst*, Carbohydrate Research, **2000**, *328*, 449-457

[Hibbitts2015] E. I. Gürbüz, D. D. Hibbitts, E. Iglesia, *Kinetic and Mechanistic Assessment of Alkanol/Alkanal Decarbonylation and Deoxygenation Pathways on Metal Catalysts*, Journal of the American Chemical Society, **2015,** *137*, 11984-11995

[Huang2014] Z. Huang, J. Chen, Y. Jia, H. Liu, C. Xia, H. Liu, *Selective hydrogenolysis of xylitol to ethylene glycol and propylene glycol over copper catalysts*, Applied Catalysis B: Environmental, **2014**, *147*, 377-386

[Huang2016] Y. Huang, P.-Y. Chao, T.-Y. Cheng, Y. Ho, C.-T. Lin, H.-Y. Hsu, J.-J. Wong, T.-C. Tsai, *Design of sulfonated mesoporous silica catalyst for fructose dehydration guided by difructose anhydride intermediate incorporated reaction network*, Chemical Engineering Journal, **2016**, *283*, 778-788

[Huber2017] G. W. Huber, 2017 Project Peer Review, *Production of α,ω diols from biomass*, U.S. Department of Energy (DOE) and Bioenergy Technologies Office (BETO), **2017**

[Isbell1944] H. J. Isbell, *Interpretations of some reactions in the carbohydrate field in terms of consecutive electron displacement*, Journal of Research of the National Bureau of Standards, **1944**, *32*, 45

[Isbell1969] H. J. Isbell, *Transformations of sugars in alkaline solutions*, Carbohydrate Research, **1969**, *9*, 163-175

[Isikgor2015] F. H. Isikgor, C. R. Becer, *Lignocellulosic biomass: a sustainable platform for the production of bio-based chemicals and polymers*, Polymer Chemistry, **2015**, *6*, 4497-4559

[Jang2000] D. O. Jang, Y. H. Joo, D. H. Cho, *Efficient Synthesis of Epoxides from Vicinal Diols Via Cyclic Sulfates*, Synthetic Communications, *30 (24)*, **2000**

[Jin2015] X. Jin, J. Shen, W. Yan, M. Zhao, P. S. Thapa, B. Subramaniam, R. V. Chaudhari, *Sorbitol Hydrogenolysis over Hybrid Cu/CaO-Al_2O_3 Catalysts: Tunable Activity and Selectivity with Solid Base Incorporation*, ACS Catalysis, **2015**, *5*, 6545-6558

[Kellner1981] C. S. Kellner, A. T. Bell, *The kinetics and mechanism of carbon monoxide hydrogenation over aluminated-supported ruthenium*, Journal of Catalysis, **1981**, *70 (2)*, 418-432

[Khym1958] J. X. Khym, L. P. Zill, *Separation and analysis of polyhydroxy substances*, Patent US 2818851 A, **1958**

[Kobayashi2015] H. Kobayashi, H. Yokoyama, B. Feng, A. Fukuoka, *Dehydration of sorbitol to isosorbide over H-beta zeolites with high Si/Al ratios*, Green Chemistry, **2015**, *17*, 2732-2735

[Kokoh2011] A. Habrioux, K. Servat, S. Tingry, B. Kokoh *Catalytic Strategies for Converting Lignocellulosic Carbohydrates to Fuels and Chemicals*, Aqueous Pretreatment of Plant Biomass for Biological and Chemical Conversion to Fuels and Chemicals: 61-102, **2013**, Wiley

[Kolomnikov1974] I. S. Kolomnikov, V. P. Kukolev, M. E. Vol'pin, *Hydrogen Transfer from Organic Compounds Catalysed by Transition Metal Complexes*, Russian Chemical Reviews, **1974**, 43 (5), 903-932

[Kornberg1948] A. Kornberg, S. Ochoa, A. H. Mehler, *Spectrophotometric studies on the decarboxylation of ß-keto acids*, Journal of Biological Chemistry, **1948**, *174*, 159-172

[Kühne2013] B. Kühne, *Einfluss der Reaktionsbedingungen auf die Hydrierung von Ketodisacchariden*, Masterthesis, TU Darmstadt, **2013**

[Kühne2018] B. Kühne, H. Vogel, R. Meusinger, S. Kunz, M. Kunz, *Selective -C-O- hydrogenolysis over Cu based catalysts; identification of the reaction mechanism and key intermediates*, Catalysis Science & Technology, **2018**, *8*, 755-767

[Kuusisto2005] J. Kuusisto, J.-P. Mikkola, P. P. Casal, H. Karthu, J. Väyrynen, T. Salmi, *Kinetics of the catalytic hydrogenation of D-fructose over a CuO-ZnO catalyst*, Chemical Engineering Journal, **2005**, *115*, 93-103

[Kunz2002] T. Rose, M. Kunz, *Production of Isomalt*, Landbauforschung Völkenrode, **2002**, *241*, 75-80

[Paley1950] L. A. Paley, *Methods of purifying sugar juice*, Patent US 2522797 A, **1950**

[Li2013] J. Li, A. Spina, J. A. Moulijn, M. Makkee, *Sorbitol dehydration into isosorbide in a molten salt hydrate medium*, Catalysis Science and Technology, **2013**, *3*, 1540-1546

[Lia2012] X. Lia, K. Li, X. Xiang, S.-G. Wang, X. She, Y. Zhu, Y. Li, *Mediatory role of K, Cu and Mo over Ru/SiO_2 catalysts for glycerol hydrogenolysis*, Journal of Industrial and Engineering Chemistry, **2012**, *18*, 818-821

[Liang2014] D. Liang, C. Liu, S. Deng, Y. Zhu, C. Lv, *Aqueous phase hydrogenolysis of glucose to 1,2-propanediol over copper catalysts supported by sulfated spherical carbon*, Catalysis Communications, **2014**, *54*, 108-113

[Lichtenthaler2004] F. W. Lichtenthaler, S. Peters, *Carbohydrates as green raw materials for the chemical industry*, C. R. Chimie, **2004**, *7*, 65-90

[Liu2010] S. Wang, Y. Zhang, H. Liu, *Selective Hydrogenolysis of glycerol to Propylene Glycol on Cu-ZnO Composite Catalysts: Structural Requirements and Reaction Mechanism*, Chemistry – An Asian Journal, **2010**, *5*, 1100-1111

[Liu2014] S. Liu, M. Tamura, Y. Nakagawa, K. Tomishige, *One-Pot Conversion of Cellulose into n-Hexane over the Ir-ReO_x/SiO_2 Catalyst Combined with HZSM-5*, ACS Sustainable Chemistry & Engineering, **2014**, *2 (7)*, 1819-1827

[Luyken2018] H. Luyken, BASF SE, *Wärmegekoppelte Destillation*, wikipedia entry from 17th january 2016 with calculation of energy savings in a multi-stage distillation and personal discussion in 2018

[Ma2008] L. Ma, D. He, Z. Li, *Promoting effect of rhenium on catalytic performance of Ru catalysts in hydrogenolysis of glycerol to propanediol*, Catalysis Communications, **2008**, *9*, 2489-2495

[Ma2009] L. Ma, D. He, *Hydrogenolysis of Glycerol to Propanediols Over Highly Active Ru-Re Bimetallic Catalysts*, Topics in Catalysis, **2009**, *52*, 834-844

[Ma2010] L. Ma, D. He, *Influence of catalyst pretreatment on catalytic properties and performanecs of Ru-Re/SiO_2 in glycerol hydrogenolysis to propanediols*, Catalysis Today, **2010**, *149*, 148-156

[Maitlis1981] J. Cook, P. M. Maitlis, *Formaldehyde as a Hydrogen-donor to Aldehydes and Ketones in Metal-catalysed Reactions in Water*, Journal of the Chemical Society, Chemical Communications, **1981**, *17*, 924-925

[Makkee1985] M. Makkee, A. P. G. Kieboom, H. van Bekkum, Hydrogenation of D-fructose and D-fructose/D-glucose mixtures, Carbohydrate Research, **1985**, 138 (2), 225-236

[Maris2007a] E. P. Maris, R. J. David, *Hydrogenolysis of glycerol over carbon-supported Ru and Pt catalysts*, Journal of Catalysis, **2007**, *249*, 328-337

[Maris2007b] E. P. Maris, W. C. Ketchie, M. Murayama, R. J. Davis, *Glycerol hydrogenolysis on carbon-supported PtRu and AuRu bimetallic catalysts*, Journal of Catalysis,**2007**, *251*, 281-294

[Michaud1990] C. Michaud, D. F. Brodie, *Ion Exchange Resin – Methods of Degradation*, Water Conditioning & Purification, **1990**, 44-51

[Miyazawa2006] T. Miyazawa, Y. Kusunoki, K. Kunimori, K. Tomishige, *Glycerol conversion in the aqueous solution under hydrogen over Ru/C + an ion-exchange resin and its reaction mechanism*, Journal of Catalysis, **2006**, *260*, 213-221

[Montassier1983] D. K. Sohounloue, C. Montassier, J. Barbier, *Catalytic hydrogenolysis of sorbitol*, Reaction Kinetics and Catalysis Letters, **1983**,*22*, 391-397

[Montassier1988] C. Montassier, D. Giraud, J. Barbier, *Polyol Conversion by Liquid Phase Heterogeneous Catalysis Over Metals* (Hrsg.: M. Guisnet*et al.*), Elsevier, Amsterdam, **1988**, 165-170

[Montassier1991] C. Montassier, J.C. Ménézo, L.C. Hoang, C. Renaud, J. Barbier, *Aqueous polyol conversions on ruthenium and on sulfur-modified ruthenium*, Journal of Molecular Catalysis, **1991**, *70* (1), 99-110

[Montassier1995] C. Montassier, J. M. Dumas, P. Granger, J. Barbier, *Deactivation of supported copper based catalysts during polyol conversion in aqueous phase*, Applied Catalysis A: General, **1995**, *121 (2)*, 231-244

[Murthy1993] V. S. Murthy, A. S. Gaitonde, S. P. Rao, *One-Pot Conversion of 1,2-Diols to Epoxides: Convenient Preparation of Methyl 2,3-Anhydro-5-O-trityl-β-D-lyxofuranoside and Methyl-2,3-Anhydro-4,6-O-benzylidene-α-D-manno-pyranoside*, Synthetic Communications, *23 (3)*, **1993**

[Musser1993] M. T. Musser, *Adipic Acid*, Ullmann's Encyclopedia of Industrial Chemistry, 5th ed, *Vol. A1* (Eds.: B. Elvers, S. Hawkins, W. Russey, G. Schulz), Wiley-VCH, Weinheim, **1993**, p. 271

[Musser2005] M. T. Musser, *Adipic Acid*, Ullmann's Encyclopedia of Industrial Chemistry, Wiley-VCH, Weinheim, **2005**

[Nielsen2013] M. Nielsen, E. Alberico, W. Baumann, H.-J. Drexler, H. Junge, S. Gladiali, M. Beller, *Low-temperature aqueous-phase methanol dehydrogenation to hydrogen and carbon dioxide*, Nature, **2013**, *495*, 85-89

[Nikolla2011] E. Nikolla, Y. Román-Leshkov, M. Moliner, M. E. Davis, *„One-Pot" Synthesis of 5-(Hydroxymethyl)furfural from Carbohydrates using Tin-Beta Zeolite*, ACS Catalysis, **2011**, *1*, 408-410

[Otomo2015] R. Otomo, T. Yokoi, T. Tatsumi, *Synthesis of isosorbide from sorbitol in water over high-silica aluminosilicate zeolites*, Applied Catalysis A: General, **2015**, *505*, 28-35

[Palkovitz2012] R. Palkovitz, A. M. Ruppert, K. Weinberg, *Hydrogenolysis Goes Bio -From Carbohydrates and Sugar Alcohols to Platform Chemicals*, Angewandte Chemie, **2012**, *51*, 2564-2601

[Palkovitz2014] K. Tajvidi, P. J. C. Hausoul, R. Palkovitz, *Hydrogenolysis of Cellulose over Cu-Based Catalysts – Analysis of the Reaction Network,* ChemSusChem, **2014**, *7*, 1311-1317

[Palkovitz2015] P. J. C. Hausoul, L. Negahdar, K. Schute, R. Palkovitz, *Unravelling the Ru-Catalyzed Hydrogenolysis of Biomass-Based Polyols under Neutral and Acidic Conditions*, ChemSusChem, **2015**, *8*, 3323-3330

[Pronin1987] Y. E. Kupsevich, O. G. Larionov, I. D. Stal'naya, L. A. Nakhapetyan, A. Y. Pronin, *Chromatographic Separation of Glucose and Fructose*, Russian Chemical Reviews, **1987**, *56 (3)*, 510-522

[Ravenelle2010] R. M. Ravenelle, F. Schüßler, A. D'Amico, N. Danilina, J. A. van Bokhoven, J. A. Lercher, C. W. Jones, C. Sievers, *Stability of Zeolites in Hot Liquid Water*, The Journal of Physical Chemistry C, **2010**, *114*, 19582-19595

[Rennovia2010] T. R. Boussie, E. L. Dias, Z. M. Fresco, V. J. Murphy, J. Shoemaker, R. Archer, H. Jiang, *Production of adipic acid and derivatives from carbohydrate-containing materials*, Rennovia Inc., Patent WO2010144862 A2, **2010**

[Rose2011] M. Rose, R. Palkovitz, *Cellulocse-Based Sustainable Polymers: State of the Art and Future Trends*, Macromolecular Rapid Communications, **2011**, *32 (17)*, 1299-1311

[Ruddlesden1981] J. F. Ruddlesden, A. Steward, D. J. Thompson, R. Whelan, *Diastereoselective Control in Ketose Hydrogenations with Supported Copper and Nickel Catalysts*, Faraday Discussions of the Chemical Society, **1981**, *72*, 397-411

[Schichtel2009] B. J. Schichtel, *Hydrierung von Isomaltulose und Fructose an Ruthenium-Träger-Katalysatoren im Batch- und Trickle-Bed-Reaktor*, Dissertation, TU Darmstadt, **2009**

[Schulz1950] H. Schulz, H. Wagner, *Synthese und Umwandlungsprodukte des Acroleins*, Angewandte Chemie, **1950**, *62 (5)*, 105-118

[Schuster1989] L. Schuster, W. Himmele, *Verfahren zur Herstellung niederer mehrwertiger Alkohole*, BASF Patent DE 3818198 A1, **1989**

[Sexton1982] B. A. Sexton, K. D. Rendulic, A. E. Huges, *Decomposition pathways of C1 to C4 alcohols adsorbed on platinum (111)*, **1982**, *121 (1)*, 181-198

[Shanks2014] M. R. Nolan, G. Sun, B. H. Shanks, *On the selective acid-catalysed dehydration of 1,2,6-hexanetriol*, Catalysis Science & Technology, **2014**, *4*, 2260-2266

[Shell1956] R. R. Whetstone, S. A. Ballard, *1,2,6-Hexanetriol*, Shell Dev., Patent US 2768213 (A), **1956**

[Shinmi2009] A. Shimao, S. Koso, N. Ueda, Y. Shinmi, I. Furikado, K. Tomishige, *Promoting Effect of Re Addition to Rh/SiO_2 on Glycerol Hydrogenolysis*, Chemistry Letters, **2009**, *38 (6)*, 540-541

[Shinmi2010] Y. Shinmi, S. Koso, T. Kubota, Y. Nakagawa, K. Tomishige, *Modification of Rh/SiO_2 catalyst for the hydrogenolysis of glycerol in water*, Applied Catalysis B: Environmental, **2010**, *94* (3-4), 318-326

[Südzucker1991] H. Fritz, M. Vogel, *Verfahren zur Herstellung eines glucose-, fructose- und saccharosearmen Inulooligosaccharid-Produktes*, Südzucker AG, Patent EP 0440074 B1, **1991**

[Südzucker1998] H. Degelmann, J. Kowalczyk, M. Kunz, M. Schüttenhelm, *Verfahren zur Hydrierung von Zuckern*, Südzucker AG, Patent EP 0854148 A1, **1998**

[Südzucker2011] Geschäftsbericht Südzucker AG 2010/11, p.59, **2011**

[Synvina2017] P. Schiffer, *Synvina – The Joint Venture of BASF and Avantium*, Bio-Based World Quarterly, **2017**, *Issue #6*

[Szedlacsek2013] H. Szedlacsek, Dissertation, TU Darmstadt, **2013**, p. 68

[Tess1957] R. W. Tess, R. D. Harline, T. F. Mika, *1,2,6-Hexanetriol in Alkyd Resins*, Industrial & Engineering Chemistry Research, **1957**, *49 (3)*, 374-378

[Titirici2008] M.-M. Titirici, M. Antonietti, N. Baccile, *Hydrothermal carbon from biomass: a comparison of the local structure from poly- to monosaccharides and pentoses/hexoses*, Green Chemistry, **2008**, *10*, 1204-1212

[Tomishige2011] Y. Amada, Y. Shinmi, S. Koso, K. Tomishige, *Direct hydrogenolysis of 1,3-propanediol over Ir-ReO_x/SiO_2 catalyst*, Applied Catalysis B: Environmental, **2011**, *105*, 117-127

[Tomishige2012] Y. Amada, H. Watanabe, M. Tamura, Y. Nakagawa, K. Okumura, K. Tomishige, *Structure of ReO_x clusters attached on the Ir metal surface in Ir-ReO_x/SiO_2 for the hydrogenolysis reaction*, The Journal of Physical Chemistry C, **2012**, *116*, 23503-23514

[Tomishige2013] K. Chen, M. Tamura, Z. L. Yuan, Y. Nakagawa, K. Tomishige, *One-pot conversion of sugar and sugar polyols to n-alkanes without C-C- dissociation over the Ir-ReO_x/SiO_2 catalyst combined with H-ZSM-5*, ChemSusChem, **2013**, *6*, 613-621

[Tomishige2014] K. Tomishige, M. Tamura, Y. Nakagawa, *Role of Re Species and Acid Cocatalyst on Ir-ReO_x/SiO_2 in the C-O Hydrogenolysis of Biomass-Derived Substrates*, The Chemical Record, **2014**, *14 (6)*, 1041-1054

[Tomishige2017] K. Tomishige, Y. Nakagawa, M. Tamura, *Selective hydrogenolysis and hydrogenation using metal catalysts directly modified with metal oxide species*, Green Chemistry, **2017**, *19*, 2876-2924

[VDI1994] VDI-Wärmeatlas (VDI heat atlas), H. Kurt, 7. Auflage, VDI-Verlag GmbH, Düsseldorf, **1994**, p. Db 5

[Vilcocq2013] L. Vilcocq, A. Cabiac, C. Especel, E. Guillon, D. Duprez, *Transformation of Sorbitol to Biofuels by Heterogeneous Catalysis: Chemical and Industrial Considerations*, Oil & Gas Science and Technology – Rev. IFP Energies nouvelles, **2013**, *68* (5), 841-860

[Vilcocq2014] L. Vilcocq, A. Cabiac, C. Especel, S. Lacombe, D. Duprez, *New insights into the mechanism of sorbitol transformation over an original bifunctional catalytic system*, Journal of Catalysis, **2014**, *320*, 16-25

[Vogel2002] H. Vogel, *Verfahrensentwicklung*, Wiley-VCH, Weinheim, **2002**

[Vogel2005] M. Bicker, S. Endres, L. Ott, H. Vogel, *Catalytic conversion of carbohydrates in subcritical water: A new chemical process for lactic acid production*, Journal of Molecular Catalysis A: Chemical, **2005**, *239* (1-2), 151-157

[Vogel2014] H. Vogel, *Chemie erneuerbarer kohlenstoffbasierter Rohstoffe zur Produktion von Chemikalien und Kraftstoffen,* Chemie Ingenieur Technik, **2014**, *86*, 1-16

[Wang1995] K. Wang, M. C. Hawley, T. D. Furney, *Mechanism Study of Sugar and Sugar Alcohol Hydrogenolysis Using Diol Model Compounds,* Industrial & Engineering Chemistry Research, **1995**, 34 (11), 3766-3770

[Wang2010] S. Wang, Y. Zhang, H. Liu, *Selective Hydrogenolysis of Glycerol to Propylene Glycol on Cu-ZnO Composite Catalysts: Structural Requirements and Reaction Mechanism*, Chemistry an Asian Journal, **2010**, *5* (5), 1100-1111

[Wang2016] J. Xi, Q. Xia, Y. Shao, D. Ding, P. Yang, X. Liu, G. Lu, Y. Wang, *Production of hexane from sorbitol in aqueous medium over Pt/NbOPO$_4$ catalyst,* Applied Catalysis B: Environmental, **2016**, *181*, 699-706

[Werpy2004] T. Werpy, G. Peterson, Top Value Added Chemicals from Bio-mass. Results of Screening for Potential Candidates from Sugars and Synthesis Gas, Vol. 1, US Department of Energy, **2004**.

[Yamaguchi2014] A. Yamaguchi, O. Sato, N. Mimura, M. Shirai, *Intramolecular dehydration of mannitol in high-temperature liquid water without acid catalysts*, RSC Advances, **2014**, *4*, 45575-45578

[Zartman1933] W. H. Zartman, H. Adkins, *Hydrogenolysis of Sugars,* Journal of the American Chemical Society, **1933**, *55 (11)*, 4559-4563

[Zevnik1963] F. C. Zevnik, R. L. Buchanan, *Generalized correlation of process investment*, Chemical Engineering Progress, **1963**, *59* (2), 70-78

[Zhang2014] Q. Zhang, T. Wang, Y. Xu, Q. Zhang, L. Ma, *Production of liquid alkanes by controlling reactivity of sorbitol hydrogenation with a Ni/HZSM-5 catalyst in water*, Energy Conversion and Management, **2014**, *77*, 262-268

[Zhang2016] J. Zhang, F. Lu, W. Yu, R. Lu, J. Xu, *Effects of alkaline additives on the formation of lactic acid in sorbitol hydrogenolysis over Ni/C catalyst*, Chinese Journal of Catalysis, **2016**, *37*, 177-183

[Zhao2010] L. Zhao, J. H. Zhou, Z. J. Sui, X. G. Zhou, *Hydrogenolysis of sorbitol to glycols over carbon nanofibers supported on ruthenium catalyst*, Chemical Engineering Science, **2010,** *65*, 30-35

[Zhou2010] Z. Zhou, X. Li, T. Zeng, W. Hong, Z. Cheng, W. Yuan, *Kinetics of Hydrogenolysis of Glycerol to Propylene Glycol over Cu-ZnO-Al_2O_3 Catalysts*, Chinese Journal of Chemical Engineering, **2010**, *18* (3), 384-390

[Zhu2014] Y. Zhu, X. Kong, X. Li, G. Ding, Y. Zhu, Y.-W. Li, *Cu Nanoparticles Inlaid Mesoporous Al_2O_3 As a High-Performance Bifunctional Catalyst for Ethanol Synthesis via Dimethyl Oxalate Hydrogenation*, ACS Catalysis, **2014**, *4* (10), 3612-3620

9. Appendix

9.1. Identification of deoxygenated reaction intermediates with combined ^{13}C-NMR, GC, GC-MS, and HPLC analysis

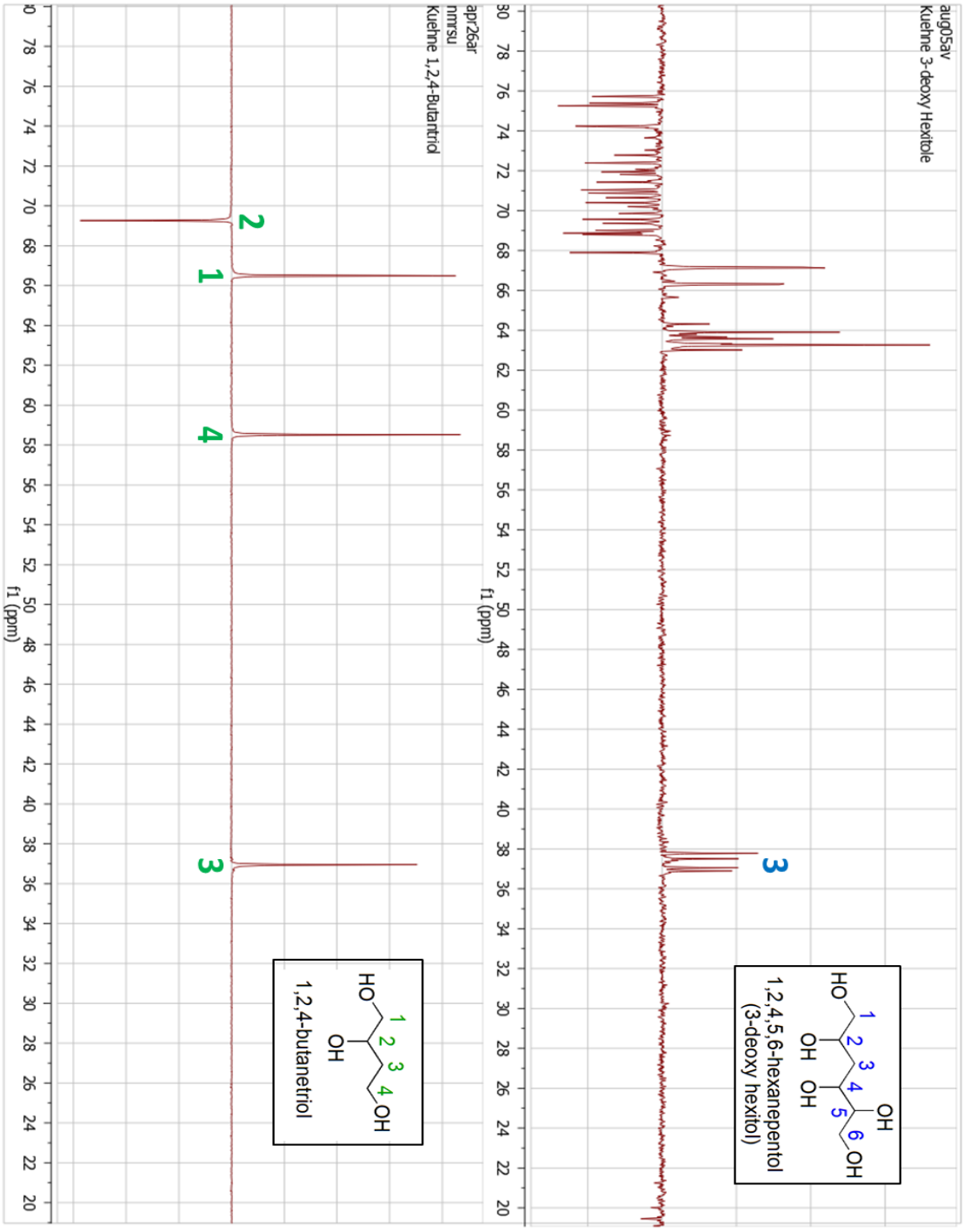

Figure 9-1: Identification of 3-deoxy hexitols (1,2,4,5,6-hexanepentols) by ^{13}C-NMR analysis (DEPT) in comparison with 3-deoxy tetritols (1,2,4-butanetriol, a standard purchased from Sigma-Aldrich as reference). Carbon atoms with one or three C-H bonds are facing down from the base line, while carbon atoms with two C-H bonds face upwards. The 3-deoxy hexitol shows four different isomeric carbon atoms at the 3-position that result from three chiral carbon atoms ($3^2 = 8$ diastereomers: however, enantiomers are not separated which results in four visible diastereomers). The corresponding GC chromatogram is shown in **Figure 9-2**.

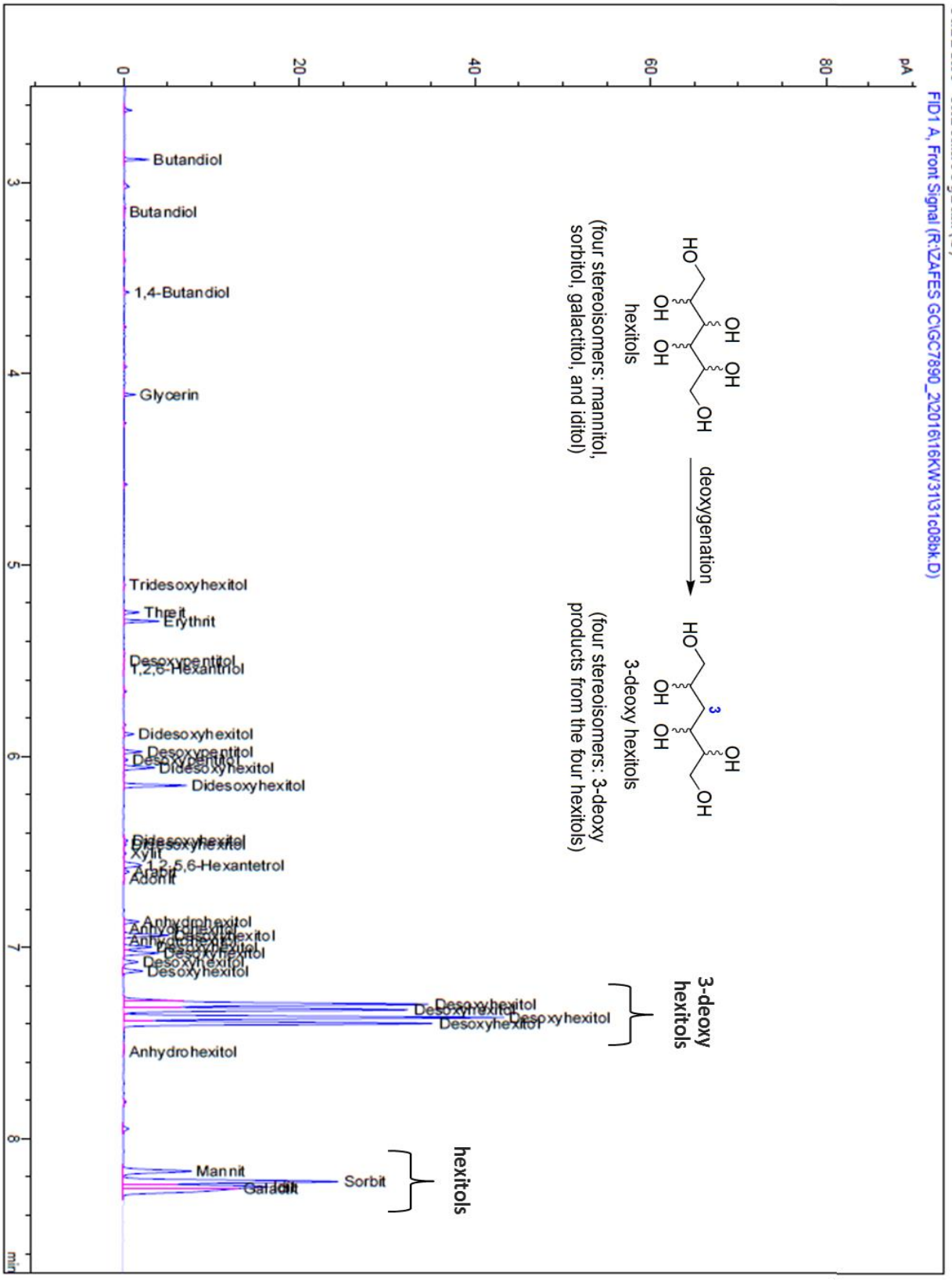

Figure 9-2: GC chromatogram of the polyol mixture that was analyzed by NMR analysis for identification of the 3-deoxy hexitols (1,2,4,5,6-hexanepentols). The polyol mixture was isolated by chromatography from a reaction mixture resulting from hydrogenolysis of sorbitol using a Cu-Raney catalyst at 180 °C, 150 bar H_2 and 5 h reaction time (**Figure 9-3**). Four different monodeoxy hexitols are detected at about 7.4 min retention time, which are identified as 3-deoxy hexitols by ^{13}C-NMR analysis (see **Figure 9-1**).

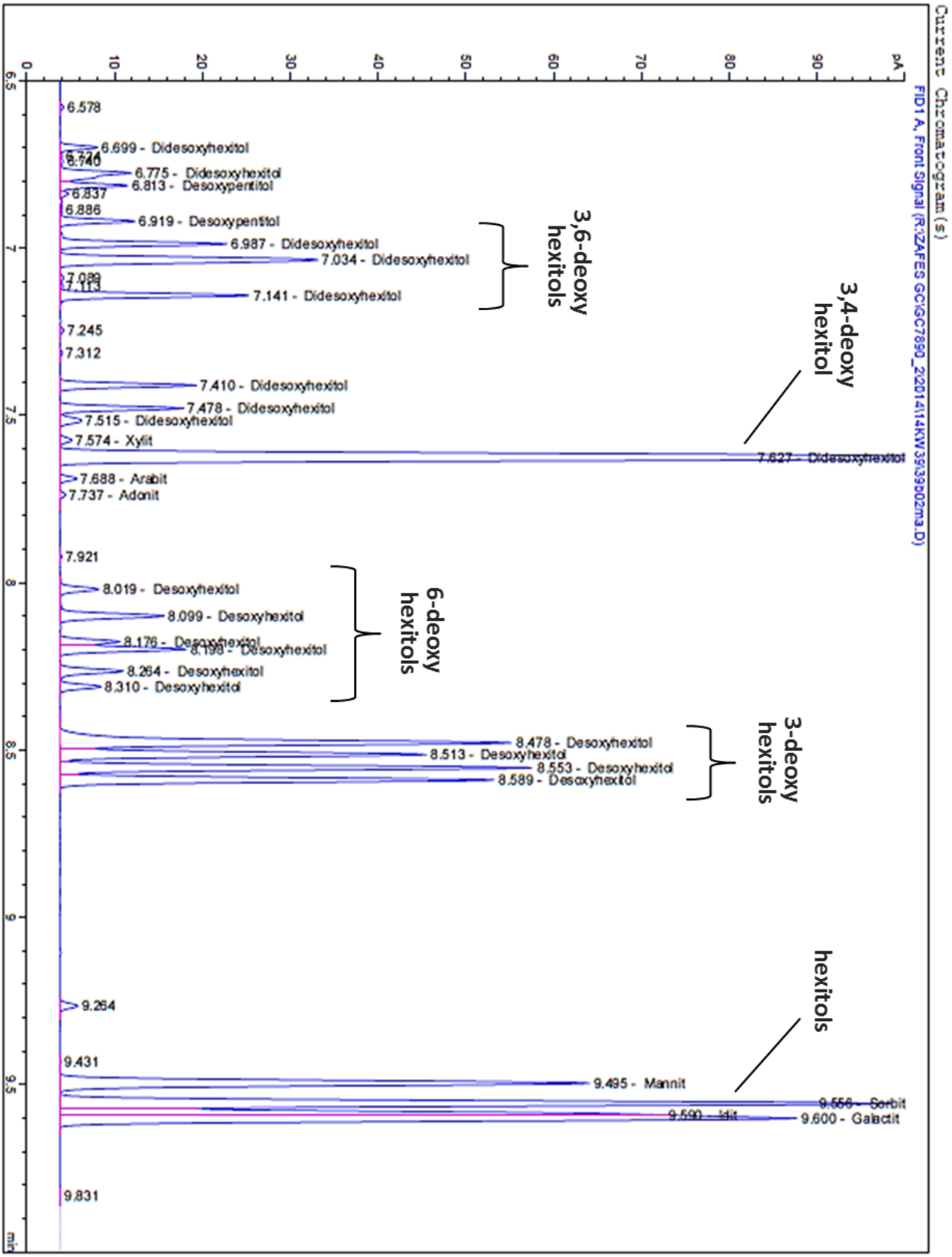

Figure 9-3: GC chromatogram for the conversion of mannitol over Cu-Raney at 180 °C, 150 bar H_2 and 5 h reaction time. Four stereoisomers of 3-deoxy hexitols (1,2,4,5,6-hexanepentols) are detected at a retention time of 8.5 to 8.6 min. Six stereoisomers of 6-deoxy hexitols (1,2,3,4,5-hexanepentols) are detected at 8.0 to 8.3 min. The same 6-deoxy stereoisomers are obtained from rhamnose hydrogenation as shown in **Figure 9-4**.

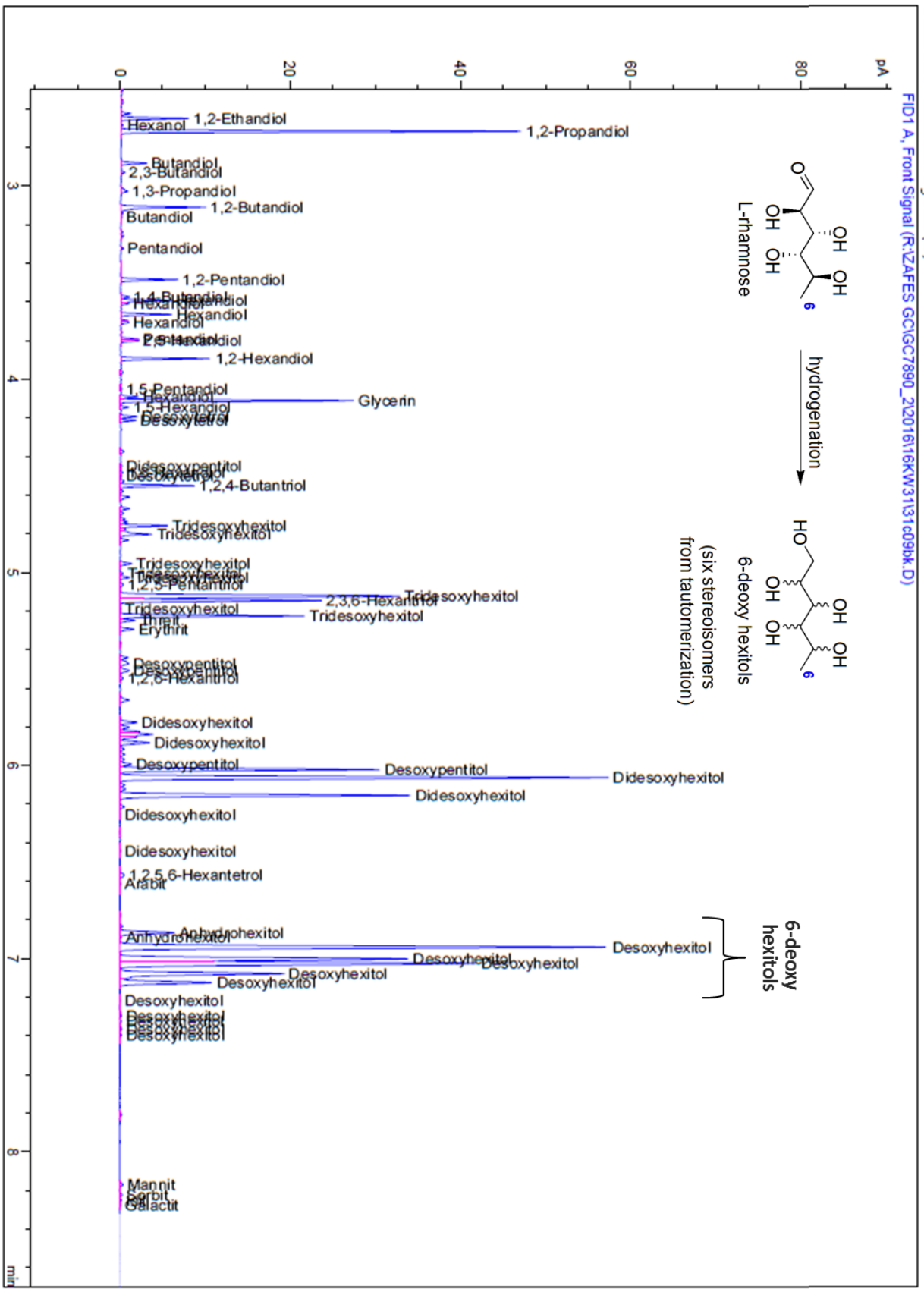

Figure 9-4: GC chromatogram of the product mixture obtained from rhamnose hydrogenation to 6-deoxy hexitols (1,2,3,4,5-hexanepentols, catalyst: Cu-Raney at 70 °C and 150 bar H_2) and subsequent hydrogenolysis at 180 °C, 150 bar H_2 and 5 h reaction time. Six different stereoisomers of 6-deoxy hexitols are formed from the 6-deoxy sugar rhamnose.

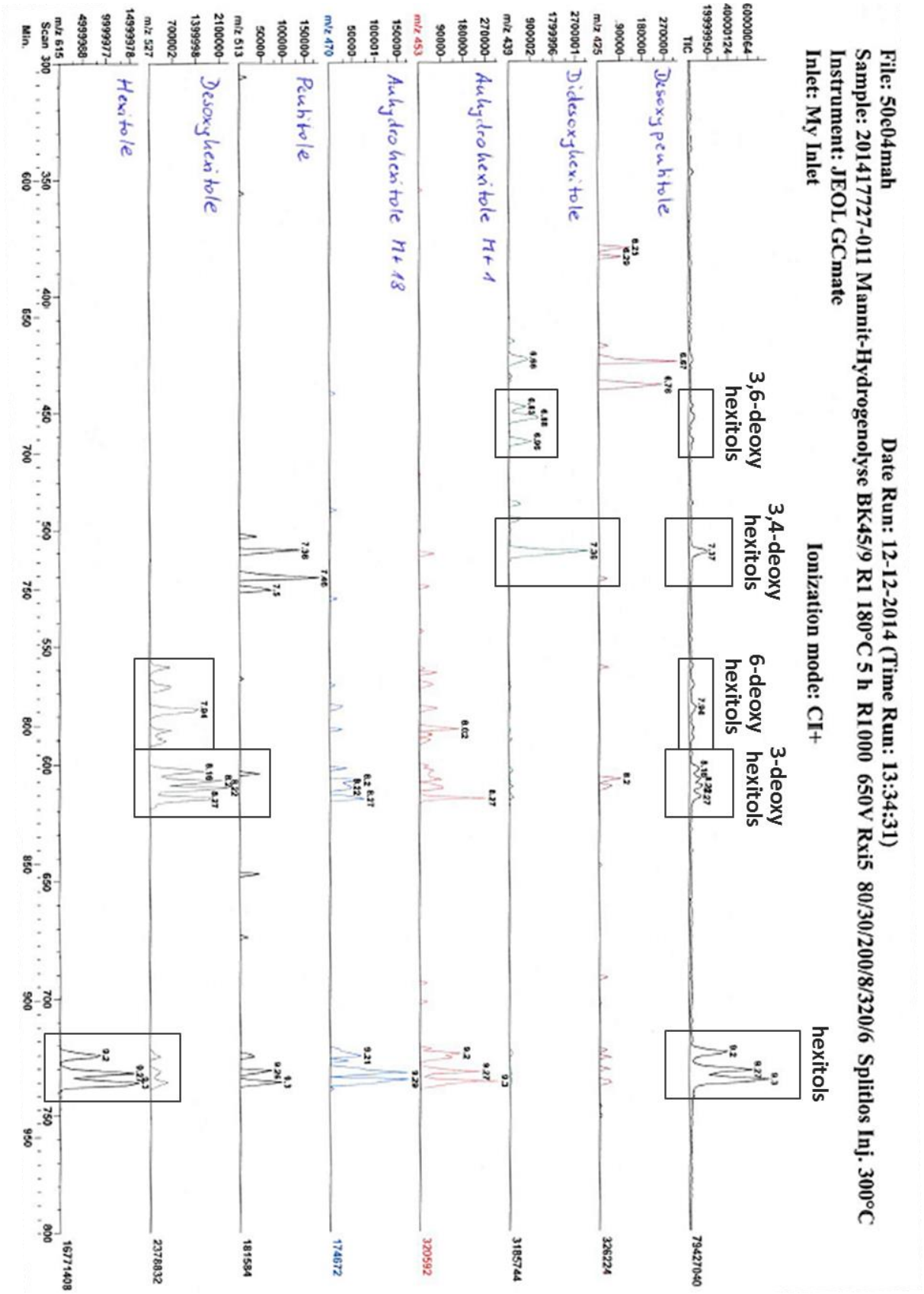

Figure 9-5: GC-MS analysis of the polyol mixture shown in **Figure 9-3**. 3-deoxy and 6-deoxy hexitols (labeled as Desoxy-hexitole) are detected with a mass-to-charge-ratio of 527 m/z which accounts for the M+1 form (with an added proton) of the TMS-derivatives (see chapter 4.1 for silylation). The M+1 species of the 3,4-deoxy and 3,6-deoxy hexitols (as Didesoxyhex-itole) are detected with a 439 m/z ratio.

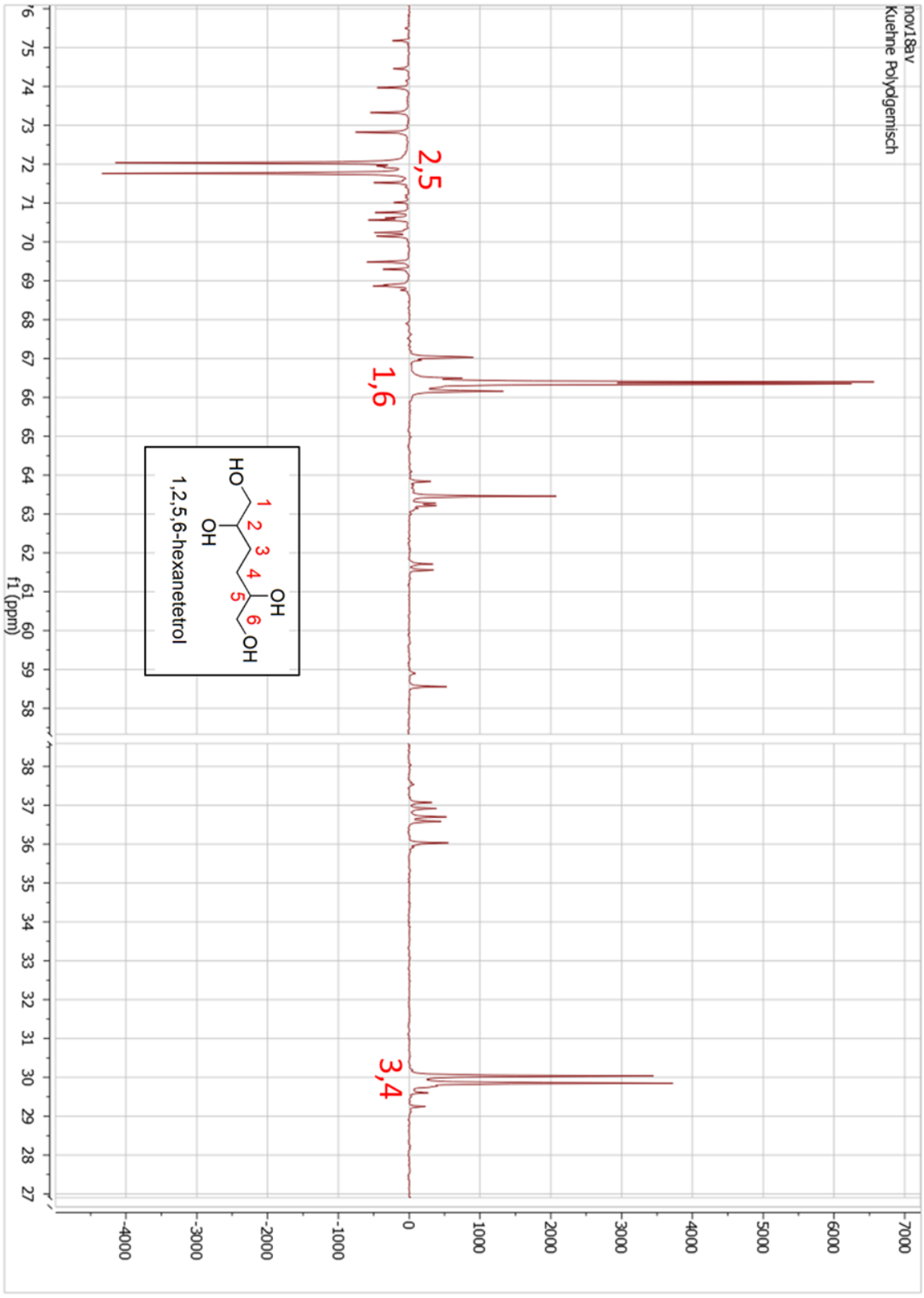

Figure 9-6: Identification of the 3,4-dideoxy hexitol (1,2,5,6-hexanetetrol) by ^{13}C-NMR analysis (DEPT). Carbon atoms with one or three C-H bonds are facing down from the base line, while carbon atoms with two C-H bonds face upwards. The 1,2,5,6-hexanetetrol shows two different isomeric carbon atoms for each position in the molecule that result from two chiral carbon atoms ($2^2 = 4$ diastereomers: however, enantiomers are not separated which results in two visible diastereomers). The GC chromatogram is shown in **Figure 9-7**.

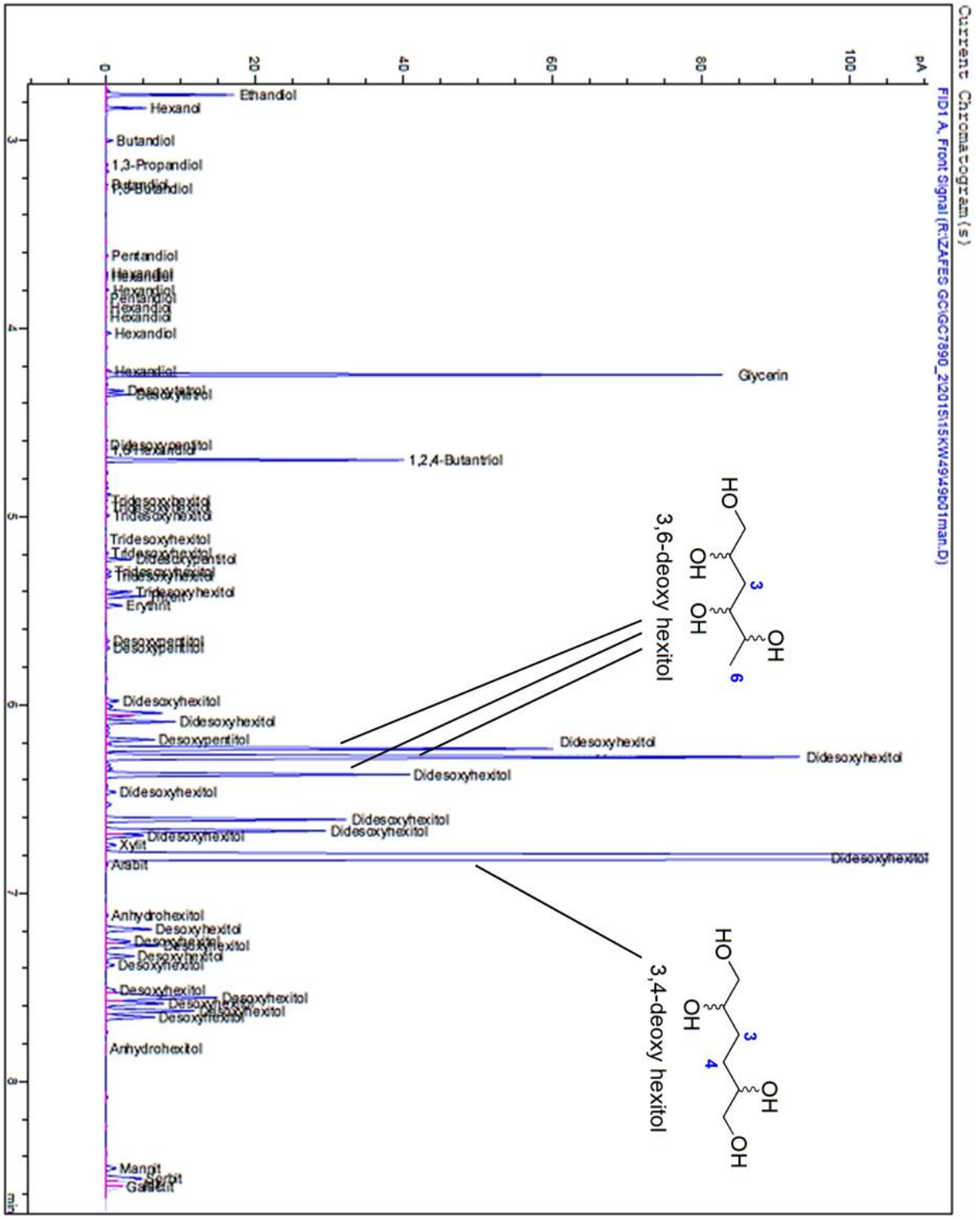

Figure 9-7: GC chromatogram of the polyol mixture that was analyzed by NMR analysis for identification of the 3,4-deoxy hexitols (1,2,5,6-hexanetetrol). The polyol was isolated by chromatography from a reaction mixture resulting from hydrogenolysis of sorbitol using a Cu-Raney catalyst at 180 °C, 150 bar H_2 and 40 h reaction time. The 3,4-deoxy hexitol (1,2,5,6-hexanetetrol) is detected at a retention time of 6.8 min and was identified by NMR analysis as shown in **Figure 9-6**.

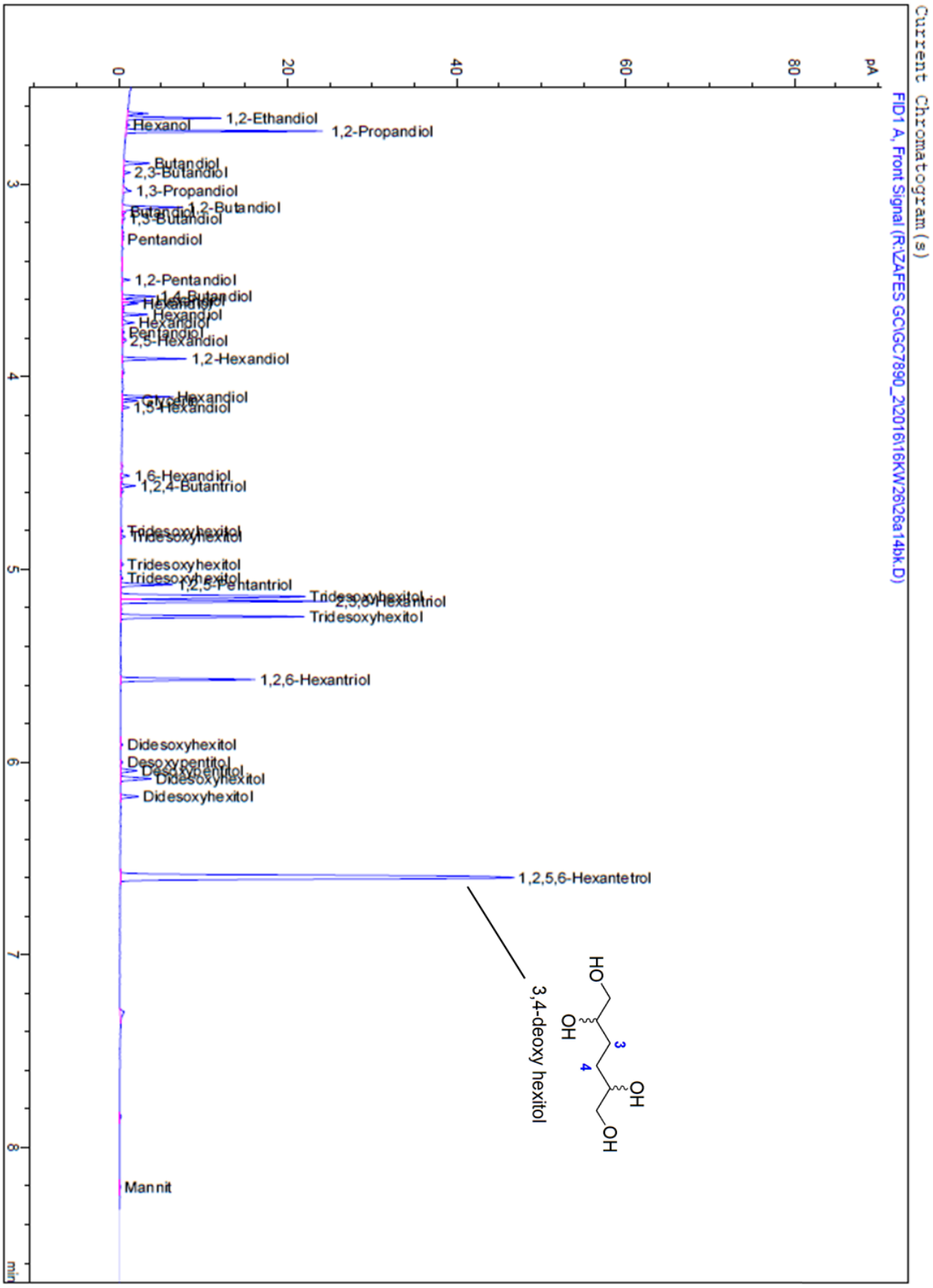

Figure 9-8: GC chromatogram for the conversion of mannitol over Cu-Raney at 180 °C, 150 bar H_2 and 40 h reaction time. The 3,4-deoxy hexitol (1,2,5,6-hexanetetrol) is detected at a retention time of 6.6 min. The polyol mixture shown in **Figure 9-7** was obtained by chromatographic separation from this aqueous polyol solution.

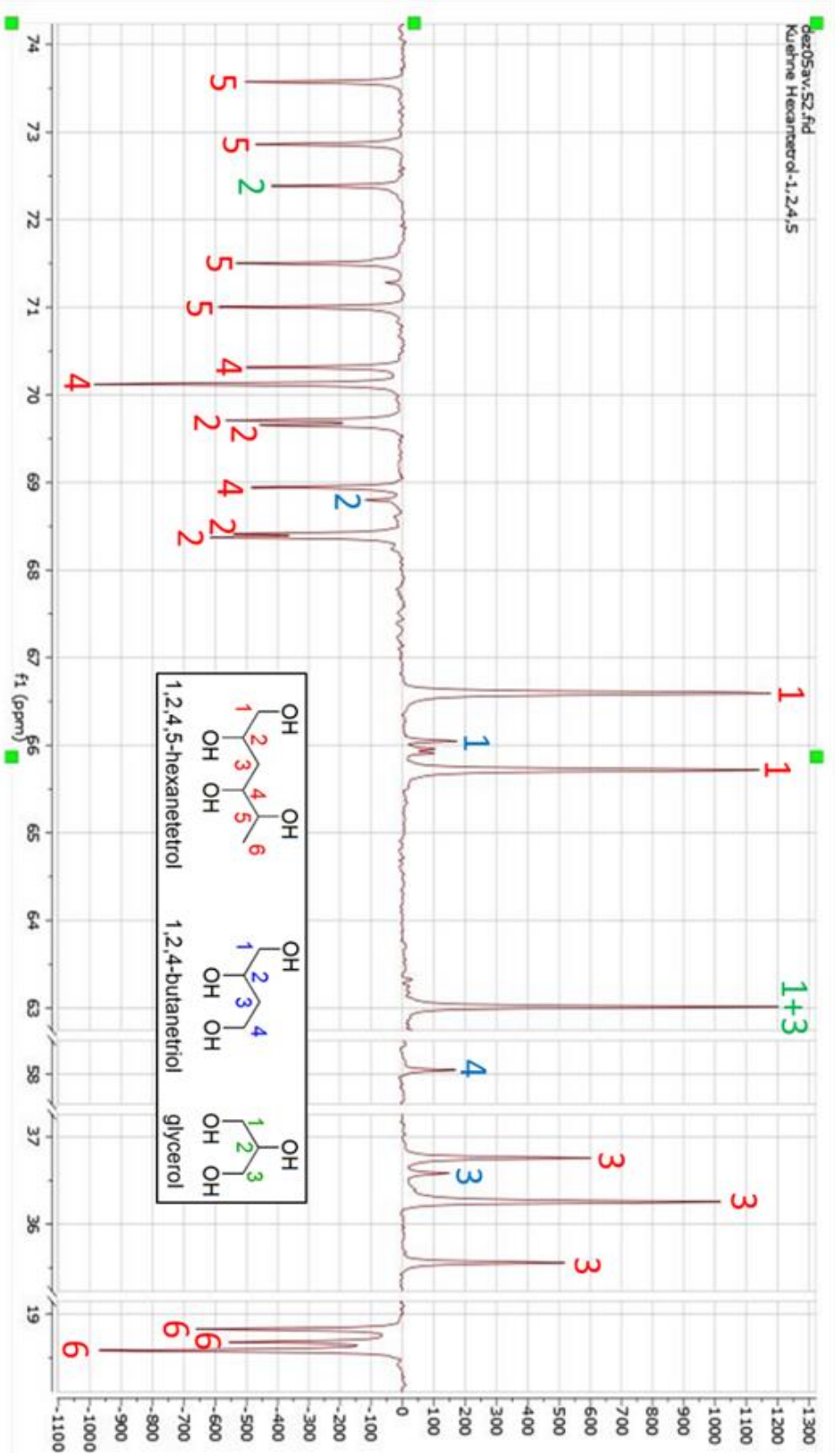

Figure 9-9: Identification of the 3,6-dideoxy hexitol (1,2,4,5-hexanetetrol) along with 1,2,4-butanetriol and glycerol by ^{13}C-NMR analysis (DEPT). Carbon atoms with one or three C-H bonds are facing down from the base line, while carbon atoms with two C-H bonds face upwards. 1,2,4,5-hexanetetrol shows four different isomeric carbon atoms for each position in the molecule that result from three chiral carbon atoms (2^3 = 8 diastereomers: however, enantiomers are not separated which results in four visible diastereomers). The GC chromatogram is shown in **Figure 9-10**.

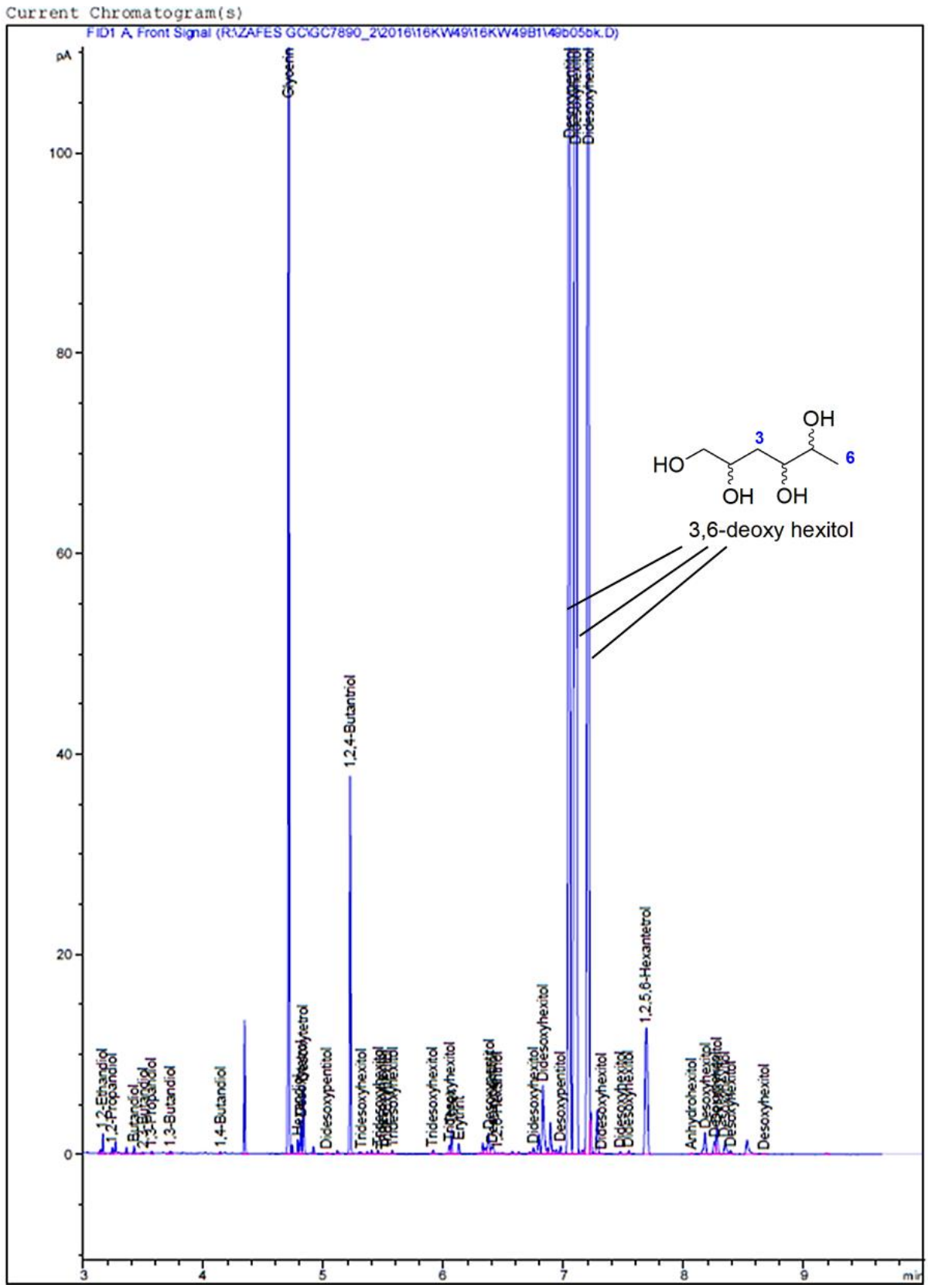

Figure 9-10: GC chromatogram of the polyol mixture that was analyzed by NMR analysis for identification of the 3,6-deoxy hexitols (1,2,4,5-hexanetetrols). The polyols were isolated by chromatography from a reaction mixture resulting from hydrogenolysis of rhamnose over a Cu-Raney catalyst at 180 °C, 150 bar H_2 and 20 h reaction time. The 3,6-deoxy hexitols are detected at a retention time of 7.0 to 7.2 min and were identified by NMR analysis as shown in **Figure 9-9**.

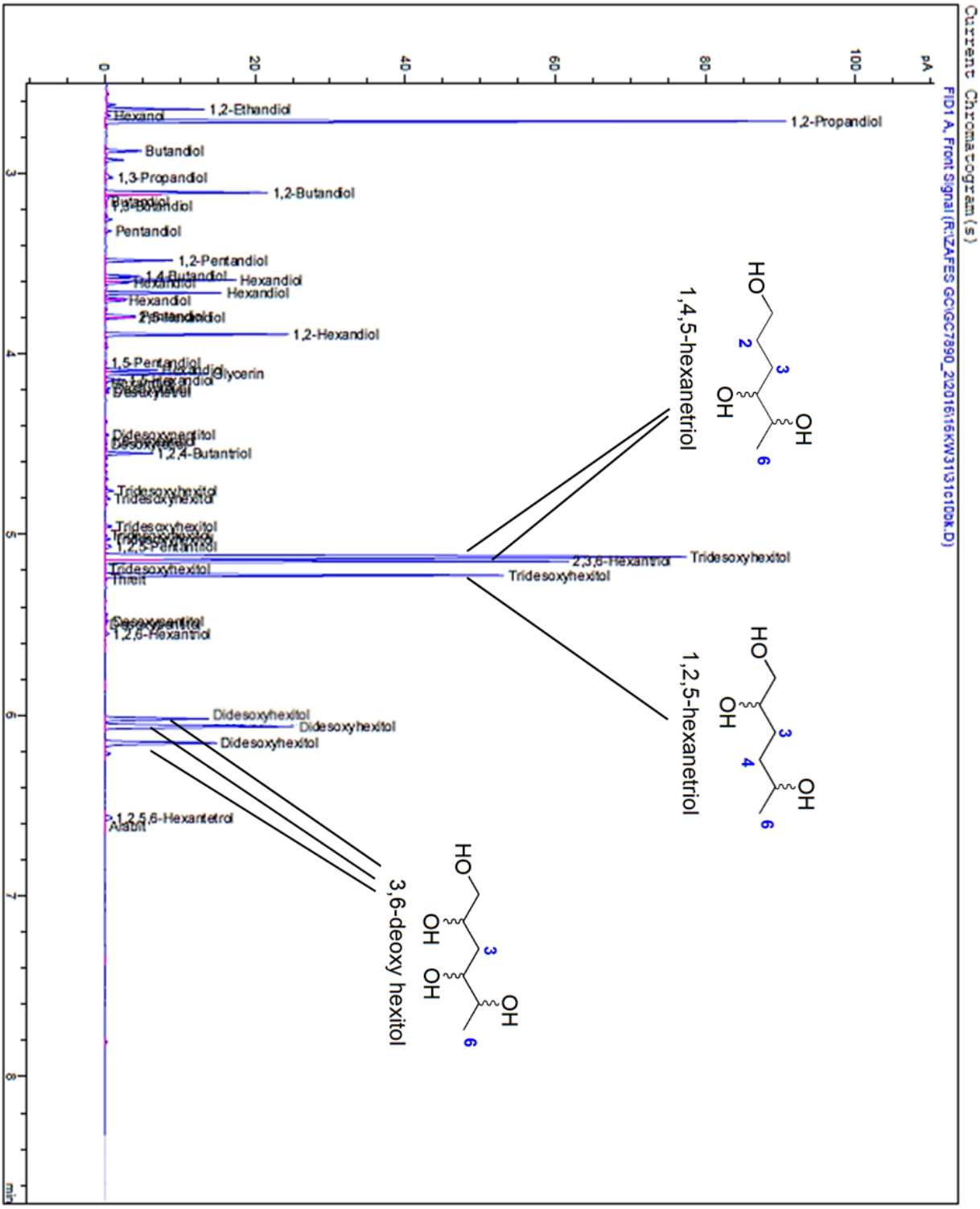

Figure 9-11: GC chromatogram for a polyol solution obtained from rhamnose hydrogenolysis over Cu-Raney at 180 °C, 150 bar H_2 and 20 h reaction time. Three peaks for 3,6-deoxy hexitols (1,2,4,5-hexanetetrols) are detected at a retention time of 6.0 to 6.2 min. The peak in the middle is twice as large as the two others which is a clear indication that two stereoisomers are co-eluted which means that four stereoisomers are formed. This is in line with the detected four stereoisomers in NMR analysis as shown in **Figure 9-9**. The same three 3,6-deoxy hexitols are obtained as intermediate products from hexitols (**Figure 9-3** and **Figure 9-5**).

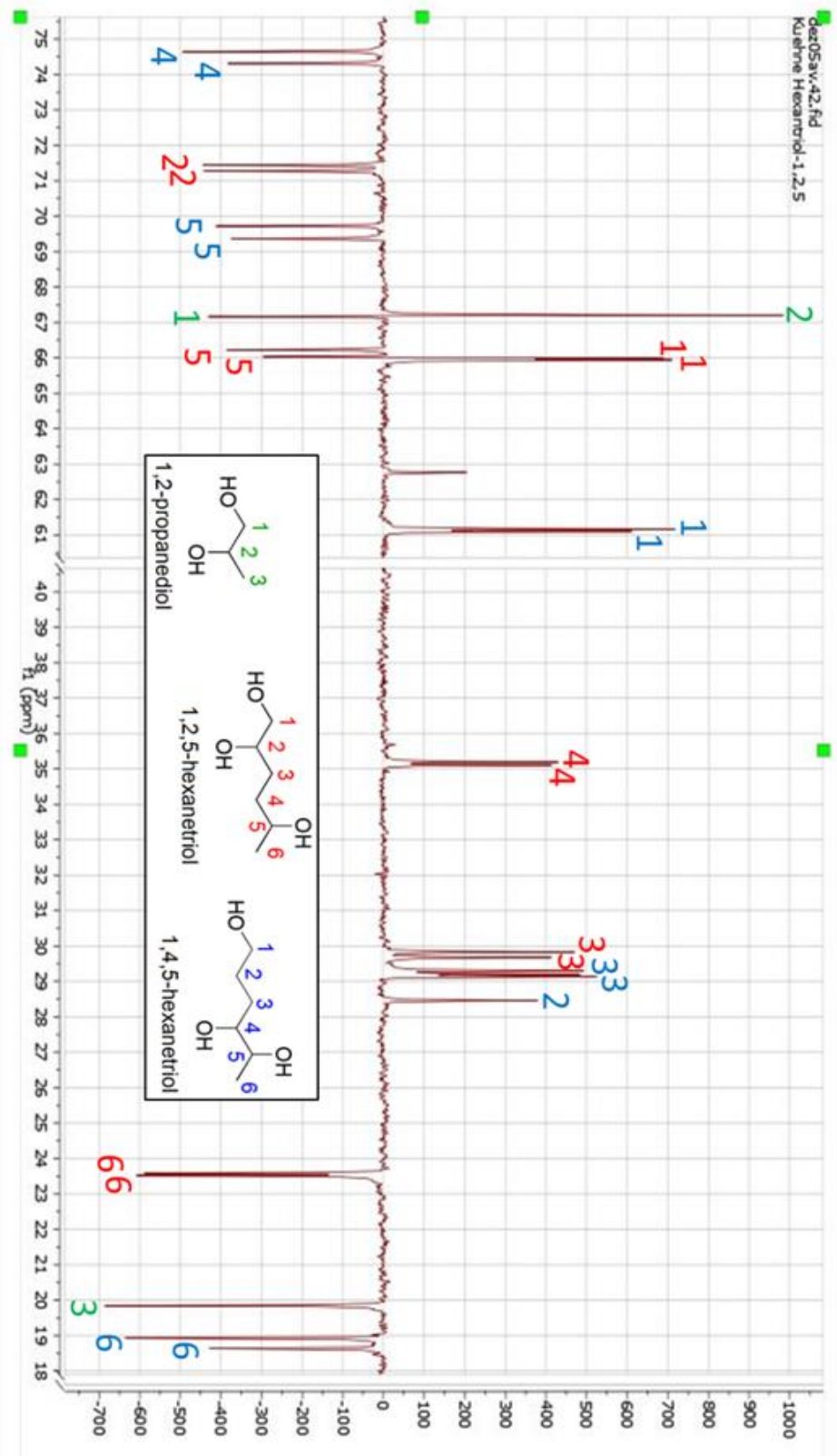

Figure 9-12: Identification of the two hexanetriol isomers 1,2,5-hexanetriol and 1,4,5-hexanetriol along with 1,2-propanediol by ^{13}C-NMR analysis (DEPT). Carbon atoms with one or three C-H bonds are facing down from the base line, while carbon atoms with two C-H bonds face upwards. Both hexanetriols show two different isomeric carbon atoms for each position in the molecule that result from two chiral carbon atoms ($2^2 = 4$ diastereomers: however, enantiomers are not separated which results in two visible diastereomers). The GC chromatogram is shown in **Figure 9-13**.

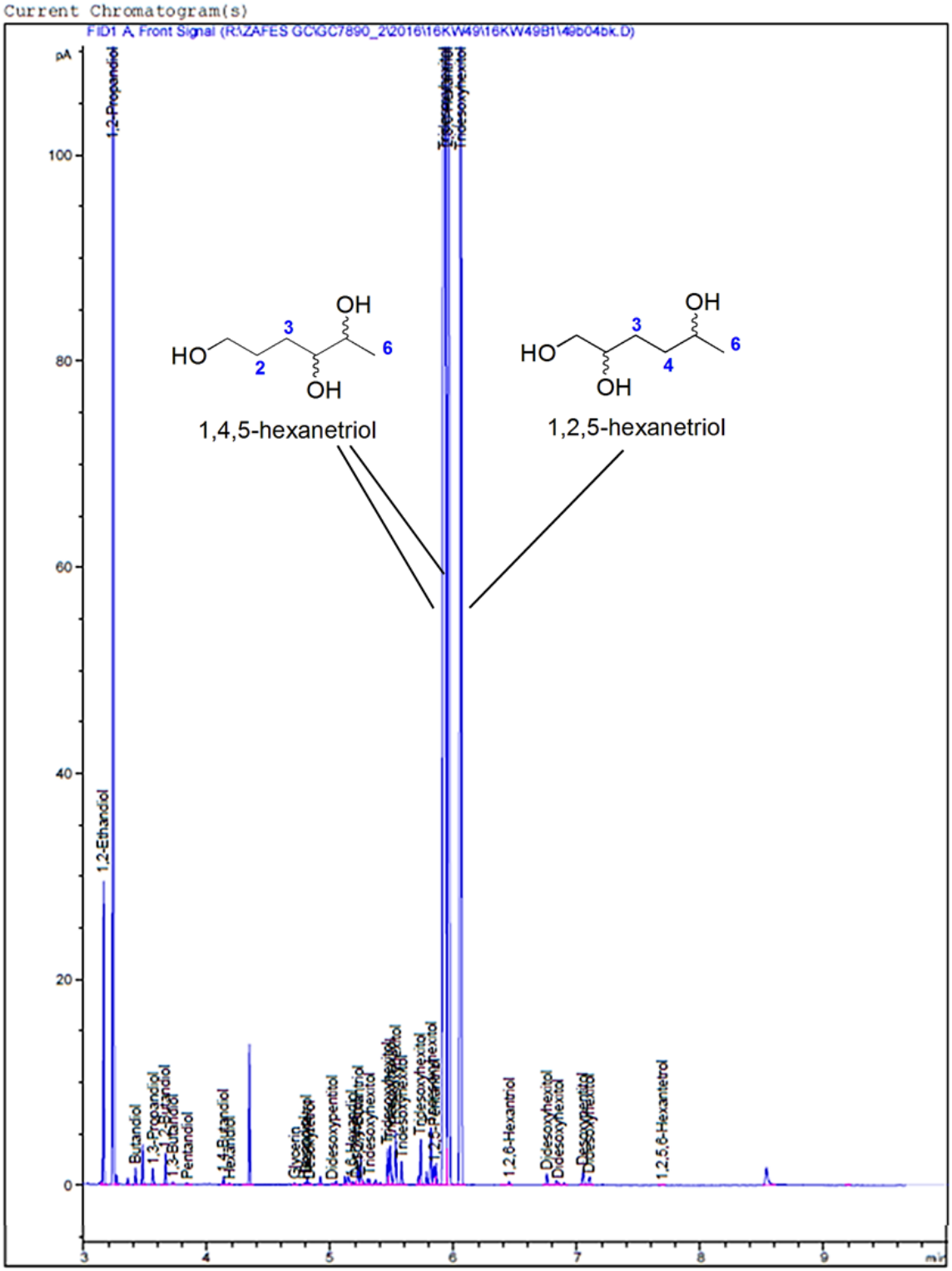

Figure 9-13: GC chromatogram of the polyol mixture that was analyzed by NMR analysis for identification of the 1,2,5- and 1,4,5-hexnaetriols. The polyols were isolated by chromatography from a reaction mixture resulting from mannitol hydrogenolysis over Cu-Raney at 180 °C, 150 bar H_2 and 40 h (**Figure 9-8**). The hexanetriols are detected at a retention time of 5.9 to 6.1 min and were identified by NMR analysis as shown in **Figure 9-12**. Three peaks are detected, similar to the reaction mixture shown in **Figure 9-8** at a retention time of 5.2 min. The first two peaks are partly co-eluted (no base line separation) which indicates that the two compounds are stereoisomers. **Figure 9-14** and **Figure 9-15** show that the co-eluted stereoisomers are the 1,4,5-hexanetriol.

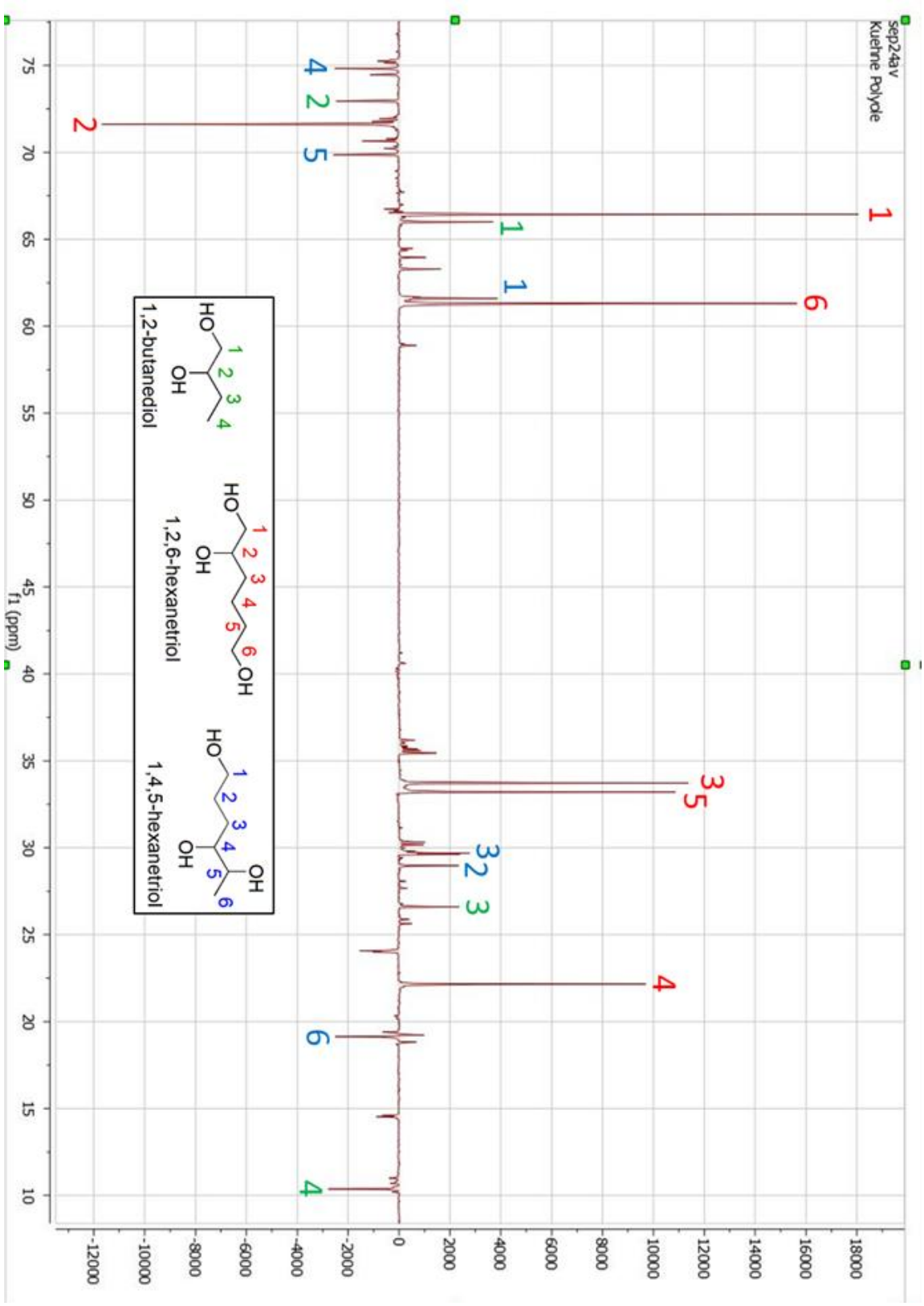

Figure 9-14: Identification of the two hexanetriol isomers 1,2,6-hexanetriol and 1,4,5-hexanetriol along with 1,2-butanediol by ^{13}C-NMR-analysis (DEPT). Carbon atoms with one or three C-H bonds are facing down from the base line, while carbon atoms with two C-H bonds face upwards. The GC chromatogram is shown in **Figure 9-13**.

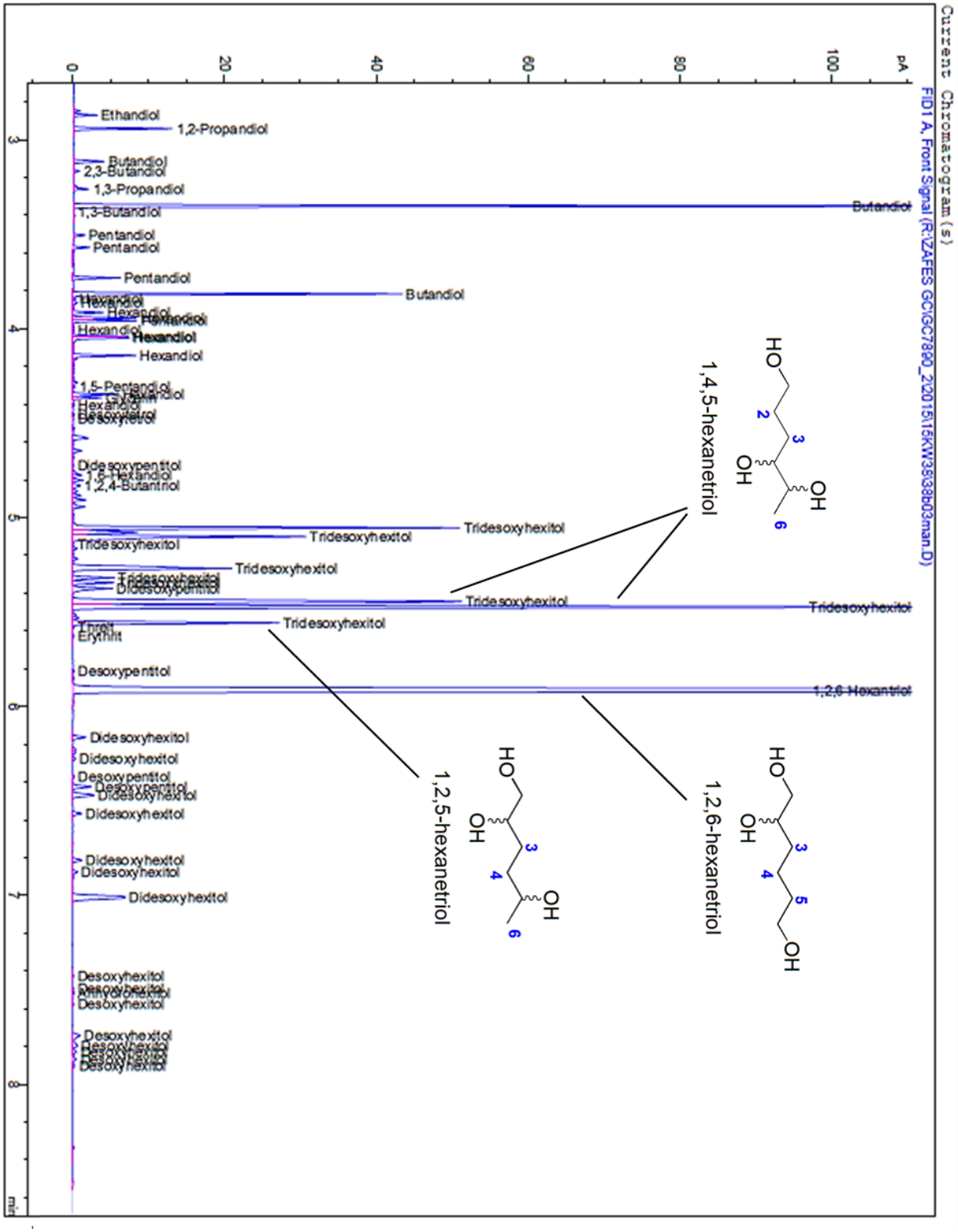

Figure 9-15: GC chromatogram of the polyol mixture that was analyzed by NMR analysis for identification of the 1,2,6- and 1,4,5-hexanetriols (**Figure 9-15**). The polyols were isolated by chromatography from a reaction mixture resulting from hydrogenolysis of mannitol using a Cu-Raney catalyst at 180 °C, 150 bar H_2 and 40 h reaction time as shown in **Figure 9-8**. 1,4,5- and 1,2,6-hexanetriols are the main components and detected at a retention time of about 5.5 and 5.9 min, respectively. The 1,2,6-hexanetriol was identified using a standard reference, purchased from Sigma-Aldrich.

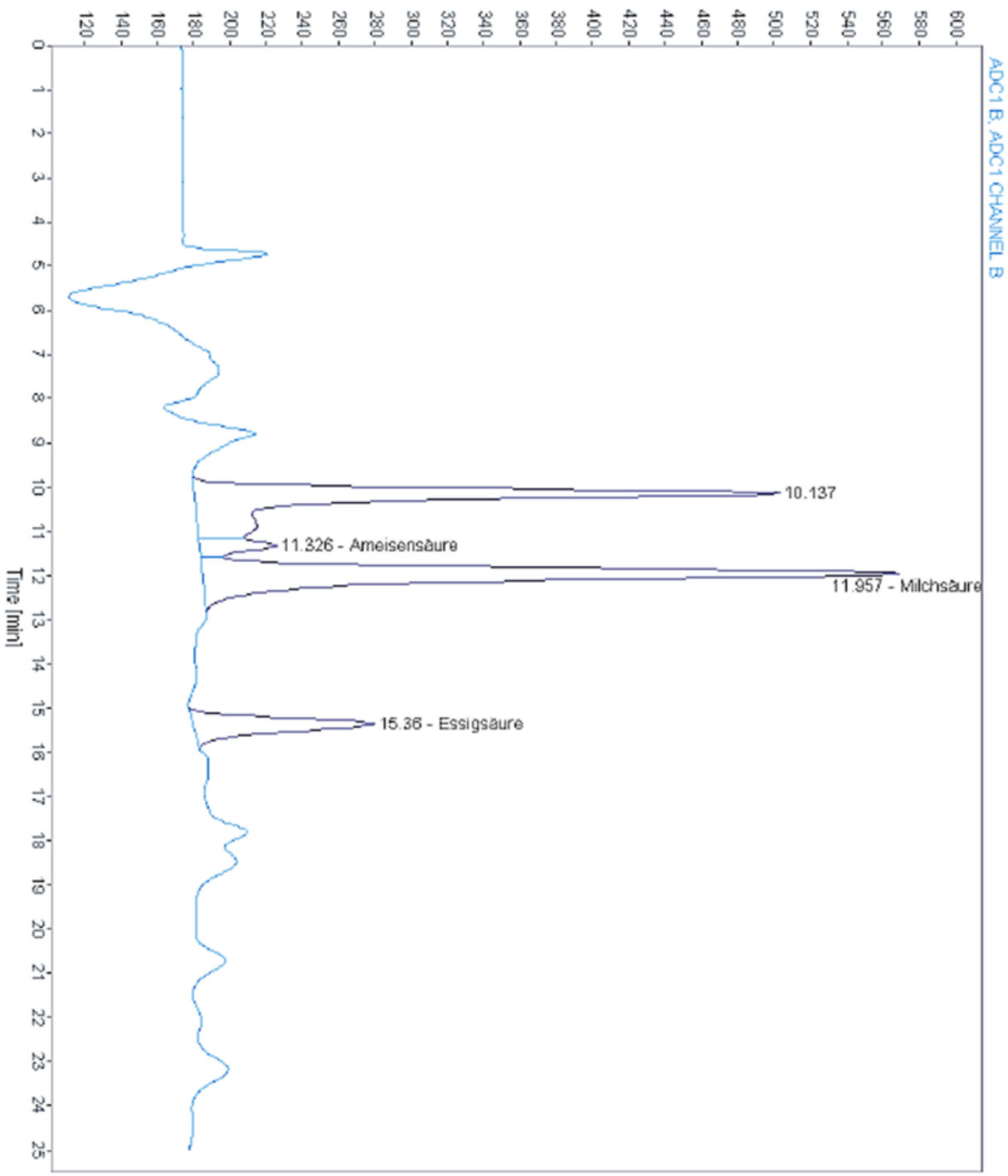

Figure 9-16: Verification of formic acid (at 11 min retention time), acetic acid (15,5 min), and lactic acid formation (12 min) with HPLC-analysis. One additional unidentified acid is detected at a retention time of 10 min. The product mixture was obtained from mannitol hydrogenolysis over Cu-Raney at 180 °C without H_2 atmosphere (instead 25 bar N_2 were used) and 5 h reaction time.

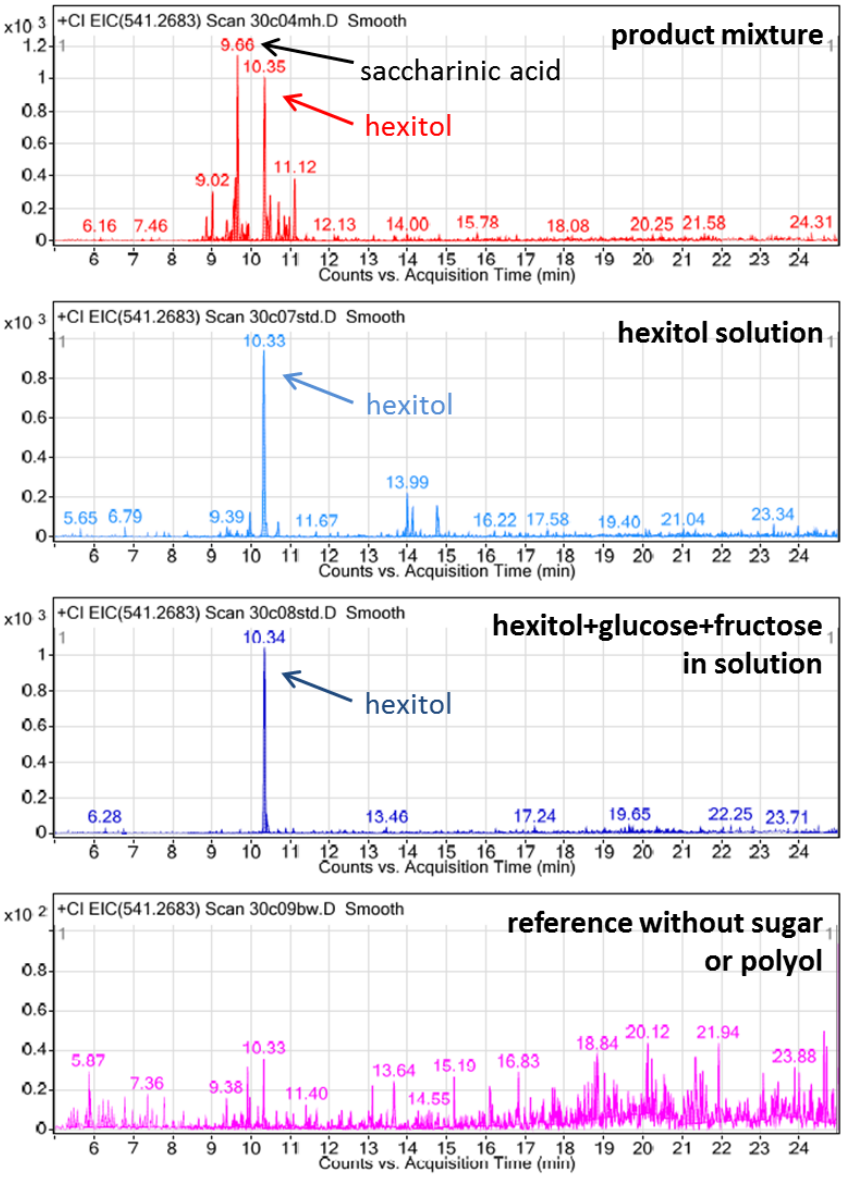

Figure 9-17: Identification of saccharinic acids with a mass of 541,2 m/z for the TMS-derivated molecule (OH-groups protected with trimethylsilyl-groups, see chapter 4.1) via GC-MS. The mass-to-charge-ratio only fits a deoxygenated aldonic acid (saccharinic acid, M+1 ion after addition of a proton) and is only detected in the product mixture. Hence, formation of an unknown artifact from hexitols or sugars such as glucose or fructose can be excluded.

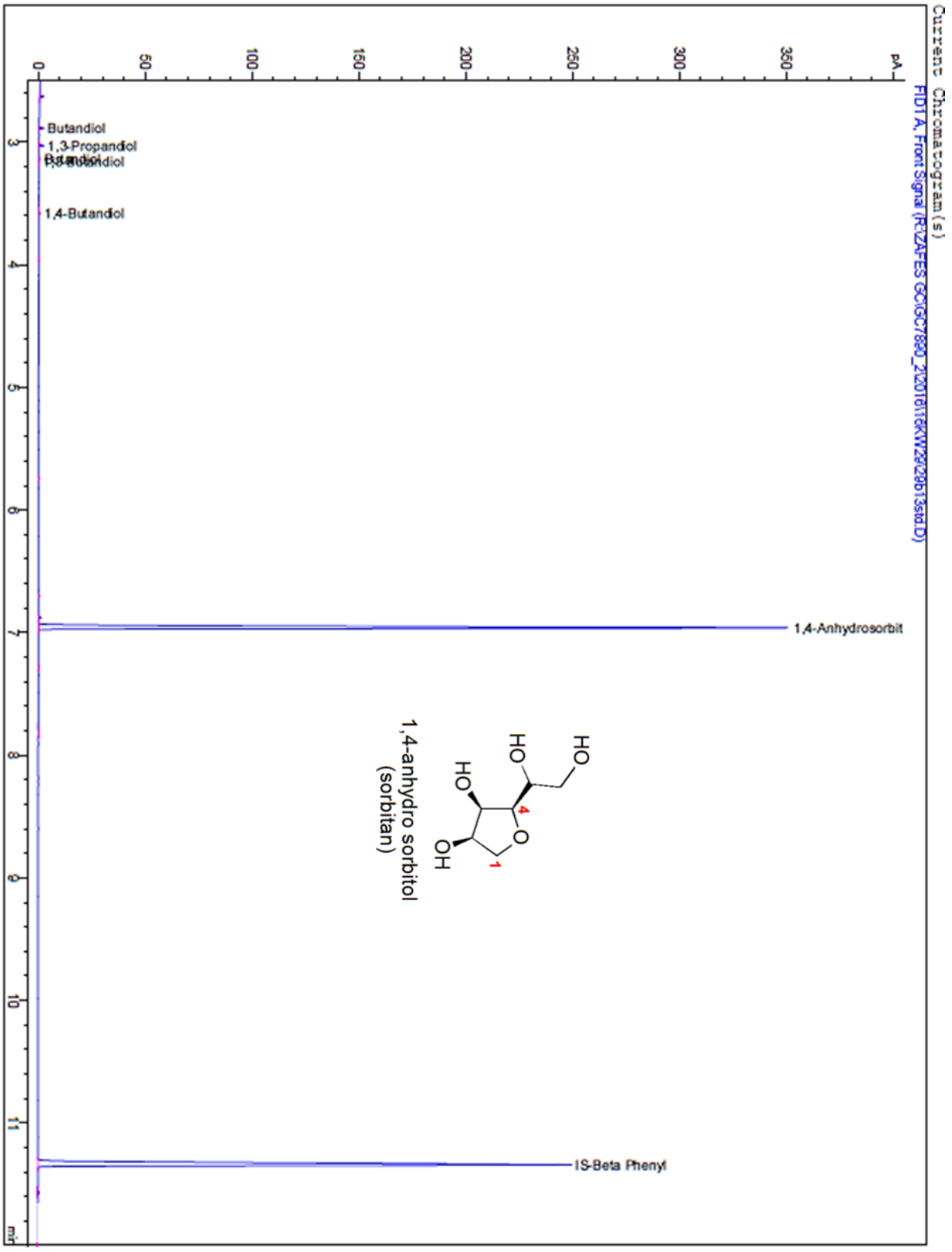

Figure 9-18: GC chromatogram of 1,4-anhydro sorbitol (sorbitan, a stereoisomer to 1,4-anhydro mannitol (mannitan)) purchased from Sigma Aldrich.

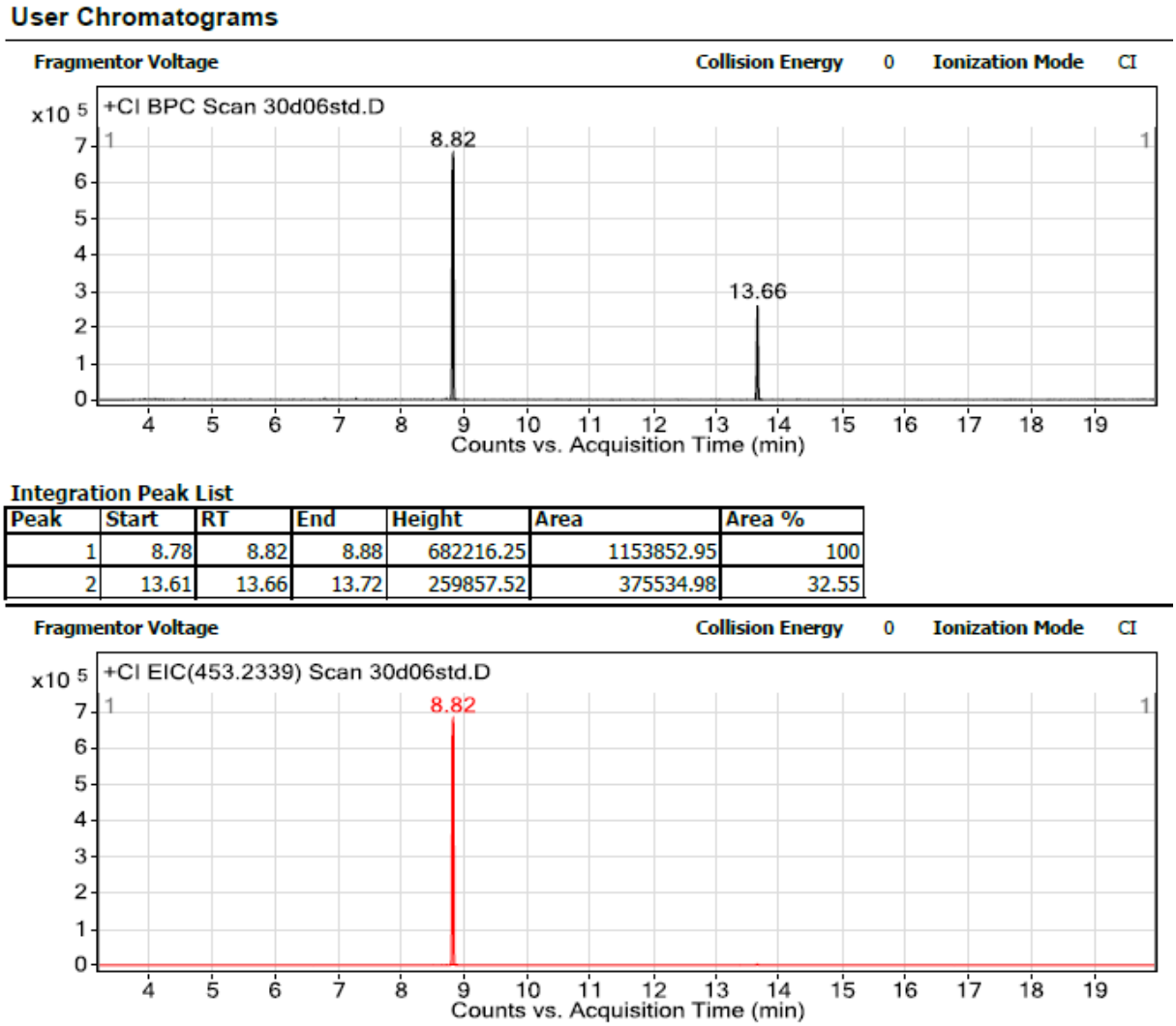

Figure 9-19: GC-MS spectrum of 1,4-anhydro sorbitol (sorbitan, purchased from Sigma Aldrich) shown in **Figure 9-18** with a mass-to-charge-ratio of 453,2 m/z (M+1 ion).

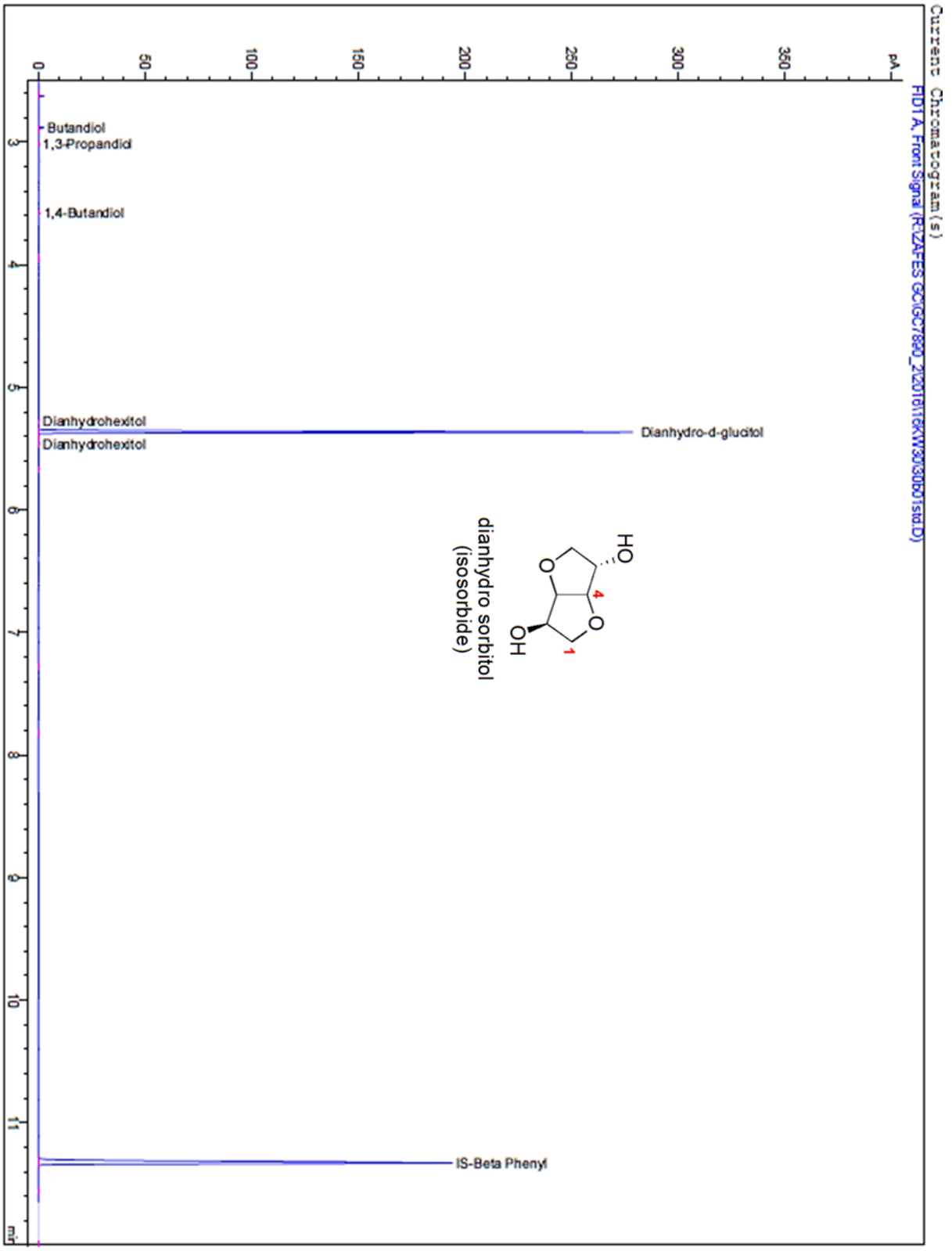

Figure 9-20: GC chromatogram of a dianhydro sorbitol standard (isosorbide, a stereoisomer to dianhydro mannite (isomannide)) purchased from Sigma Aldrich (as Dianhydro-d-glucitol).

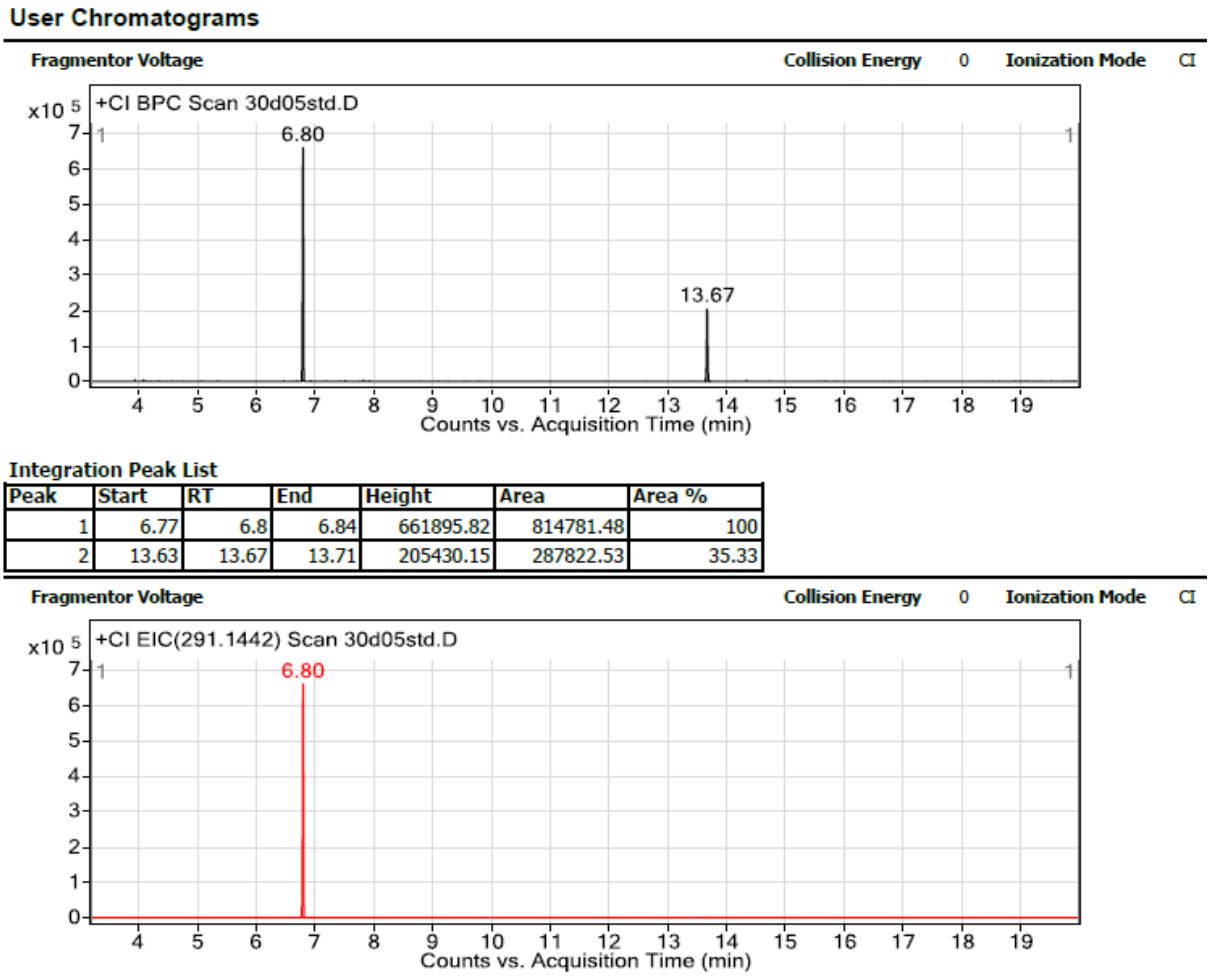

Figure 9-21: GC-MS spectrum of dianhydro sorbitol (isosorbide, purchased from Sigma Aldrich) shown in **Figure 9-20** with a mass-to-charge-ratio of 291,1 m/z (M+1 ion).

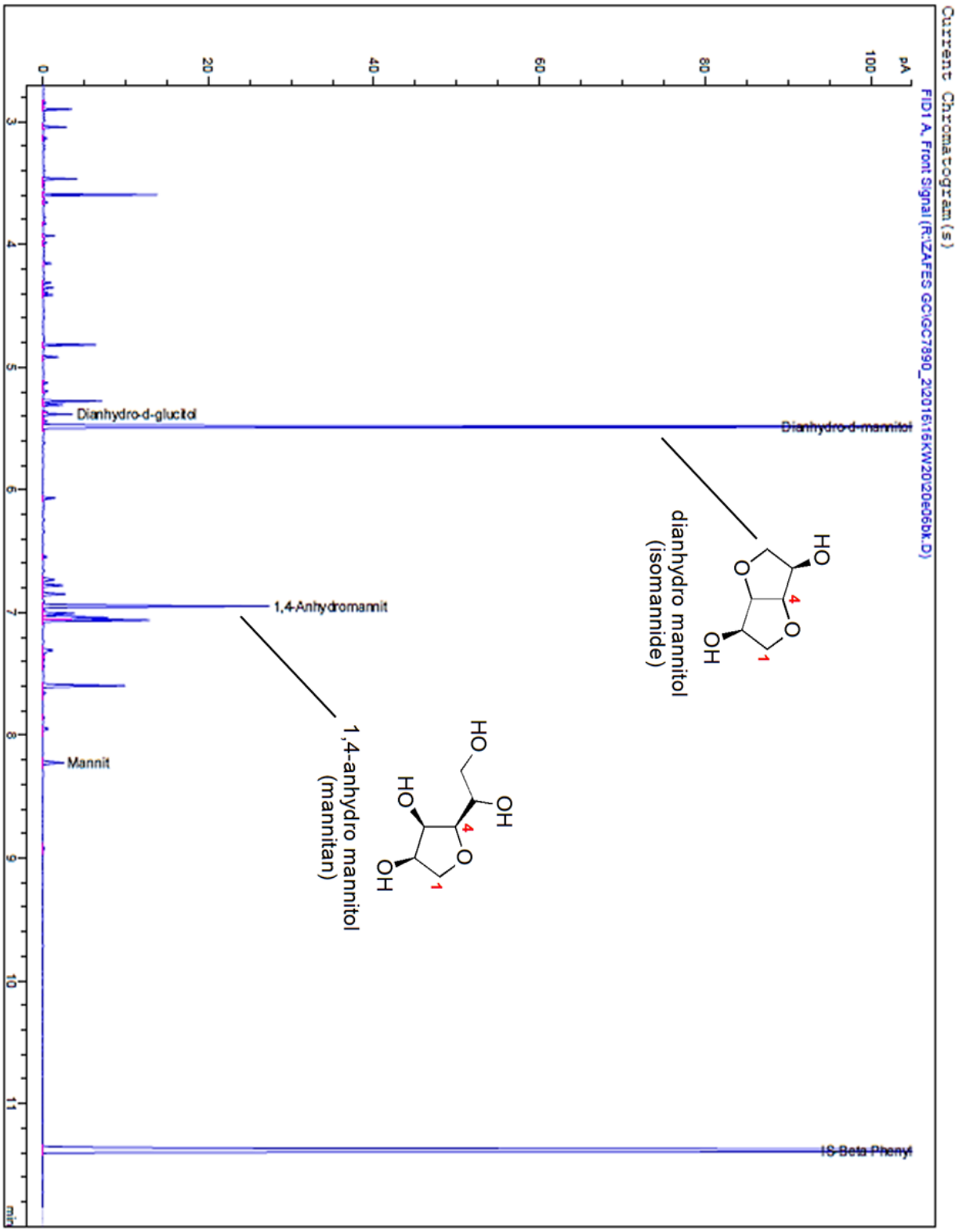

Figure 9-22: GC chromatogram of the product mixture obtained from mannitol hydrogenolysis (aqueous 7.5 wt-% mannitol solution) over an acidic H-ZSM-5 zeolite at 220 °C, 150 bar H_2 and 5 h reaction time. The main product is isomannide (dianhydro-d-mannitol, 5.5 min) along with mannitan (1,4-anhydro-mannitol) at 7.0 min retention time. The peak of the reactant, mannitol, is shown at 8.2 min retention time.

9.2. GC-chromatograms of product mixtures obtained from hydrogenolysis over Cu- and Ru-based catalysts

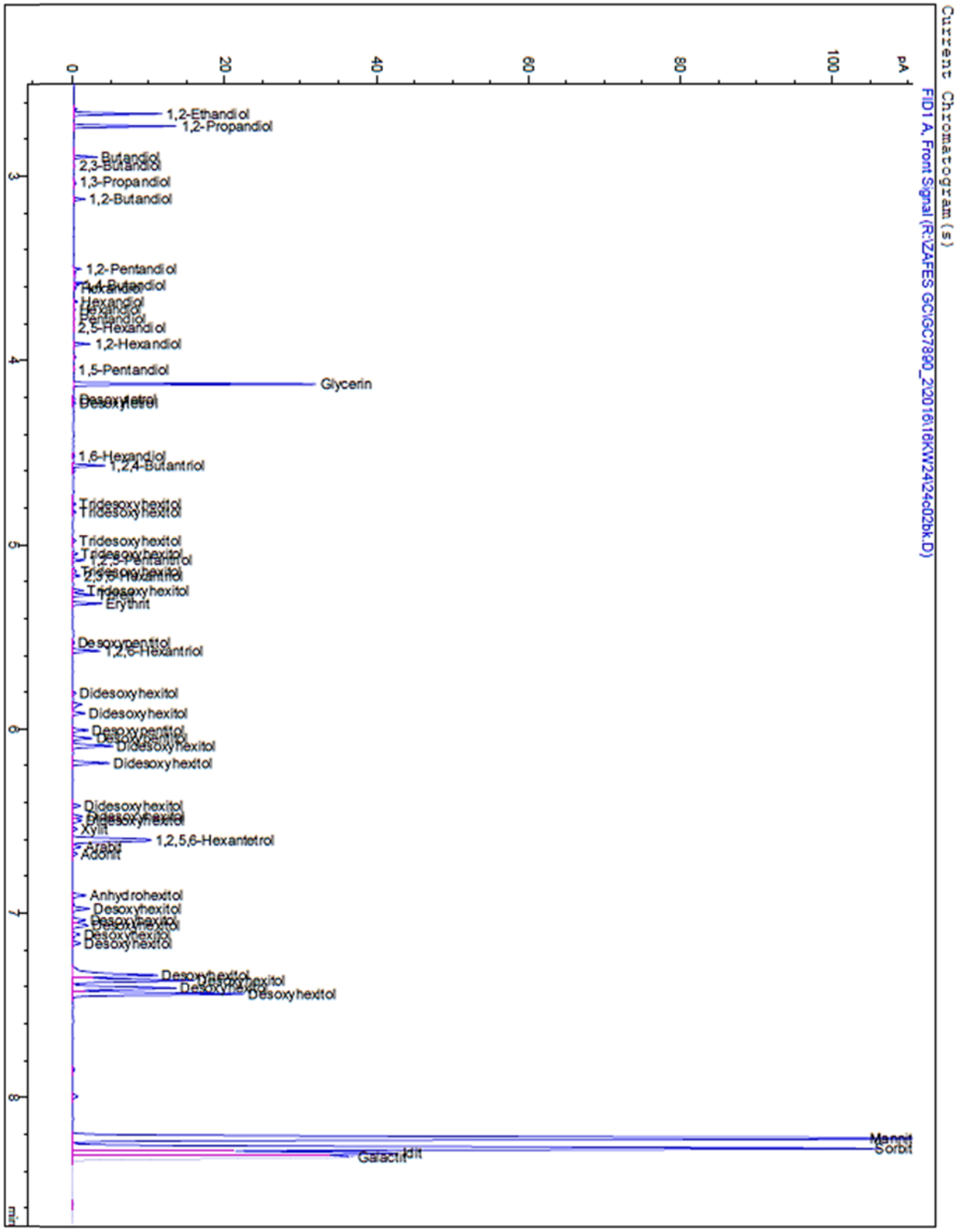

Figure 9-23: GC chromatogram of the product mixture obtained from mannitol hydrogenolysis (aqueous 7.5 wt-% mannitol solution) over Cu/ZnO at 180 °C, 150 bar H_2 and 5 h reaction time. The main products are 3-deoxy hexitols (four stereoisomers at 7.4 min retention time), the 3,4-deoxy hexitol (1,2,5,6-hexanetetrol, at 6.6 min), ethanediol and 1,2-propanediol (2.7 min), and glycerol (4.2 min).

Figure 9-24: GC chromatogram of the product mixture obtained from mannitol hydrogenolysis (aqueous 7.5 wt-% mannitol solution) over Cu/ZnO at 220 °C, 150 bar H_2 and 5 h reaction time. The main products are 3,4-deoxy hexitol (1,2,5,6-hexanetetrol, at 7.0 min retention time), ethanediol and 1,2-propanediol (2.8 min), and glycerol (4.3 min).

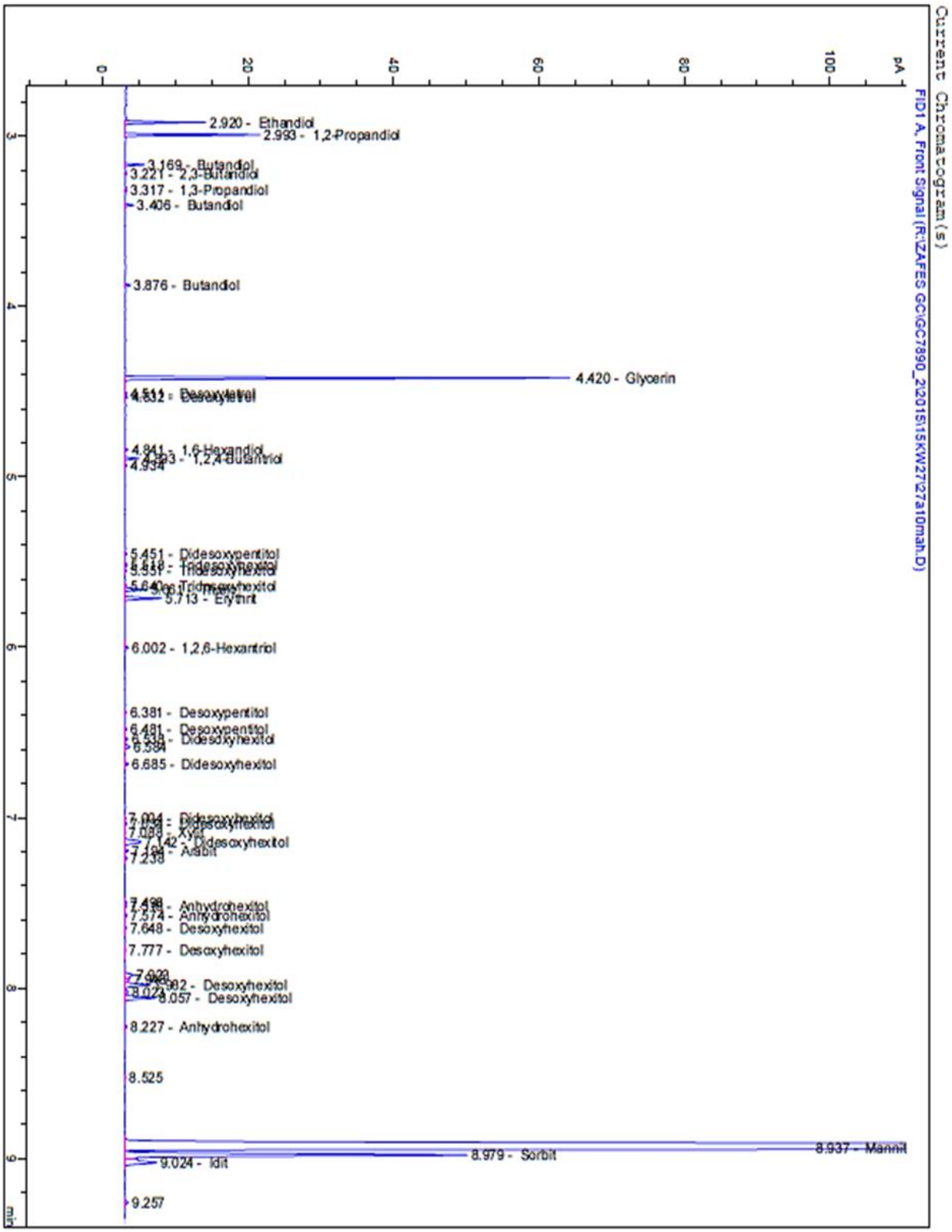

Figure 9-25: GC chromatogram of the product mixture obtained from mannitol hydrogenolysis (aqueous 7.5 wt-% mannitol solution) over Cu/Al_2O_3 at 180 °C, 150 bar H_2 and 5 h reaction time. The main product is glycerol (4.5 min retention time).

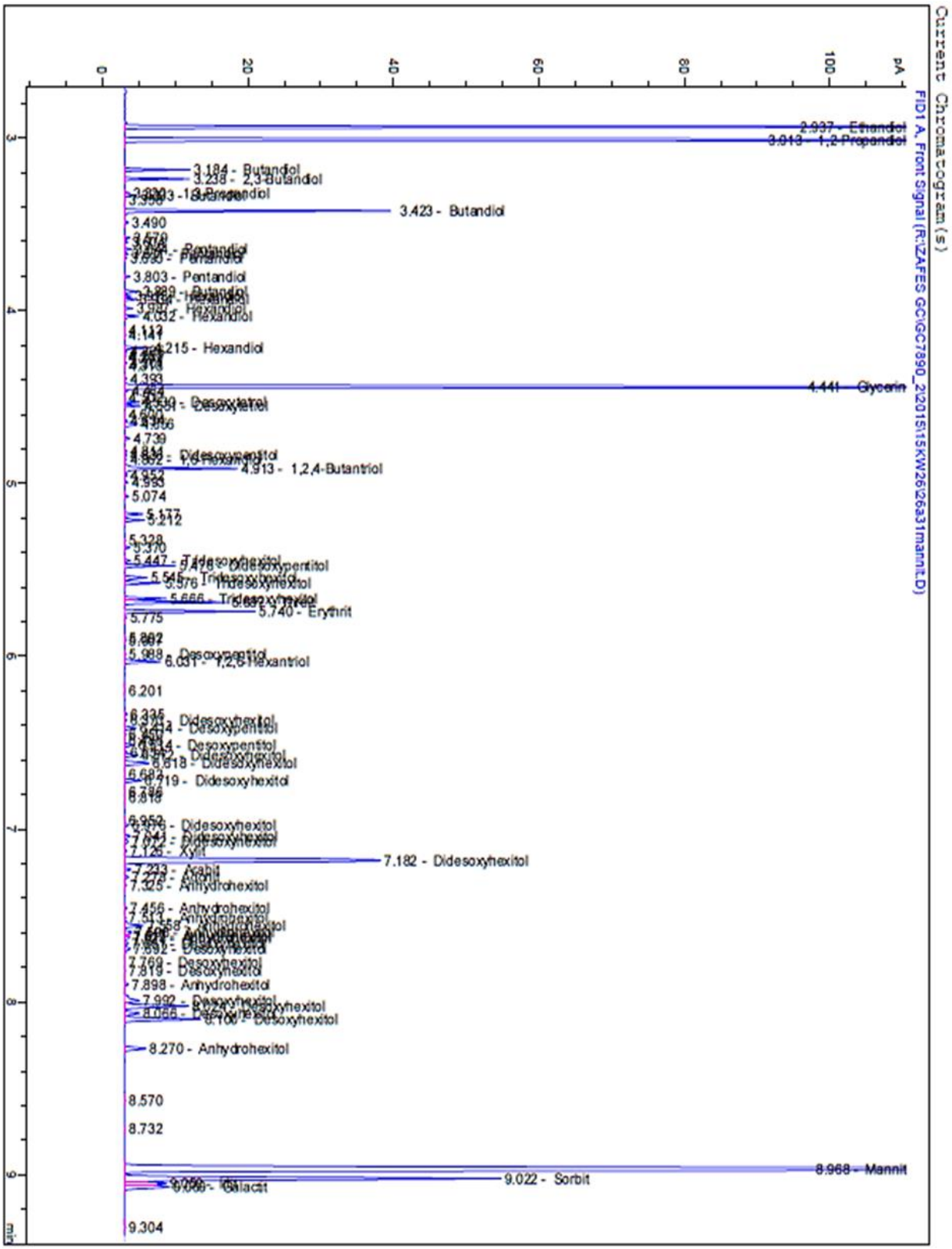

Figure 9-26: GC chromatogram of the product mixture obtained from mannitol hydrogenolysis (aqueous 7.5 wt-% mannitol solution) over Cu/Al_2O_3 at 220 °C, 150 bar H_2 and 5 h reaction time. The main products are ethanediol and 1,2-propanediol (3 min retention time), and glycerol (4.5 min).

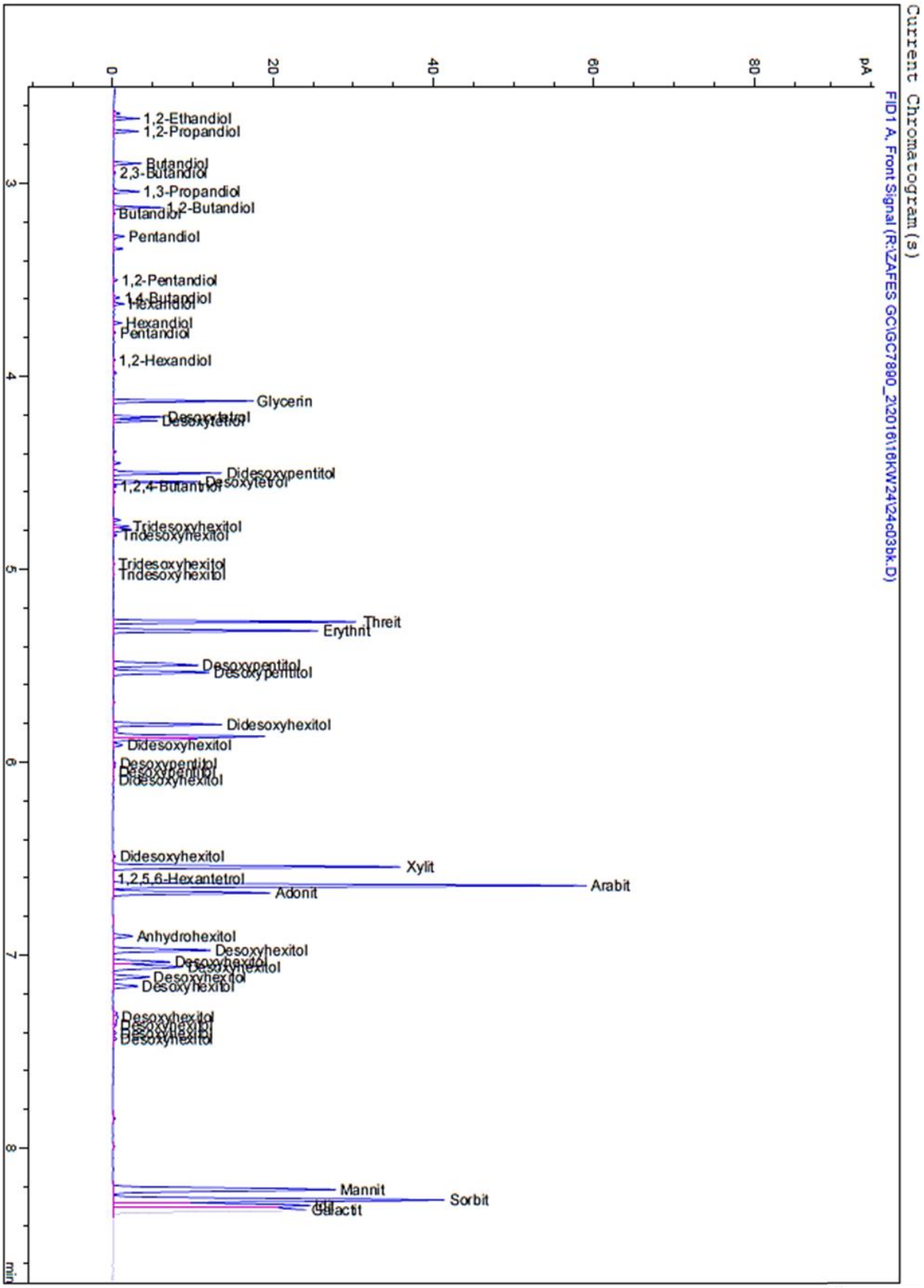

Figure 9-27: GC chromatogram of the product mixture obtained from mannitol hydrogenolysis (aqueous 7.5 wt-% mannitol solution) over Ru/Al_2O_3 at 180 °C, 150 bar H_2 and 5 h reaction time. The main products are C5 polyols (xylitol, arabitol, as well as ribitol (labeled as Adonit)) at 6.6 min retention time.

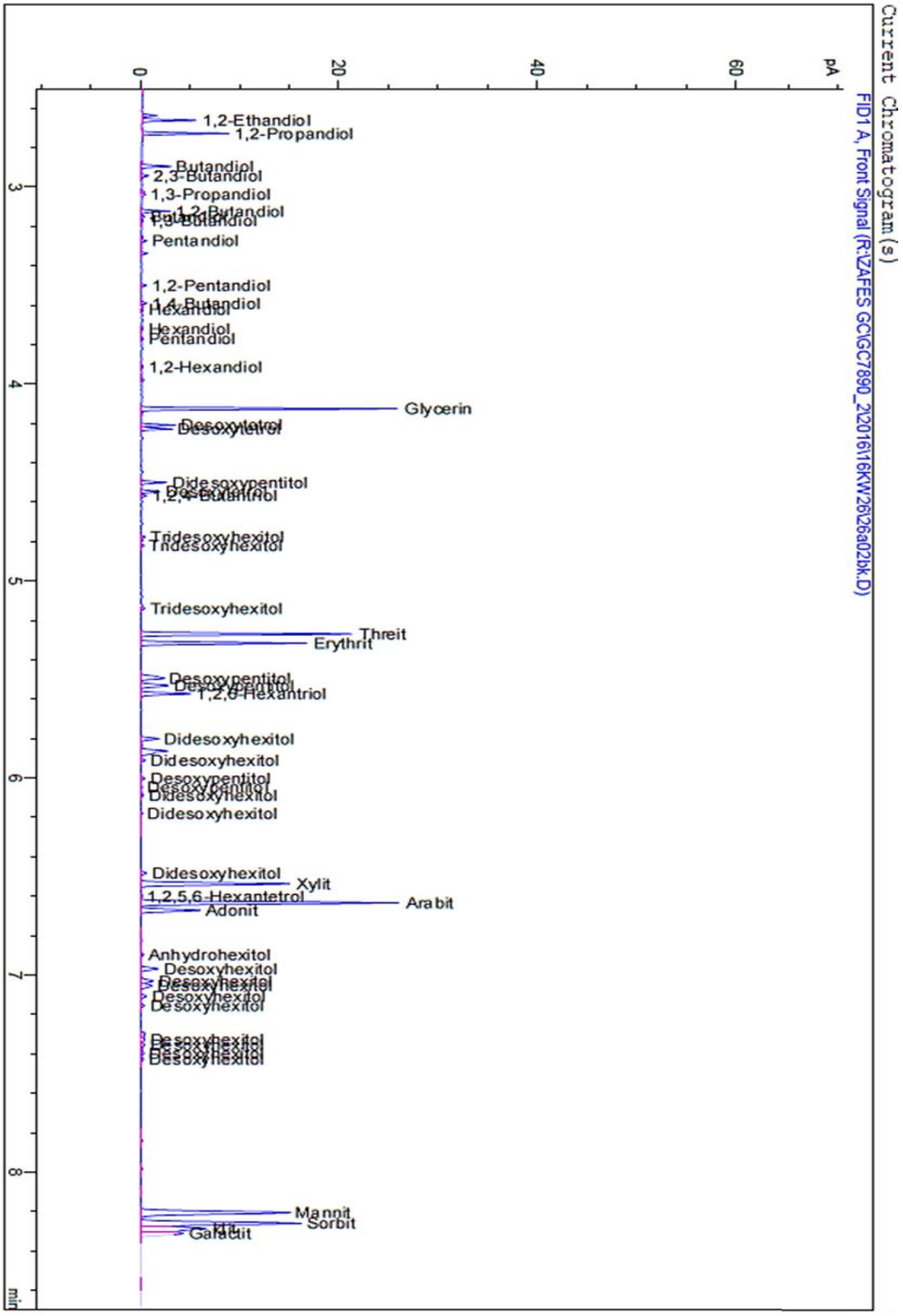

Figure 9-28: GC chromatogram of the product mixture obtained from mannitol hydrogenolysis (aqueous 7.5 wt-% mannitol solution) over Ru/Al_2O_3 at 220 °C, 150 bar H_2 and 5 h reaction time. The main products are gaseous C1 polyols and only 13 mol-% of the applied carbon is left in the liquid phase. The liquid phase composition mainly accounts for C5 polyols (xylitol, arabitol, and ribitol (labeled as Adonit)) at 6.6 min retention time, the C4 polyols erythritol and threitol (5.3 min), and the C3 polyol glycerol (3.1 min).

9.3. BET analysis of the Cu-Raney and supported Cu/Al_2O_3 catalyst before and after hydrogenolysis reactions

Quantachrome QuadraWin - Data Acquisition and Reduction
for QuadraSorb SI
©2000-13, Quantachrome Instruments. All rights reserved.
version 6.0

Quantachrome

Analysis			Report			
Operator:	admin	Date:10/1/2016	Operator:	operator	Date:2016/11/14	
Sample ID:	BK_CuAl2O3	Filename:	BK_CuAl2O3.QPS			
Sample Desc:		Comment:				
Sample weight:	0.7602 g					
Analysis Time:	2186.2 min	End of run:	10/1/2016 23:06:39	Instrument:	QuadraSorb Station 4	
Void Vol.:	He Mode,Cell: 9mm small bulb	Run mode:	Standard	Instrument version:	6.01	
Cold Zone Vol.:	6.6861	Warm Zone Vol.:	7.4086			
Thermal delay:	180 sec	He evac time:	3 min			
Outgas Time:	2.0 hrs	OutgasTemp:	300.0 C			
Analysis gas:	Nitrogen	Bath Temp:	77.3 K			
Press. Tolerance:	variable/variable (ads/des)	Equil time:	variable/60 sec (ads/des)	Equil timeout:	variable/120 sec (ads/des)	

Multi-Point BET

Data Reduction Parameters Data

Adsorbate	Nitrogen		Temperature	77.350K		
	Molec. Wt.:	28.013	Cross Section:	16.200 Å²	Liquid Density:	0.808 g/cc

Multi-Point BET Data

Relative Pressure [P/Po]	Volume @ STP [cc/g]	1 / [W((Po/P) - 1)]	Relative Pressure [P/Po]	Volume @ STP [cc/g]	1 / [W((Po/P) - 1)]
1.39021e-01	43.4217	2.9753e+00	2.38743e-01	50.9971	4.9204e+00
1.59085e-01	44.9247	3.3693e+00	2.78952e-01	54.2705	5.7036e+00
1.78901e-01	46.4103	3.7562e+00	2.99265e-01	56.0074	6.1011e+00
1.98896e-01	47.9395	4.1438e+00			

BET summary

Slope =	19.491
Intercept =	2.674e-01
Correlation coefficient, r =	0.999999
C constant=	73.885
Surface Area =	176.252 m²/g

Figure 9-29: BET analysis of the fresh Cu/Al_2O_3 catalyst (purchased from Sigma Aldrich) before it was applied for six hydrogenolysis reactions of 5 h reaction time, each, for the conversion of mannitol at 180 to 220 °C and 150 bar H_2. A surface area of 176 m^2/g was calculated from N_2 adsorption.

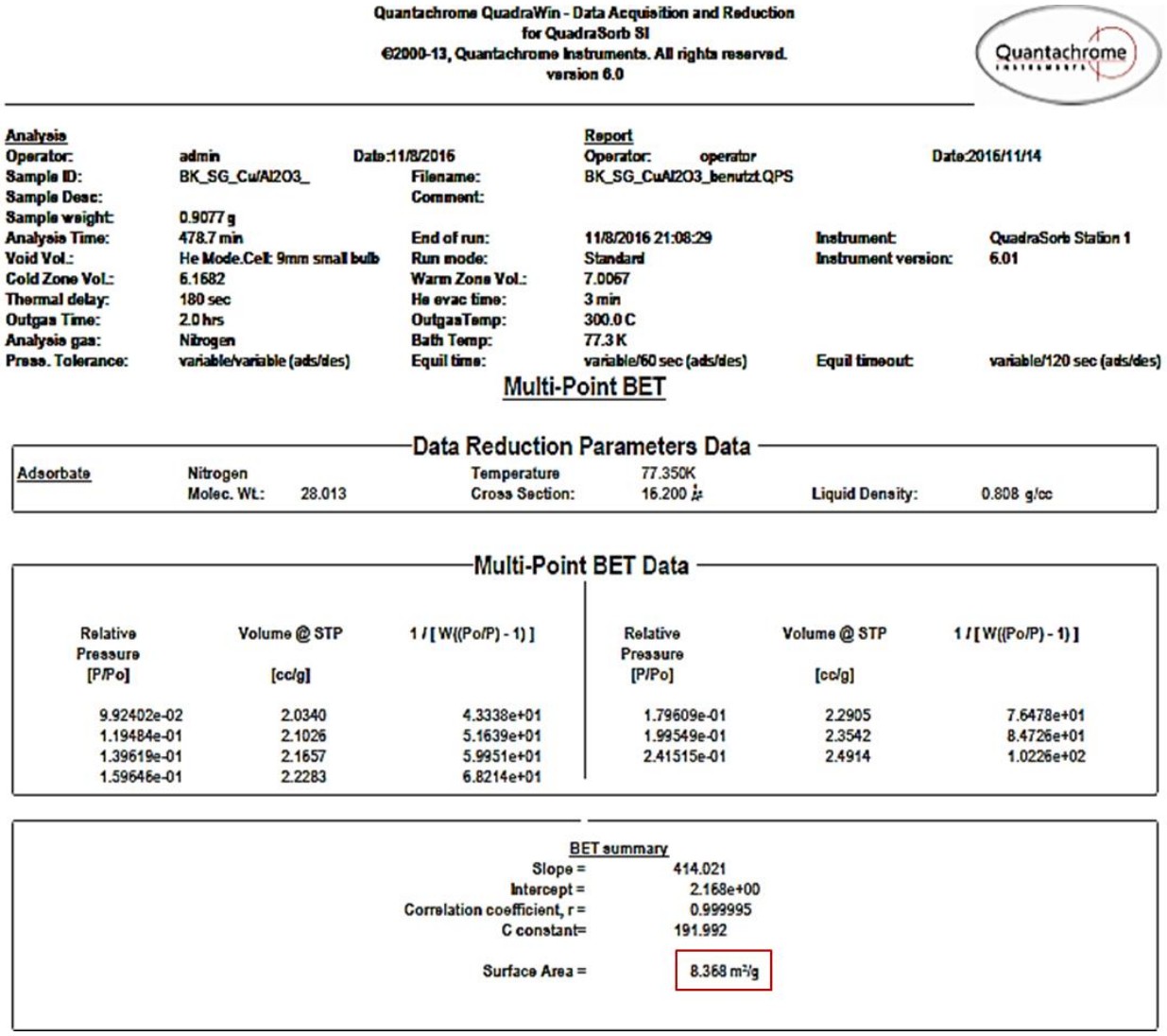

Quantachrome QuadraWin - Data Acquisition and Reduction
for QuadraSorb SI
©2000-13, Quantachrome Instruments. All rights reserved.
version 6.0

Quantachrome

Analysis			Report			
Operator:	admin	Date:11/8/2016	Operator:	operator	Date:2016/11/14	
Sample ID:	BK_SG_Cu/Al2O3_	Filename:	BK_SG_CuAl2O3_benutzt.QPS			
Sample Desc:		Comment:				
Sample weight:	0.9077 g					
Analysis Time:	478.7 min	End of run:	11/8/2016 21:08:29	Instrument:	QuadraSorb Station 1	
Void Vol.:	He Mode.Cell: 9mm small bulb	Run mode:	Standard	Instrument version:	6.01	
Cold Zone Vol.:	6.1682	Warm Zone Vol.:	7.0067			
Thermal delay:	180 sec	He evac time:	3 min			
Outgas Time:	2.0 hrs	OutgasTemp:	300.0 C			
Analysis gas:	Nitrogen	Bath Temp:	77.3 K			
Press. Tolerance:	variable/variable (ads/des)	Equil time:	variable/60 sec (ads/des)	Equil timeout:	variable/120 sec (ads/des)	

Multi-Point BET

Data Reduction Parameters Data

Adsorbate	Nitrogen		Temperature	77.350K		
	Molec. Wt.:	28.013	Cross Section:	16.200 Å²	Liquid Density:	0.808 g/cc

Multi-Point BET Data

Relative Pressure [P/Po]	Volume @ STP [cc/g]	1 / [W((Po/P) - 1)]	Relative Pressure [P/Po]	Volume @ STP [cc/g]	1 / [W((Po/P) - 1)]
9.92402e-02	2.0340	4.3338e+01	1.79609e-01	2.2905	7.6478e+01
1.19484e-01	2.1026	5.1639e+01	1.99549e-01	2.3542	8.4726e+01
1.39619e-01	2.1657	5.9951e+01	2.41515e-01	2.4914	1.0226e+02
1.59646e-01	2.2283	6.8214e+01			

BET summary

Slope =	414.021
Intercept =	2.168e+00
Correlation coefficient, r =	0.999995
C constant=	191.992
Surface Area =	8.368 m²/g

Figure 9-30: BET analysis of the used Cu/Al_2O_3 catalyst (purchased from Sigma Aldrich) after it was applied for six hydrogenolysis reactions of 5 h reaction time, each, for the conversion of mannitol at 180 to 220 °C and 150 bar H_2. A surface area of 8 m^2/g was calculated from N_2 adsorption.

Quantachrome QuadraWin - Data Acquisition and Reduction
for QuadraSorb SI
©2000-13, Quantachrome Instruments. All rights reserved.
version 6.0

Analysis
Operator: admin
Sample ID: Ben SMR479
Date:5/19/2016
Filename:

Report
Operator: admin
Date:2016/06/01
Ben SMR477 nach alk Wäsche.QPS

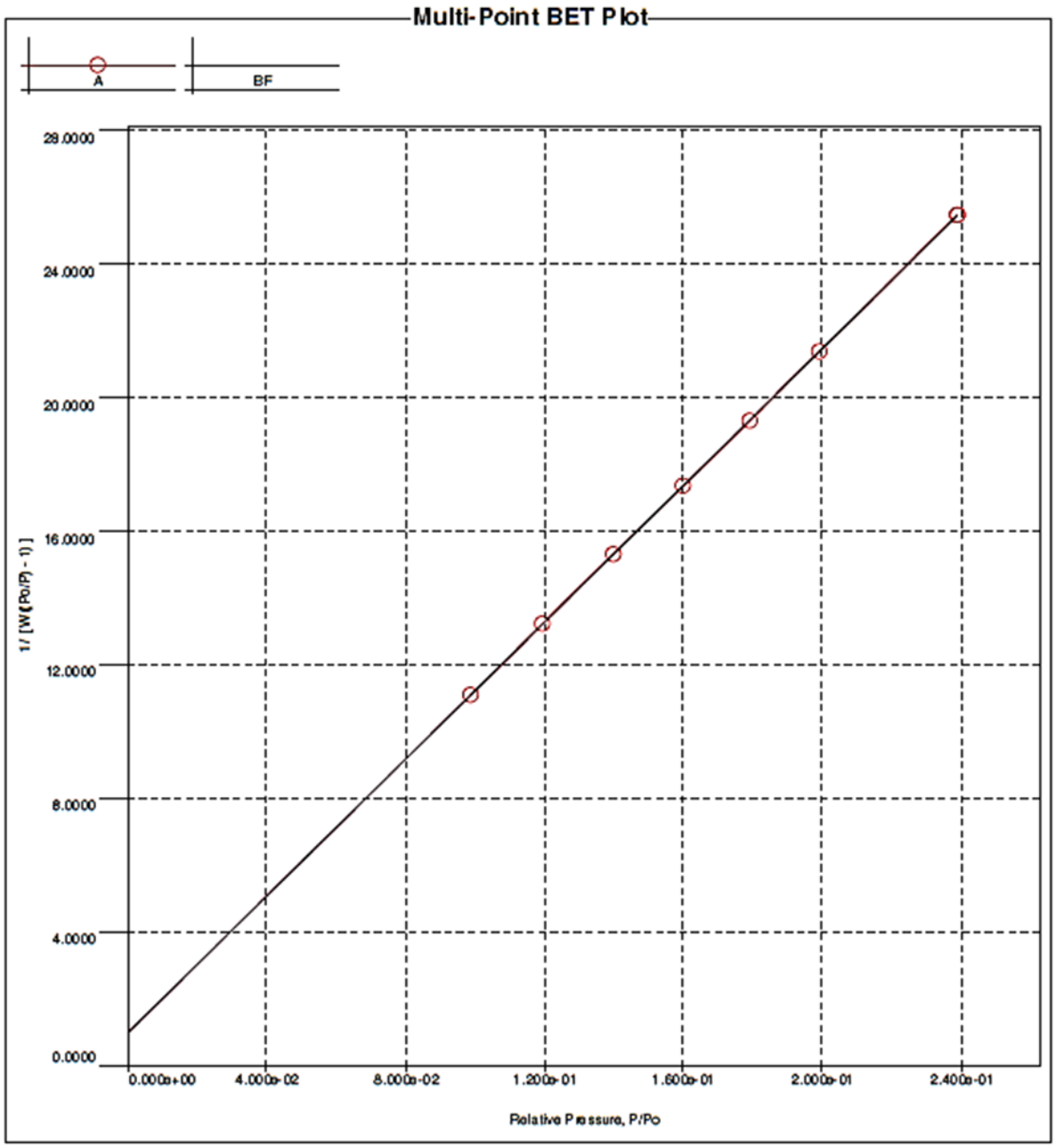

MBET summary

Slope =	102.414
Intercept =	9.851e-01
Correlation coefficient, r =	0.999997
C constant =	104.967
Surface Area =	33.680 m²/g

Figure 9-31: BET analysis of the fresh Cu-Raney catalyst (provided from Südzucker) before it was applied for six hydrogenolysis reactions of 5 h reaction time, each, for the conversion of mannitol at 180 to 220 °C and 150 bar H_2. A surface area of 34 m^2/g was calculated from N_2 adsorption.

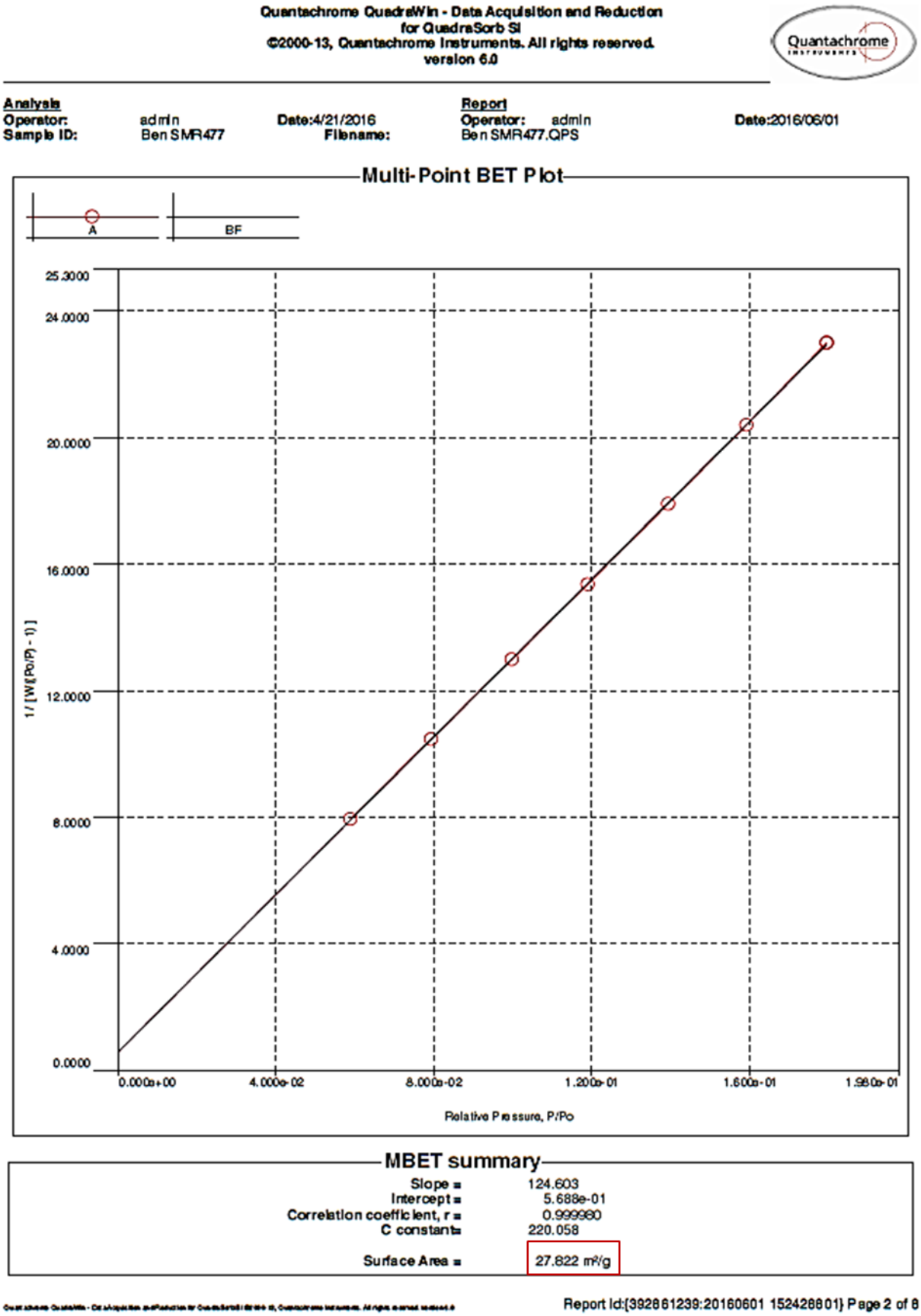

Figure 9-32: BET analysis of the used Cu-Raney catalyst (provided from Südzucker) after it was applied for about 200 h time-on-stream at hydrogenolysis conditions (180 to 220 °C at 150 bar H_2). A surface area of 28 m^2/g was calculated from N_2 adsorption.

9.4. Calculation (rough estimation) of fix costs and operating costs for an industrial process based on experimental data from laboratory experiments and literature

9.4.1. Calculation of capital investment for a 20.000 tons chemical plant

ISBL (location-independent capital investment: pure chemical plant) and OSBL (location-dependent invest: also includes auxiliary plants, e.g. storage buildings, cooling towers, and disposal facilities) for a 20.000 tons chemical plant are calculated using the method of specific units under consideration of each unit's complexity [Vogel2002]. One unit is defined as a complete reaction or separation unit, including all pumps, compressors, heat exchangers and main tanks. The ISBL costs arise from equation 9.1.

$$\boldsymbol{ISBL}\ (€) = Q\ (€\ a\ t^{-1}\ unit^{-1})\ x\ \frac{\boldsymbol{i}}{\boldsymbol{i(0)}}\ x\ capacity\ (t\ a^{-1})\ x\ \sum_{1}^{n}\ [N(units)\ x\ CF] \qquad \text{Eq. 9.1}$$

with Q : base factor for petrochemical intermediates, 60 € / (t a^{-1}) *x* unit in 1995 [Vogel2002]

$\frac{\boldsymbol{i}}{\boldsymbol{i(0)}}$: cost index, considers inflation rate (2,1 % → $1{,}021^{23}$) to adapt the base factor for 2018

capacity: production of 20.000 tons per year

N : Number of units, the process concept (see **Figure 7-1**) requires 8 units in total

CF: complexity-factor

To estimate a chemical plant's complexity, correction factors were defined from Zevnik *et al.* that corresponds to the temperature and pressure in each unit, as well as the used material (e.g. aluminium or stainless-steel) [Zevnik1963]. These factors are assessed based on diagrams and values, shown in **Figure 9-33**, to calculate the complexity-factor CF as defined in equation 9.2.

$$\boldsymbol{CF} = 2\ x\ 10^{(F_T + F_P + F_M)} \qquad \text{Eq. 9.2}$$

with CF : complexity-factor

F_T: correction factor for operating temperature

F_P: correction factor for operating pressure

F_M: correction factor for material

Table 9-1: Calculation of complexity-factors (*CF*) for each unit of the process concept shown in **Figure 7-1**. The complexity-factor *CF* is based on the correction factors F_T, F_P, and F_M that are estimated from the diagrams shown in **Figure 9-33** [Zevnik1963].

Hydrogenation unit *N* (units) = 1		**Hydrogenolysis unit** *N* (units) = 1		**Absorption, SMB unit, and four evaporators** *N* (units) = 6	
F_T	0.04	F_T	0.06	F_T	0
F_P	0.22	F_P	0.23	F_P	0
F_M	0.40	F_M	0.40	F_M	0.40
CF	**9.14**	***CF***	**9.80**	***CF***	**5.02**

The ISBL costs arise to ~ 95 mio. € when the equations 9.1 and 9.2 are applied with the corresponding values and complexity-factors for each unit:

$$\boldsymbol{ISBL}\ (€) = 60\ (€\ a\ t^{-1}\ unit^{-1})\ x\ 1.021^{23}\ x\ 20.000\ (t\ a^{-1})\ x\ (1\ \text{x}\ 9.14 + 1\ \text{x}\ 9.80 + 6\ \text{x}\ 5.02)$$
$$= 95.000.000\ €$$

When the construction of auxiliary plants, e.g. storage buildings, cooling towers, and disposal facilities are also considered, the OSBL costs are taken into account. The OSBL costs are roughly calculated by multiplication of the ISBL costs with the factor 1.33:

$$\boldsymbol{OSBL}\ (€) = 1.33\ x\ ISBL\ (€) = 126.300.000\ €$$

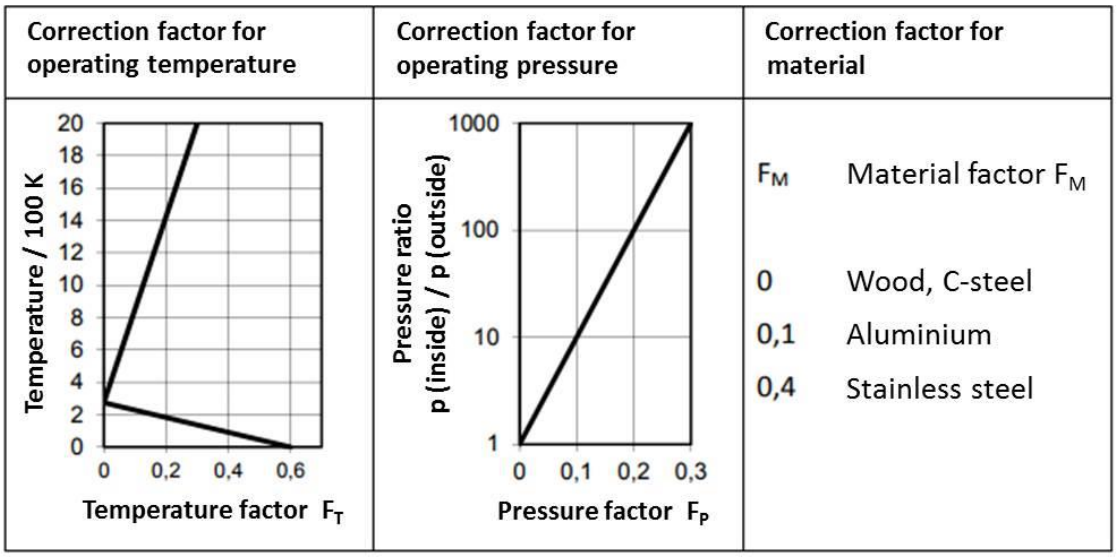

Figure 9-33: Correction factors for temperature, pressure and material of a unit according to Zevnik [Zevnik1963].

9.4.2. Calculation of operating and production costs for a 20.000 tons chemical plant

Main operating cost factors for an industrial chemical plant are depreciation (payback of capital investment, OSBL, over several years), maintenance, raw materials (here: sugars and hydrogen), steam as an energy source of the multiple heat exchangers, and waste water treatment. Hereby, steam is a much cheaper energy source than electricity, in particular for countries with expensive costs per kWh like Germany [Vogel2002]. The depreciation is mainly affected by the desired time (number of years) for the payback of the capital investment, OSBL, which includes the chemical plant with all units as shown in **Figure 7-1** and auxiliary plants such as storage buildings and waste treatment facilities. Usually the payback of the invest should be finished after ten years. Hence, 10 % of the OSBL costs are priced on the production costs for 20.000 tons per year (depreciation costs) [Vogel2002].

A payback after twelve years results in a depreciation of 8.3 % of the OSBL per year. The maintenance cost is usually in the range of 3-5 % of the OSBL per year, which is also priced on the production of 20.000 tons per year [Vogel2002]. **Table 7-1** in chapter 7 shows the estimated costs considering "average values" (average case) and lower priced values (best case) that depend e.g. on different raw material prices in different countries, better heat-coupling, or lower depreciation and maintenance costs. The calculation of each expense is based on a capacity of 20.000 tons per year and performed using the following equations.

$$\textbf{\textit{Depreciation costs}}\ (€/kg) = \frac{OSBL\ (€)}{N\ (a)\ x\ 20.000\ (t\ a^{-1})\ x\ 10^3\ (kg\ t^{-1})}$$
$$= 0.63\ €/kg\ (payback\ after\ 10\ years)$$
$$or\ \ 0.48\ €/kg\ (payback\ after\ 12\ years)$$

with *N (a)*: Number of years for payback of the capital investment (OSBL) [Vogel2002].

$$\textbf{\textit{Maintenance costs}}\ (€/kg) = \frac{OSBL\ (€)\ x\ maintenance\ factor\ (\%)}{20.000\ (t\ a^{-1})\ x\ 10^3\ (kg\ t^{-1})}$$
$$= 0.32\ €/kg\ (5\ \%\ per\ year)$$
$$or\ \ 0.19\ €/kg\ (3\ \%\ per\ year)$$

with *maintenance factor*: Percentage of OSBL costs, usually 3-5 % per year [Vogel2002].

$$\textbf{\textit{Raw materials costs}}\ (€/kg) = \frac{Tonnage\ sugar\ as\ feed\ (t\ a^{-1})}{20.000\ (t\ a^{-1})}\ x\ sugar\ price\ (€/kg)$$
$$= \frac{1}{mass\ yield\ of\ products}\ x\ sugar\ price\ (€/kg)$$
$$= \frac{1}{0.45}\ x\ 0.41\ (€/kg)$$
$$= 0.91\ €/kg$$

with *Tonnage sugar as feed*: dependent on mass yield of deoxy polyols from sugars (45 wt-%)*.

sugar price: estimated 0.41 €/kg [Vogel2002].

* The C-balance is 80 mol-% (see **Figure 5-9** in chapter 5.1.2). Hexanetriols, glycols and the 1,2,5,6-hexanetetrol account for ~77 mol-% of the total amount of carbon (77 mol-% of the C-balance; 33 mol-% for hexanetriols, 11 mol-% for glycols, and 33 mol-% for the 1,2,5,6-hexanetetrol) in the liquid phase (see **Figure 5-9** in chapter 5.1.2).

Hence, only about 45 wt-% of the applied sugar is yielded in the three product streams as shown in the following equation.

$$Mass\ yield\ of\ products\ (wt\ \%) = \frac{\sum[S_{\boldsymbol{Product}}\ (mol\ \%)\ x\ M_{\boldsymbol{Product}}\ (g\ \ mol^{-1})]}{M_{Glu}\ (g\ \ mol^{-1})}$$

$$= \frac{0.8\ x\ (0.33\ x\ M_{\boldsymbol{Hexanetriols}} + 0.11\ x\ \overline{M}_{\boldsymbol{Glycols}} + 0.33\ x\ M_{\boldsymbol{1,2,5,6-HTO}}}{M_{\boldsymbol{Glu}}\ (g\ \ mol^{-1})}$$

$$= 0.45 = 45\ wt\ \%$$

with $M_{\boldsymbol{Glu}}$: 180 g/mol (molar mass of glucose (or fructose, respectively))

$M_{\boldsymbol{Hexanetriols}}$: 134 g/mol

$\overline{M}_{\boldsymbol{Glycols}}$: 69 g/mol for a mixture of ethanediol and 1,2-propanediol

$M_{\boldsymbol{1,2,5,6-HTO}}$: 150 g/mol

$$Tonnage\ sugar\ as\ feed\ (t\ \ a^{-1}) = \frac{20.000\ (t\ \ a^{-1})}{0.45} = 44.400\ (t\ \ a^{-1})$$

$$\boldsymbol{Hydrogen\ costs}\ (€/\boldsymbol{kg}) = \frac{H_2\ consumption\ per\ year\ (t\ \ a^{-1})}{20.000\ (t\ \ a^{-1})}\ x\ H_2\ price\ (€/kg)$$

$$= 0.13\ €/kg\ (based\ on\ H_2\ price\ in\ Europe)$$

$$or\ \ 0.04\ €/kg\ (based\ on\ H_2\ price\ in\ USA)$$

with *H_2 consumption per year*: dependent on number of hydrogenation and hydrogenolysis steps. It is assumed that 4 mol H_2 are consumed in average for the conversion of sugars (1 mol H_2 for hydrogenation of sugars to hexitols and 3 mol H_2 in average for multiple -C-O- and/or -C-C- bond cleavage steps to hexanetriols, glycols, 1,2,5,6-hexanetetrol, and various mono alcohols as minor side products)*.

H_2 price: estimated 1.35 €/kg in Europe and ~0.40 €/kg in USA [Boulamanti2017].

* The H_2 consumption results from the following equation:

$$H_2\ consumption\ per\ year\ (t\ \ a^{-1}) = Tonnage\ sugar\ as\ feed\ (t\ \ a^{-1})\ x\ \frac{M_{\boldsymbol{H_2}}\ (g\ \ mol^{-1})}{M_{\boldsymbol{Glu}}\ (g\ \ mol^{-1})}\ x\ 4$$

$$= 44.400\ (t\ \ a^{-1})\ x\ \frac{2\ (g\ \ mol^{-1})}{180\ (g\ \ mol^{-1})}\ x\ 4$$

$$= approx.\ 2000\ (t\ \ a^{-1})$$

$$\textbf{Steam costs}\ (€/kg) = \frac{Amount\ of\ steam\ (t\ a^{-1})}{20.000\ (t\ a^{-1})}\ x\ \frac{Steam\ price\ (€\ t^{-1})}{10^3\ (kg\ t^{-1})}\ x\ factor_{\textbf{heat-coupl.}}$$

$$= 0.49\ €/kg\ (with\ factor_{\textbf{heat-coupl.}}: 0.50)$$

$$or\ \ 0.25\ €/kg\ (with\ factor_{\textbf{heat-coupl.}}: 0.25)$$

with $Amount\ of\ steam$: Steam amount for heating the aqueous polyol solution up to hydrogenolysis temperature (180 °C) and for evaporation of water in downstream process. 16 bar steam is chosen, which equals 200 to 250 °C (superheated steam).

Steam price: estimated 32 €/t, which was adapted for 2018 from 20 €/t in 1995 [Vogel2002] by consideration of an inflation rate of 2.1 % (20 €/t $x\ 1.021^{23}$ = 32 €/t).

$factor_{\textbf{heat-coupl.}}$: factor that considers a reduction of energy and thus, the amount of steam, by heat-coupling of evaporators. Energy savings of about 50 % and more are possible in a heat-coupled multi-stage evaporator when compared to one large single tower [Luyken2018]. For this process, the factor is assumed to vary between 0.5 and 0.25, depending on the amount of stages.

$$Amount\ of\ steam\ (t\ a^{-1}) = \frac{Evaporated\ water\ (t\ a^{-1})}{\Delta H_{\textbf{vap,16 bar steam}}\ (kWh\ t^{-1})}\ x\ \Delta H_{\textbf{vap,water at 100°C}}\ (kWh\ t^{-1})$$

$$+ \frac{\dot{Q}_{\textbf{heating,water in H-200}}\ (kWh\ a^{-1})}{\Delta H_{\textbf{vap,16 bar steam}}\ (kWh\ t^{-1})}$$

$$= 513.000\ (t\ a^{-1})$$

$$+ 93.000\ (t\ a^{-1})\ =\ 606.000\ (t\ a^{-1})$$

with $\Delta H_{\textbf{vap,16 bar steam}}$: 534 kWh/t [Vogel2002]. $\Delta H_{\textbf{vap,water at 100°C}}$: 627 kWh/t [Vogel2002].

For a rough calculation of steam costs, the major energy sources are estimated: heating in the hydrogenolysis section and evaporation of water in the downstream process. The required heat capacity $\dot{Q}_{\textbf{heating,water in H-200}}$ to heat the hexitols solution up to hydrogenolysis conditions (180 °C) is estimated as follows. The mass stream exits the hydrogenation reactor R-100, shown in **Figure 7-1** in chapter 7, at 90 °C and consists of 30 wt-% hexitols (in total with water: about 150.000 t/a). This mass stream is diluted with the same amount of pure water (with an estimated 20 °C), which results in a mass stream of 300.000 t/a at 55 °C (15 wt-% hexitols). This stream needs to be heated up to 180 °C to enable hydrogenolysis (deoxygenation) conditions.

$$\dot{Q}_{\textbf{heating,water in H-200}} = c_{\textbf{p,water at 180°C/250bar}}\ x\ \dot{m}_{\textbf{hexitols solution}}\ x\ T_{\textbf{180°C}}$$

$$- c_{\textbf{p,water at 55°C/200bar}}\ x\ \dot{m}_{\textbf{hexitols solution}}\ x\ T_{\textbf{55°C}}$$

$$\dot{Q}_{\boldsymbol{heating,water\ in\ H-200}} = c_{\boldsymbol{p,water\ at\ 180°C/250bar}}\ x\ 3x10^{8}\ kg\ a^{-1}\ x\ 453\ K - c_{\boldsymbol{p,water\ at\ 55°C/200bar}}\ x\ 3x10^{8}\ kg\ a^{-1}\ x\ 328\ K$$

$$= 1.77x10^{11}\ kJ\ a^{-1} \quad \text{(this equals 6.15 MW)}$$

$$= 4.9x10^{7}\ kWh\ a^{-1}$$

with $c_{\boldsymbol{p,water\ at\ 55°C/200bar}}$: 4.14 kJ kg^{-1} K^{-1}, $c_{\boldsymbol{p,water\ at\ 180°C/250bar}}$: 4.3 kJ kg^{-1} K^{-1} [VDI1994].

The amount of water, that has to be evaporated in the downstream process, is calculated as follows.

$$Evaporated\ water\ (t\ a^{-1}) = evaporation\ before\ SMB^{*}\ (t\ a^{-1}) + dewatering\ of\ the\ 3\ product\ streams\ after\ SMB\ (t\ a^{-1})$$

$$= 237.000^{*}\ (t\ a^{-1}) + \sum\left(\frac{Feed_{\boldsymbol{Sugar}}\ (t\ a^{-1})}{M_{\boldsymbol{Glu}}\ (g\ mol^{-1})}\ x\ \frac{C-balance\ (mol\ \%)\ x\ S_{\boldsymbol{Product}}\ (mol\ \%)\ x\ M_{\boldsymbol{Product}}\ (g\ mol^{-1})}{ratio_{\boldsymbol{Product}}\ in\ product\ stream\ (wt\ \%)}\right)$$

$$= 237.000^{*}\ (t\ a^{-1}) + \frac{Feed_{\boldsymbol{Sugar}}\ (t\ a^{-1})}{M_{\boldsymbol{Glu}}\ (g\ mol^{-1})}\ x\ \frac{0.80\ (mol\ \%)\ x\ 0.33\ (mol\ \%)\ x\ M_{\boldsymbol{Hexanetriols}}\ (g\ mol^{-1})}{0.1\ (wt\ \%)} + \frac{Feed_{\boldsymbol{Sugar}}\ (t\ a^{-1})}{M_{\boldsymbol{Glu}}\ (g\ mol^{-1})}\ x\ \frac{0.80\ (mol\ \%)\ x\ 0.11\ (mol\ \%)\ x\ M_{\boldsymbol{Glycols}}\ (g\ mol^{-1})}{0.1\ (wt\ \%)} + \frac{Feed_{\boldsymbol{Sugar}}\ (t\ a^{-1})}{M_{\boldsymbol{Glu}}\ (g\ mol^{-1})}\ x\ \frac{0.80\ (mol\ \%)\ x\ 0.33\ (mol\ \%)\ x\ M_{\boldsymbol{1,2,5,6-HTO}}\ (g\ mol^{-1})}{0.1\ (wt\ \%)}$$

$$= 237.000^{*}\ (t\ a^{-1}) + 200.000\ (t\ a^{-1}) = 437.000\ (t\ a^{-1})$$

with $Feed_{\boldsymbol{Sugar}}$: 44.400 t/a

$M_{\boldsymbol{Glu}}$: 180 g/mol (molar mass of glucose (or fructose, respectively))

$M_{\boldsymbol{Hexanetriols}}$: 134 g/mol

$\overline{M}_{\boldsymbol{Glycols}}$: 69 g/mol for a mixture of ethanediol and 1,2-propanediol

$M_{\boldsymbol{1,2,5,6-HTO}}$: 150 g/mol

* The amount of water, that is evaporated before the SMB unit (237.000 t/a), is required to increase the concentration of polyols from ~11 wt-% after the hydrogenolysis reactor to ~60 wt-% to operate the SMB unit (see **Figure 7-1** in chapter 7). This number includes the water formed as a side product during deoxygenation reactions to deoxy polyols and side products, such as mono alcohols (in total: about 12.000 t/a).

Hence, in total about 606.000 t/a of 16 bar steam are required to heat the hexitols solution in H-200 (see **Figure 7-1** in chapter 7) and evaporate 437.000 t/a of water (under the chosen operating conditions) in the downstream process.

$$\boldsymbol{Water\ treatment\ plant}\ (€/kg) = \frac{M_{Sugar}\ (g\ mol^{-1})}{\bar{M}_{Products}\ (g\ mol^{-1})}\ x\ \frac{(1-S)}{S}\ x\ C\ content\ x\ C\ price$$

$$= 0.55\ €/kg$$

with M_{Sugar}: 180 g/mol (molar mass of glucose or fructose, respectively)

$\bar{M}_{Products}$: Approx. 132 g/mol for a mixture of the polyols in the 3 product streams. As 77 mol-% of the carbon in the liquid phase consists of these products, the averaged molecular weight is 0.33 / 0.77 *x* $M_{Hexanetriols}$ + 0.11 / 0.77 *x* $M_{Glycols}$ + 0.33 / 0.77 *x* $M_{1,2,5,6\text{-}HTO}$ ~ 132 g/mol

$M_{Hexanetriols}$: 134 g/mol

$\bar{M}_{Products}$: 69 g/mol for a mixture of ethanediol and 1,2-propanediol

$M_{1,2,5,6-HTO}$: 150 g/mol

S: Selectivity for the polyols in the 3 product streams, which is 62 mol-% (80 mol-% is the carbon yield the products account for ~77 mol-% from this amount of carbon. Hence, the selectivity is 0.80 *x* 0.77 = 0.62)

$C\ content$: Carbon content in the reactant, which is 40 wt-% for sugar (glucose or fructose).

$C\ price$: Approx. 1.61 €/kg C, which was adapted for 2018 from ~ 1 €/kg C in 1995 [Vogel2002] by consideration of an inflation rate of 2.1 % (1.0 €/kg C $x\ 1.021^{23}$= 1.61 €/kg C).

The calculations shown in this chapter determine the costs for production of sugar based deoxy C6 polyols (1,2,5,6-hexanetetrol and hexanetriols) and glycols, on a 20.000 tons scale as shown in **Table 7-1** in chapter 7. These numbers are approximations based on rough estimations for costs of the feedstock, rough calculation of the product streams (and product composition), heat capacity for heating of water in the hydrogenolysis section, and the evaporation of water in the downstream process. These are the main factors that contribute to production costs aside from depreciation and maintenance in an industrial process. **Table 7-1** in chapter 7 shows that, based on these numbers, the minimum production cost would be between 2.43 and 3.03 €/kg for bio-based 1,2,5,6-hexanetetrol and hexanetriols. Such calculations, in particular for ISBL / OSBL and thus, depreciation and maintenance costs, have a deviation of about ± 30 % to ± 60 % [Vogel2002].

9.4.3. Comparison of conversion rates for hydrogenation and hydrogenolysis reactions

The comparison of conversion rates for hydrogenation and hydrogenolysis reactions in the conceptual process design, shown in chapter 7, was based on hydrogenation runs using a Ni-Raney catalyst and 40 h hydrogenolysis experiments as shown in **Figure 5-9** in chapter 5.1.2. The amount of converted reactant (reducing sugar or hexitol, respectively) was standardized per one hour reaction time and one kilogram of catalyst (Ni-Raney or Cu-Raney, respectively). The conversion rate for sugar hydrogenation over Ni-Raney was calculated to be about 320 g h^{-1} kg_{cat}^{-1} (which equals 30 µmol min^{-1} g_{cat}^{-1} as shown in **Figure 9-34**), compared to 10.6 g h^{-1} kg_{cat}^{-1} of hexitol conversion in hydrogenolysis experiments over Cu-Raney. The conversion rate for the hydrogenolysis reaction results from equation 9.3.

Conversion rate for hydrogenolysis reaction

(Conversion of hexitols over Cu-Raney based on **Figure 5-9** in chapter 5.1.2): Eq. 9.3

$$Conv.\ rate\ = \frac{42\ g_{sorbitol}\ x\ 10^6\ \mu mol\ mol^{-1}}{182\ g\ mol^{-1}\ x\ \ 40\ h\ x\ 60\ min\ h^{-1}\ x\ \ 100\ g_{cat}} = 0.96\ \mu mol_{sorbitol}\ min^{-1}\ g_{cat}^{-1}$$

$$= 10.5\ g_{hexitols}\ h^{-1}\ kg_{cat}^{-1}$$

Hence, the hydrogenation is about 30 times faster than the hydrogenolysis reaction. The amount of sugar that needs to be hydrogenated in a chemical plant with capacity of 20.000 tons per year is about 44.440 tons (see chapter 9.4.2). Thus, the resulting catalyst amount for the hydrogenation and hydrogenolysis reactor, based on Ni- and Cu-Raney catalysts, are shown in equations 9.4 and 9.5.

Catalyst amount (Ni-Raney) for hydrogenation reactor: Eq. 9.4

$$Catalyst\ amount\ = \frac{44.400\ tons\ (sugar)\ x\ 10^6\ g\ ton^{-1}}{8000\ h\ a^{-1}\ x\ \ 320\ g\ h^{-1}\ kg_{cat}^{-1}\ x\ \ 10^3\ kg\ ton^{-1}} = 17.1\ tons$$

Catalyst amount (Cu-Raney) for hydrogenolysis reactor: Eq. 9.5

$$Catalyst\ amount\ = \frac{44.400\ tons\ (sugar)\ x\ 10^6\ g\ ton^{-1}}{8000\ h\ a^{-1}\ x\ \ 10.6\ g\ h^{-1}\ kg_{cat}^{-1}\ x\ \ 10^3\ kg\ ton^{-1}} = 525\ tons$$

The density of both Cu-Raney and Ni-Raney in the catalyst basket was ~2.0 (about 200 g per 100 ml catalyst basket). Based on equations 9.4 and 9.5, the volume of the hydrogenation reactor would be approximately 9 m³, whereas the hydrogenolysis reactor requires almost 270 m³ of catalyst. Hence, the amount of Cu-Raney is not feasible for an industrial realization of the hydrogenolysis reaction at a 20.000 tons a year scale. The conversion rate (and possibly the selectivity) of the hydrogenolysis catalyst needs to be improved.

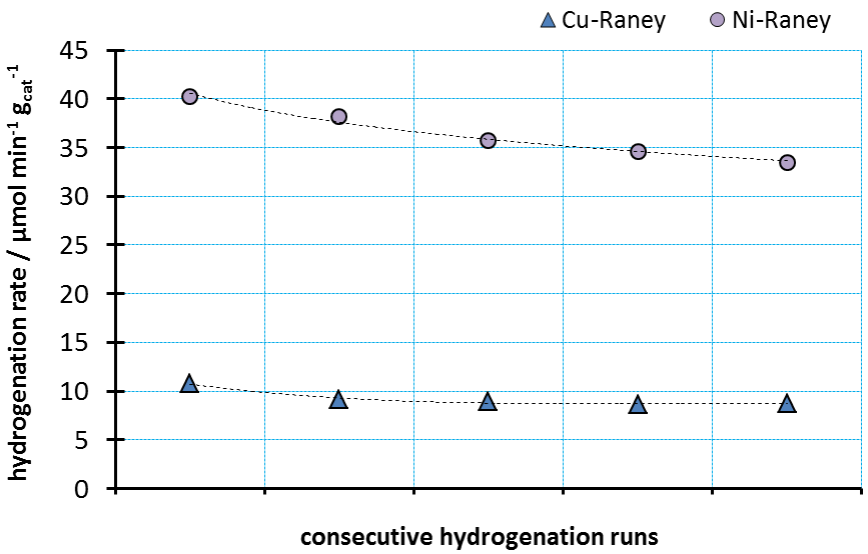

Figure 9-34: Conversion rates for Cu-Raney and Ni-Raney for the hydrogenation of isomaltulose (fructose building block) at 70 °C and 150 bar H_2. The hydrogenation rate is standardized per one gram of catalyst and results in conversion rates between 40 and 33 µmol min^{-1} g_{cat}^{-1} for the Ni-Raney catalyst. A conversion rate of 30 $\mu mol_{fructose}$ min^{-1} g_{cat}^{-1} equals to about 320 $g_{fructose}$ h^{-1} kg_{cat}^{-1}.

Declaration on the dissertation

I hereby declare that I have prepared this dissertation autonomously and only with the specified references, sources and aids. All passages taken from references are identified as such. This work has not yet been provided, in the same or similar form, to any examining office.

Darmstadt, 11th April 2018

(Benjamin Bernhard Kühne)

Curriculum Vitae

Personal data

Name:	Benjamin Bernhard Kühne
Address:	Apostelbräustr. 16 67549 Worms
Date of birth:	28th July 1988
Place of birth:	Mainz

Academic and school education

01/2014 – 06/2018	Doctoral thesis (dissertation) Working group: Prof. Dr.-Ing. Herbert Vogel Technische Universität Darmstadt Cooperation with Südzucker CRDS (Central Department for Research, Development, and Services) Supervision: Prof. Dr. Markwart Kunz
04/2013 – 11/2013	Masters thesis Südzucker CRDS Offstein, supervision: Prof. Dr. Markwart Kunz Research for working group: Prof. Dr.-Ing. Herbert Vogel Technische Universität Darmstadt
09/2008 – 11/2013	Academic chemistry studies Technische Universität Darmstadt
08/1999 – 06/2008	Immanuel-Kant-Gymnasium, Rüsselsheim

Professional activity

Since 01/2017	Process Engineer BASF SE Ludwigshafen
01/2014 – 12/2016	Research associate Working group: Prof. Dr.-Ing. Herbert Vogel Technische Universität Darmstadt
04/2013 – 11/2013	Trainee / Graduate Südzucker CRDS Offstein

Darmstadt, 11th April 2018